ABSTRACT

Title of Document: URBAN PARTICLE AND POLLUTANT CAPTURE VIA STORMWATER FILTER FACILITIES AND THE CONCOMITANT WATER QUALITY AND HYDROLOGICAL BENEFITS.

Houng Li, Doctor of Philosophy, 2007

Directed By: Professor Allen P. Davis
Department of Civil and Environmental Engineering.

Bioretention and sand filters are increasingly adopted as stormwater best management practices (BMPs) to remedy hydrology and water quality impairment from urban development. However, connection between BMP hydrological and water quality benefits and limits of BMP media (pollutant breakthrough, clogging, and long-term pollutant accumulation) are still unclear. This study investigated these issues through field hydrological and water quality monitoring, media core collection and analysis, and laboratory column tests.

Results indicate that bioretention facilities can achieve substantial hydrological benefits through delaying / reducing peak flows and decreasing runoff volume. Bioretention effluents exhibited good water quality for nearly all monitored pollutants except for copper and phosphorus, the latter of which may be attributed to media organic matter dissolution. Bioretention effectively removed suspended solids, lead,

and zinc from runoff. The runoff volume reduction promotes pollutant mass removal and links BMP water quality benefits with hydrological performance. However, effluent nutrients (phosphorus, nitrogen species) and Total Organic Carbon levels were slightly higher than those of the influent. Chloride was significantly exported.

Laboratory column tests show that bioretention media is limited by clogging and particle breakthrough is not expected. Clay components in urban runoff play an important role in media clogging. A bioretention filtration model is developed, which describes the column test results and can be used to predict bioretention performance. The investigation concludes that urban particles cannot penetrate into bioretention media for more than 5 to 20 cm.

Media analyses indicate that most captured metals affiliated with the trapped urban particles and the media collected within the top BMP layer. A small fraction of captured metals are soluble-exchangeable; the majority of the metal / media and metal / trapped urban particle affiliations are stronger. Substantial metal accumulation at the BMP surface was observed, suggesting maintenance needs. Captured phosphorous showed weaker media affiliations compared to those of the metals.

Based on these discoveries, a shallow bioretention design is recommended, which can substantially reduce construction costs and increase the popularity of bioretention, resulting in more hydrological and water quality benefits.

URBAN PARTICLE AND POLLUTANT CAPTURE VIA STORMWATER FILTER FACILITIES AND THE CONCOMITANT WATER QUALITY AND HYDROLOGICAL BENEFITS

By

Houng Li

Dissertation submitted to the Faculty of the Graduate School of the
University of Maryland, College Park, in partial fulfillment
of the requirements for the degree of
Doctor of Philosophy
2007

Advisory Committee:
Professor Allen P. Davis, Chair
Professor Robert L. Hill
Associate Professor Kaye L. Brubaker
Associate Professor Patrick Kangas
Associate Professor Eric A. Seagren

Dedication

This dissertation is dedicated to my dearest wife, Chiu, Chen, for all she has done, and does, and is.

A heartfelt thank is also offered to my family and friends in Taiwan, Canada, United Kingdom, and United States, who always sincerely wish me well.

Acknowledgements

I would like to express my gratitude to my advisor, Dr. Allen P. Davis and the dissertation committees, Dr. Kaye L. Brubaker, Dr. Robert L. Hill, Dr. Patrick Kangas, and Dr. Eric A. Seagren for their professional comments that have improved the quality of this work. The inspiring courses taught by Dr. Oliver J. Hao, Dr. Bruce James, and Dr. Alba Torrents at the University of Maryland have prepared me for this research, to whom I owe a heartfelt appreciation too. I also would like to thank Navid Ariaban, Walter Caldwell, Craig Carson, Chen Chiu, Katie DiBlasi, Kevin J. Edwards, Howard P. Grossenbacher, Philip Jones, Ameya Pradhan, Rebecca C. Stack, Jim H. Stagge, Mark Wilcox, and Lan Zhang for their help with field sample collections, Maria Chang for her help in the laboratory experiments, Reagan Colaco , Mehmet Melih Demirkan, Kelly R. Flint, Ruxandra M. Floroiu, Chi-hsu Hsieh, Hunho Kim, and Xueli Sun for laboratory equipment demonstrations, the Prince George's County (MD)'s Public Works for providing the bioretention media, and the District of Columbia Department of Health (DOH), Environmental Health Administration and Prince George's County (MD), Department of Environmental Resources for financial support.

Gratefulness is also extended to my schoolmates for their companion and support to Chao-jen Chang, Eunyoung Hong, Kwee-len Lee and her family, Wei Xian and her family, and Sue-ming Yang. I thank my undergraduate advisor Dr. Jhy-Chern Liu and my master degree advisor Dr. Ching-Yuan Chang, as well as Dr. Hwong-Wen Ma for their mentoring and recommendation that helped me gain the admission to the University of Maryland and be able to initiate this doctoral research thereafter.

Table of Contents

.

List of Tables

List of Figures

Chapter 1: Introduction

1.1 **The Impact of Urban Development on Watershed Hydrology**

As impervious land area increases with urban development, the concomitant impact on the hydrologic cycle and water quality of watersheds can be enormous. First, development significantly alters the watershed hydrology (Figure 1-1, Schueler 1987), reducing the interception of rainfall from vegetation, infiltration, and ground water recharge, and increases surface runoff. A major impact of the imperviousness increase of a watershed is the decrease of infiltration and the buffer capacity against large precipitation. Without the pervious area to absorb precipitation through infiltration, more precipitation can be converted to rapid runoff. As such, the pattern of surface runoff changes accordingly.

Figure 1-2 illustrates the hydrograph of a stream before and after development. Before the development, the pervious areas provide the land the buffer capacity against the impact of the precipitation. The stream flow rates change in a gradual manner with time, with a higher baseflow supporting the aquatic ecosystem and proper water uses (drinking, recreation, fishing, irrigation, etc.) After development, the buffer capacity is lost, which provokes higher and more rapid peak discharge, and a lower baseflow and possibly longer dry period. The hydrological changes lead to complex challenges. First, the higher and more rapid discharge increase the probability of flood and channel erosion. The decrease of the infiltration interrupts the recharge of groundwater and surface water, which are valuable water resources

for many areas. The lower baseflow and longer dry period for streams endanger aquatic and riparian ecology and limit the water uses.

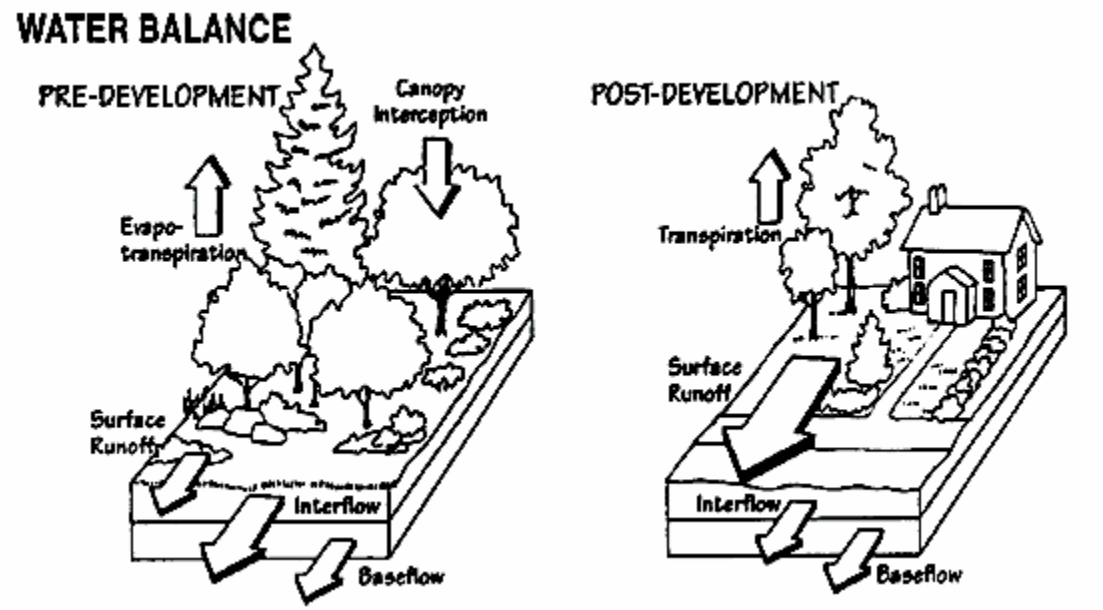

Figure 1-1. Comparison of water balance of a watershed before and after development (Schueler 1987).

Unfortunately, the frequency and intensity of precipitation, which are important components of the hydrologic cycle, are also changing toward an extreme pattern because of global warming. Research indicates that climate change is leading to higher frequency of flood and drought (Lehner et al. 2006), which aggravates these negative hydrological impacts of urban development. As such, remedies addressing the improvement of flood control capability and groundwater / surface water recharge should be examined and carefully adopted in a prompt manner.

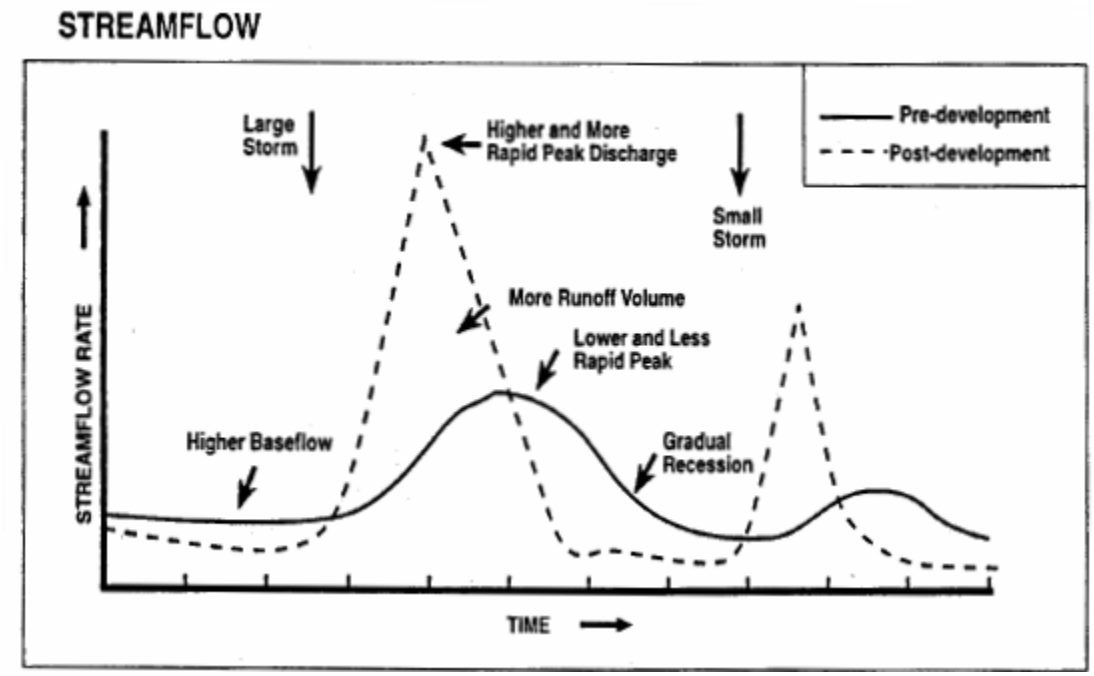

Figure 1-2. Comparison of hydrograph before and after development (Schueler 1987).

1.2 **The Impact of Urban Development on Water Quality**

Development also impairs water quality in local watersheds via point source and nonpoint source pollution. Point source discharges are directly from the outfalls of factories, industries, and municipal wastewaters. Prior to proper treatment, the pollutant loadings of point source discharges are generally much higher than nonpoint sources. One major pollutant in point source discharges is organic waste, which, if discharged without proper treatment into receiving water bodies, will be degraded by local microorganisms, stimulating significant oxygen consumption. Downstream ecology will be negatively affected as a result, accompanied with aesthetically unpleasant appearance and odor. Other pollutants such as organic solvents, heavy metals, and toxic substances also take part in rendering the receiving water unsuitable for drinking, irrigation, recreation, and many other uses.

The 1977 enacted Clean Water Act (CWA) in the United States regulates point source pollution via creating a permit program, the National Pollutant Discharge Elimination System (NPDES), which requires treatment and removal of major pollutants before discharging from point sources. Since then, point source water pollution has been significantly reduced through the checks and balances originating from NPDES enforcement. Table 1-1 illustrates a comparison of water quality parameters in urban runoff to that of treated domestic wastewater (after secondary treatment), which accounts the shift of the major pollution loading from point source to nonpoint source for receiving water bodies. For the United States and other territories in which point source water pollution is well-regulated, the front line of water pollution prevention has notably been reallocated to nonpoint source discharges.

USEPA promulgated the NPDES stormwater permit application regulation in 1990 (Stormwater program, Phase I), which addressed stormwater runoff discharges that flow directly into municipal separate storm sewer system (MS4s) serving a population of 100,000 or more. That covered 173 cities, 46 counties, and other USEPA or State designated systems such as state highway departments (USEPA 1999a). It also covered 11 categories of industries, including construction activity that disturbs 5 or more acres of land. The CWA requires these NPDES permits to prohibit non-stormwater from entering regulated MS4s, and to reduce the pollutant discharge to the maximum extent practicable. The Phase II program, which was initially published in 1999, expanded the Phase I program to smaller MS4s and construction that disturbs less than 5 acres of land (USEPA 2005).

Table 1-1. Comparison of water quality parameters in urban runoff with treated (after secondary treatment) domestic wastewater (USEPA 1999a).

Pollutant	Urban runoff (separate sewer)		Domestic wastewater (after secondary)
	Range	Typical	Typical
TSS (mg/L)	20-2890	150	20
TP (mg/L)	0.02-4.30	0.36	2
TN (mg/L)	0.4-20.0	2	30
Pb (μg/L)	10-1200	180	50
Cu (μg/L)	10-400	50	30
Zn (μg/L)	10-2900	20	80
Fecal Coliform (#/100 mL)	400-50000	-	200

Nonetheless, our knowledge for improving stormwater quality is still limited. Inherently, both the stormwater quality and flow quantity vary temporally and spatially and are not readily predictable (Davis and McCuen 2005), which render related studies a formidable challenge. Even so, a number of best management practices (BMPs) have been developed to mitigate stormwater pollution and restore post-development hydrology to pre-development hydrology, such as detention basins (dry), retention ponds (wet), filter facilities (e.g., sand filters and bioretention), vegetative practices (e.g., green roofs, grassed swales), constructed wetlands, and others (Davis 2005). Among these, the use of porous media (sands, gravel, soil, or others) as adsorptive filters to capture urban particulate and dissolved pollutants is a commonality shared by many stormwater BMPs. Additionally, some filter-type BMPs can also promote infiltration and simultaneously improve the post-development hydrology. Two representative BMP filtration facilities (bioretention and sand filters) are introduced in the following sections.

1.3 **Biortention for Treatment of Urban Stormwater Runoff**

Bioretention, also known as "rain garden," is an innovative stormwater BMP developed in the early 1990s to abate urban runoff pollutants and promote infiltration. Bioretention generally consists of a porous soil media layer covered with a thin layer of hardwood mulch (Figure 1-3). A variety of vegetation (grasses, shrubs, and small trees) are planted in a bioretention cell to promote evaportranspiration, biological activity, and pollutant uptake, as well as to maintain soil porosity and permeability. The bioretention facility is usually designed to a size of about 5% of the runoff drainage area (Davis and McCuen 2005), which can promote infiltration and compensate the hydrological impact after land development (Davis 2007a).

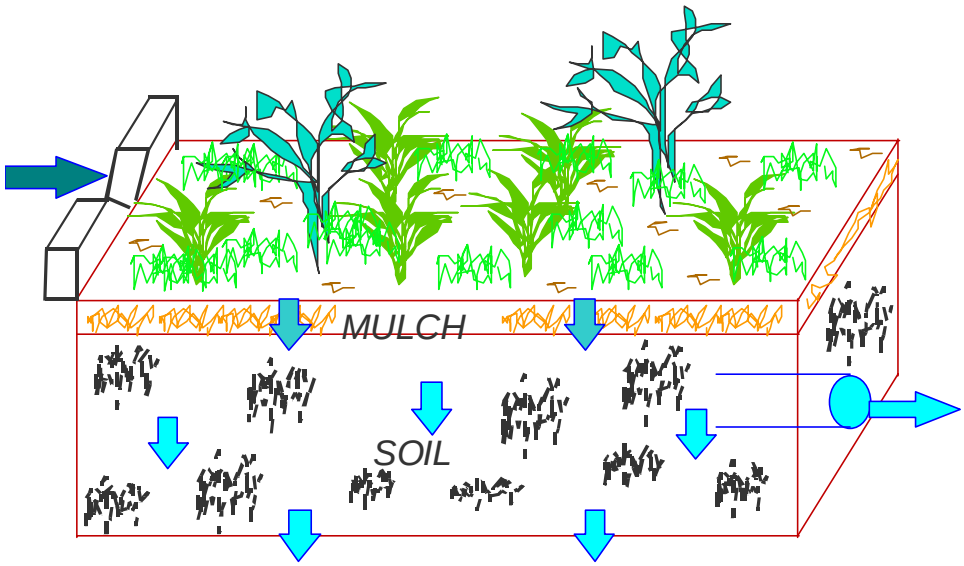

Figure 1-3. Basic bioretention components (Davis 2007a).

Previous laboratory and field bioretention studies have demonstrated its performance in water quality improvement, particularly in total suspended solids (TSS) and heavy metal removal (Davis et al. 2003, Hsieh and Davis 2005). For

nutrient pollutants (e.g., nitrogen and phosphorus species), the reported removal efficiencies were divided, from good (Davis et al. 2006), variable (Hsieh and Davis 2005), moderate, insignificant, and even exporting (Dietz and Clausen 2005, 2006), which may be attributed to their stronger sensitivity to the media and local watershed characteristics as compared to TSS and heavy metals. Nonetheless, good performance in controlling persistent pollutants, the encouragement of infiltration, the aesthetically pleasant appearance, and more natural appearance make bioretention an appealing BMP that is gaining more and more adoption in stormwater management.

1.4 Sand Filters for Treatment of Urban Stormwater Runoff

A sand filter is also used as a stormwater BMP to improve runoff quality. Sand filters can be built underground to accommodate limited space use, which is a preferred option for densely populated areas. An example of a sand filter is shown in Figure 1-4. A pretreatment well is usually placed in front to protect the filter bed from direct impact of diverted runoff. However, an underground sand filter needs a significant amount of concrete to construct, which increases the construction costs. A concrete filter bed bottom also limits the promotion of infiltration and hydrological improvement.

In contrast to bioretention, the sand filter is a mature technology, which has been fully developed for water and wastewater treatment. As a result, this work focused more on bioretention, instead of sand filters. The performance for stormwater quality improvement through sand filters has also been demonstrated in related studies (e.g., Urbonas 1999 and Barrett 2003). Nevertheless, the variability of incoming runoff characteristics in both quality and quantity and the infeasibility of a backwash process

for filter cleaning prompt new challenges for stormwater sand filter operation and maintenance.

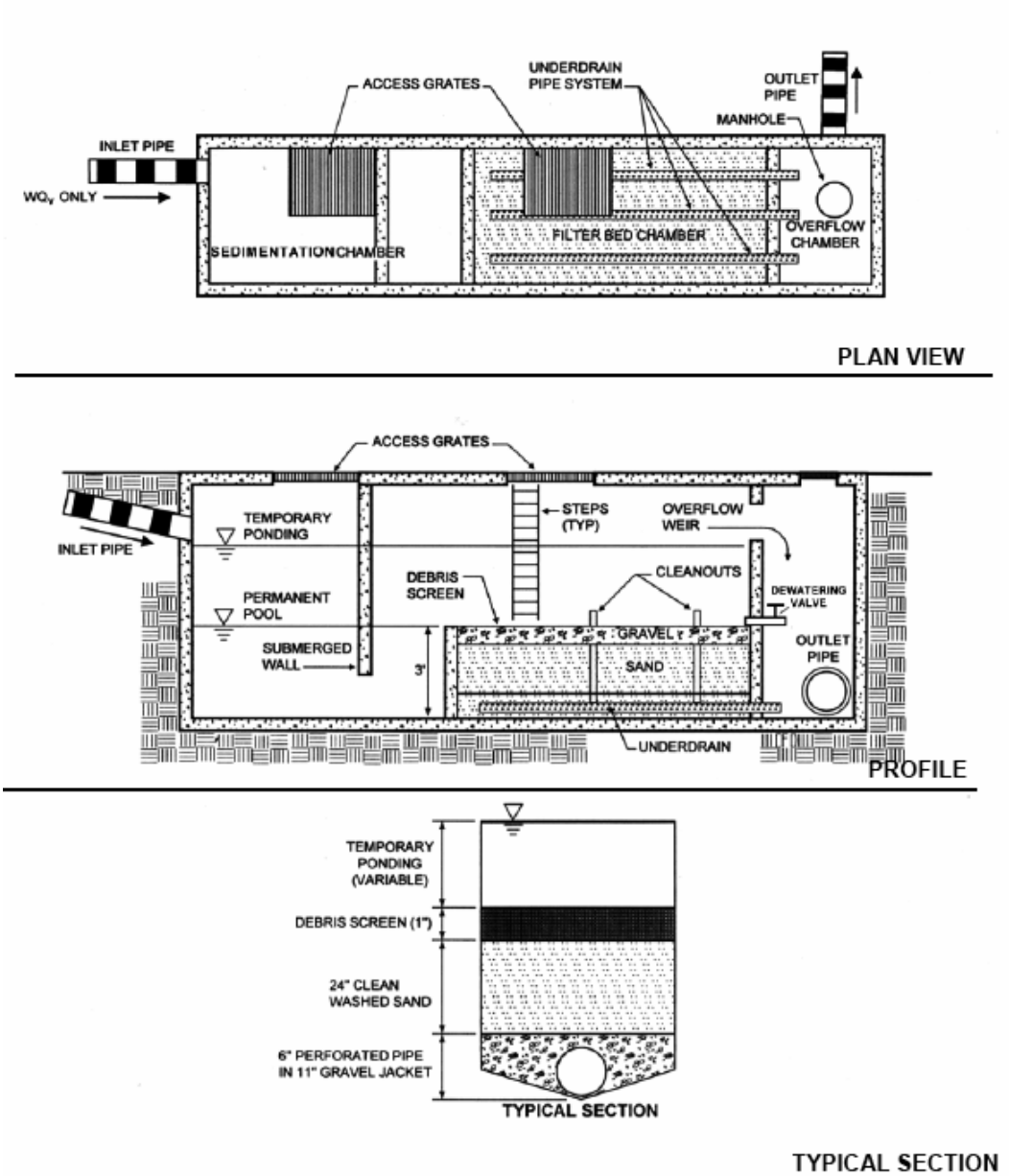

Figure 1-4. An underground sand filter for stormwater runoff treatment (MDE 2000).

1.5 Long Term Issues of BMP Filters for Treatment of Urban Stormwater Runoff

As many stormwater BMP filters are put on line for their water quality and hydrological benefits, several key long term issues remain. The first is the fate of the captured pollutants inside the BMP filter media. Whether these captured pollutants (especially persistent pollutants) will hold onto the media, or leach out with subsequent storm events, is a crucial factor for determining long term BMP performance. Risk of long term captured pollutant accumulation also plays a decisive role in BMP maintenance frequency. Different maintenance measures are currently adopted for BMP filters, including entire or partial replacement of the porous media. Understanding the spatial profile and fate of the captured pollutants can help identify the proper maintenance action, as well as modification of BMP design.

Several physical factors also determine the design and maintenance requirements of BMP filters. For example, as a filtering device, is the BMP filter a breakthrough limited filter or a clogging limited one? The performance of water and wastewater sand filters have been thoroughly investigated (McGhee 1991, Tchobanoglous et al. 2003). However, the performance of soil media BMP filters such as bioretention is still unknown.

The penetration depth of incoming urban particles inside the bioretention porous media is also a key factor for its design and maintenance. A comprehensive bioretention filtration modeling theory that can provide clear insight to these aspects is now required.

Finally, the hydrological benefits of the infiltration-promoting BMP filters have not been adequately and quantitatively addressed in the field scale, which can have

tremendous impact on local watersheds in the long run. The correspondence of water quality improvement through field bioretention facilities with the local hydrology has not been established.

1.6 Research Objectives, Benefits, and Approaches

This study had four major objectives:

1. To quantitatively estimate the hydrological benefits, water quality improvement and their correlations for field bioretention facilities.
2. To provide insight on the performance of bioretention media (breakthrough limited or clogging limited) for urban particle capture and the particle penetration depth.
3. To determine the fate and spatial profile of the captured pollutants in BMP filter media.
4. To assess the risk for long term pollutant accumulation within BMP filter media.

Field bioretention monitoring for pollutant abatement and hydrological improvement were performed (Chapter 3). Laboratory bioretention column tests were completed to determine whether bioretention media is clogging limited or breakthrough limited for urban particle capture, as described in Chapter 4. Based on observations from the column tests, a bioretention filtration theory and model were developed to estimate the particle penetration and filter life expectancy (Chapter 5). To determine the fate and spatial profile of the captured pollutants within BMP filters, media core samples were taken from field BMPs with subsequent laboratory media

analyses to examine the captured pollutant at different media depth with time, which is described in Chapter 6. These discoveries can be employed in modifying the design and maintenance of the BMP filters. Optimization of design and maintenance can reduce BMP construction and maintenance costs and maximize their hydrologic and water quality benefits; the resulting cost-effectiveness can promote their popularity and therefore achieve more environmental gains. Eventual benefits are improved water quality and hydrological conditions for post-development watersheds, as illustrated in Figure 1-5.

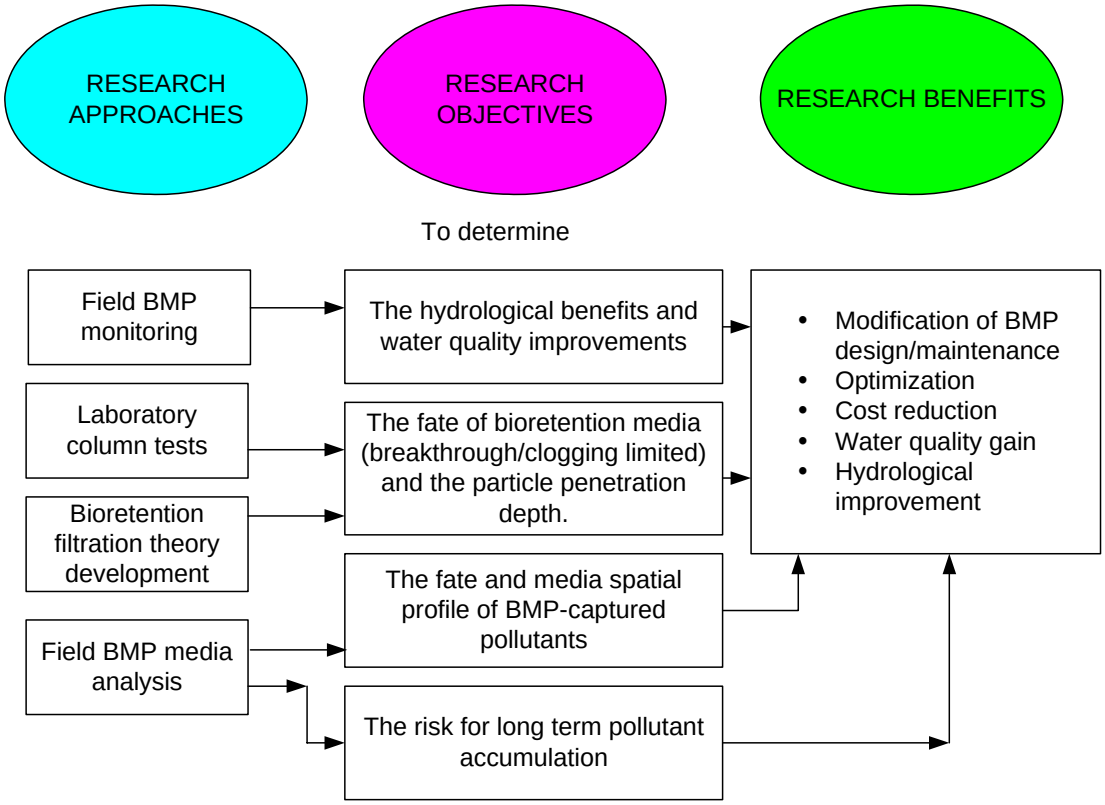

Figure 1-5. The research objectives, approaches, and benefits of this work.

Chapter 2: Background and Rationale for Research

2.1 Urban Stormwater Pollution and Treatment

A great variety of urban stormwater pollutants have been identified; pollutant types and concentrations are largely dependent on land uses (Davis and McCuen 2005). Transportation systems, particularly highways, have been noted as one of leading causes of the stormwater quality impairment (Barrett et al. 1998), contributing organic pollutants, heavy metals (such as copper and zinc from worn tire treads and brake pads), urban particles (from roadway construction and maintenance, worn tires and pavement, sediments, and others), hydrocarbons and fuel additives from vehicle fluid leakage, and atmospheric deposition from traffic emissions (Barrett et al. 1998, Furumai et al. 2002). As such, traffic activity in different land uses significantly affects runoff quality. Aside from traffic, residential areas contribute heavy metals (cadmium, copper, lead, and zinc) from house siding and pesticides / herbicides from inappropriate pest control and lawn maintenance, as well as nutrients (nitrogen and phosphorus species) from fertilizer uses (Davis and McCuen 2005). Runoff to surface water bodies can erode particles from uplands; the resulting turbidity increases have been associated with elevated concentrations of bacteria, *Giardia*, *Cryptosporidium*, and other microorganisms (Gannon and Busse 1989, Atherholt et al. 1998). Stormwater pollution occurs at different land use areas with different pollutant patterns. Overall, stormwater pollutant sources vary temporally and spatially and are subject to many environmental conditions such as temperature,

season, traffic activity, construction, land uses, etc. A summary of common urban stormwater pollutant concentrations for different land uses are listed in Table 2-1.

Table 2-1. Typical pollutant concentrations in urban stormwater runoff for different land uses (USEPA 1999a).

	Median event mean concentration for land use		
Pollutants	Residential	Mixed	Commercial
Biological oxygen demand (mg/L)	10	7.8	9.3
Chemical oxygen demand (mg/L)	73	65	57
Total suspended solid (mg/L)	101	67	69
Total lead (μg/L)	144	114	104
Total copper (μg/L)	33	27	29
Total zinc (μg/L)	135	154	226
Total Kjeldahl nitrogen (μg/L)	1900	1288	1179
Nitrate and nitrite (μg/L)	736	558	572
Total phosphorus (μg/L)	383	263	201
Soluble phosphorus (μg/L)	143	56	80

Obviously, concentrations of these pollutants can be used to determine the quality of stormwater, which is also very important in judging the performance of stormwater BMPs. The water quality requirement depends on the purpose or use (for example, drinking, fishing, irrigation, and recreation) of the receiving water bodies. Other than humans, the receiving water quality required for wildlife species (e.g., fishes, aquatic plants, and smaller animal life) to thrive also needs to be considered. As such, two fundamental questions in stormwater management are to properly define water quality that reflects all of the uses and users of the water (Davis and McCuen 2005), and to integrate individual BMPs in the same watershed (Zhen et al. 2006). Table 2-2 includes some stormwater quality criteria for TSS and total phosphorus (TP) (Davis 2007b); other than TSS and TP, water quality criteria of other pollutant species for aquatic life protection (COMAR 2006) and drinking water maximum contaminant level (MCL, USEPA 2003) are also listed. Additionally, pathogen indicator criteria

(*E. Coli.* and Fecal Coliform) for recreational water bodies are incorporated as well (USEPA 1986).

Table 2-2. List of water quality criteria.

Pollutant	Criteria			
	Drinking water MCL [a]	Aquatic life protection [c]	Pathogen indicator [f]	Stormwater criteria [g]
As (µg/L)	10	340 [d] / 150 [e]	-	-
Be (µg/L)	4	-	-	-
Cd (µg/L)	-	2	-	-
Cl^- (µg/L)	250 [b]	-	-	-
Cr (µg/L)	100	-	-	-
Cu (µg/L)	-	13 [d] / 9 [e]	-	-
E.Coli,# /100mL	126	-	126	-
Fecal Coliform (#/100mL)	200	-	200	-
Hg (µg/L)	2	1.4 [d]/ 0.77 [e]	-	-
Pb (µg/L)	15	65 [d] / 2.5 [e]	-	-
Zn (µg/L)	5000 [b]	120 [d, e]	-	-
NO_3^- (mg/L as N)	10	-	-	-
NO_2^- (mg/L as N)	1	-	-	-
TSS (mg/L)	20	-	-	20
TP (mg/L as P)	0.2	-	-	0.2

[a] USEPA 2003, [b] secondary standard, [c] COMAR 2006, [d] acute, [e] chronic, [f] USEPA 1986, [g] Davis 2007b.

Similar to the unit processes and unit operations in water works and wastewater treatment plants, stormwater BMPs attempt to treat runoff quality for designated uses of the receiving water bodies, while improving post-development watershed hydrology. However, it is unlikely to integrate as many different unit processes / operations into a single BMP to achieve multiple water parameter (pollutant) targets as those of water works and wastewater treatment plants; trade-offs often occur between water parameter targets for BMP selection and design. Among these parameters, TSS (total suspended solids) is often a primary target that measures aquatic particulate matters for stormwater BMPs. Phosphorus is also another important parameter for areas in which eutrophication is of concern.

2.2 Water Quality Performance Criteria of BMP Facilities

Pollutant removal efficiencies are the most commonly used indices for water quality improvement through stormwater BMPs. Removals are calculated from the pollutant concentration/mass reduction based on event averages, grab samples, statistical correlations of inlet / outlet pollutant levels, or others (Strecker and Quigley 1999, Barrett 2005), and are also know as "percent removal" (for they are often expressed in percentage). Most BMP monitoring studies report the percent removal because it is intuitively straightforward and readily understandable. Nonetheless, significant shortcoming results from the use of percent removal. BMPs do not function with an uniform pollutant removal efficiency throughout a wide range of influent pollutant levels. For instance, a BMP which demonstrates a high pollutant percent removal under highly contaminated influent conditions, can perform with poor percent removal under low influent pollutant levels (Strecker et al. 2000).

The decrease of BMP pollutant removal efficiencies under low influent pollutant levels has been demonstrated and in some cases, a minimum achievable effluent level through BMP implementation has been observed for many pollutants, e.g., for detection ponds (Strecker et al. 2000), and sand filters (Barrett 2005). As a result, the use of pollutant removal efficiencies may underestimate BMP performance under clean influent conditions and warrants caution. Some studies suggest that other indices such as effluent quality should be used together with percent removal; others recommended that BMP performance requirement should not use percent removal, but effluent quality (e.g., Strecker et al. 2000, 2001, 2004). A review of pollutant treatment efficiencies for field bioretention and sand filters are listed in Table 2-3.

Table 2-3. List of pollutant treatment efficiencies for field bioretention and sand filters.

	TSS (mg/L)	Copper (µg/L)	Lead (µg/L)	Zinc (µg/L)	TP (mg/L as P)	O&G [e] (mg/L)	NO_3^-—N (mg-N/L)	NH_4^+-N (mg-N/L)	TKN (mg-N/L)	TN (mg-N/L)	Source
Bioretention											
Input [a]	138-162	-	96-114	-	2.84-3.62	16-23	1.98-2.86	1.96-2.43	-	-	Hsieh and Davis (2005)
Output	1-45	-	<2-26	-	<0.05-2.14	<1	1.83-2.84	1.16-2.24	-	-	
Removal	72-99%	-	80->98%	-	37-99%	>99%	2-7%	5-10%	-	-	
Input [b]	18	-	39	-	<0.05	63	0.11	0.09	-	-	Hsieh and Davis (2005)
Output [b]	16	-	<2	-	<0.05	<0.5	0.10	<0.05	-	-	
Removal [b]	10%	-	>95%	-	-	>99%	10%	>44%	-	-	
Input	-	-	-	-	0.009-0.015	-	0.7-0.9	0.04	0.5-0.6	1.3-1.6	Dietz and Clausen (2006)
Output	-	-	-	-	0.039-0.043	-	0.3-0.4	0.01	0.4-0.5	0.7-0.9	
Removal [c]	-	-	-	-	-108%	-	67%	82%	26%	51%	
Input	-	-	-	-	0.1	-	0.3-0.5	0.22-0.24	0.8-1.0	1.27-1.35	Hunt et al. (2006)
Output	-	-	-	-	0.6-3.0	-	0.3	1.54-2.82	4.1-4.9	4.38-5.23	
Removal [c]	-	99%	81%	98%	13-75%	-	13-75%	-	-	40%	
Input	-	-	-	-	-	-	-	-	-	-	UNHSC (2006)
Output	-	-	-	-	-	-	-	-	-	-	
Removal [d]	97%	-	-	99%	-	-	44%	-	-	-	
Input	13-100	5-36	4-240	62-190	0.19-3.84	-	0.07-0.20	-	-	-	Davis (2007b)
Output	<4-64	3-15	<2-77	<30-670	<0.03-2.19	-	0.01-0.05	-	-	-	
Removal [d]	47%	57%	83%	62%	76%	-	83%	-	0.5-0.6%	-	
Sand filter											
Input	12-884	30-135	-	40-890	0.05-1.4	-	-	-	0.4-28	2.4-30	Urbonas (1999)
Output	4-40	16-35	-	8-59	0.04-0.14	-	-	-	0.2-2.9	1.6-8.2	
Removal	8-96%	0-71%	-	50-98%	5-92%	-	-	-	0-90%	-130-84%	
Input [b]	90	21	21	236	0.41	-	0.63	-	3.02	3.72	Barrett (2003)
Output [b]	9	10	3	48	0.25	-	1.10	-	1.48	2.91	
Removal [b]	90%	50%	87%	80%	39%	-	-74%	-	51%	22%	
Input	-	-	-	-	-	-	-	-	-	-	UNHSC (2006)
Output	-	-	-	-	-	-	-	-	-	-	
Removal [d]	49%	-	-	81%	-	-	6%	-	-	-	

[a] Synthetic runoff input (with a duration of 6hr), [b] Mean values, [c] Pollutant mass removal, [d] Median values, [e] oil and grease.

2.3 Interactions between Stormwater Filtration Media, Pollutants, and Seeping Runoff

As mentioned, porous media have been extensively used in stormwater BMPs as adsorptive filters and can successfully remove many types of runoff pollutants. However, the fate of captured pollutants in stormwater filters has not adequately been addressed, particularly for more novel and recent designs such as bioretention. Even for early-adopted infiltration system designs such as detention / retention basins, the results from previous studies were few and divided. One reason is that the primary goal for stormwater infiltration systems was not for pollutant retention (Mikkelsen et al. 1997) in the early days, but for improvement of post-development hydrology. Another reason is that the complexity of the different porous media used in the stormwater filtration facilities, including gravels, sands, and soils of a variety of textures, complicates the interactions between the media and different types of captured pollutants. Further, the pollutant loading pattern varies in different localities.

Several studies investigated the potential risk of groundwater and soil pollution from stormwater detention / retention basins, with different conclusions. Fischer et al. (2003) suggested risks from petroleum hydrocarbons and pesticides leakage. Mikkelsen et al. (1997) studied the fate of polyaromatic hydrocarbons (PAH), heavy metals, and adsorbed organically bound halogen (AOX) in infiltration systems and did not find a considerable risk for groundwater contamination from stormwater infiltration, but projected that long term (30 yr) accumulation eventually will reach environmentally critical levels. Bardin et al. (2001) reported no surrounding ground

water and soil contamination near infiltration basins. As such, the fate of media-captured pollutants needs to be addressed for risk consideration for stormwater BMPs.

Captured pollutants in the porous media of stormwater infiltration system have a variety of fates and implications to surrounding soils and groundwater. Persistent pollutants such as heavy metals can accumulate to environmentally critical levels. Nutrients such as phosphorus and nitrogen species have higher potential for biological transformations, such as intake / excretion by plants or microorganisms, nitrification, and denitrification. PAH and AOX can accumulate, but also can be slowly degraded through different biological pathways (Cookson 1995). The hydraulic designs (e.g., wet or dry basins, basin depth), hydrological conditions (e.g., antecedent dry weather period), climate, and media characteristics affect the micro-scale biosphere of the porous media through oxygen levels, temperature, pH, and other factors, which vary the plant / microbial ecology and metabolic pathways, and therefore select the intermediate and end products from the biodegradation of the captured pollutants.

The type of the porous media selected for a BMP also significantly affects the fate of the captured pollutants, as well as the media constituents. Gravels and sands are large in size and weight, and are relatively inert, having less mobility, surface area per unit volume, and binding ability with captured pollutants. Soil media are small in size and chemically active, having higher mobility, surface area per unit volume, and pollutant adsorption capability. As such, soil media have greater pollutant capture potential than gravels and sands. However, the association between the media and

seeping runoff is dynamic and interactive. Physically, small-sized soil media is more likely to leak out of BMP facilities than sands and gravels and may contribute turbidity and color in the effluents as a result. Chemically, the higher surface area per unit volume provides soil media with higher chance to release the media content to the effluent during infiltration and weathering processes. A previous study has identified iron export from bioretention cells and estimated its sources from the iron-rich in situ soil or cell soil media, and the effluent samples bore a light red color (Hunt et al. 2006). Although this phenomenon may also occur during natural infiltration process, the possible addition of effluent turbidity and colors from stormwater filtration facilities using soil media may prompt aesthetical issues for the effluent.

Aside from media adsorption of dissolved pollutants, particulate pollutants in urban runoff are mostly captured and retained through filtration, which is discussed in the following sections.

2.4 Stormwater Filtration Using Porous Media

Depth filtration, which uses porous media (particularly sands, gravels, and anthracite) in water / wastewater treatment, is considered as a mature technology with thorough research investigations. As TSS is captured during the filtration process, the headloss increase (clogging) can lead to a demand for backwash (for rapid sand filters) or a top-scratching (for slow sand filters or intermittent sand filters) maintenance, and the penetration of TSS can lead to effluent quality degradation (breakthrough). The clogging limit and breakthrough limit decide the maintenance frequency for conventional sand filters (Figure 2-1, Tchobanoglous et al. 2003), as

well as for stormwater BMP filters. However, significant differences occur between sand filters at water works and stormwater filters at urban areas, such as media types, filter inflow patterns (flow rate and water quality), degrees of media saturation, and maintenance procedures. These differences address the needs for the development of stormwater filtration theory.

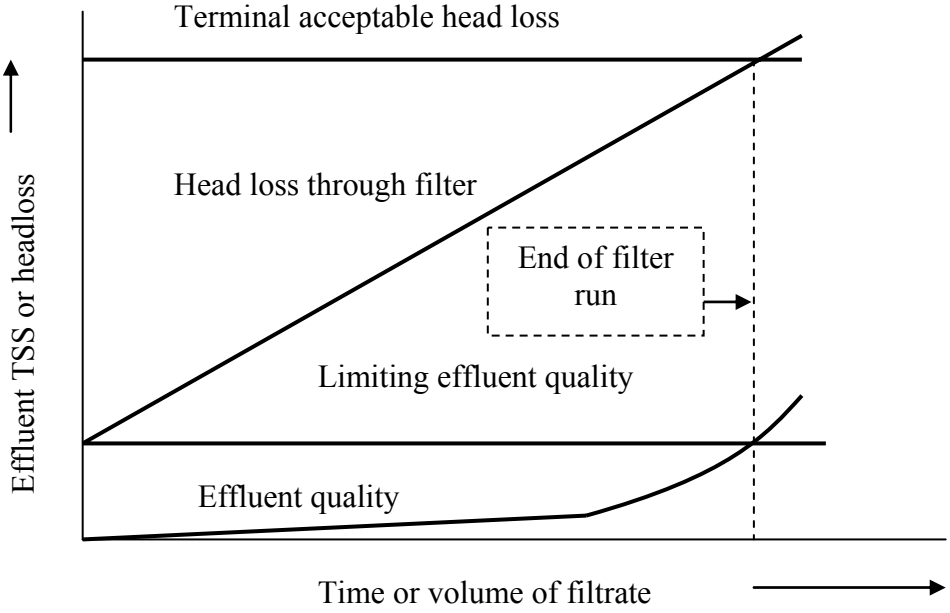

Figure 2-1. Conceptual sketch for filter breakthrough limit and clogging limit (Tchobanoglous et al., 2003).

To date, stormwater filtration through porous media has not been adequately discussed in theory, even after its adoption in practice. This "missing link" implies tremendous opportunity for stormwater BMP filter improvement. As previously mentioned, the great fluctuations in both stormwater quality and quantity render BMP studies a difficult task. Other factors, such as the complexity of BMP filter media composition, also produce significant difference between the conventional filters and

the BMP filters and restrict the direct application of existing filtration theory to stormwater BMP filters, which are discussed in the following sections

2.4.1. Depth filtration stages

Understanding the evolution of the typical filtration stages in terms of effluent quality and filtrate volume (or time) can help in properly using depth filtration theory developed from rapid / slow sand filter studies and applying filtration theory for stormwater filtration facilities. Figure 2-2 illustrates the filtration stages for a typical breakthrough limited sand filter. The fresh media of a clean sand filter have a larger pore size and a smaller surface area to volume ratio in the beginning, and may result relatively higher effluent TSS levels, compared to the media that have been loaded for a considerable period. As captured influent TSS deposit inside the media pore space and slow down the subsequent TSS penetration, the deposit also acts as new surface. The new surface often has a higher surface area to volume ratio and is more chemically active than the pristine media. These factors allow better trapping for TSS and other pollutants. The progress of the effluent TSS level improvement from a clean filter is referred as the "ripening" stage. Additives such as diatoms and polymers are used in the influents of some sand filters to shorten the ripening stage (McGhee 1991, Tchobanoglous et al. 2003).

After the filter is ripened, the working stage begins, until significant TSS penetration makes the effluent TSS (breakthrough limited) or the headloss (clogging limited) due to the TSS capture reach unacceptable levels. Afterwards, maintenance procedures (backwashing, media replacing, or top-scratching) are needed. For field stormwater filtration facilities, monitoring for the effluent TSS levels and headloss is

not done as readily as that of sand filters in water works and wastewater treatment plants. A prediction model based on stormwater filtration theory development is needed.

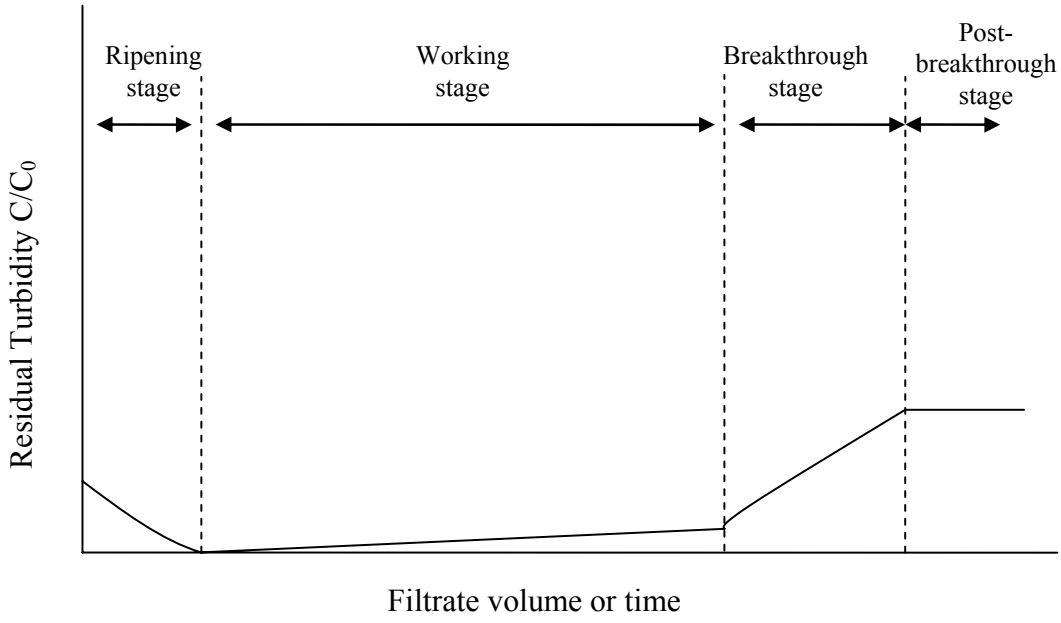

Figure 2-2. An illustration of filtration stages (Adin and Rebhun 1977)

2.4.2. Classical filtration theory- the microscopic model

Several microscopically-derived models have been proposed for clean filters, such as the Yao, pore velocity (PV), Yao-Habibian (YH), and Rajagolplan and Tien (RT) filtration equations, which have been broadly discussed (e.g., Yao et al. 1971, Kau and Lawler1995, Logan et al. 1995, Cushing and Lawler 1998). For example, Yao's model is:

$$\frac{C}{C_0} = \exp\left[-\frac{3}{2}\frac{(1-\theta)}{d_c}\alpha\eta L\right] \tag{2-1}$$

$$\eta = 4N_{Pe}^{-2/3} + \frac{3}{2}N_R^2 + N_G \quad (2\text{-}2)$$

where as C_0 and C represent the influent / effluent particle concentrations, θ is the filter bed porosity, d_c is the diameter of the spherical collector (media particle), α is the sticking coefficient (defined as the ratio of the rate particles stick to a collector to the rate they strike the collector), η is the single collector collision efficiency, as calculated in Equation (2-2), L is the bed depth, $N_{Pe}=u^* d_c/D_p$ is the Peclet number, $N_R=d_p/d_c$ is the interception number, and $N_G=U_p/u^*$ is the gravitation number. u^* is the characteristic velocity (defined as the approach velocity in the Yao model), D_p is the colloid (suspended particle) diffusion coefficient, d_p is the suspended particle diameter, $U_p=g(\rho_p - \rho_f) d_p^2/18\mu$ is the particle settling velocity, g is the gravitational constant, ρ_p is the suspended particle density, ρ_f is the fluid density, and μ is the fluid viscosity. The three terms at the right hand side of Equation (2-2) represent the single collector efficiency achieved via the mechanisms of diffusion, interception, and sedimentation, respectively, as illustrated at Figure 2-3.

This model was developed using a mass balance based on the particles removed by an isolated spherical collector, assuming that a packed bed is an assemblage of isolated spheres. The PV model is similar to the Yao model, but uses pore velocity instead of approach velocity. The YH model is a modification of the Yao model incorporating a correction factor for the diffusion term into account for the collision efficiency η (Logan et al. 1995). The RT model also has a similar form to the Yao model, but all terms are based on the flow in a concentric sphere space surrounding the collectors.

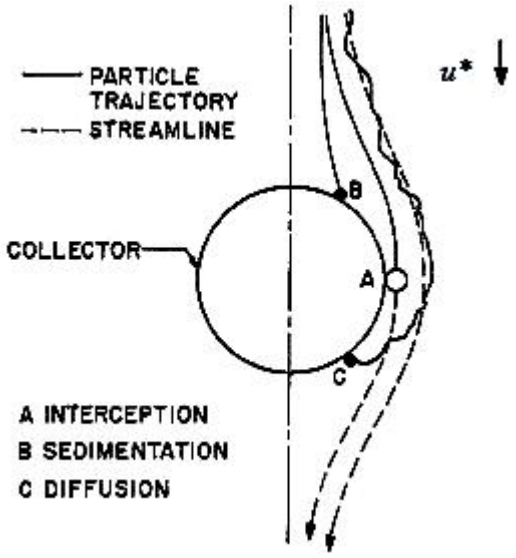

Figure 2-3. Filtration mechanisms of depth filtration (Yao et al. 1971).

The microscopic model provides a heuristic concept of depth filtration mechanisms. The collision efficiency η can be computed as the sum of the collision efficiencies of interception, sedimentation, and diffusion (AWWA 1999). Further, it established that the removal efficiency of a clean bed filter depends on the incoming particle size and identified a critical particle size of 1 μm (under rapid sand filter conditions), which has the lowest opportunity to be captured compared to other particles larger or smaller than that (O'Melia and Ali 1978).

The microscopic models, however, do not account for the accumulation of the solids deposited in the filter and is used for clean beds. In addition, the collector efficiency listed above is based on mono-dispersed systems; the overall collector efficiency is the sum (weighed according to the particle numbers) of each pair of the media collector size and suspended particle size. Also, the sticking coefficient α must be determined through column experiments (Tufenkji and Elimelech 2004).

These factors limit the field application of the microscopic model. Furthermore, in stormwater filtration facilities which use topsoil as one of the media constituents, such as bioretention, the fine sized and chemically active media with a high surface area to volume ratio render the filters "ripened" almost right after their installation, which violates the use of the microscopic "clean filter" model. Therefore, this research does not use the microscopic model in the stormwater filtration theory development.

2.4.3. Classical filtration theory- the macroscopic model

Another form of classic depth filtration models were developed many years ago (Bohart and Adams 1920, Herizig et al. 1970) and have been modified for different applications (Adin and Rebhun 1977; Chaudhry 1987a, 1987b; Saatci 1989, 1990; Akgiray and Saatci 1998). These one-dimensional models, also known as the macroscopic model (AWWA 1999), begin with a mass balance for an infinitesimal control volume in the filter bed:

$$-q\frac{\partial C}{\partial Z}=\frac{\partial(\varepsilon C)}{\partial t}-D\frac{\partial^2 C}{\partial Z^2}+\frac{\partial \sigma}{\partial t} \qquad (2\text{-}3)$$

where q represents the downward water flow rate per unit area of the filter media (approach velocity), C is the TSS concentration of water being transported through the media, Z is the media depth, ε is the media porosity, D is the dispersion coefficient, consisting of diffusion and hydrodynamic dispersion coefficients, and σ is the specific deposit (mass of TSS deposited per unit volume of the media). This equation consists of an advection term $q(\partial C/\partial Z)$, an accumulation term of pore-suspension $\partial(\varepsilon C)/\partial t$, a dispersion term $D(\partial^2 C/\partial Z^2)$, and accumulation term of solid

deposition $\partial\sigma/\partial t$. With the assumptions of neglecting the dispersion term $D(\partial^2 C/\partial Z^2)$ and the accumulation term of pore-suspension $\partial(\varepsilon C)/\partial t$, the mass balance becomes:

$$q\frac{\partial C}{\partial Z}+\frac{\partial \sigma}{\partial t}=0 \tag{2-4}$$

which is the mass balance for the macroscopic model. From Equation (2-4), the decrease of TSS in the filtrate stream along the seeping path (the first term) approximately equals the increase of specific deposit (the second term).

Iwasaki (1937) proposed the relationship between TSS decrease and the media depth (the first term) as:

$$\frac{\partial C}{\partial Z}=-\lambda C \tag{2-5}$$

where λ is the filter coefficient with the dimension of reciprocal length. It is generally assumed that λ is independent of suspension concentration, but dependent on time, position, and specific deposit σ. Many studies have tried to formulate the variation of λ with σ (Tien 1989). For example, a simple linear relationship:

$$\lambda=\lambda_0+b\sigma_v \tag{2-6}$$

where λ_0 is the clean bed filter coefficient, b is an empirical constant which can be positive or negative, and σ_v is the volumetric specific deposit (the volume of deposited particles per unit filter volume), which can be derived from σ via TSS density.

2.4.4. Cake filtration

Most stormwater filtration facilities have a design media depth > 0.7 m (MDE 2000), which implies that the designated filtration mechanism is depth filtration.

However, cake filtration may occur under several conditions. For example, if the size ratio of the media to the incoming suspended solids is relatively small (MacDowell-Boyer et al. 1986, Teng and Sansalone 2004), or if the resistance at the filter media surface becomes excessive as suspended solids are deposited, a TSS cake layer will form and grow. The concerns here are the headloss increase due to the cake layer growth, as well as the pollutant spatial profile change as a result of the cake formation. Several models have been developed to describe cake filtration (e.g., Grace 1953, Willis and Tosun 1980, Tien and Bai 2003). However, most of the cake filtration theory was developed from the assumption that the cake layer grows on a septum, not a porous media layer, which makes its connection with the depth filtration model difficult.

2.5 Hydrological Benefits of Infiltration-Promoting BMPs

As previously mentioned, the initial development of stormwater BMPs was aimed at improving post-development hydrology. Infiltration-type BMPs intercept runoff from impervious land areas before the stormwater conveyance system, providing buffer capacity for sudden runoff surges (which has been compromised during urban development, as previously mentioned), and therefore compensate for post-development hydrology to some degree. During these processes, the peak runoff flows are delayed and reduced, and the discharging runoff volume decreases as the infiltration volume increases. As a result, risks of flood and channel erosion diminish and groundwater recharges are promoted through more infiltration. To quantify the performance of the post-development hydrology restoration via stormwater BMPs, three metrics have been proposed to measure the hydrological benefits (Davis 2007a).

The peak flow rate ratio of effluent to influent R_{peak}, the peak discharge time span ratio of effluent to influent R_{delay}, and the effluent/influent volume ratio f_V, were used to describe the restoration of hydrological conditions, which are defined as:

$$R_{peak} = \frac{q_{peak-out}}{q_{peak-in}} \tag{2-7}$$

$$R_{delay} = \frac{t_{q-peak-out}}{t_{q-peak-in}} \tag{2-8}$$

$$f_v = \frac{V_{out}}{V_{in}} \tag{2-9}$$

where $q_{peak\text{-}out}$ and $q_{peak\text{-}in}$ represent the peak flow rates of the effluent and influent, $t_{q\text{-}peak\text{-}out}$ and $t_{q\text{-}peak\text{-}in}$ represent the time elapsed between the beginning of influent flow and the peak effluent and influent flows, and V_{out} and V_{in} represent the effluent and influent runoff volume. Through providing the buffer capacity for runoff surges with extra infiltration opportunity, as mentioned, a successful BMP facility can amend its serving drainage area to simulate the pre-development hydrology and achieve lower R_{peak} and higher R_{delay} values (to reduce and delay peak flow for flood protection and channel erosion prevention), as well as lower f_v values (by promoting groundwater recharge and/ or evapotranspiration).

However, these metrics have only been used in investigating the hydrological benefits for field bioretention facilities with lined bottoms (Davis 2007a). To date, application of these metrics for bioretention facilities without surrounding liners (which is more common for field bioretention) have not been adequately addressed. Such an application is attempted in this study. The details of the three metrics and their application in field bioretention facilities (without liners) are described in Chapter 3.

Chapter 3: Hydrological and Water Quality Benefits of Bioretention: Field Studies

3.1 Introduction

This chapter presents hydrological and water quality benefits of bioretention through a field study of two bioretention facilities for one year. As previously mentioned, bioretention is capable of improving post-development hydrology through runoff storage and infiltration, which delay / decrease runoff peak flows and reduce the discharge volume to drainage networks. This advantage reduces the impact of flood and channel erosion for storm drainage systems. Bioretention media are also capable of capturing and/ or transforming runoff pollutants and thus improving water quality in receiving water bodies. On the other hand, the natural mix of bioretention media also has the potentials to release its composition substances at minor background concentrations and this process warrants careful examination. As such, a variety of pollutants, including particulate matter, heavy metals, nutrients, organic matters, and pathogen indicators were monitored at both inputs and outputs at two bioretention sites. Additionally, it is established that bioretention can effectively intercept urban particulate pollutants. However, small to substantial amount of TSS are still detected in the outflow (e.g., Hsieh and Davis 2005, Hunt 2006), which may come from media leaching or seepage runoff particles. This chapter also attempts to identify their source through field studies.

3.2 Methodology

3.2.1. Site description

Two bioretention cells located in College Park (CP) and Silver Spring (SS), Maryland, USA, shown in Figure 3-1, were monitored. Both sites are part of the Anacostia watershed. Cell CP is among 5 bioretention facilities (11 cells) serving Comcast Center parking lots at the University of Maryland campus. The drainage area is a high-use land consisting of 90 % of imperious surface such as asphalt parking lots, roads and concrete sidewalks for commuter students and athletic event visitors. These 5 bioretention facilities, including Cell CP, were retrofitted into the storm drain network to improve local hydrology and water quality in spring 2004. Cell CP is trapezoid in shape (length = 50.3 m, width = 2.4 m / 4.8 m, and cell area = 181 m^2) as shown in Figure 3-2 and serves a designed drainage area of approximately 0.28 ha, producing a cell surface area: drainage area ratio = 6%. The cell has a sloped surface, with an average ponding storage depth of 15 cm. Two 15-cm perforated PVC pipes run the length of Cell CP below the media, collecting and conveying infiltrated water to nearby Campus Creek, a small first order stream that runs through the University of Maryland campus. The cell media depth is between 0.5 and 0.8 m. Approximately 400 g of Cell CP media sample was manually taken (with nitrile gloves and pre-cleaned shovels), double bagged, and sent to the University of Delaware Soil Testing Program for characterization in December 2005. The result indicates a sandy loam with a pH of 7.3 and an organic matter content of 5.7 %, as shown in Table 3-1.

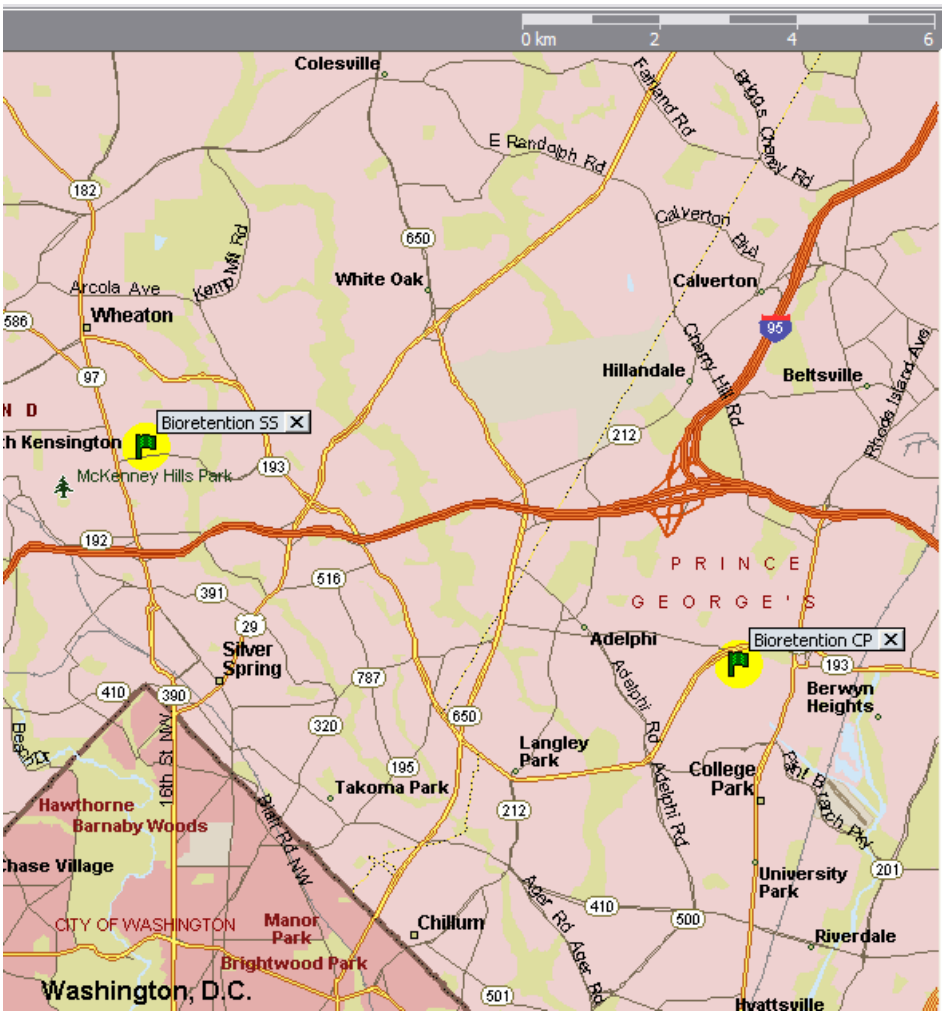

Figure 3-1 Locations of the monitored bioretention cells (Microsoft Streets and Trips 2005).

Cell SS is among three bioretention sites serving as a runoff drainage retrofit of a health service facility complex of Montgomery County, MD since its completion in March 2006. The drainage area consists of 90% impervious surface such as asphalt parking lots and driveways for inpatients, working commuters, and visitors. Cell SS has a designed drainage area of 0.45 ha, however, field observation during rainfalls indicates that runoff flows are often directed to peripheral lawns and thus decrease the cell inflow. Cell SS is a triangular basin structure (side = 18, 18, and 12 m), as shown in Figure 3-3, with an estimated surface area = 102 m^2, producing a cell surface area:

drainage area = 2%. (The actual ratio is considered to be larger since less runoff inflow is diverted into the cell than the design drainage, as mentioned). A 30 cm ponding storage depth is created with a discharge riser. A group of 15-cm perforated PVC pipes runs underneath the cell media through the cell to the exit riser to collect and convey infiltrated water to the storm drain. The riser opening is about 30 cm higher than the media surface. The cell media depth is 0.9 m. A Cell SS media sample was also collected and sent to the University of Delaware Soil Testing Program for characterization using the same method as Cell CP at the same date (although Cell SS was completed at March 2006, the media was in place by December 2005). The result indicates a sandy clay loam with a pH of 7.7 and an organic matter content of 12.2 %, as shown in Table 3-1.

Figure 3-2. Cell CP at the University of Maryland campus (March 2006).

Figure 3-3. Cell SS at Silver Spring, MD and its serving parking lot (August 2006).

Table 3-1 Media characterization of the monitored bioretention cells.

	CP media	SS media
Characteristics		
Soil texture:		
Sand (%)	80	54
Silt (%)	13	26
Clay (%)	7	20
Texture	Sandy loam	Sandy clay loam
pH	7.3	7.7
Organic matter (%)	5.7	12.2

3.2.2. Monitoring and analysis methodology

Cell CP intercepts incoming runoff through a 20-cm Tracom Cutthroat flume for influent rate measurement and water sampling. The cell underdrain directs infiltrated water to a discharge manhole with a 20-cm PVC pipe, which is outfitted with a 20-cm Thel-Mar plug-in weir for effluent rate measurement and water quality sampling. Two ISCO 6712FR refrigerated auto-samplers were assigned to the influent and effluent. Each auto-sampler was equipped with bubble flow meter (ISCO 730) positioned at the flow measurement device. One factory-calibrated ISCO 674 Tipping Bucket Rain Gauge with 0.0254-cm sensitivity was connected with the influent auto-sampler to record rain fall. The layout of Cell CP monitoring devices is shown in Figure 3-4.

A similar layout was also deployed for Cell SS, as shown in Figure 3-5. A 23-cm Parshall flume was used for influent rate measurement and water quality sampling. A 15-cm Thel-Mar plug-in weir was outfitted in the discharge pipe at the bottom of the exit riser for effluent rate measurement and water quality sampling. The installation of the auto-samplers, bubble flow meters, and rain gauge is equivalent to that at Cell CP. The discharge equations and resolutions of the flow measurement devices are summarized in Table 3-2. The sizes of the effluent pipes limited the flow measurement devices, particularly in Cell SS. In high precipitation or strong intensity events, the effluent flow rates sometimes exceeded the weir ranges and were reported as the maximum measurable flow rates with a “larger than” note. The input and output flow rates lower than the flow rate measurement ranges at both sites were reported as no flow.

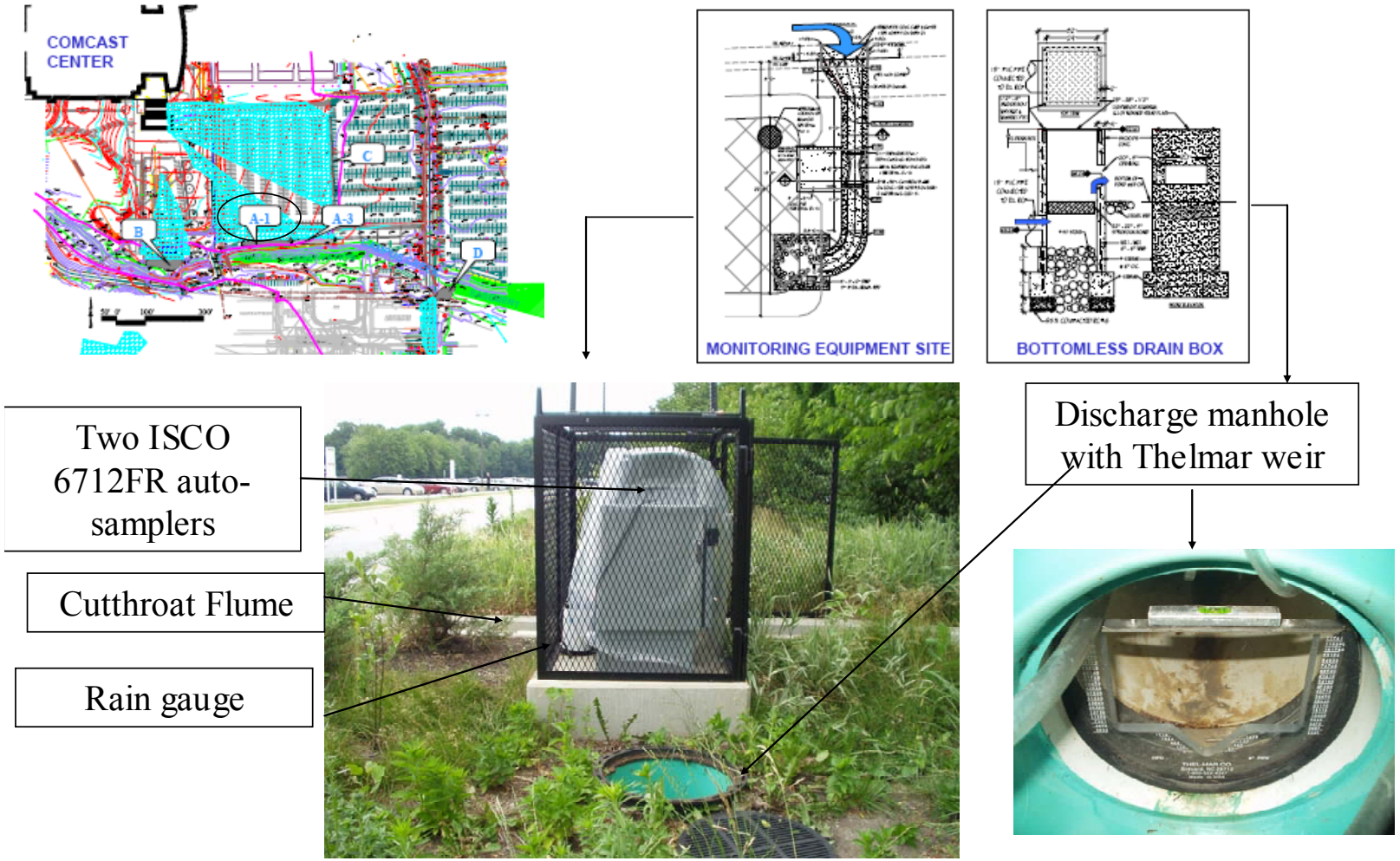

Figure 3-4. Monitoring devices layout in Cell CP, University of Maryland.

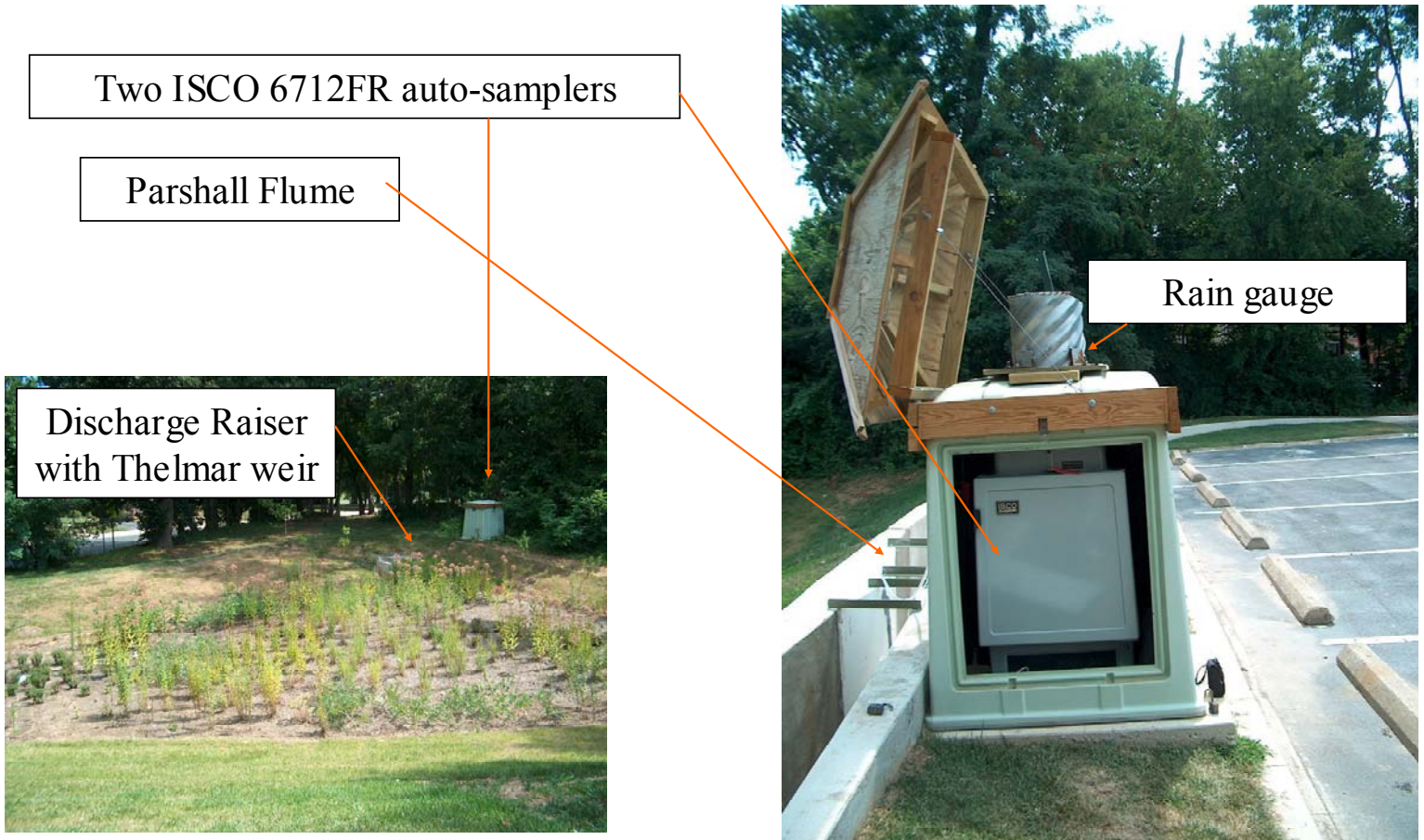

Figure 3-5. Monitoring devices layout in Cell SS, Silver Spring, MD.

Table 3-2. Discharge equations and weir resolutions for flow measurement devices.

	Device	Discharge equation[1]	Weir resolution
Cell CP			
Input	20-cm Cutthroat flume[2]	$Q = 80.4H^{1.83}$	H = 0.06-1.00 Q = 0.5-81.0
Output	20-cm Thel-Mar weir[3]	$Q = 129H^{2.63.}$	H = 0.026-0.431 Q = 0.002-5.651
Cell SS			
Input	23-cm Parshall flume[4,5]	$Q = 86.9H^{1.53}$	H = 0.06-2.00 Q = 1.17-245.00
Output	15-cm Thel-Mar weir[3]	$Q = 101H^{2.57}$	H = 0.022-0.293 Q = 0.002-2.147

[1] Q = flow rate in liter/s, H = water head in ft. [2] Merkley (2004). [3] Provided by the manufacturer .
[4] Grant and Dawson (2001). [5] Blaisdell (1994).

Stormwater monitoring began in April, 2006 and concluded in February, 2007, and included both hydrological monitoring and water quality sampling. Hydrological monitoring (precipitation and influent / effluent rates) occurred for 14 events for Cell CP and 40 events for Cell SS. (Cell SS is equipped with an AC power line and was able to process more monitoring.) Every 2 min, the auto-samplers recorded water level and converted to runoff flow rate Q and volume V_e according to the discharge equations programmed into the samplers (Table 3-2) and simple numerical integration of flow measurements over time:

$$V_e = \int_0^t Q(t)dt = \sum_{t=0}^{t} Q(t)\Delta t \tag{3-1}$$

Among these hydrological monitoring events, 8 events were chosen as water quality sampling (2 events per season). The 8 events were selected based on the following criteria: 1) the events occurred on the same date for both Cells CP and SS, and 2) both cell input and output ends generated measureable flows (i.e., generated flow rates were within the ranges of the flow rate measurement devices).

During a water quality sampling event, flow-weighted composite sampling was employed for both inputs and outputs of Cells CP and SS, and the flow-weighted composite samples were directly analyzed for pollutant levels to obtain the pollutant event mean concentration (EMC) of that event. The samplers were programmed to trigger when measurable flow rates were detected and to continue taking flow-weighted composite samples until the collector turned off the program after the rain event. The programming of each sampler is listed in Table 3-3. Additionally, one field blank was processed for each cell.

Table 3-3. Programming for the auto-samplers for water collection.

	Trigger criteria	Sample proportion
Cell CP		
Input	$H \geq 2.0$ cm[1]	10 mL sample/6-20 L runoff [2]
Output	$H \geq 0.5$ cm[1]	10 mL sample/10-30 L runoff [2]
Cell SS		
Input	$H \geq 2.0$ cm[1]	10 mL sample/10-20 L runoff [2]
Output	$H \geq 0.5$ cm[1]	10 mL sample/5-10 L runoff [2]

[1]H = water head, [2]depended on anticipated rainfall amount.

The auto-samplers were set at a temperature < 4 ˚C during water quality sampling events to preserve collected samples. Each sampler contained one 9-L HDPE container and one to three 10-L glass containers (depended upon the anticipated rainfall intensity from weather forecasts). These containers were acid-washed and thoroughly rinsed with deionized water before the rainfall event. The samples were picked up and delivered to the laboratory subcontractor within 24 hours at the Washington Suburban Sanitary Commission (WSSC) laboratory, Silver Spring, MD, where the analyses were carried out. Before the delivery, each sample was transferred to the sample containers (a 1-L glass bottle, a 200-mL glass bottle, a 1-L

plastic bottle, and two 100-mL sterilized containers for each sample) which were pre-cleaned and supplied by the laboratory subcontractor. Nitrile gloves were always used during the sample collection and transfer. Once the sampling was done, all bottles were marked with codes, stored in coolers, then delivered to the WSSC laboratory. The water quality parameters analyzed by the WSSC laboratory included total arsenic, total cadmium, chloride, total chromium, total copper, *E. Coli.*, Fecal Coliforms, total lead, total mercury, nitrogen species, Oil &Grease (O&G), phosphorus, total organic carbon (TOC), total suspended solids (TSS), and total zinc. The analytical methods used by the WSSC laboratory are listed in Appendix 2. Additionally, another 100 mL was transferred to a 200-mL pre-cleaned plastic container for each sample and delivered to the Environmental Engineering Laboratory, University of Maryland for dissolved copper analyses.

Dissolved copper samples were processed through separating particulate copper from the water samples with a 0.2 μm pore size, 25-mm diameter membrane disk filter (Pall Corporation), a 25-mm Easy Pressure syringe filter holder (Pall Corporation) and a 60 mL, Luer-Lok syringe (Becton Dickerson & Co.). The separation processes were finished within 6-8 hour after sample collection. One laboratory blank was used for each sampling event with deionized water. Dissolved copper levels were analyzed on a Perkin-Elmer 5100ZL atomic absorption spectrophotometer on the furnace module, against four standards in the range between 4 and 200 μg/L, according to Standard Method 3110 (APHA et al. 1995). Analytical standards were prepared using 1000 mg/L stock solutions (Fisher Scientific or VWR Scientific Products). A standards check was performed after every 10 analyzed

samples with an acceptable difference ≤ 5 %. The detection limit for copper concentrations is 2 μg/L.

3.2.3. Quality control

As mentioned, field blanks were employed by pouring deionized water into a cleaned bottle at both sites after every water quality monitored event, and were then subjected to the same delivery and laboratory procedures as the runoff samples to verify that no contamination occurred during handling, and that the baseline for measuring various constituents was sufficiently low. For all measured constituents, the residual concentrations in the field blanks were negligible. During the analyses of dissolved copper, standards were checked regularly to ensure that the standards curve still applied to the samples, as previously mentioned.

3.2.4. Data handling and statistical analyses

Probability plots for hydrologic and water quality parameters were created by ranking the measured values. The plotting position for each value on the probability scale p was calculated from:

$$p = \frac{i - \alpha}{(n + 1 - 2\alpha)} \tag{3-2}$$

where i is the i th smallest number among a sample size n, and α represents a constant that describes the plotting position function. The most commonly adopted α value is 0 (the Weibull plotting position) for the simplicity and its application to return periods (Harter 1984). However, the Weibull plotting position may introduce bias at the extremities when tested against know distributions, and α = 3/8 is the best known compromise during the tests (Cunnane 1978). Since this study does not use the

concept of yearly maximum return periods, a value $\alpha = 3/8$ of was employed. Data were plotted on a log scale and often described by straight line (with some deviation at the extremes), implying their log-normal distribution nature, which is also commonly used for stormwater parameters approximation (Van Buren et al. 1997).

Paired Student's t Test and Wilcoxon Matched-Pairs Signed-Ranks Test (McCuen 1985, Zar 1996) were used to determine if Cell CP or SS is making a statistically significant improvement on the pollutant levels. To this end, an input ΔA was used:

$$\Delta A = A_{\text{inf luent}} - A_{effluent} \tag{3-3}$$

where $A_{influent}$ represents input pollutant EMC to the cell, and $A_{effluent}$ represents output pollutant EMC. The two statistical tests examine whether the pollutant removal for the cell is greater than zero. Therefore, the hypotheses of the tests are:

$$H_0 : \mu_{\Delta A} = 0 \tag{3-4}$$

$$H_a : \mu_{\Delta A} > 0 \tag{3-5}$$

where $\mu_{\Delta A}$ represents the mean value of ΔA.

The paired Student's t Test assumes that:

1. The scale of the data measurement has an equal-interval scale property.
2. The pair-differences are randomly drawn from the source population.
3. The source population from which the pair-differences have been drawn is normally distributed.

The test statistic, t, can be calculated as (Zar 1996):

$$t = \frac{\overline{\Delta A} - 0}{S / \sqrt{n}} \tag{3-6}$$

where $\overline{\Delta A}$ and S represent the sample mean and standard deviation of ΔA, and n represents the number of paired samples. The critical value of the t test statistic is a function of the 5% level (5% was used in this study) of significance and the degrees of freedom $\nu = n - 1$, and can be found in t distribution tables. If the calculated t value is greater than the critical value, the null hypothesis H_0 can be rejected and the bioretention cell is successfully removing the analyzed pollutant.

The Wilcoxon Matched-Pairs Signed-Ranks Test is similar to the parametric Paired Student's t test in purpose and thus serves as an alternative analysis. However, it is a non-parametric test and does not assume a normal distribution of the source population. It only requires that the data be paired and that the pair difference is continuous, independent, and is representative of the source population.

The test statistic, T is the lesser of the sums of the positive and negative differences between the ranks of the values in the samples from the two groups. T is obtained as follows (McCuen 1985):

1. Compute the magnitude of the difference between each pair ΔA.
2. Rank the differences in absolute value in descending order.
3. Place the sign of the difference on the rank.
4. Compute the sum of the ranks of the positive differences, S_p, and the sum of the ranks of the negative differences, S_n.

The value of the test statistic, T is the lesser of the absolute values of S_p and S_n. The critical T value is obtained from statistical tables through the sample size n and the 5% level of significance. If the calculated T value is less than the critical value,

the null hypothesis H_0 can be rejected and the bioretention cell is successfully removing the analyzed pollutant.

3.3 Results and Discussion

3.3.1. Storm events characterization

The monitored storm events in this study are assumed to be "typical" Maryland storms in a hope to draw generalized conclusions from the monitored results. Kreeb (2003) analyzed the rain fall intensity, duration, and frequency for 10, 352 storm events at 15 weather stations within the State of Maryland; the frequency of an average Maryland storm that is expected to produce given rainfall depths and durations are listed in Table 3-4 in terms of probabilities. The hydrological monitoring and water quality sampled storm events at Cells CP and SS are to compared with Kreeb (2003)'s results in an attempt to determine if these events are representative storms for the State of Maryland.

Table 3-4 indicates that about 33% of the rainfall events in Maryland are expected to have precipitation less than 0.254 cm. Among these small events, more than 87% have a duration less than 2 hr. As a result, about one third of Maryland storms have a low rainfall and short duration. The other two-thirds are more evenly distributed between different rainfall depths and durations.

Figure 3-6 lists a comparison between Kreeb (2003)'s results, the hydrological monitoring events, and water quality sampled events at Cell CP for rainfall depth and duration. The hydrological monitoring events had similar profiles in rainfall depth and duration with typical Maryland storms except for a higher chance for the 0.255-

0.635 cm rainfall depth and a lower chance for large events (> 2.54 cm; no monitored event falls in this category). However, water quality sampled events had lower rainfall depth (< 1.28 cm), which is believed due to the ranges of the flow rate measurement devices. (If the flow rate was higher than the weir range, pollutant mass loading estimates would become difficult and the sampling was most likely to be aborted, the groundwater surge from nearby Campus Creek at Cell CP also compounded this situation.) Figure 3-6 also indicates that the water quality sampling campaigns did not successfully collect samples for the events with 3-7 hr and > 24 hr durations. However, the frequency for rainfall events with 3-7 hr and > 24 hr durations is also relatively low for typical Maryland storms. The rainfall depth and duration of all monitored events at both cells are listed in Appendix 1.

Table 3-4. Frequency of storm events for 15 stations at the State of Maryland (Kreeb 2003).

	Rainfall Depth (cm)					
Event Duration	0.0254-0.254	0.255-0.635	0.636-1.27	1.28-2.54	> 2.54	Sum
0-2 hr	0.2857	0.0214	0.0167	0.0043	0.0008	0.3289
2-3 hr	0.0164	0.0257	0.0221	0.0089	0.0025	0.0756
3-4 hr	0.0085	0.0223	0.0198	0.0083	0.0038	0.0627
4-7 hr	0.0099	0.0351	0.0475	0.0221	0.0087	0.1233
7-13 hr	0.0058	0.0337	0.0629	0.0528	0.0266	0.1818
13-24 hr	0.0024	0.007	0.0397	0.0611	0.0515	0.1617
>24 hr	0	0.0009	0.0043	0.0172	0.0435	0.0659
Sum	0.3287	0.1461	0.213	0.1747	0.1374	1

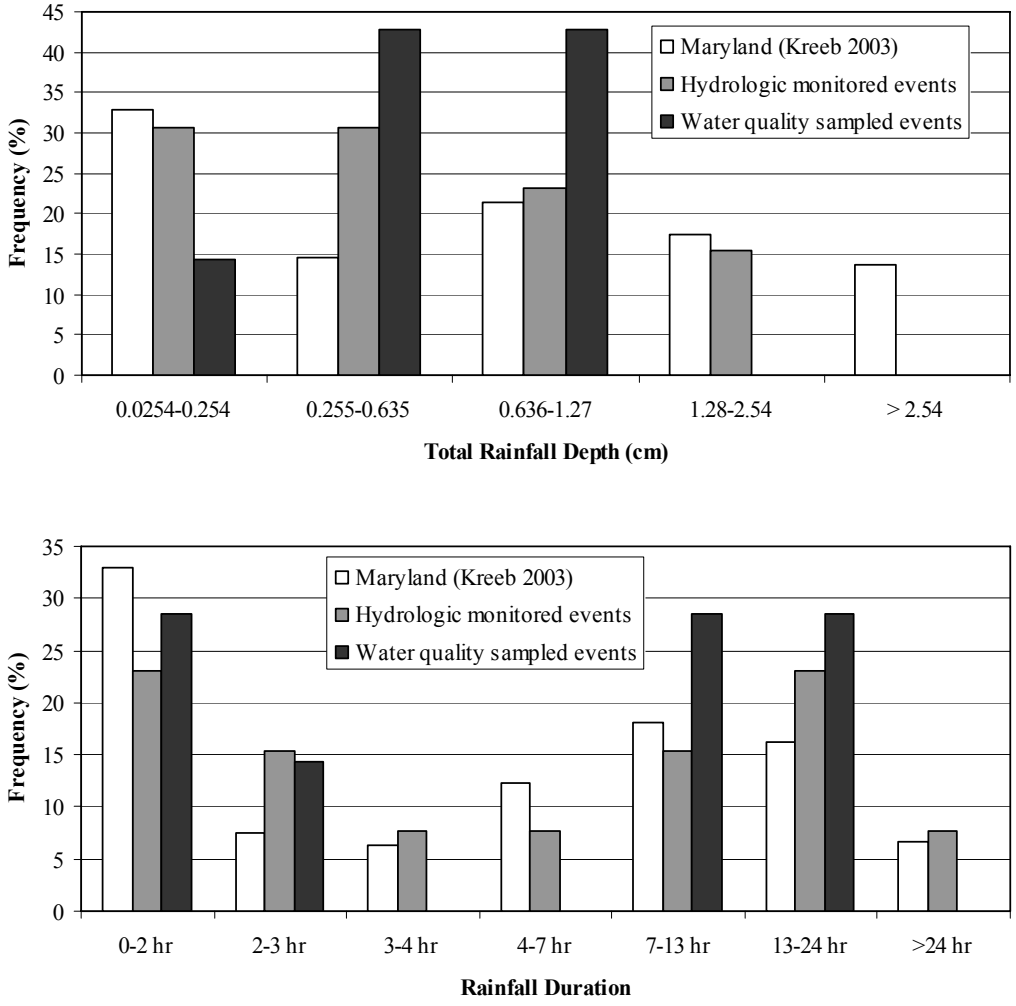

Figure 3-6. Rainfall depth and duration patterns for Maryland (Kreeb 2003) and Cell CP storm events.

Figure 3-7 lists the comparison between Kreeb (2003)' results and the Cell SS storm events. Likewise, the hydrological monitoring events exhibited similar rainfall depth and duration profiles with typical Maryland storms. However, the water quality sampled events had higher precipitation (>1.28 cm). As previously mentioned, Cell SS has a larger capacity for storage and infiltration, which results in less effluent in small events. In order to collect effluent samples, larger storms were more likely to

be used for water quality monitoring. Like Cell CP, the events with 3-7 hr durations were not used in the water quality monitoring. It is possible that the predominance of small or large storms at both cells may produce outliers and should be noted. However, the hydrological monitored storms closely resemble the distribution of rainfall depth and storm durations in the state of Maryland (Kreeb 2003) and appears to be representative.

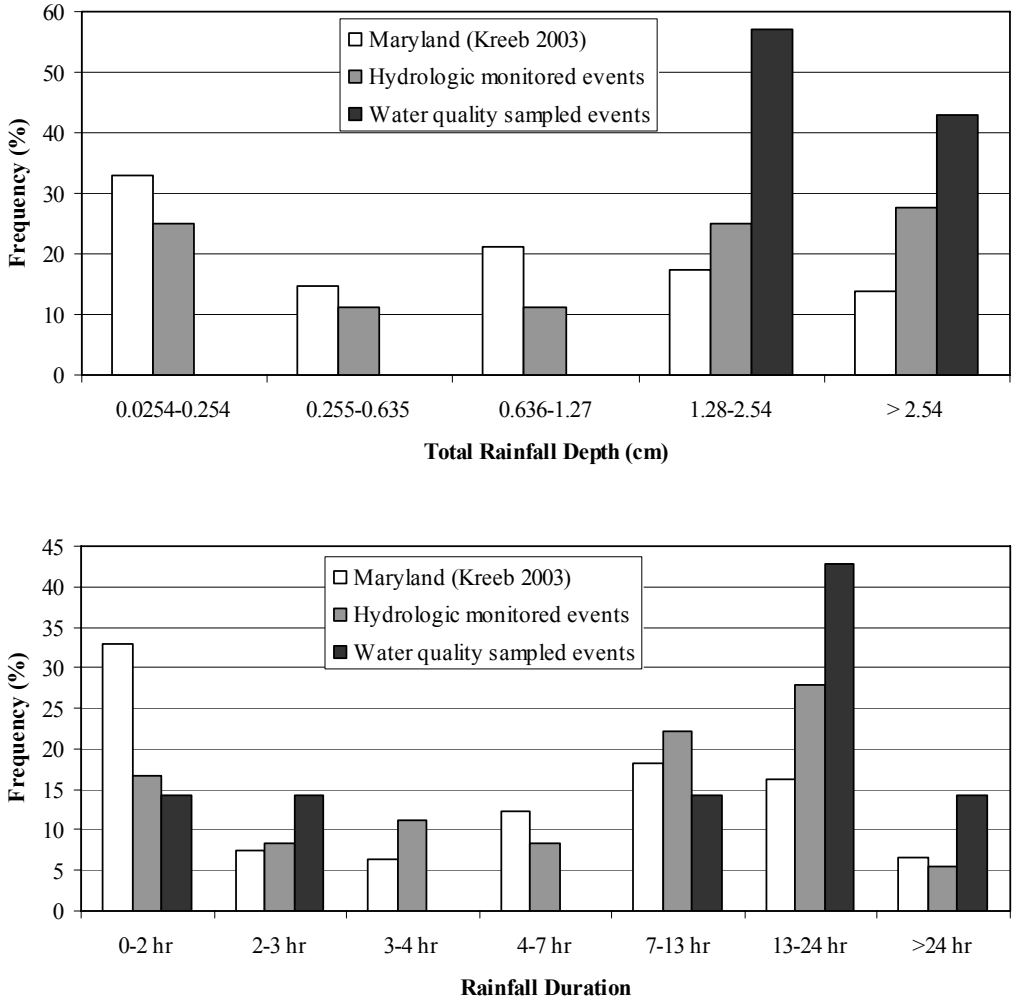

Figure 3-7. Rainfall depth and duration patterns for Maryland (Kreeb 2003) and Cell SS storm events.

3.3.2. Hydrological benefits

Typical hydrographs for Cells CP and SS can be used to illustrate the hydrological benefits of bioretention, as shown in Figure 3-8. Cells CP and SS delayed and reduced the runoff peak flows, and diminished the runoff volume through infiltration. However, in many events, more complicated hydrological conditions occurred, such as multiple peak flow, varying rainfall intensity and event durations, and overlapping rainfall events. To be clear, two rainfall events were separated with a dry period greater than 6 hours.

It appears that the ground water level near Cell CP became elevated during intense or long duration events because of the nearby Campus Creek, compounding the effluent volume measurement in some events. The variety of rainfall patterns can be exemplified with the following data: During the 14 monitoring events, Cell CP received 0.03-2.05 cm rainfall (median = 0.45 cm) with event duration of 0.2-24.9 hr (median = 4.6 hr), resulting rainfall intensity of 0.03-1.14 cm/hr (0.08 cm/hr) and influent of 0.003-0.683 m^3/m^2 (normalized with the cell surface area, median = 0.061 m^3/m^2). One event was a wintry mix in which the precipitation could not be registered on the rain gauge and only the runoff flow rates were recorded.

During the 40 monitoring events, Cell SS received 0.03-5.36 cm rainfall (1.46 cm) with event duration of 0.03-32.3 hr (median = 8.0 hr), resulting a rainfall intensity of 0-3.20 cm/hr (0.16 cm/hr) and influent of 0-0.822 m^3/m^2 (0.136 m^3/m^2). Three of four winter events were wintry mix in which the precipitation could not be registered on the rain gauge and only the runoff flow rates were recorded; one winter event had snow accumulation in both the rain gauge and inflow Parshall flume and

the precipitation and runoff flow rates were unable to be recorded. All event hydrological data are listed in Appendix 1.

In the smallest 3 (CP) and 12 (SS) events that generated incoming runoff from the drainage areas, no measurable underdrain effluent was detected, indicating that the entire runoff volume was stored through infiltration and holding by the soil. The pollutant discharge of these events was therefore zero.

Figures 3-9 and 3-10 demonstrate the rainfall amount as a function of event duration for Cells CP and SS, respectively. The trend lines drawn for the "zero discharge" events approximately serve as the boundary between the flow and no flow events. In Cell CP, the intercept and slope of the line are 0.05 cm and 0.029 cm/hr (the trend line has a best fit equation of $y = 0.05 + 0.029\,x$ through curve fitting using the least squares method), implying that Cell CP can treat a rainfall ≤ 0.05 cm or with an intensity ≤ 0.029 cm/hr in its drainage area without discharge. Similarly, Figure 3-10 indicates that Cell SS can completely treat a rainfall ≤ 0.25 cm or with an intensity ≤ 0.034 cm/hr (the trend line equation: $y = 0.25 + 0.034\,x$). Events that could not generate incoming runoff were not included in the estimate. Cell SS exhibited excellent runoff treatment capability; as previously mentioned, Kreeb 2003 indicates that the probability of rainfall depth <0.254 cm in Maryland is about 33%. As a result, Cell SS is able to manage more than one third of rainfall events in its drainage area without discharge. The probability of the zero discharge events in Cell CP cannot be directly estimated from Kreeb's data (2003) since 0.05 cm is much smaller than the minimal literature rainfall depth category, but is clearly lower than that of Cell SS.

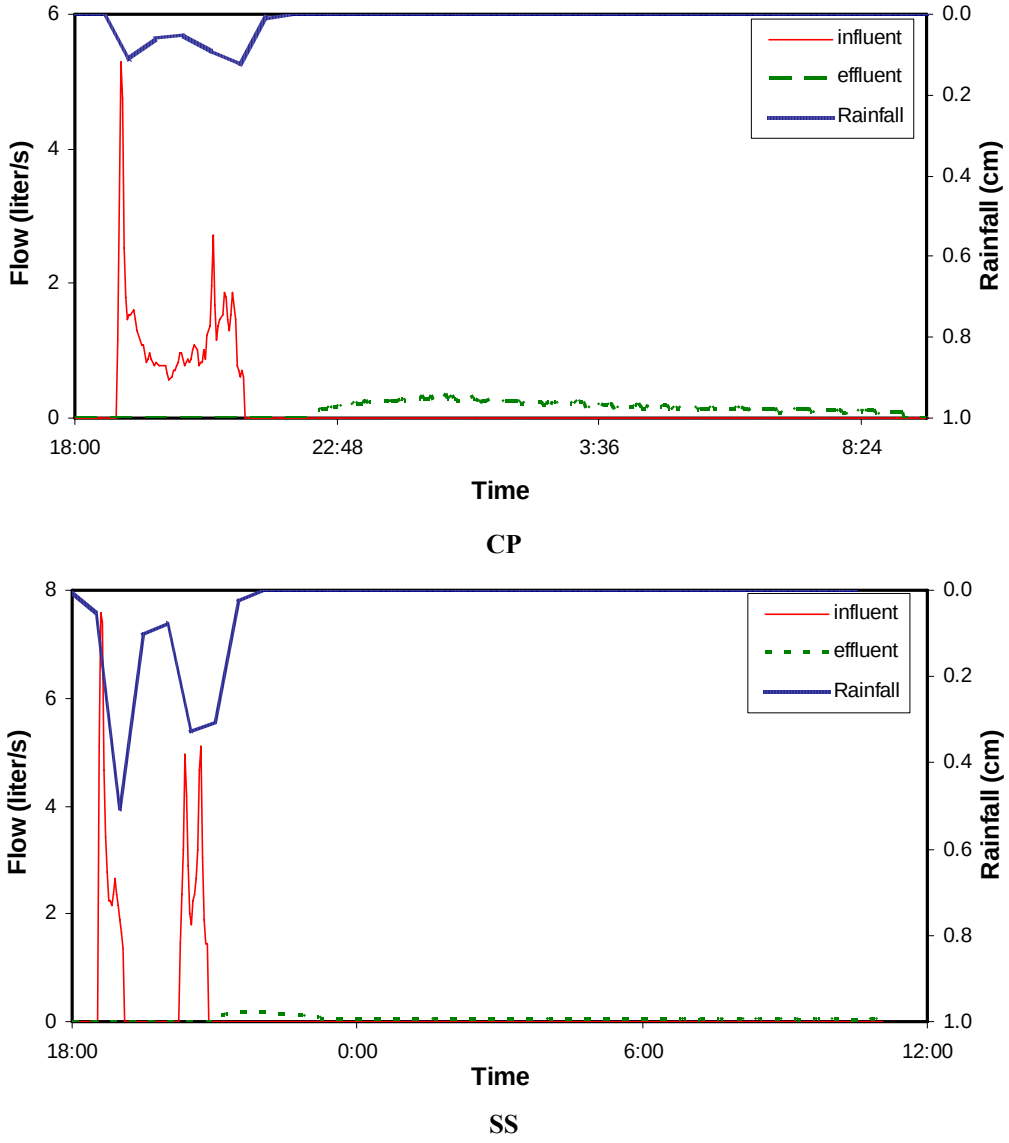

Figure 3-8. The hydrographs of Cells CP and SS for the event on 4/3/2006.

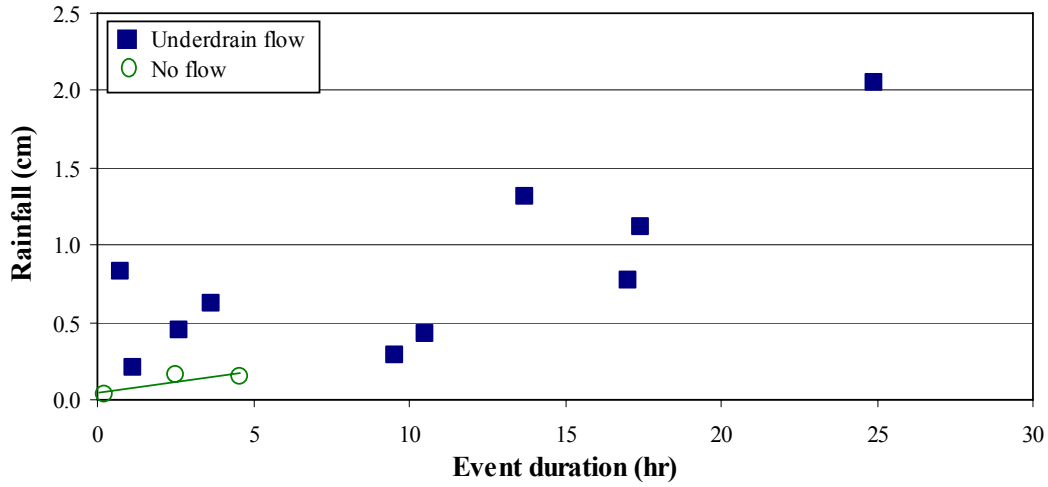

Figure 3-9. Rainfall depth and event duration for Cell CP events with and without generating underdrain flow.

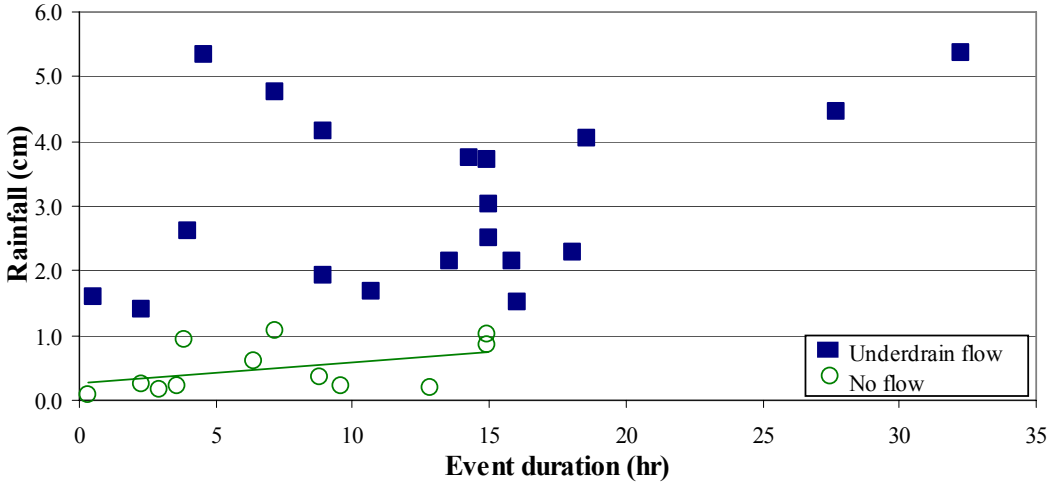

Figure 3-10. Rainfall depth and event duration for Cell SS events with and without generating underdrain flow.

As mentioned, Cell SS has a lower cell surface area to drainage area ratio (2%) than Cell CP (6%), although the actual ratio at Cell SS is considered to be larger than 2% since less runoff inflow is diverted into the cell than the design drainage (which implies a smaller actual drainage area). Nonetheless, Cell SS still handled a higher hydraulic loading (0-0.822 m^3/m^2, median = 0.136 m^3/m^2 or 13, 913 L) compared to

Cell CP (0.003-0.683 m^3/m^2, median = 0.061 m^3/m^2 or 10, 987 L) during the observation period. However, Cell SS still indicated better hydrological performance than Cell CP in terms of managing inflow without discharge. It is believed that the larger cell volume (in terms of the media depth, since the hydraulic loadings are normalized with the cell area) of Cell SS (0.9 m) provides larger runoff storage capacity than that of Cell CP (0.5-0.8m). Cell SS is also designed with a higher ponding depth (0.30 m, compared to 0.15 m of Cell CP) to handle higher hydraulic loadings and to overcome infiltration resistance from the thicker media depth. Moreover, the designed maximum Darcy hydraulic gradients (calculated by the designed ponding depth and media depth, a hydraulic gradient higher than that will cause runoff overflow and treatment bypass) of the two cells are similar (Cell CP: 1.2-1.3, Cell SS: 1.3). Cell CP media is sandy loam and the Cell SS media is sandy clay loam. The higher clay content in Cell SS (20%, Table 3-1) compared to Cell CP (7%) presumably renders Cell SS media with a lower hydraulic conductivity (which was not measured in this study). As such, the effluent flow rates (normalized to the cell areas) in Cell SS are lower than those of Cell CP, resulting in longer runoff hydraulic retention time, which favors runoff pollutant removal. However, higher ponding storage and cell volume also imply higher construction cost; a deep media design may also be inappropriate at areas with elevated groundwater level and stormwater drainage infrastructure.

Three performance metrics have been proposed to measure restoration of post-development hydrology through bioretention in terms of peak flow delay, peak flow reduction, and runoff volume reduction (Davis 2007a). The peak flow delay is

described using the peak delay ratio, R_{delay}, which is defined as the elapsed time to peak for the output flow, $t_{q\text{-}peak\text{-}out}$, based on the input runoff start time, and the time to peak flow for the input, $t_{q\text{-}peak\text{-}in}$:

$$R_{delay} = \frac{t_{q-peak-out}}{t_{q-peak-in}} \tag{3-7}$$

By delaying the flow peaks ($R_{delay} > 1$), bioretention produces hydrological responses more similar to undeveloped land. Larger R_{delay} values reflect better restoration.

Davis (2007a) proposed that $R_{delay} \geq 6$ as one criterion for hydrological restoration, based on the estimate for sheet flow time of concentration, T_c:

$$T_c = \frac{0.938}{i^{0.4}}\left(\frac{nL}{\sqrt{S}}\right)^{0.6} \tag{3-8}$$

where n represents Manning's roughness coefficient, L is the flow path length, i is the rainfall intensity, and S is the drainage area slope. Comparing T_c for a light underbrush forest ($n \approx 0.4$) and a paved drainage area ($n \approx 0.02$) at the same flow path length, rainfall intensity, and slope, the T_c ratio equals $(0.4/0.02)^{0.6} = 6$, which constitutes the target value.

For the events in which no output flow was observed, $t_{q\text{-}peak\text{-}out}$ and R_{delay} values mathematically approach infinity. Since the target value is 6, these events were arbitrarily assigned a R_{delay} value of 6 in Davis' study (2007a) so that they can be included in the data set. However, in this study, a R_{delay} value of 200 was used instead, since a significantly larger value can reflect R_{delay} is approaching infinity (other R_{delay} values ranges from 1 to 180 in both cells). For events in which the incoming peak flow occurred at exactly the event beginning ($t_{q\text{-}peak\text{-}in} = 0$, including two events at Cell SS and none at Cell CP), R_{delay} values also approach infinity; a

R_{delay} value of 200 was also used for these events. The probability plots for R_{delay} values of Cells CP and SS are shown in Figure 3-11.

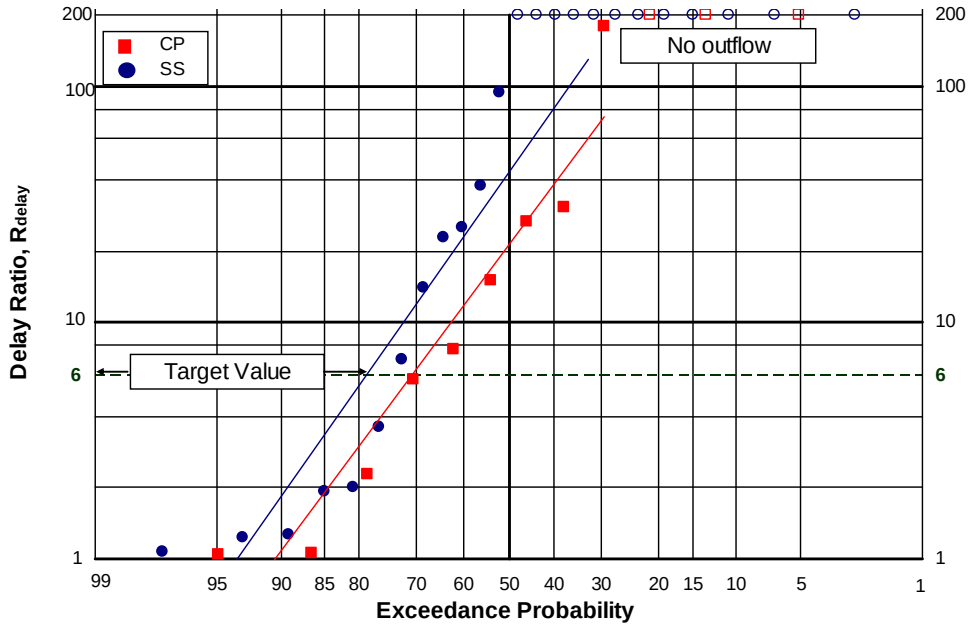

Figure 3-11. The peak delay ratio R_{delay} of Cells CP and SS for monitored storms.

Figure 3-11 indicates excellent peak delay performance from Cells CP and SS; over 70% of events are predicted to produce a $R_{delay} \geq 6$ at both cells (70% at Cell CP and 78% at Cell SS). The median R_{delay} values are 21 (Cell CP) and 147 (Cell SS); all events had $R_{delay} > 1$. Cell SS had larger R_{delay} values compared to Cell CP because of its larger media volume, as previously mentioned.

For comparison, the target value of $R_{delay} \geq 6$ can be expected to be met in 31-38% of rainfall events, and peak delay ($R_{delay} > 1$) is expected for 75-88% of rainfall events at field bioretention facilities (Davis 2007a). Compared with these data, Cells CP and SS exhibited better hydrological performance in delaying runoff peak flows. The literature R_{delay} data were obtained from two lined bioretention cells (Davis 2007a),

whose hydrological performance is believed to be limited because their infiltration function was restricted by the liner. Those cells have a cell surface area:drainage area of 2% and media depth of 0.9-1.2 m, similar to Cell SS (2% and 0.9 m), but had a smaller area ratio and a larger media depth compared with Cell CP (6% and 0.5-0.8 m). As such, infiltration function may be of critical importance for bioretention design.

Another restoration metric proposed by Davis (2007a) describes the peak flow rate reduction using the peak flow reduction ratio, R_{peak}:

$$R_{peak} = \frac{q_{peak-out}}{q_{peak-in}} \tag{3-9}$$

where $q_{peak\text{-}in}$ is the peak inflow (L/sec) and $q_{peak\text{-}out}$ is the corresponding peak outflow (L/sec). A $R_{peak} < 1$ indicates peak reduction. The proposed target R_{peak} value is $R_{peak} \leq 0.33$, which was derived from comparing the Rational Method runoff coefficient c for undeveloped land (0.3) to that of a highly impervious area (c=0.9) (Davis 2007a).

Two events at Cell CP had effluent flow rates exceeding the weir range (5.6 L/s) during event durations of 25 and 14 hours; it is believed that this was caused by increased groundwater level elevation from nearby Campus Creek. The 15-cm effluent discharge pipe at Cell SS is relatively small for flow rate determination; the measurable effluent range (with the 15-cm Thel-mar plug-in weir) is less than 2.1 L/s, as mentioned. As such, eight events had flow rates exceeding that value at Cell SS. The effluent rates, volume, and R_{peak} were estimated with the upper limit of the weir range and included in data set for these events. The probability plots for R_{peak} values of Cells CP and SS are shown in Figure 3-12.

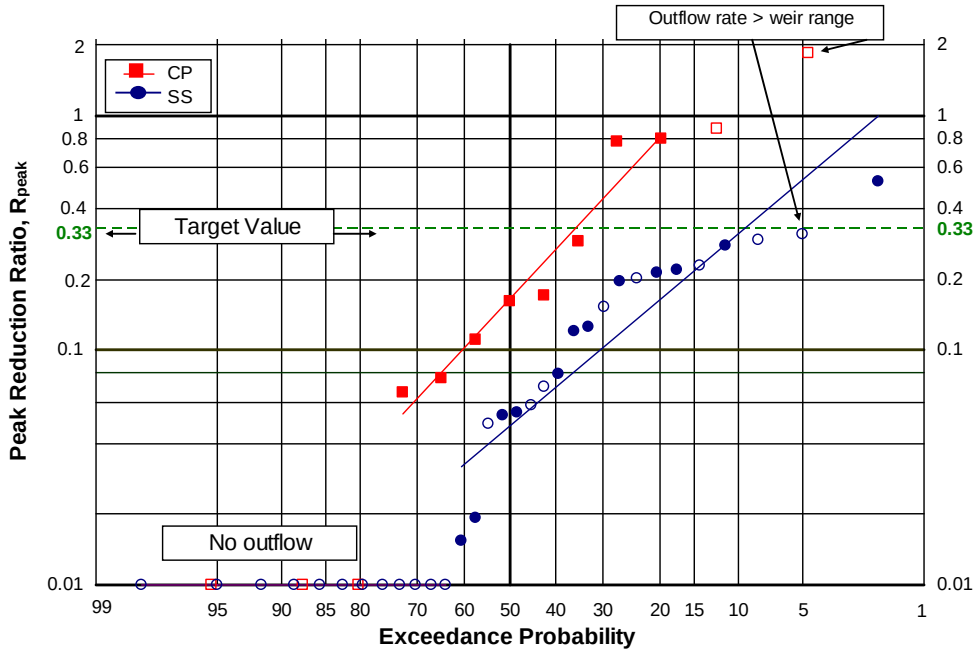

Figure 3-12. The peak reduction ratio R_{peak} of Cells CP and SS for monitored storms.

Figure 3-12 indicates excellent peak reduction capability from both cells. The predicted exceedance probability for the cells to achieve the target value is >65% (CP) and >90% (SS). All measurable events had peak reduction (R_{peak} < 1), with median R_{peak} values of 0.16 (CP) and 0.05 (SS). Again, Cell SS exhibited better hydrological performance compared to Cell CP because of its relatively larger media volume. For comparison, Davis (2007a) noted exceedance probabilities for lined field bioretention facilities to meet this target value as 30-42%, and median R_{peak} values of 0.40-0.48 have been reported (Davis 2007a). It is believed that the better performance for Cells CP and SS is a result of the fact that they are not lined and have better infiltration, as mentioned. Other literature documented an average bioretention peak flow reduction of 85% (R_{peak} =0.15, UNHSC 2006).

The third restoration metric as measures of successful low impact development (LID) performance proposed by Davis (2007a) is the fraction of input water measured leaving each system after 24 hours, f_{V24}:

$$f_{V24} = \frac{V_{out-24}}{V_{in}} \tag{3-10}$$

where V_{in} is the input stormwater runoff volume (L) to a bioretention cell and V_{out-24} was the corresponding outflow volume (L) leaving the cell after 24 hrs. It was noted that sometime outflows continued from the underdrains for many hours or even days at very low flow rates, as illustrated in Figure 3-8. Because of the practical challenges of measuring low flows for extended times, an outflow volume is defined after 24 hrs of flow. A $f_{V24} < 1$ indicates runoff volume reduction and ground water recharge, and the target f_{V24} value proposed is $f_{V24} < 0.33$ with the same rationale of R_{peak} (Davis 2007a). The probability plots for f_{V24} values of Cells CP and SS are shown in Figure 3-13, which projects that 70% (CP) and 75% (SS) of the events are expected to show $f_{V24} < 1$, indicating runoff flow reduction. The events with effluent volume > runoff volume ($f_{V24} > 1$) are assumed to have been caused by groundwater surge from the nearby creek or other cells during intense or long-duration rainfall events, particularly at Cell CP. The median f_{V24} values are 0.7 (CP) and 0.1 (SS). Sixty percent (CP) and 65% (SS) of the events are expected to achieve the target value ($f_{V24} < 0.33$). Cell SS indicated better runoff volume reduction compared to Cell CP, because of its larger cell volume, as mentioned. Literature f_{V24} values for bioretention are 0.18 to 0.23 (median values), and the probability to meet the target value is expected to be 55-62% (Davis 2007a).

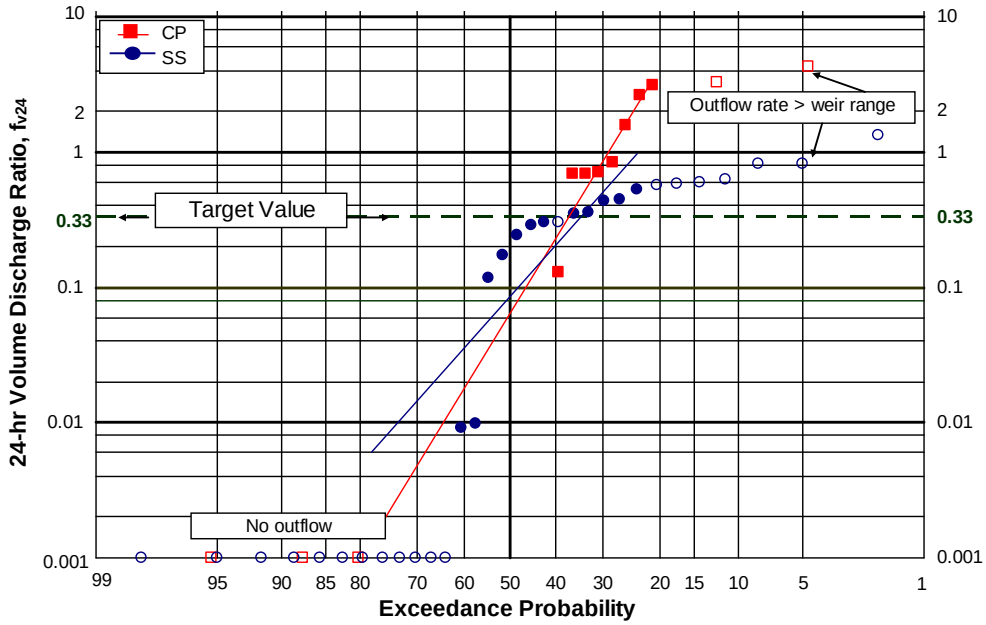

Figure 3-13. The 24-hr volume discharge ratio f_{V24} of Cells CP and SS for monitored storms.

Judging from the three metrics, Cells CP and SS exhibited very good performance to restore post-development hydrology through delaying / reducing peak flows and runoff volume reduction, which provides significant hydrological benefits such as flood control, channel erosion protection, and groundwater recharge. At Cell CP, precipitation appears to be an important factor for cell hydrology. Of the events which could not reach the target values of R_{delay} and R_{peak}, precipitation was 0.43-1.12 cm (the median precipitation at Cell CP = 0.46 cm). Similarly, of the events which could not achieve the target f_{V24} value, the precipitation depth was 0.20-2.05 cm. As such, high precipitation can render poor hydrological performance for bioretention, even when the precipitation amount is still within the design water quality volume (which is about 2.5 cm rainfall in Maryland, MDE 2000). The length of rainfall duration also played as an important role for determining cell hydraulic performance.

The events that could not reach the R_{delay} ,R_{peak}, and f_{V24} targets at Cell CP had rainfall durations of 10.5-24.9, 0.7-17.4, and 0.7-24.9 hr, respectively. (The median rainfall duration at Cell CP is 4.6 hr).

These phenomena were also observed at Cell SS. Events that could not reach R_{delay} ,R_{peak}, and f_{V24} targets had precipitation of 4.04, 1.68-4.04, and 1.60-5.33 cm, respectively, and rainfall durations of 18.6, 10.6-19.7, and 0.50-27.7 hr, respectively. (The median precipitation and rainfall duration of Cell SS are 1.5 cm and 8 hr). As such, the precipitation patterns have strong effects on cell hydrological performance. The cell hydrological performance can be enhanced with larger cell surface area to drainage area ratio and media volume, as previously discussed. Of course, the trade-off between construction cost, construction availability, and performance requires detailed analysis for individual sites. One goal of this study is to provide quantitative tools for such analysis and design decisions.

Hunt (2006) found significantly higher field bioretention outflow: inflow volume ratios in winter than at other times of a year and concluded the seasonal difference as a result of lower evapotranspiration (ET) rates in winter, compared to those of warmer seasons. In this study, the f_{V24} values at both cells did not exhibit significant seasonal difference as mentioned above, which may be attributed to different vegetation growth conditions in these cells. Further, ET phenomena were not obvious during the rainfall events, in which the hydrological monitoring was conducted. However, estimates of ET water flux are important for judging bioretention vegetation performance, which may require hydrological, soil monitoring, and lysimetric methods, as well as micrometeorological and remote sensor monitoring for

parameters such as solar radiation, wind, and temperature (Jacob et al. 2002, Drexler et al. 2004); therefore is beyond the scope of this research and warrants further study.

3.3.3. Water quality results

Results of the water quality monitoring are listed in Table 3-5. The inflow runoff pollutants concentrations at both cells are generally at the lower end compared to literature values (Table 3-6), which may be attributed to different local runoff characteristics under different land use conditions. Concentrations of particulate pollutants (TSS) and heavy metals were generally reduced after treatment, which also agrees with previous studies (Davis et al. 2003, Hsieh and Davis 2005). Concentrations of nutrients (nitrogen species and TP) and chloride were generally increased after treatment, which agrees with some previous studies of bioretention (Dietz and Clausen 2005, 2006, Hunt et al. 2006) and grassed swales (Stagge 2006). It is believed that the additional nutrients originate from the plants and animals living the top-soil / mulch media, which are also responsible for TOC concentration increases; additional chloride may come from the application of de-icing reagents as road maintenance during snow seasons, which serves as a chloride source inside the media, dissolving out as chloride ion in subsequent storm events. The affiliation between pollutants and media affects the pollutant capture and is discussed in Chapter 6.

Table 3-5. Results of the water quality monitoring of the 8 events at both sites.

BMP	Pollutant	Influent EMC			Effluent EMC			EMC percent removal (%)			Pollutant mass removal (%)		
		Median	Min[1]	Max[2]	Median	Min[1]	Max[2]	Median	Min[1]	Max[2]	Median	Min[1]	Max[2]
Cell CP	TSS (mg/L)	47	7	200	3	1	10	88	39	99	92	-59	99
	Chromium (µg/L)	3	<2	14	3	2	5	12	<-40	85	29	<-265	97
	Copper (µg/L)	18	9	42	15	9	35	11	-84	53	34	-226	92
	Lead (µg/L)	3	<2	18	<2	<2	7	55	-97	85	84	-49	97
	Zinc (µg/L)	42	15	174	11	6	17	71	22	94	72	-103	99
	Chloride (mg/L)[3]	4	2	143	28	4	448	-314	-918	-60	-193	-2290	72
	TN (mg /L as N)	1.4	0.1	4.9	1.6	0.9	3.2	-28	-961	34	-18	-2994	88
	Nitrate (mg/L as N)	0.33	0.09	2.59	0.80	0.27	2.04	-136	-556	21	-71	-872	85
	Nitrite (mg/L as N)	0.03	<0.02	0.12	0.03	<0.02	0.08	12	-48	58	55	<-325	88
	TKN (mg/L as N)	1.1	<0.2	2.2	0.8	0.5	1.2	10	<-182	62	-6	<-832	91
	TP (mg/L as P)	<0.1	<0.1	0.7	0.3	0.1	0.5	-77	<-287	59	-36	-1180	95
	TOC (mg/L)[4]	3.3	1.6	11.4	9.2	6.5	17.5	-215	-492	-35	-77	-1856	59
	E Coli. (#/100mL)[5]	92	43	308	13	1	1145	71	-272	99	94	-1131	>99
	Fecal Coliform (MPN/100mL)[5]	140	80	900	37	4	1600	77	-78	96	96	-488	99
Cell SS	TSS (mg/L)	16	6	150	3	<1	30	78	13	98	88	50	99
	Chromium (µg/L)	<2	<2	6	<2	<2	3	>46	46	65	>88	<55	>94
	Copper (µg/L)	12	7	19	11	5	17	-2	-38	74	63	<13	99
	Lead (µg/L)	<2	<2	7	<2	<2	3	60	>0	61	81	<67	95
	Zinc (µg/L)	15	7	67	5	2	11	68	24	>89	92	<56	>99
	Chloride (mg/L)	3	<1	13	3	2	16	<-6	<-960	83	63	-775	99
	TN (mg /L as N)	0.9	0.1	1.2	0.6	0.3	1.1	-15	-567	76	44	<-284	99
	Nitrate (mg/L as N)	0.27	0.06	0.72	<0.05	<0.05	0.29	68	14	>91	96	>32	99
	Nitrite (mg/L as N)	<0.02	<0.02	0.05	<0.02	<0.02	0.04	-5	-8	>62	>87	68	99
	TKN (mg/L as N)	0.5	<0.2	0.9	0.5	0.3	1.1	-29	<-282	58	33	<-120	99
	TP (mg/L as P)	<0.1	<0.1	0.2	<0.1	<0.1	0.1	24	<-20	55	<38	<31	95
	TOC (mg/L)[3]	3.4	1.8	7.9	7.0	1.0	21.5	-141	-598	88	-4	<-476	99
	E Coli. (#/100mL)[5]	4	1	2420	29	1	5475	>-126	-1008	50	-69	-232	94
	Fecal Coliform (MPN/100mL)[5]	8	<2	>1600	32	<2	1600	0	-438	>0	14	-61	88

[1] Minimum, [2]Maximium, [3] 7 events available, [4] 6 events available, [5] 4 events available.

Table 3-6. Comparison of the water quality results from the bioretention influents of this study to some EMC data for highway stormwater runoff studies..

Reference	Site	Land use	TSS (mg/L)	Cu (µg/L)	Pb (µg/L)	Zn (µg/L)	TN (mg N/L)	TP (mg P/L)
This study [a] (MD, USA)	Cell CP	Institutional	47	18	3	42	1.4	<0.1
	Cell SS	Institutional	16	12	<2	15	0.9	<0.1
Stotz (1987)[b]	A81, FRG [c]	Rural	137	97	20	360	-	0.25
	A6, FRG	Rural	181	117	2	620	-	0.35
	A8, FRG	Rural	152	58	24	320	-	0.31
Sansalone and Buchberger (1997)	Millcreek, OH, USA	Urban	-	43-325	37-97	459-15244	-	-
Barrett et al. (1998) [b]	W35. TX, USA	Commercial/ Residential	129	37	53	222	1.07 [d]	-
	CH, TX, USA	Rural/ Residential	91	7	15	44	0.71 [d]	-
	WC, TX, USA	Commercial/ Residential	19	12	3	24	0.37 [d]	-
Wu et al. (1998) [b]	HB, NC, USA	Rural/ Residential	283	24.2	21	-	3.67 [e]	0.43
	NC49, NC, USA	Rural/ Residential	93	11.5	14	-	1.40 [e]	0.52
	I85, NC, USA	Rural/ Residential	30	4.6	6.5	-	1.14 [e]	0.31
Flint (2004) [b]	US1, MD, USA	Urban	405 (32-10000)	100 (14-740)	190 (6-2300)	1300 (80-30000)	5.1 (0.3-41.5)	0.6 (0.2-3.6)

[a] Median EMC, [b] Mean of EMC, [C] Federal Republic of Germany, [d] NO_3 only, [e] NO_3 + TKN

Data were available from the subcontractor laboratory for only four events for *E. Coli.* and Fecal Coliform. Some indicated indicator organism removal and others indicated export. As such, results of runoff pathogen indicator (*E Coli.* and Fecal Coliform) treatment are inconclusive. Compared to physical and chemical pollutants, many other factors can affect pathogen indicator capture, such as microbial growth and decay, as well as indigenous pathogen species living in the media. The ecology of microbiological communities in soil media is extremely complicated and little understood. A single gram of soil may contain more than 10^9 bacterial cells and

organisms that belong to tens of thousands of different species (Eldor 2007). As such, the survival of runoff pathogen in bioretention media warrants further studies.

Figures 3-14 to 3-17 present the pollutant EMC ratios of the influents and the corresponding effluents (C/C_0) of monitored events at Cells CP and SS, respectively, which provide overall pictures of pollutant levels of the monitored cells. As previously mentioned, the pollutant removal at the monitored cells is mixed. TSS and heavy metals (Cr, Cu, Pb, and Zn) were removed from the runoff; nutrients (nitrogen species and TP), organic matter (TOC), and chloride were added to the discharge runoff from the cell media in terms of concentration increases, and indicator organism removals were mixed (removal at CP but export at SS). As, Cd, Hg, and O&G levels at cell inflow and outflow were nearly all below the detection limits at both cells and are not included in the plots.

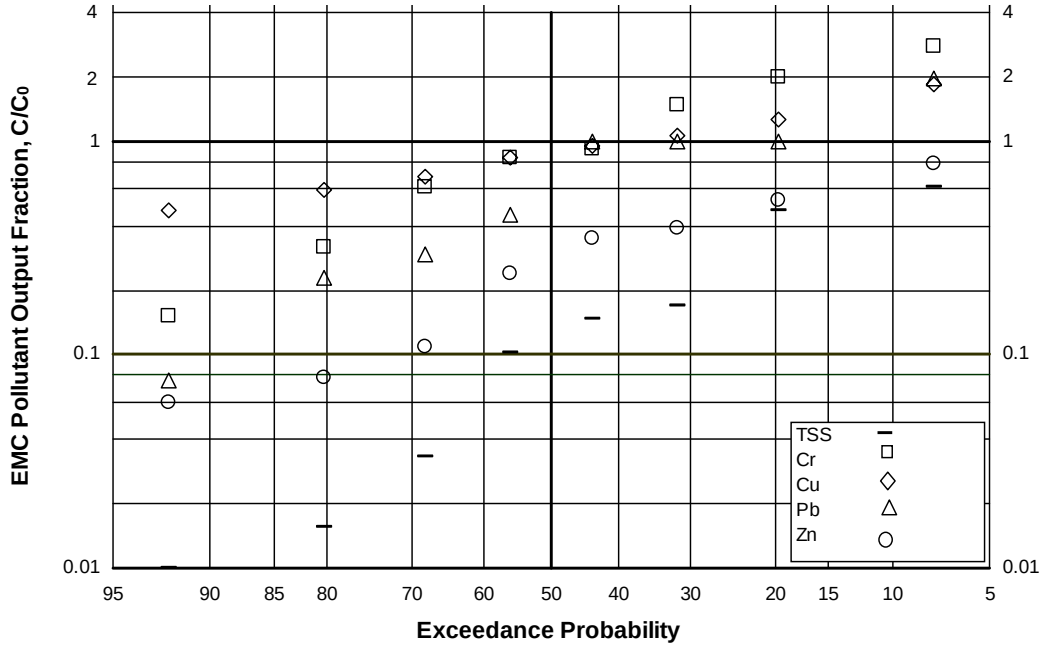

Figure 3-14. C/C_0 values for metals and TSS from monitored events at Cell CP.

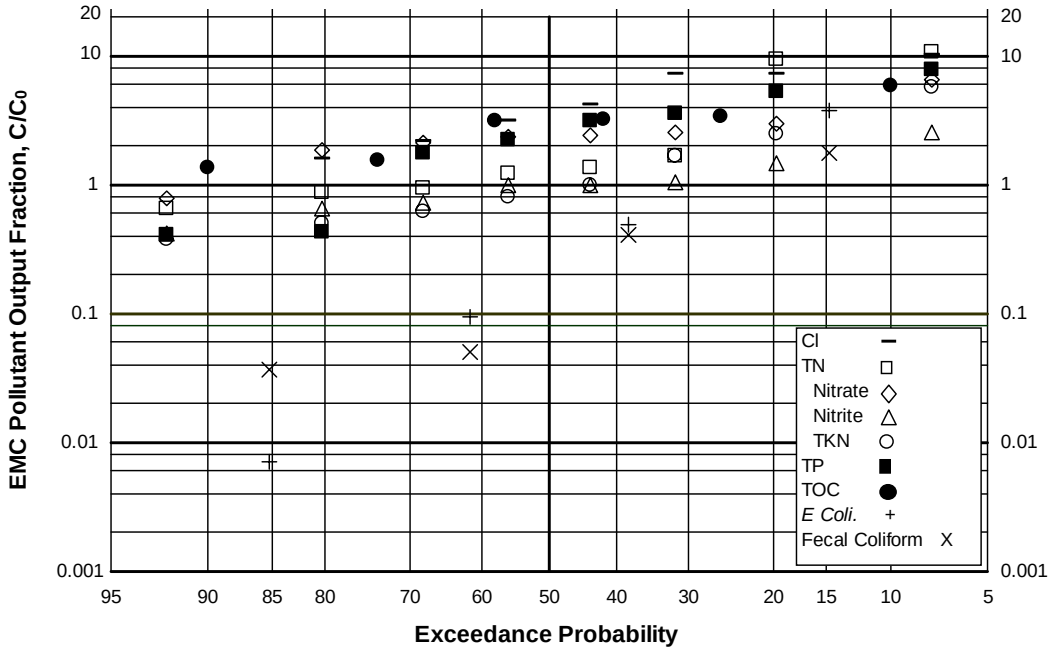

Figure 3-15. C/C_0 values for other pollutants from monitored events at Cell CP.

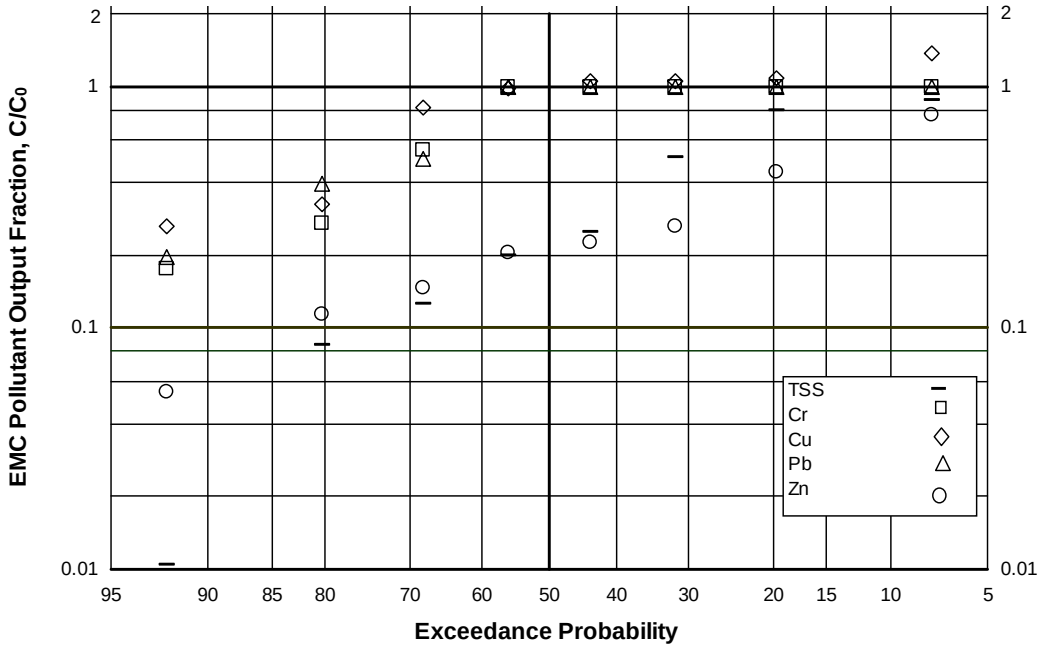

Figure 3-16. *C/C_0* values for metals and TSS from monitored events at Cell SS.

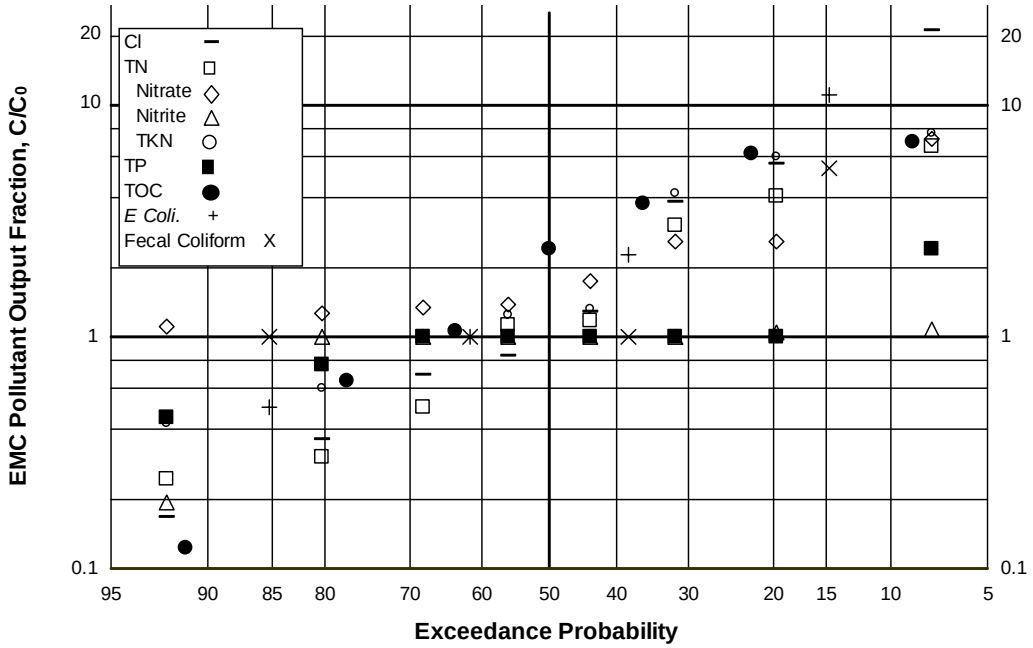

Figure 3-17. C/C_0 values for other pollutants from monitored events at Cell SS.

Similar results are also reflected through the statistical tests. Results of the Paired Student's t Test for the input / output pollutant levels at both cells are listed in Table 3-7, which indicate that TSS and zinc were significantly removed through Cell CP. Other input pollutant levels did not show significant difference from output pollutant levels at Cell CP. All monitored pollutant did not exhibit statistically significant differences between influent and effluent levels at Cell SS.

Results of the non-parametric Wilcoxon Matched-Pairs Signed-Ranks Test are listed in Table 3-8. At Cell CP, TSS and zinc were significantly removed by the media while nitrate, chloride, and TOC were significantly exported; other pollutants did not show significant differences between the input and output concentrations. At Cell SS, TSS and zinc exhibited significant removal; the other pollutants did not have statistically significant differences between their input and output concentrations.

As previously mentioned, a significant number of rainfall / runoff events can be treated completely with bioretention cells because they are small enough to be assimilated entirely by the bioretention media. However, the data present via Figures 3-14 to 3-17 and Tables 3-5 to 3-8 do not include these small events and thus underestimate the performance. The presentation of water quality performance for stormwater BMP is problematic and has not been standardized because of the complicated non-point source pollution nature (Davis 2007b). The most traditional metric of evaluation is the EMC percent removal:

$$\text{EMC Percent Removal} = (1 - \frac{EMC_{out}}{EMC_{in}}) \times 100\% \tag{3-11}$$

However, EMC percent removed may be misleading since the size of the rainfall event is not considered. As mentioned, the pollutant mass capture can also be achieved through flow attenuation, particularly in small events. As such, pollutant mass removal is also used:

$$\text{Pollutant Mass Removal} = (1 - \frac{M_{out}}{M_{in}}) \times 100\% \tag{3-12}$$

The pollutant mass input (M_{in}) and output (M_{out}) for the cell can be calculated by integrating the product of the pollutant concentration and flow rate during a runoff event:

$$Mass = M = \int_0^t C(t)Q(t)dt \tag{3-13}$$

The data for the influent and effluent pollution concentrations, as well as pollutant EMC percent removal and mass removal are summarized in Table 3-5 and Appendix 2.

Table 3-7. Test results of the Paired Student's t Test for the monitored water quality parameters.

Pollutants	College Park (CP) bioretention					Silver Spring (SS) bioretention				
	N*	df	$t_{computed}$	$t_{df, 0.05}$	Significant difference in population means?	N*	df	$t_{computed}$	$t_{df, 0.05}$	Significant difference in population means?
TN	8	7	-0.572	1.895	No	8	7	0.373	1.895	No
Nitrate	8	7	-2.202	1.895	No	4	3	2.10	2.353	No
Nitrite	5	4	1.510	2.132	No	2	1	-9.00	6.314	No
TKN	7	6	1.335	1.943	No	5	4	0.42	2.132	No
TP	4	3	0.249	2.353	No	2	1	2.23	6.314	No
Cl	7	6	-1.511	1.943	No	6	5	0.56	2.015	No
TSS	8	7	2.590	1.895	Yes (removal)	6	5	1.42	2.015	No
TOC	6	5	-5.665	2.015	No	7	6	-1.43	1.943	No
E Coli.	4	3	-0.701	2.353	No	3	2	-1.03	2.920	No
Fecal Coliform	4	3	-0.526	2.353	No	3	2	-1.00	2.920	No
As	-	-	-	-	-	-	-	-	-	-
Cr	6	5	1.594	2.015	No	1	0	-	-	-
Cu	8	7	0.707	1.895	No	7	6	0.35	1.943	No
Pb	3	2	0.935	2.920	No	1	0	-	-	-
Zn	8	7	2.633	1.895	Yes (removal)	5	4	1.94	2.132	No

* = The total number of applicable samples in the combined data sets used for comparison.

Table 3-8. Test results of the Wilcoxon Matched-Pairs Signed-Ranks Test for the monitored water quality parameters.

Pollutants	College Park (CP) bioretention				Silver Spring (SS) bioretention			
	N *	T computed	T 0.05	Significant difference in population means?	N *	T computed	T 0.05	Significant difference in population means?
TN	8	11.0	6	No	8	16.0	6	No
Nitrate	8	5.0	6	Yes (export)	4	0.0	-	-
Nitrite	5	3.0	1	No	2	0.0	-	-
TKN	7	8.0	4	No	5	5.0	1	No
TP	4	5.0	-	-	2	0.0	-	-
Cl	7	0.0	4	Yes (export)	6	8.0	2	No
TSS	8	0.0	6	Yes (removal)	6	0.0	2	Yes (removal)
TOC	6	0.0	2	Yes (export)	7	7.0	4	No
E Coli.	4	4.0	-	-	3	1.0	-	-
Fecal Coliform	4	4.0	-	-	3	0.0	-	-
As	-	-	-	-	-	-	-	-
Cr	6	4.0	2	No	1	-	-	-
Cu	8	12.0	6	No	7	10.5	4	No
Pb	3	1.0	-	-	1	-	-	-
Zn	8	0.0	6	Yes (removal)	5	0.0	1	Yes (removal)

* = The total number of applicable samples in the combined data sets used for comparison.

Figures 3-18 to 3-21 list the pollutant mass input to output ratios (M_{out}/ M_{in}) at both cells as a comparison to the pollutant EMC ratios of the influents and the corresponding effluents (C/C_0). In Cell CP, the trend of M_{out}/ M_{in} (Figures 3-18 and 3-19) and C/C_0 (3-14 and 3-15) are similar; however, M_{out}/ M_{in} (3-20 and 3-21) and C/C_0 (3-16 and 3-17) ratios at Cell SS exhibited much better pollutant mass removal compared to pollutant concentration reduction. Table 3-5 also shows that the pollutant mass removals were generally higher, compared to the EMC percent removals for almost all pollutants at both cells (particularly at Cell SS), indicating that the good hydrologic performance (in terms of runoff volume reduction) of bioretention facilities also promotes water quality improvement. Hunt et al. (2006)

also identified the correlation between hydrological and water quality benefits for field bioretention facilities. However, pollutant mass removal cannot completely account for small events in this study, since the sampling protocol for the water quality monitoring was to sample storm events in which both cell input and output had measurable flows at the two sites, as mentioned.

Table 3-5 also indicates that Cell SS had higher pollutant removal efficiencies (both EMC percent removal and mass removal) compared to Cell SS for nearly all pollutants. It is believed that the higher clay content of the Cell SS media renders the media with a higher surface area / volume ratio, providing higher pollutant adsorption capacity. The higher organic matter content in Cell SS media (12%, compared to 6% of Cell CP media, Table 3-1) may also help the media microbial community growth, which assisted biodegradation of captured pollutants. The longer runoff hydraulic retention time design of Cell SS, as discussed above, is also considered as favorable in helping pollutant capture and biodegradation. For example, nitrate removal efficiencies at Cell SS (EMC percent removal = 68%, pollutant mass removal = 96%, median values, Table 3-5) were significantly higher than those of Cell CP (-136% and -71%), which is believed to be associated with the factors stated above that enhanced microbial denitrification.

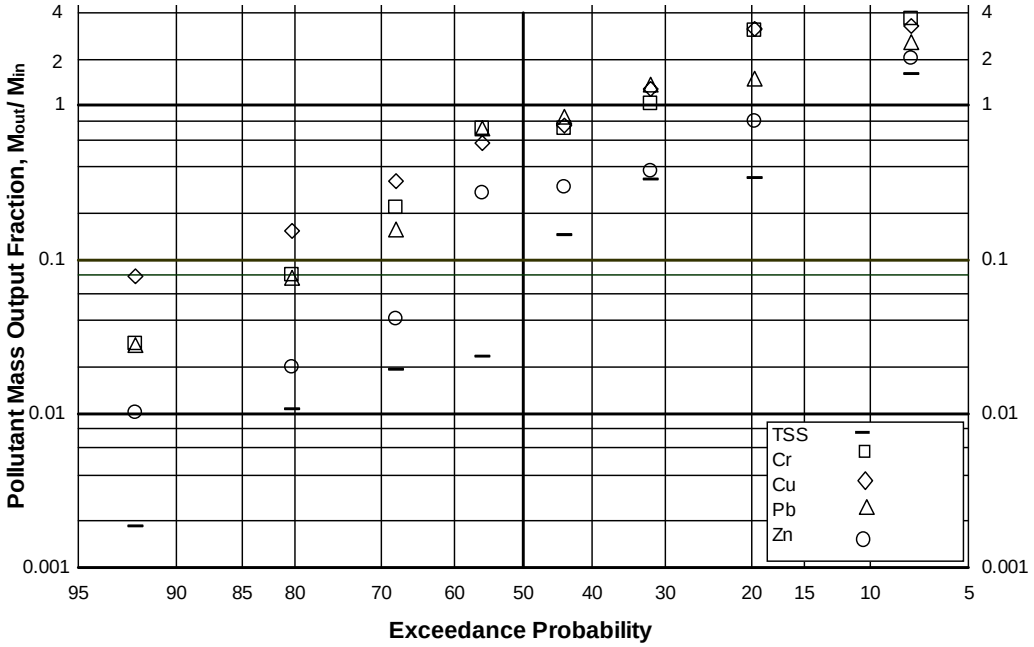

Figure 3-18. M_{out}/ M_{in} values for metals and TSS from monitored events at Cell CP.

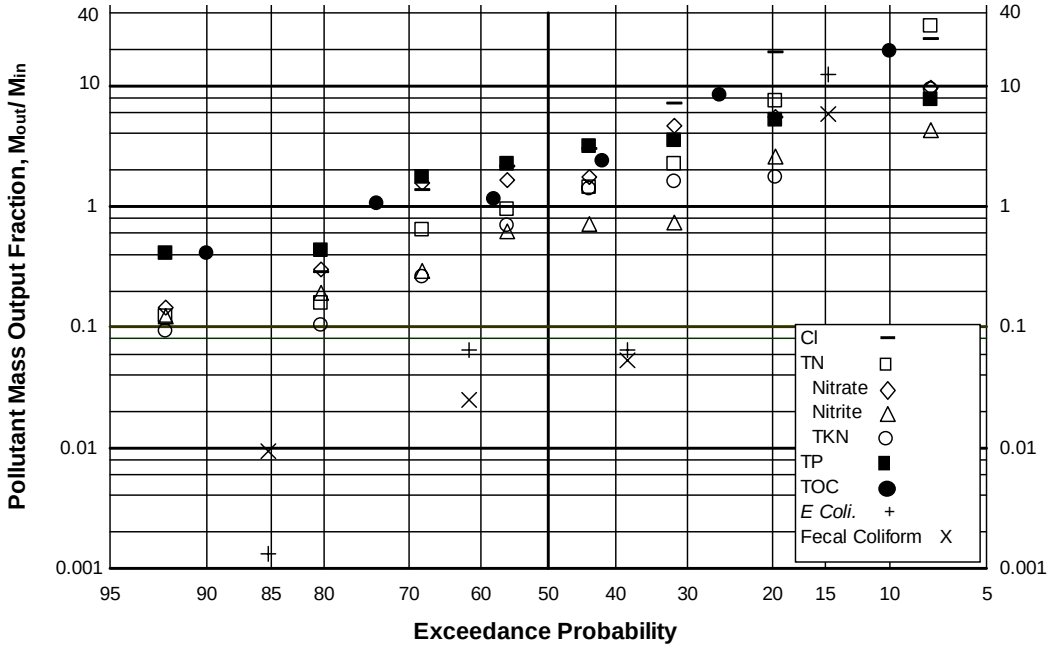

Figure 3-19. M_{out}/ M_{in} values for other pollutants from monitored events at Cell CP.

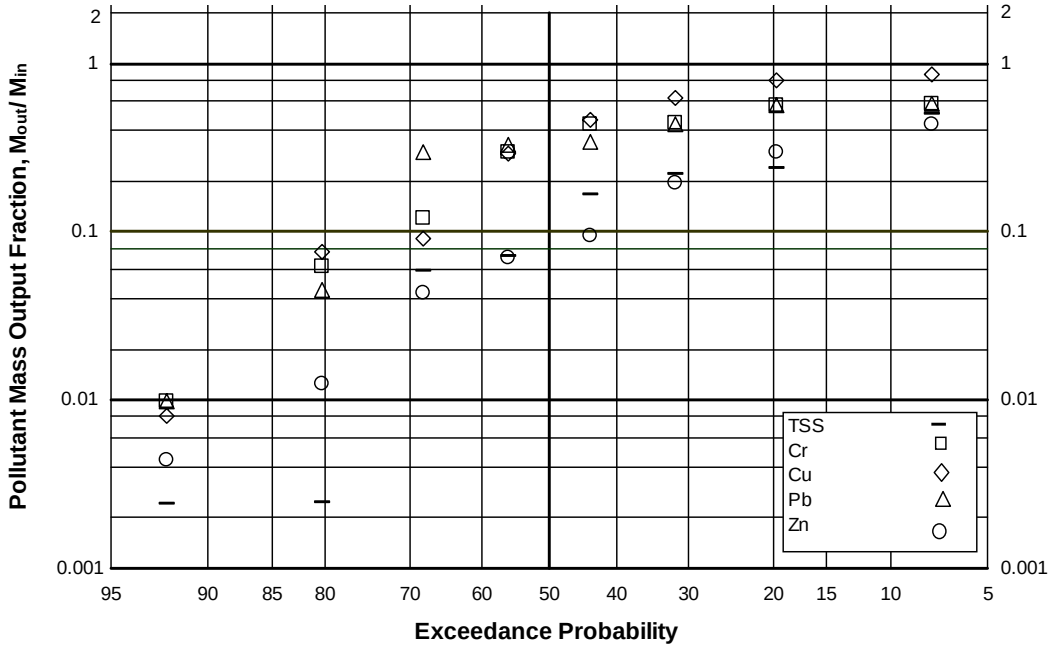

Figure 3-20. M_{out}/ M_{in} values for metals and TSS from monitored events at Cell SS.

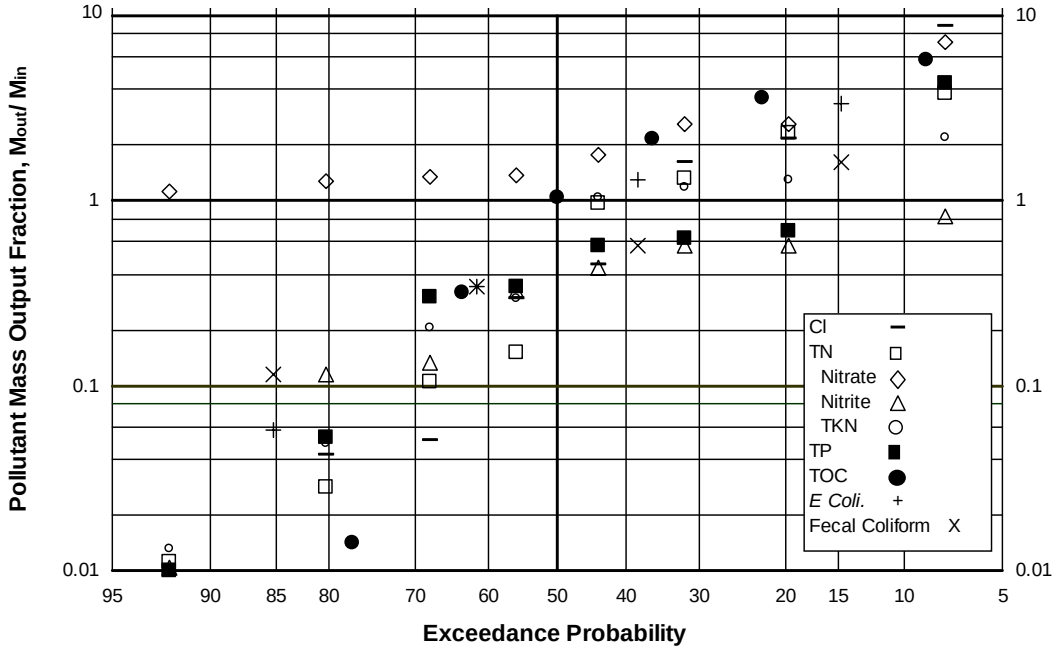

Figure 3-21. M_{out}/ M_{in} values for other pollutants from monitored events at Cell SS.

The third metric that can be employed in evaluating BMP water quality performance is effluent water quality, regardless of influent pollutant levels and EMC / mass removal contribution. Presentation of water quality data using probability plots can focus on the treatment outcome and anticipated TMDL (total maximum daily load) requirement (Davis 2007b). To this end, the water quality criteria from Table 2-2 are used as target pollutant concentrations, which consist of a stormwater quality criterion used by a previous study (Davis 2007b), the aquatic life protection criteria (acute, COMAR 2006), the drinking water MCL (USEPA 2003), and the pathogen indicator criteria for recreational water bodies (USEPA 1986). For pollutants with overlapped regulated criteria, a smaller value was used to cover wider water use.

Figures 3-22 and 3-23 present the TSS and zinc data, which demonstrate good removal and effluent quality. The median effluent TSS values are 3 mg/L at both cells (the target value = 20 mg/L), and the median output zinc levels are 11 μg/L (CP) and 5 μg/L (SS); the target zinc concentration is 120 μg/L. Over 95% (CP) and 85% (SS) of the effluent TSS concentrations and over 95% (both cells) of the effluent zinc concentrations are expected to meet the target values. For comparison, literature effluent TSS and zinc concentrations for field bioretention facilities are 13-18 mg/L and 44-48 μg/L, respectively, and the non-exceedance probabilities for TSS and zinc target values are 58-72% and 78->95% (Davis 2007b).

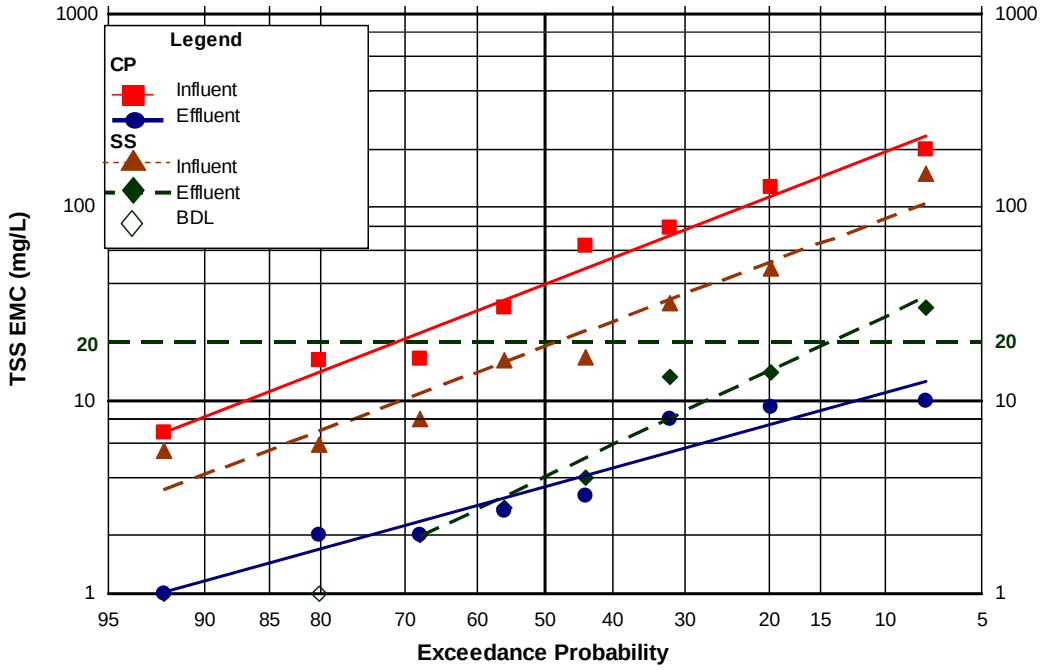

Figure 3-22. TSS probability plot for Cells CP and SS (BDL= below detection limit).

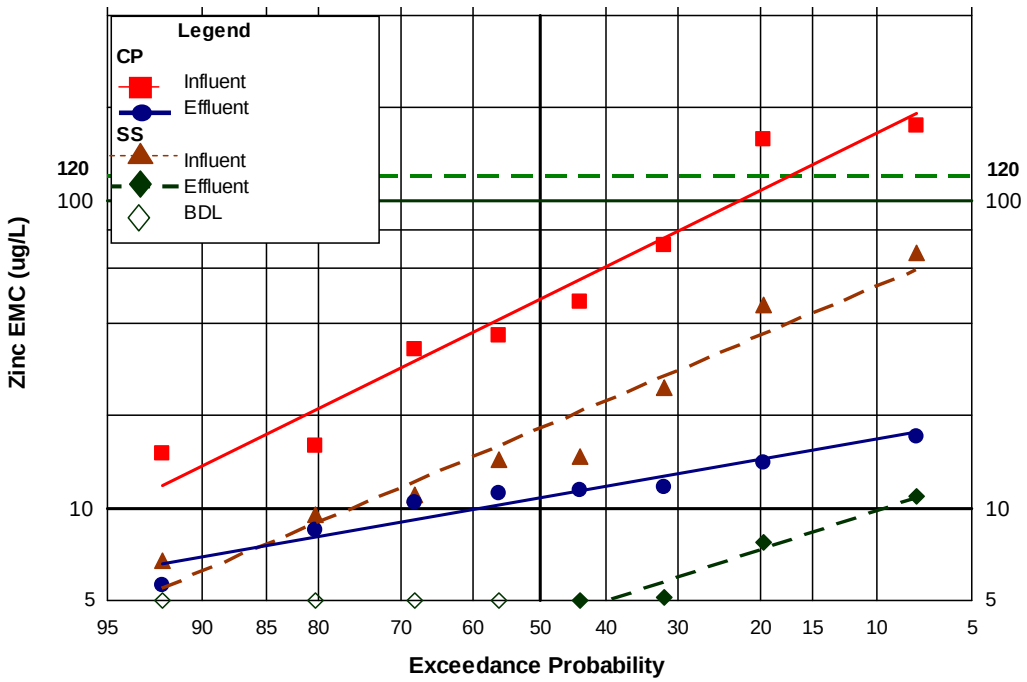

Figure 3-23. Zinc probability plot for Cells CP and SS (BDL= below detection limit).

The probability plots of other pollutants are listed in Appendix 2. With similar procedures, the comparison between the effluent pollutant concentrations, water quality criteria (from Table 2-2), and some literature values are listed in Table 3-9.

Table 3-9. Comparison of effluent water quality with the water quality criteria for the 8 events at both sites.

BMP	Pollutant	Water quality criteria (1) [a]	Median effluent EMC		Non-exceedance probability to (1), %	
			This study	Literature [b]	This study	Literature [b]
Cell CP	TSS (mg/L)	20	3	13-18	>95	58-72
	Chromium (µg/L)	100	3	-	>95	-
	Copper (µg/L)	13	15	3-4	35	91-96
	Lead (µg/L)	65	<2	<2-4	>95	>93
	Zinc (µg/L)	120	11	44-48	>95	78->95
	Chloride (mg/L)	250	28	31-125 [c]	>95	65-85 [c]
	TN (mg /L as N)	-	1.6	-	-	-
	Nitrate (mg/L as N)	10	0.80	0.02	>95	-
	Nitrite (mg/L as N)	1	0.03	-	>95	>80 [c]
	TKN (mg/L as N)	-	0.8	-	-	-
	TP (mg/L as P)	0.2	0.3	0.15-0.17	30	62-70
	TOC (mg/L)	-	9.2	-	-	-
	E Coli. (#/100mL)	126	13	-	>70	-
	Fecal Coliform (MPN/100mL) [5]	200	37	-	70	-
Cell SS	TSS (mg/L)	20	3	13-18	>85	58-72
	Chromium (µg/L)	100	<2	-	>95	-
	Copper (µg/L)	13	11	3-4	75	91-96
	Lead (µg/L)	65	<2	<2-4	>95	>93
	Zinc (µg/L)	120	5	44-48	>95	78->95
	Chloride (mg/L)	250	3	31-125 [c]	>95	65-85 [c]
	TN (mg /L as N)	-	0.6	-	-	-
	Nitrate (mg/L as N)	10	<0.05	0.02	>95	-
	Nitrite (mg/L as N)	1	<0.02	-	>95	>80 [c]
	TKN (mg/L as N)	-	0.5	-	-	-
	TP (mg/L as P)	0.2	<0.1	0.15-0.17	85	62-70
	TOC (mg/L)	-	7.0	-	-	-
	E Coli (#/100mL)	126	29		>65	-
	Fecal Coliform (MPN/100mL)	200	32	-	70	-

[a] Table 2-2, [b] Davis 2007b for bioretention, [c] Stage 2006 for grassed swales.

Table 3-9 shows that both cells indicated good effluent quality (with a non-exceedance probability to the target value > 80%) for nearly all pollutants (except

copper and pathogen indicators at both cells, and TP at Cell CP). Among these pollutants, the non-exceedance probabilities to the target value are 35% (CP) and 75 % (SS) for copper, >70% (CP) and >65% (SS) for *E. Coli.*, 70% (both cells) for fecal coliforms, and 30% (CP) for TP. Overall, the effluent water quality is fair to good at both cells except for the copper and TP levels at Cell CP. Although chloride was substantially exported, as discussed above, the non-exceedance probabilities to the target value (250 mg/L) for effluent chloride concentrations at both cells are >95%. Cell SS exhibited better performance in controlling effluent pollutant levels compared to Cell CP, which may be attributed to its clay-rich media and long hydraulic retention time design. The poor performance for copper and TP control in some media is investigated further through media analysis in Chapter 6.

3.3.4. Pollutant mass load and release per unit drainage area

Data of annual pollutant mass load per unit drainage area (L_{in}, in kg/ha-yr) are essential in watershed stormwater management for integrated BMP system design and deployment. L_{in} can be estimated using the *simple method* (Davis and McCuen 2005):

$$L_{in} = \frac{PC_F R_V C}{100} \tag{3-14}$$

where P is the average annual precipitation (1067 mm/yr for the State of Maryland, MDE 2000), C_F is a factor that corrects for events that do not produce runoff, in this study, a typical value = 0.9 for impervious area (Davis and McCuen 2005) was used; R_V is the runoff coefficient for the drainage area (= 0.9 for Cells CP and SS), and C is the input pollutant EMC in mg/L (median values were used in this study).

Data of annual pollutant mass release per unit drainage area after BMP treatment (L_{out}, in kg/ha-yr) are of equal importance for BMPs integration in watershed

stormwater management. L_{out} can be estimated through the pollutant mass input to output ratios (M_{out}/ M_{in}) measured in field BMPs:

$$L_{out} = (L_{in})\left(\frac{M_{out}}{M_{in}}\right) \tag{3-15}$$

Median M_{out}/ M_{in} values were used in this study. Table 3-10 lists the L_{in}, M_{out}/ M_{in}, and L_{out} values for Cells CP and SS, which provide a pollutant mass inventory basis for watershed management or Total Maximum Daily Loads (TMDLs) development for nonpoint source pollution control. However, it should be noted that the annual pollutant mass load and release per unit drainage area are subject to changes in land use and BMP conditions.

Table 3-10. Comparison of effluent water quality with the water quality criteria for the 8 events at both sites.

Cell	Pollutant	Input EMC (mg/L) [a]	Output EMC (mg/L) [a]	M_{out}/ M_{in} (-) [a]	Pollutant mass load L_{in} (kg/ha-yr)	Pollutant mass release L_{out} (kg/ha-yr)
CP	TSS	47	3	0.08	406	32
	Chromium	3 [b]	3 [b]	0.71	0.026	0.018
	Copper	18 [b]	15 [b]	0.66	0.156	0.103
	Lead	3 [b]	<2 [b]	0.16	0.026	0.004
	Zinc	42 [b]	11 [b]	0.28	0.363	0.102
	Chloride	4	28	2.93	35	101
	TN	1.4	1.6	1.18	12	14
	Nitrate	0.33	0.80	1.71	3	5
	Nitrite	0.03	0.03	0.45	<1	<1
	TKN	1.1	0.8	1.06	10	10
	TP	<0.1	0.3	1.36	<1	<1
	TOC	3.3	9.2	1.77	29	50
SS	TSS	16	3	0.12	138	17
	Chromium	<2 [b]	<2 [b]	0.12	<0.017	<0.002
	Copper	12 [b]	11 [b]	0.37	0.104	0.038
	Lead	<2 [b]	<2 [b]	0.19	<0.017	<0.003
	Zinc	15 [b]	5 [b]	0.08	0.130	0.010
	Chloride	3	3	0.37	26	10
	TN	0.9	0.6	0.56	8	4
	Nitrate	0.27	<0.05	0.04	2	<1
	Nitrite	<0.02	<0.02	0.13	<1	<1
	TKN	0.5	0.5	0.67	4	3
	TP	<0.1	<0.1	0.62	<1	<1
	TOC	3.4	7.0	1.04	29	31

[a] Median values, [b] in µg/L.

3.3.5. Dissolved copper and metal toxicity reduction

The dissolved copper data were used to calculate the copper partition coefficient on the solid phase and liquid phase at both the influent and effluent streams according to the method adopted by Sansalone and Buchberger (1997). The partition coefficient between particulate-bound mass and dissolved mass K_d ((L/kg) is defined as:

$$K_d = \frac{C_s}{C} \tag{3-16}$$

where C_s is the particulate-bound metal element mass (mg metal/kg of dry solids TSS) and C is dissolved metal element concentration (mg/L). The following relationship is employed by Sansalone and Buchberger (1997) to obtain K_d values for runoff-carried metal species:

$$f_d = \frac{1}{1 + K_d m} \tag{3-17}$$

where f_d is the ratio of dissolved metal concentration to total metal (dissolved metal + particulate-bound metal) concentration and m is TSS level. Equation (3-17) can be also expressed as:

$$K_d = \left(\frac{1 - f_d}{f_d}\right)\left(\frac{1}{m}\right) \tag{3-18}$$

The f_d and calculated K_d values for copper at both cells are listed at Table 3-11 with a comparison of Sansalone and Buchberger's results for highway runoff particles at Cincinnati, Ohio (1997) and Sauvé et al.'s summary results for soils from 452 studies (2000). In some samples, the TSS levels were lower than the detection limit (1 mg/L), therefore Equation (3-18) is unavailable. Additionally, the copper levels in several samples were too low to determine dissolved or even total copper

concentrations. Further, only the results in which the dissolved copper concentrations of the laboratory blanks were below the detection limit were adopted, as mentioned. As such, only 18 samples (including input and output) were used in K_d calculation at the two cells. It should be noted that the sample holding time can affect the K_d values because partitioning is a dynamic process. As such, this study used a 6-8 hours sample holding time, compared to the holding time "within hours" (not specified) in Sansalone and Buchberger's studies (1997). Samples with a holding time longer than that were not used in dissolved copper analyses.

Table 3-11. The calculated f_d and K_d for cell input/output particles and copper affiliation and literature values comparison.

Event date		f_d			K_d (L/kg)×10^4			
		Input	Output	Literature value for highway runoff [1]	Input	Output	Literature value for highway runoff particle [1]	Literature value for soil [2]
Cell CP	04/03/06	0.26	0.38	0.31-0.71	2.3	82.2	0.1-1.8	0.007-82.9 (average = 4.8)
	04/21/06	0.32	0.17		7.2	504		
	06/24/06	-	0.60		-	8.5		
	07/04/06	0.27	0.34		16.4	19.3		
	02/25/07	0.40	0.16		0.8	262		
	Average	0.31	0.33		6.7	175		
Cell SS	04/03/06	0.23	0.26		6.8	-		
	04/21/06	0.69	0.21		0.3	12.3		
	06/24/06	0.17	0.33		15.2	51.9		
	07/04/06	-	0.40		-	10.6		
	09/14/06	0.53	0.53		10.9	43.5		
	Average	0.41	0.35		8.3	29.6		

[1] Sansalone and Buchberger (1997), [2] Sauvé et al. 2000.

It should be also noted that the filter pore size in dissolved copper determination can affect the analysis results. The 0.2 μm filter used in this study enabled the K_d estimate for smaller particles, compared to the 0.45 μm filter used by Sansalone and

Buchberger (1997). It is assumed that small particles can adsorb more metals because of their large specific surface area, compared to large particles of the same composition. As such, the calculated K_d values from a 0.2 μm filtration process should be higher than those from a 0.45 μm filtration process.

Results from Table 3-11 indicate that the input and output runoff had similar f_d values at both cells (0.31-0.41), which are also close to the literature f_d values for highway runoff (0.31-0.71, Sansalone and Buchberger 1997). Input runoff particles had higher, but the same order of magnitude of K_d values (average 6.7×10^4 L/kg at Cell CP and 8.3×10^4 L/kg at Cell SS), compared with the literature values of 0.1×10^4 to 1.8×10^4 L/kg for highway runoff particles (Sansalone and Buchberger 1997). The difference may originate from the variety of runoff particle characteristics in different locations, as well as the filter pore size used in the analysis process.

However, the effluent particles had much higher K_d values (average 175×10^4 L/kg at Cell CP and 30×10^4 L/kg at Cell SS) than influent particles, approximately 1 or 2 orders of magnitude greater. The fact that cell input and output runoffs had similar f_d and output runoff particles had much higher K_d have two important implications:

First, dissolved metals are often considered to have higher toxicity or bioavailability (Turer et al. 2001) compared to particulate bound metals, although soil metal bioavailability is far from an accurate science (Sauvé 2002*)*, and is sensitive to biotic activity (Wen et al. 2004*)*. Since bioretention facilities are capable of reducing total metal amount (the pollutant mass removal for copper in this study is 34% at Cell CP and 63% at Cell SS), a relatively constant f_d value implies the decrease of metal toxicity for downstream and receiving water. From Equation (3-17), since f_d remains

relatively constant, and K_d significantly increases after treatment, the metal toxicity reduction is mainly accomplished through particulate (TSS) removal.

Second, it is believed that the increase of K_d values of runoff particles after runoff treatment via bioretention media is because of two factors. One is the change of chemical speciation of runoff water after treatment. As mentioned, TOC concentrations increased after the treatment, which is attributed to the organic matter dissolution from the media. Literature indicates that soil organic matter has strong affiliation with dissolved metals and can increase metal mobility (Sauvé et al. 2000), which is adverse to metal toxicity reduction. The other factor that accounts for K_d increase is that effluent particles were not entirely from input runoff particles, but partly from the erosion of the media. Literature indicates that soil particles generally have higher metal adsorption capability, compared to runoff particles in terms of higher K_d values (Table 3-11, Sansalone and Buchberger 1997, Sauvé et al. 2000). As such, media particle loss can increase average values of the metal adsorption capability and K_d for discharge particles. Figure 3-24 shows the appearance of the input and output water samples for both cells at the event on 4/3/2006. The colors of input (dark) and output (light) water samples are easily distinguished and colors of output samples are close to those of the soil media.

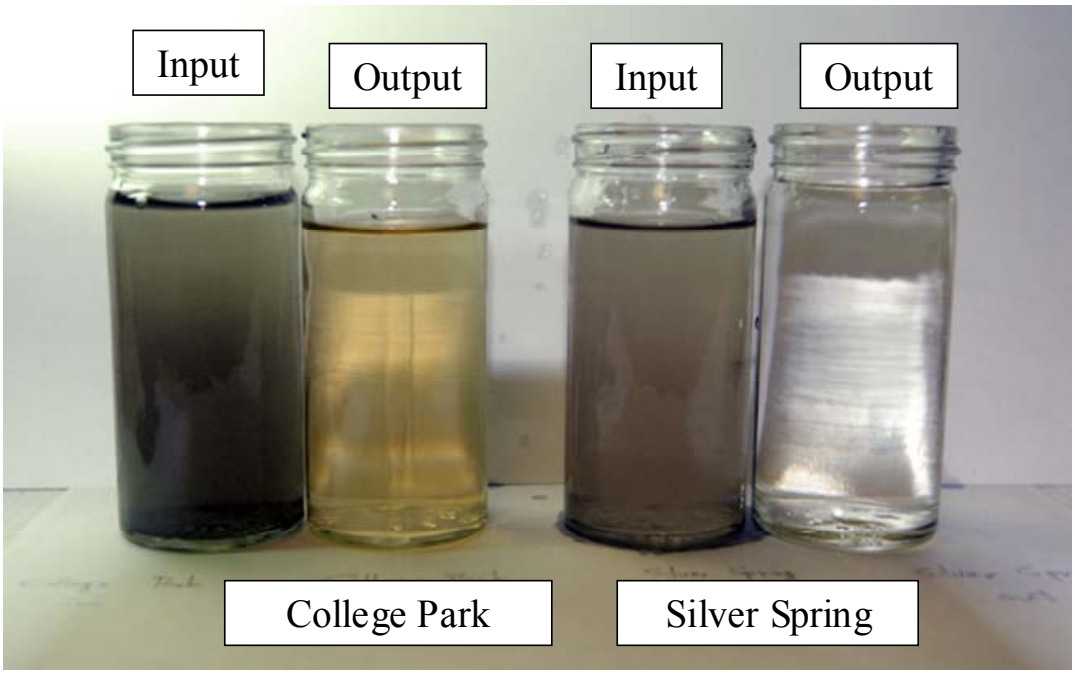

Figure 3-24. Input and output water samples for Cells CP and SS at the events of 4/3/2006.

3.4 Summary

From the field study of the two bioretention cells, it is concluded that bioretention is capable of improving post-development hydrology by delaying and reducing runoff peak flows and promoting infiltration. As such, it also helps in flood control and channel erosion protection from urbanization. The companion infiltration promotion also helps groundwater recharge. The hydrological performance is particularly good for small rain events and is reduced under extreme precipitation. A larger cell surface area: drainage area ratio and media volume can increase the performance.

From the water quality perspective, bioretention can effectively remove TSS and heavy metals from runoff. However, slight organic matter and nutrients leak-out also occur from the bioretention media to the effluent at low concentrations. Chloride is significantly exported from the monitored bioretention cells. The pathogen indicator

removal capability of bioretention is inconclusive and needs further studies. The runoff volume reduction through infiltration significantly increases the pollutant mass removal for nearly all pollutants; as such, the hydrological performance and water quality benefit of bioretention facilities are strongly correlated. Overall, the effluent water quality is fair to good for nearly all monitored pollutants except copper and TP at Cell CP.

The dissolved copper analysis indicates that the bioretention cells reduced the metal toxicity for downstream water through particulate capture and flow attenuation. The increase of K_d for output runoff particles may be attributed to the dissolution of media organic matter and media particle loss. Since the particulate removal is of critical importance, and the source of the output particles is still unclear. (Do the output particles originate from the input runoff particles or from the media loss?) The following two chapters are dedicated to examining particulate capture and movement through the bioretention media.

Chapter 4: Bioretention Filtration - Laboratory and Field Studies

4.1 Introduction

Suspended aquatic particles are usually measured as total suspended solids (TSS), which can negatively impact aquatic ecosystems and natural water quality through a variety of mechanisms (Davis and McCuen 2005). A number of toxic and otherwise important pollutants may be affiliated with stormwater solids. TSS is commonly selected as a target pollutant for stormwater BMPs, and many BMPs are designed primarily for urban particle control. Among many BMPs, bioretention has demonstrated good-to-excellent removal for TSS and heavy metals (Davis et al. 2003, Hsieh and Davis 2005, Davis 2007b).

A bioretention facility removes pollutants during ponding storage and infiltration of incoming runoff through the planting soil media. The resulting vertical profile of captured particulate pollutants in the treatment media is of great concern in bioretention design, operation, and maintenance. For example, a design media depth shallower than the pollutant penetration depth can compromise the effluent quality (pollutant breakthrough). An over-designed media depth, on the contrary, will drastically increase construction costs and increase flow resistance. An understanding of the spatial pollutant profile also assists in the selection of facility maintenance measures, such as partial or full media replacements. Of critical importance, excess deposition of urban particles may clog the media and therefore render the BMP inoperative. As a result, an understanding of filtration mechanisms

correlated with the captured-particles profile and the hydraulic conductivity in bioretention is very important.

Previous studies of filtration theory for rapid and slow sand filters have provided fundamental foundations for understanding of bioretention filtration. However, significant differences between sand filters and bioretention facilities limit the direct use of sand filter knowledge. First, sand filters usually have relatively steady inflow rates and ponding heads, while the variability of incoming runoff renders bioretention behavior much more dynamic and unsaturated media will occur during dry weather periods. Second, bioretention facilities use significantly different media than sand filters. Recent bioretention designs typically have used engineered mixtures of construction sand (50% by volume), topsoil (20-30%), and mulch (20-30%) (Davis and McCuen 2005). As such, the bioretention media are smaller than typical sand filter media (gravel/sand/anthracite) and more heterogeneous, which may limit particulate penetration and increase the possibility of clogging. As such, stratification at the bioretention media surface is more likely to occur than in sand filter media; correspondingly the suspended solids removal mechanisms (depth filtration and cake filtration) may also differ between the two. Third, sand filter media are rigid and relatively inert, while bioretention media are plastic and chemically and biologically active.

The primary factors that limit sand filter run-time are effluent quality impairment (TSS breakthrough) and headloss development (clogging) (Tchobanoglous et al. 2003). To study these limiting factors for bioretention, field and laboratory column

experiments with solids-deposit profile and headloss observations are needed. As such, the objectives of this chapter are:

1. To determine whether bioretention media are limited by clogging or TSS breakthrough.
2. To evaluate particulate depth penetration.
3. To clarify TSS removal mechanisms (depth filtration vis-à-vis cake filtration) in bioretention media.
4. To assess surface media replacement as an effective bioretention maintenance procedure.

These objectives will be addressed under both continuous and intermittent flow conditions, and for different bioretention media/TSS composition combinations (particle sizes and mineralogical composition).

4.2 Methodology

4.2.1. Soil media preparation and analysis

Two bioretention soil media samples (Soil I and Soil II) were used for column tests. Soil I was obtained through the Prince George's County (MD) Department of Public Work and Transportation. Soil II was collected during a bioretention cell maintenance procedure at the University of Maryland, College Park, MD. The collected soil was air dried and 2-mm sieved. Afterward, the soil particle size distributions (PSD) were determined using the dry sieve technique (Das 1992). Both mixes are classified as USDA sandy soils. The specific gravity of each soil media was determined using volumetric flasks as pycnometers (Das 1992). A thin layer (0.5 cm) of media sand was washed using the silica sand washing procedures (Kunze and

Dixon 1989) and packed as support of the media columns. Mechanical analysis of the sand was performed by the Soil Testing Laboratory, Department of Agronomy, University of Maryland, College Park, MD. The PSD and specific gravity data of Soil I, Soil II, and the bottom sand are shown in Table 4-1.

Table 4-1. Mechanical analysis results of the bioretention soil media used in this study.

Characteristics	Soil I	Soil II	Bottom Sand
Sand (%)	>96	>98	95
Silt (%)	<4	<2	3
Clay (%)	<4	<2	2
Soil texture	Sand	Sand	Sand
d_{10} (μm)	130	210	170
d_{50} (μm)	340	570	-
d_{60} (μm)	390	690	300
Uniformity coefficient (d_{60}/ d_{10})	2.9	3.2	1.8
Specific gravity	2.3	2.6	-

4.2.2. Suspension preparation and analysis

Soil textures and soil groups in upland watersheds are often considered for TSS trap efficiency estimates in stormwater BMP design (e.g., vegetated buffer strips, Davis and McCuen 2005) as representatives for urban particles. As such, four types of solids across the AASHTO soil classification (AASHTO 1993), sand (coarse and fine sands, 75-2000 μm, Wards Natural Science), silt (2-75 μm, 75 μm dry sieved, Wards Natural Science), and clay (<2 μm, including Kaolin (1:1 clay, EM chemicals) and Montmorillonite (2:1 clay, Ward's Natural Science)) were used in the column tests to simulate runoff suspended solids. The specific gravity of these solids was determined as described above. The PSDs for kaolin, montmorillonite, and silt were measured with an ASTM 152-H type hydrometer (Das 1992). The lower limit of the

particle size that discernable by this procedure is about 1 μm. The sands were dry sieved and only the particle fraction between 75 and 425 μm was used. The PSD and specific gravity data of these solids are listed in Table 4-2. The solids were mixed in 10^{-3} M $CaCl_2$ (Fisher Scientific) solution at different concentrations to simulate runoff in column tests.

Table 4-2. Particle size information and specific gravity of simulated runoff suspended solids used in this study.

	Kaolin	Montmorillonite	Silt	Sand
Soil texture	clay	clay	Silt	sand
diameter (μm)	<1	<1	1-75	75-425
Specific gravity	1.8	2.3	2.4	2.4

4.2.3. Column tests

A 5.08-cm-diameter Plexiglas column reactor was used as shown in Figure 4-1. At the bottom, a 0.5-cm layer of media sand was packed over a stainless steel screen. Above the bottom sand layer was a 5- or 10-cm layer of Soil I. The inflow for the column experiment was prepared in a drum with an agitator and a magnetic stirrer. Kaolin was added at about 35 or 130 mg/L in 10^{-3} M $CaCl_2$ solution. The simulated runoff suspension was fed into the soil column at flow rates at of 5, 10, and 20 cm/hr, which represent 0.3, 0.6, and 1.1 cm/hr rainfall intensity precipitation (bioretention cell area: drainage area assumed = 5% with a runoff coefficient= 0.9). Seven continuous column tests were completed under constant flow rates (Trials 1-7, Table 4-3). The clean bed hydraulic conductivity was obtained via Darcy's law by observing the water head, packing height and effluent flow rate for 20-30 minutes twice (using a constant flow rate, measuring after the water head became steady). An

average value was used for each column; to be consistent, a 10^{-3} M $CaCl_2$ solution was used as the influent in the clean bed hydraulic conductivity tests.

Before the suspension was applied, 10^{-3} M $CaCl_2$ solution was fed for at least 20 bed volumes (BV = 24 and 87 cm^3 for 5.5 and 10.5 cm packing, respectively) until the effluent filtrate TSS was less than 5 mg/L to ensure that residual small particles present in the media packing were completely flushed out. After the suspension was applied, the input and output TSS and effluent filtrate volume were measured as a function of time. Water head and surface filter cake thickness were recorded as well. The filter bed hydraulic conductivity was obtained via Darcy's law under constant flow rate conditions for continuous column tests. The kaolin used in the experiment had discernable color (white) compared with Soil I and Soil II (dark), allowing cake thickness measurement from the top of the packed media to the cake surface, reporting this value when it was larger than 1 mm (the minimum length for measurement). TSS was analyzed following Section 2540D of Standard Methods (APHA et al. 1995) using standard glass-fiber filters with a nominal pore size of 1 μm (Pall Corporation). Runs were terminated when the ponding levels were higher than the column height (25.4 cm) and overflow occurred as a result of media clogging.

The four solids plus a mixture (80% Silt+ 5% Montmorillonite+ 5% Kaolin+ 10% Sand, by mass) were used as simulated runoff suspensions in different intermittent loading column test runs with 10^{-3} M $CaCl_2$ at various TSS concentrations (Trials 8-19). The composition of the mixture attempted to simulate a representative runoff suspended particle size distribution with silt as the majority (Sansalone et al. 1998, Furumai et al. 2002). The input runoff rates were cycles of 10 or 20 cm/hr for one

day, and then stopped for one day to simulate a wet-dry weather pattern with pulse-type runoff inputs. Although the input flow was intermittent, it varied according to a piece-wise continuous pattern (pulse-type) of 0, 10, or 20 cm/hr; the hydraulic conductivity was also measured under constant flow rate conditions (10 or 20 cm/hr).

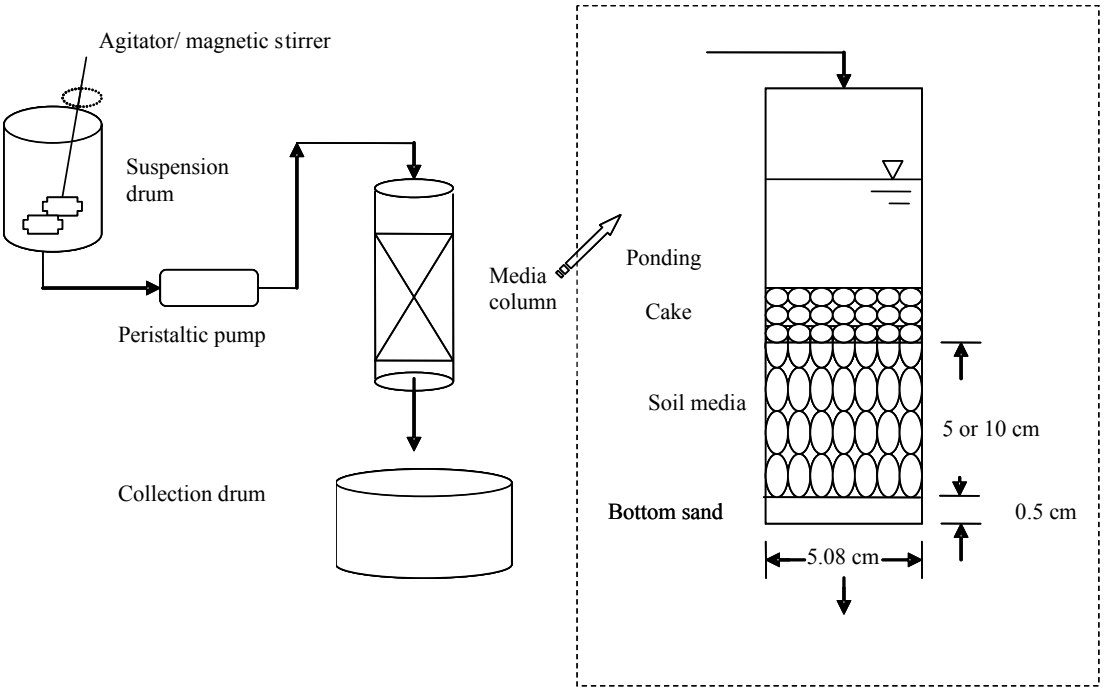

Figure 4-1. Column experiment for particle capture in soil media and stratification of the packing column reactor.

Table 4-3. Conditions for the bioretention column tests

Trial	Media	Suspended solids	Flow rate (cm/ hr)	Media depth (cm)	Input TSS (mg/L)	Media size [1] d_m (μm)	TSS size [1] d_p (μm)	d_m/d_p	Hydraulic conductivity (cm/hr)		Total solids loading (kg/m^2)
									Clean bed	At run end	
Continuous column tests											
1	Soil I	Kaolin	4.8	5.5	134±9	340	<1	>340	45	3	2.4
2			4.9	10.5	130±8	340			44	3	1.5
3			9.5	5.5	132±29	340			44	4	3.3
4			9.5	10.5	132±29	340			44	3	3.3
5			19.8	5.5	126±7	340			46	5	2.3
6			19.7	10.5	121±5	340			48	6	2.6
7			20.1	5.5	36±7	340			44	7	1.2
Intermittent column tests											
8	Soil I	Kaolin	20.8→9.0	10.5	49-1062	340	<1	>340	44	5	5.5
9			9.1→18.9	10.5	15-261				131	11	3.7
10	Soil I	Mont [1]	19.0	10.5	114-161	340	<1	>340	43	7	0.9
11			9.3	10.5	94-202				60	6	0.9
12	Soil II	Kaolin	19.6	10.5	31-195	570	<1	>570	45	8	1.0
13			10.3→19.7	10.5	48-133				52	8	1.0
14	Soil II	Mont [2]	19.6	10.5	118-166	570	<1	>570	164	7	0.9
15			9.1	10.5	110-134	570	<1	>570	48	3	0.4
16	Soil I	Silt	19.9→9.8→20.4	10.5	21-6030	340	3	113	51	9	14.5
17	Soil II	Silt	18.5	10.5	140-1774	570	3	190	49	7	6.3
18	Soil I	Sand	19.0	10.5	35-1729	340	75-425	1-5	55	7	6.4
19	Soil I	Mixture [3]	18.5→9.8	10.5	28-1535	340	<1-425	1->340	59	6	7.5
Hydraulic conductivity restoration tests											
20	Soil II	Mont [1]	-	10.5	39-588	570	<1	>570	72	1	1.8
20-1	Original media		19.9						72		
20-2	Replace top 3 cm		8.3						36		
20-3	Replace top 5 cm		9.6						39		
20-4	Replace top 7 cm		8.1						43		

[1] d_{50} or interval, [2] Montmorillonite. [3]80% silt+ 5% montmorillonite+ 5% kaolin+ 10% sand

4.2.4. Media analyses for particulate penetration depth

At the end of 8 of the intermittent loading column test runs (Trials 9-12 and 14-17), the packed column was air dried for one day. The top 5 cm and 5-10 cm layers were carefully removed and heated at 103-105 °C for three days, and then were placed in a desiccator to cool. Afterwards, the soil sample was broken up into individual particles using a mortar and a rubber tipped pestle (breaking up the soil into individual particles, but not breaking the particles themselves, Das 1992). About 40-50 g of the sample for each layer was weighed at a precision of ± 0.1 mg, then sieved with a No. 200 sieve (75 μm). The media passing through the sieve were weighed to calculate the mass percentage of media that was smaller than 75 μm after the column tests. In each penetration depth test, the media sample mass retained on a 75 μm sieve was also weighed to calculated the mass loss during the sieving process; only data with mass loss < 1% were used.

In the final column test, Soil II (as media) and montmorillonite (as simulated runoff suspended solids) were used in a hydraulic conductivity restoration test. The trial proceeded as an intermittent loading column test. After the soil column clogged (Trial 20-1), the top 3 cm Soil II layer was carefully removed with a spoon and replaced with a new 3-cm layer of Soil II. The column was than loaded as before (Trial 20-2). After 20-2, the top 5 cm soil media were replaced, followed by 20-3. Afterwards, the top 7 cm media were replaced; finally, 20-4 proceeded (Table 4-3).

4.2.5. Field bioretention observation

One bioretention facility was also chosen for field bioretention filtration observation, which located along the Anacostia River in the southeast quadrant of the District of Columbia, USA. The bioretention cell (design drainage area = 0.077 ha) is located in an active parking lot. The cell is trapezoid-shaped (sides = 2.9, 5.4, and 6.3 m, surface area = 17 m^2), with a media depth of about 1.1 m. The original media consisted of 50% (by volume) sand, 30% top soil, and 20% mulch. Seven storm events were monitored using grab samples for both cell input and output runoff from January 2005 to May 2006. TSS analyses of input and output samples were carried out using Standard Method 2540D (APHA et al. 1995) by a laboratory subcontractor. Samples were collected manually using nitrile gloves and pre-cleaned containers. This cell was also used for BMP filter media analyses, which is described at Chapter 6.

4.3 Results and Discussion

4.3.1. Bioretention filtration phenomena in the laboratory column tests

Figure 4-2 illustrates the test results of Trials 1, 5, and 7 (Soil I/Kaolin) with a media depth of 5.5 cm. Initially, flow occurred through the media without ponding. As captured particles deposited in the media, the media hydraulic conductivity and flow rate decreased and generated ponding at BV = 220 (Trial 1), then a cake layer formed at BV = 288. Hydraulic conductivity could only be measured after saturation and ponding occurred. The equivalent hydraulic conductivity of the media column, K_e reduced from a clean bed value of K_0 = 45 cm/hr to K_e = 3 cm/hr at the end of

Trial 1 (Table 4-3). Throughout the trial, the effluent TSS levels (C) remained < 7 mg/L with the influent TSS (C_0) = 134±8 mg/L ($C/C_0 < 0.06$). In all 20 column tests, C was ≤ 30 mg/L (C_0 ranged from 15 to 6030 mg/L), with a C/C_0 <0.01 to 0.26, demonstrating excellent TSS removal and effluent water quality. The hydraulic conductivity (Soil I: K_0 = 54±23 cm/hr, Soil II: K_0 = 72±46 cm/hr) reduced to 3-11 cm/hr at the end of the tests due to clogging, with K_e/K_0 ranging from 0.04-0.18. In no case was a TSS breakthrough noted. Good reproducibility was noted among the column tests comparing trials that were identical except for the media packing length. The measured clean bed hydraulic conductivity of Soil I and Soil II also showed good agreement except for Trials 9 and 14 (Table 4-3).

These results suggest that bioretention performance is limited by clogging rather than by breakthrough in regard to TSS capture. Obvious cake layer formation occurred in most experiments (15 out of 20 trials, exceptions for Trials 10-12, 14, 15), which suggests that both depth filtration and cake filtration contribute to TSS removal. Surface ponding always preceded cake formation, implying that sedimentation played an important role in initiating cake formation.

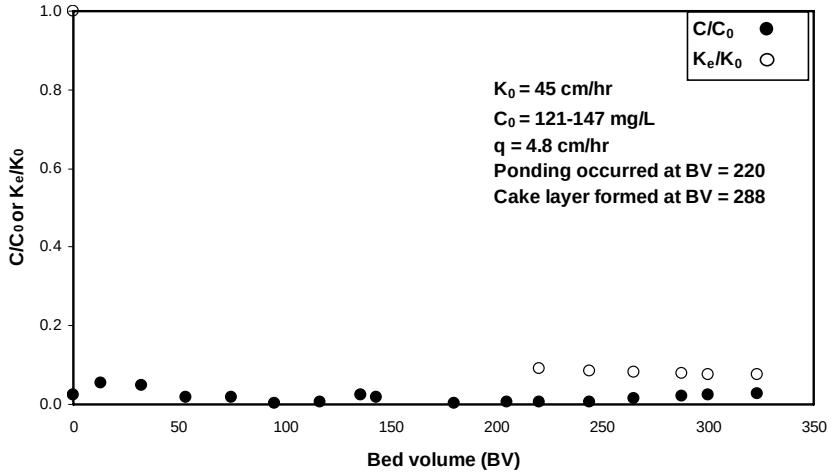

(a)

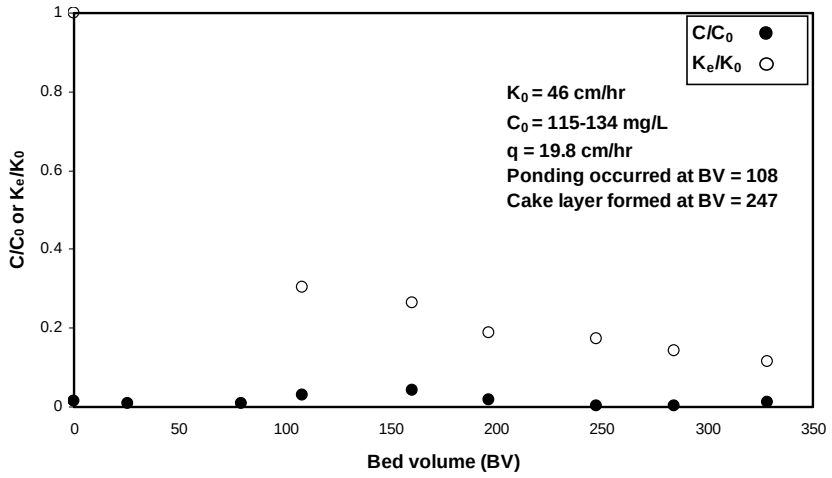

(b)

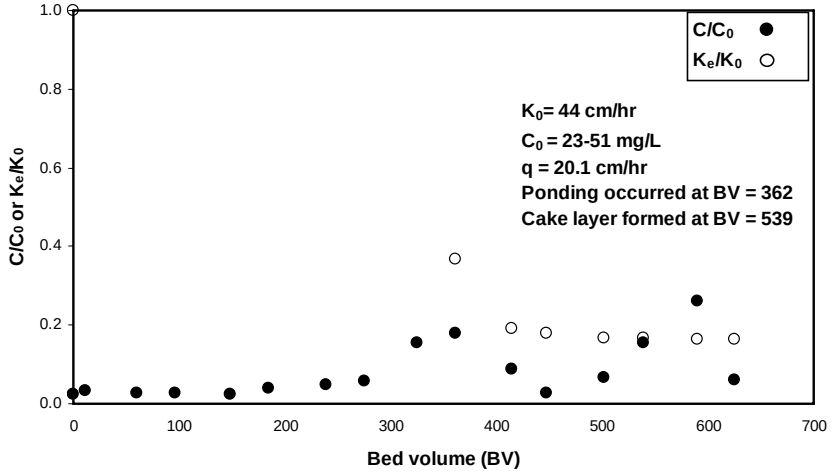

(c)

Figure 4-2. Illustrations of Trials #1 (a), 5 (b), and 7 (c) for Soil I/Kaolin, media depth = 5.5 cm.

4.3.2. Effects of media depth

From Trials 1-9 (Soil I/Kaolin), the C/C_0 values remained <0.02 when the media depth varied from 10.5 cm to 5.5 cm at different flow rates (5, 10, and 20 cm/hr). In other media/TSS combinations, a 10.5 cm media layer also successfully reduced TSS to C/C_0 below 0.02. This implies that a shallow bioretention design is feasible for particle capture. As previously mentioned, classical filtration theory (also known as the macroscopic model) describes particle removal along the media depth Z (e.g., Iwasaki 1937):

$$\frac{\partial C}{\partial Z} = -\lambda C \tag{4-1}$$

where λ is the filter coefficient with the dimension of reciprocal length and is often used in expressing filter performance. Integrating this equation with appropriate assumptions leads to classic steady state filtration theory, which includes the media depth, L (e.g., Cushing and Lawler 1998):

$$\frac{C}{C_0} = \exp\left[-\frac{3}{2}\frac{(1-\theta)}{d_c}\alpha\eta L\right] \tag{4-2}$$

where θ is the filter bed porosity, d_c is the diameter of the spherical collector (media particle), α is the sticking coefficient, and η is the single collector collision efficiency. This equation indicates a sharp exponential decrease of particle concentration throughout the media depth, and smaller media-grain sizes will result in better TSS removal and shorter media depth requirement. However, the sticking coefficient α must be determined through column experiments (e.g., Tufenkji and Elimelech 2004), and Equation (4-2) does not account for the accumulation of solids deposited in the

filter and is used for clean beds. In addition, calculation of the collector efficiency η requires a mono-disperse influent and media; the overall η for a poly-disperse system is the sum (weighted according to the particle numbers) of each pair of media grain size and suspended particle size, although a single d_{10} can provide satisfactory estimate in some studies (e.g., Martin et al. 1996). These factors limit the prediction capability of Equation (4-2) for field application. At the initial stage of filtration, studies have indicated that the clean bed filter coefficient varied as approximately the inverse 2.0 power of the filter-grain diameters (Tien 1989). As a result, for stormwater filtration facilities such as bioretention, Equations (4-1) and (4-2) predict that the fine-sized media render the filters with excellent TSS removal capability and a shallow media depth requirement; consequently no TSS breakthrough should be expected, as the experimental data had indicated.

4.3.3. Continuous vis-a-vis intermittent flow conditions

Bioretention filtration behavior under intermittent flow conditions is similar to that under continuous flow conditions, as illustrated with Trial 8 (Soil I/Kaolin, Figure 4-3). However, for the same media/TSS combination, the media columns under intermittent flow demonstrate a higher solids loading capacity (3.7-5.5 kg/m^2, Trials 8 and 9,) than under continuous flow conditions (1.2-3.3 kg/m^2, Trials 1-7) before the media columns became clogged (intermittent: K_0 = 44-131 reducing to K_e = 5-11 cm/hr; continuous: K_0 = 44-48 reducing to K_e = 3-7 cm/hr), as shown in Table 4-3. The dormant periods seemed to allow the media to "adjust" for a less-resistant flow path. Compared to chemically inert and rigid-shaped sand filter media, the plastic and chemically active bioretention media exhibited more potential to integrate

with the captured particles in shape. The media adjustment during the dry periods can smooth the flow path for the next flow loading. This may have helped the media columns to partially regain their permeability between runoff loadings. Furthermore, the difference in solids loading capacity between the two intermittent trials (8: 5.5 kg/m^2 and 9: 3.7 kg/m^2) was small despite their vast difference in TSS loading patterns (8: input flow rate q = 21→9 cm/hr, C_0 = 49-1062 mg/L; 9: q = 9→19 cm/hr, C_0 = 15-261 mg/L), which implies less significance of input flow rates and TSS variations on the media clogging as compared to the presence of dry periods.

4.3.4. Different media/TSS combinations

Figure 4-4 shows the results of Trial 10 (Soil I/Montmorillonite); the effluent TSS levels were controlled well in this trial without obvious cake formation. However, the media clogged at BV < 70, compared to BV = 195-267 for similar TSS loading pattern trials for Soil I/Kaolin (Trials 8 and 9). Thus, the same media exhibited a shorter life expectancy with Montmorillonite input than with Kaolin input. As shown in Table 4-3, the TSS inputs needed to clog the media were Montmorillonite (0.9 kg/m^2) < Kaolin (1.2-5.5 kg/m^2) < Sand (6.4 kg/m^2) < Silt (14.5 kg/m^2) for Soil I. The order for Soil II is the same (no sand trial was performed): Montmorillonite (0.4-0.9 kg/m^2) < Kaolin (1.0 kg/m^2) < Silt (6.3 kg/m^2). Generally, except for the order of sand and silt, the application of finer TSS particles to the media generated a stronger tendency to clog the media, which agrees with a previous study regarding media hydraulic conductivity and soil particle size (Boadu 2000). As for the high impact from the sand, coarse TSS particles are likely to be strained and/or settled out and remain on the surface of the bioretention media to form a cake layer. Previous studies

(McDowell-Boyer et al. 1986, Teng and Sansalone 2004) also indicate that the relative size ratio of the media diameter to infiltrating particle diameter d_m/d_p mainly determines the filtration mechanisms. However, coarse TSS particles have little impact on the effluent quality (unable to penetrate the media) and permeability reduction (due to the larger sizes) after integrating with the media. Additionally, coarse TSS particles have less pollutant adsorption capacity due to their lower surface area / volume ratios and are likely to settle along the runoff flow path before entering stormwater BMPs (except during extreme storm events).

Montmorillonite showed a higher potential to clog the media than Kaolin, which agrees with its more pronounced swelling behavior than Kaolin when wetted (Hillel 1998), which can lead to filling of greater media pore volume and will more drastically reduce the permeability. For the poly-dispersed TSS (Trial 19), the TSS input needed to clog the media was 7.5 kg/m^2, which is between those of the individual TSS types, but more near the clays. This implies that the clay components in incoming TSS assume critical responsibility for bioretention media clogging.

For the same TSS type, the differences between Soil I and Soil II were mostly indistinguishable for media clogging. The TSS inputs needed to clog the media were 1.2-5.5 kg/m^2 (Soil I) and 1.0 kg/m^2 (Soil II) for Kaolin, 0.9 kg/m^2 (Soil I) and 0.4-1.8 kg/m^2 (Soil II) for Montmorillonite, and 14.5 kg/m^2 (Soil I) and 6.3 kg/m^2 (Soil II) for Silt. This similarity is believed due to the similar clean bed conductivities of Soil I (54±23 cm/hr) and Soil II (72±46 cm/hr), even though Soil II was a coarser media.

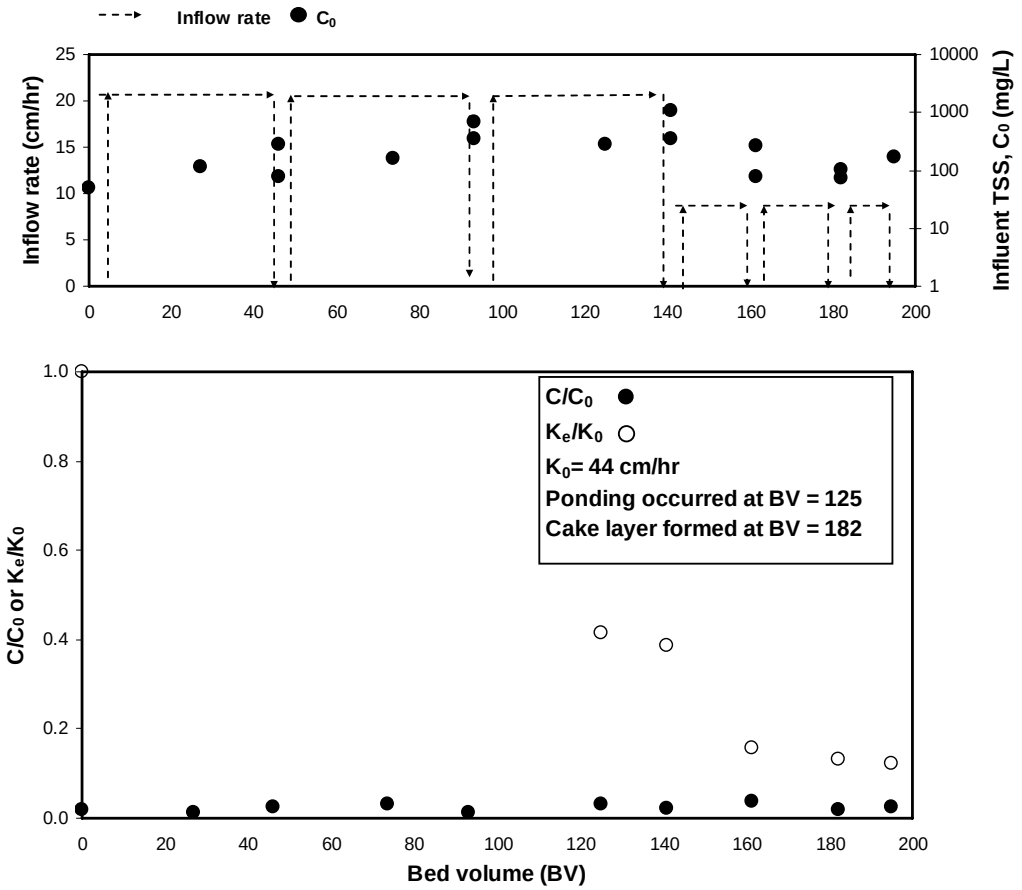

Figure 4-3. Trial 8 (Soil I/Kaolin), intermittent flow, input TSS = 49-1062 mg/L, media depth = 10.5 cm.

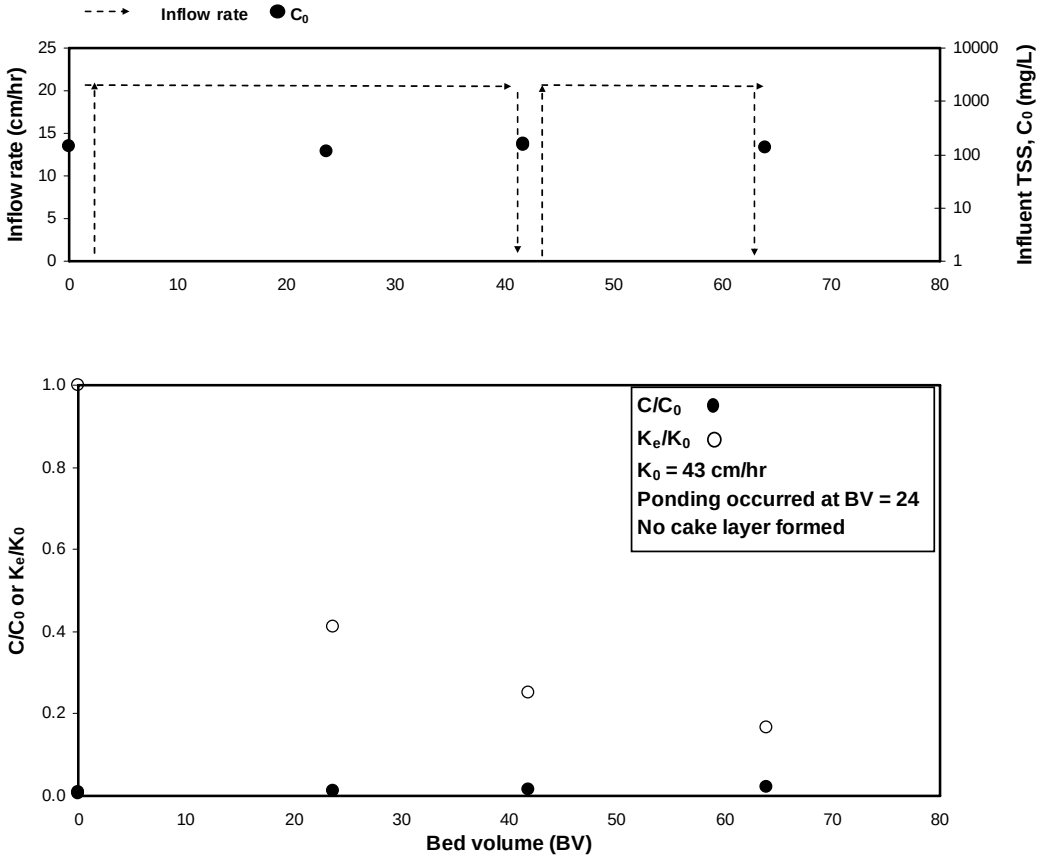

Figure 4-4. Trial 10 (Soil I/Montmorillonite), intermittent flow, input TSS=114-161 mg/L, media depth = 10.5 cm.

Suspended solids / media type also influenced the cake formation, which is indicated by the hydraulic conductivity reduction (in terms of K_e/K_0) when the cake first built up. The order for different TSS is Montmorillonite (no cake formation) < Kaolin (8-19 %) ≈ Sand (13 %) < Silt (23%) in Soil I. In Soil II, clay cake layer formation only occurred in 2 trials out of 6 for Montmorillonite (4-6%, Trial 20 counted as 4 sub-tests) and 1 out of 2 trials for Kaolin (16%). The conductivity reduction for Soil II/Silt was 26%; no test for Soil II/Sand was performed. These results suggest that the relatively larger media size for Soil II (d_{50} = 570 μm, Table 4-1) compared to Soil I (d_{50} = 340 μm) reduced the likelihood of the cake filtration. As

previously mentioned, d_m/d_p primarily determines the dominant filtration mechanism. These data indicate that coarser TSS particles had a stronger tendency to build up a cake layer in both Soil I and Soil II (although silt cake occurred before sand in terms of K_e/K_0, as discussed above).

4.3.5. TSS penetration depth and media stratification

The results of the penetration depth tests indicate that most runoff suspended solids were deposited in the top 5 cm of the media layer and the cake layer (Table 4-4), which is physical evidence that suggests a short penetration depth for incoming particles in the bioretention media. The results also agree with a previous study for long term (10-21 yr) evolution of clogging and soil pollution of stormwater infiltration basins showing that the composite media grain sizes decrease as the media depth decreases (Dechesne et al. 2005). Since the penetration distance is short, the captured TSS will deposit within a shallow depth near the surface and alter the media characteristics, including the permeability of this media "working zone", compared to the underlying relatively "pristine" section of the media. As a result, bioretention media stratification and permeability reduction occur due to solids deposition.

4.3.6. Hydraulic conductivity restoration test

Table 4-3 also shows experimental data for the hydraulic conductivity restoration test (Trial 20, Soil II/Montmorillonite). The clean bed hydraulic conductivity, K_0 = 72 cm/hr fell to 6.8 cm/hr during sub-Trial 20-1 after treating 0.5 kg/m^2 of solids. After renewing the top 3 cm layer of the 10 cm media packing, the hydraulic conductivity was restored to 36 cm/hr and then fell to 3.1 cm/hr during sub-Trial 20-

2, treating 0.6 kg/m^2. Subsequently, the 5-cm layer of top media was replaced to produce K_e = 39 cm/hr, treating 0.2 kg/m^2 and then falling to 4.2 cm/hr through sub-Trial 20-3. Finally, the 7-cm top media layer was replaced, increasing the conductivity again, this time to 43 cm/hr, which then fell to 3.5 cm/hr (sub-Trial 20-4) after collecting 0.5 kg/m^2. The hydraulic conductivity restorations to 36, 39, and 43 cm/hr resulting from removing the top 3, 5, and 7 cm top media layers without full recovery to 72 cm/hr indicates that a fraction of TSS had penetrated to the lower layers of the media and therefore reduced the media permeability. It also demonstrates the marginal effects for hydraulic conductivity restoration as the replacement depth increased. The total solids capture for each sub-trial (0.2-0.6 kg/m^2) were similar to those of Trials 14 and 15 (0.4-0.9 kg/m^2) with the same (fresh) media/TSS combination. The media replacement successfully extended the life expectancy of the media column to hold a total solids loading of 1.8 kg/m^2.

Table 4-4. Results of particulate penetration depth tests.

Trial #	Media	TSS	TSS size (d_{50}, μm)	Percentage of the media which passed 75 μm sieve (%)	
				Upper 5 cm media	5-10 cm media
9	Soil I	Kaolin	<1	3.1	2.6
10		Mont	<1	6.2	4.8
11		Mont	<1	5.2	4.6
16		Silt	3	8.8	5.1
12	Soil II	Kaolin	<1	11.5	4.6
14		Mont	<1	3.6	1.9
15		Mont	<1	4.9	3.4
17		Silt		5.4	3.7

4.3.7. TSS capture and penetration in field bioretention media

The results of input and output grab TSS concentrations from the Washington DC bioretention facility are shown in Figure 4-5. The TSS removal efficiency was good (55% to >99%), which agrees with related studies (e.g., Hsieh and Davis 2005, UNHSC 2006). Input TSS ranged from 22 to 9025 mg/L, while output TSS levels were controlled to between 10 to 225 mg/L. A surface layer at the entrance gravel zone of the facility was observed, which was an obvious collection of street particles and appeared similar to the cake layer observed in the laboratory column tests. This implies that cake filtration also occurred in the monitored bioretention facility.

To investigate further the spatial profile for captured TSS, the macroscopic depth filtration model was used (Ives 1963, Mays and Hunt 2005):

$$\frac{C}{C_0} = \frac{\sigma_v}{\sigma_{v0}} \tag{4-3}$$

where σ_v is the volumetric specific deposit (the volume of deposited particles per unit filter volume), and σ_{v0} is the volumetric specific deposit at depth = 0, respectively. Using the collected TSS concentration data, the captured particles profile in the bioretention cell media can be estimated using Equations (4-2) and (4-3), as shown by the curves in Figure 4-6. The filter coefficients λ were obtained from the field input/output TSS data and ranged from 0.007 to 0.061 cm^{-1}:

$$\lambda = -\frac{\ln \frac{C}{C_0}}{Z} \tag{4-4}$$

where the filter depth Z = 110 cm.

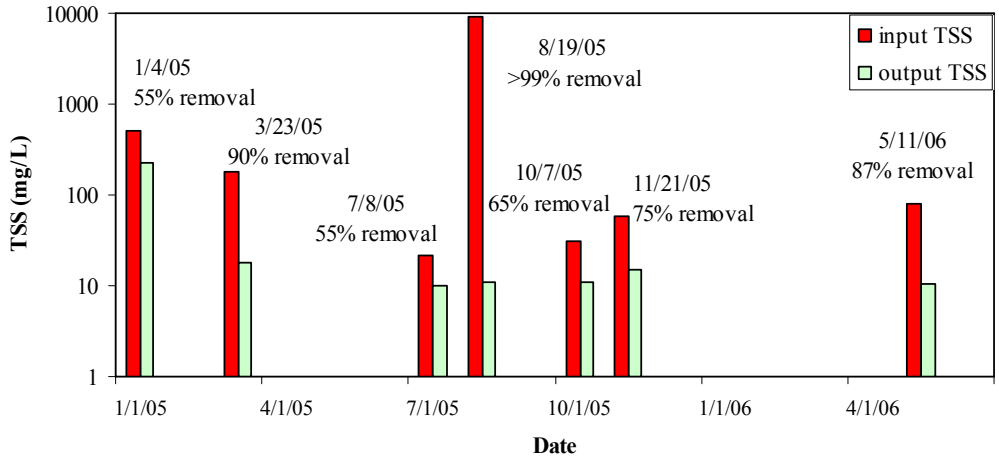

Figure 4-5. Input and output TSS of the Washington DC bioretention facility grab-samples.

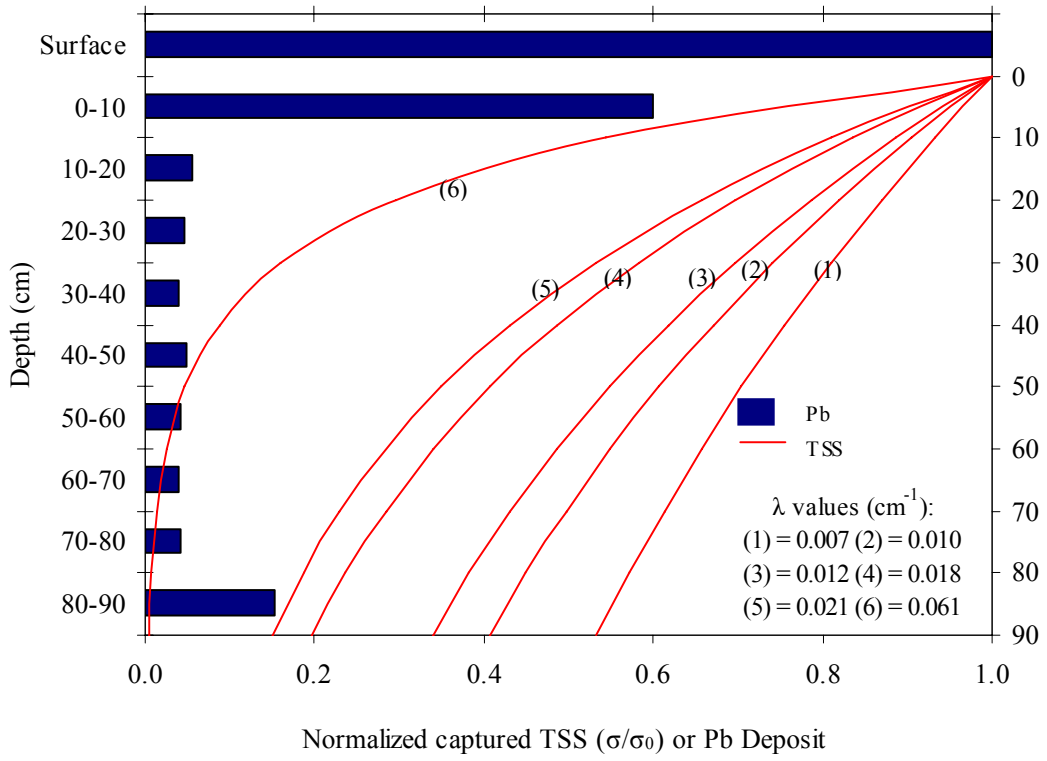

Figure 4-6. Total lead and estimated captured TSS profiles of the monitored Washington DC bioretention facility.

To examine the spatial profile of captured particulate matter in a field bioretention facility, the profile of lead may be used as a surrogate. Lead occurs mainly in particulate-bound form in urban runoff (55-82%), as compared to cadmium (4-55%), copper (29-69%), and zinc (4-46%) (Sansalone and Buchberger 1997, Dean et al. 2005), and naturally-occurring lead levels in soils are significantly less than other particulate-bound metals such as iron and aluminum. At the same bioretention facility, a 1.5-yr study conducted during approximately the same period (Dec 2004-Dec 2005) measured the media lead profile, which is described in detail in Chapter 6. The total lead (aqua regia digestion) profile is also presented in Figure 4-6 (the plot includes the surface street particle layer, which can be considered as equivalent to the cake layer that developed in the laboratory column tests). Two media samplings and analyses were performed, in December 2004 and December 2005, with averaged Pb levels used in Figure 4-6. The lead media spatial profile was clearly also top-heavy. Lead levels (21-530 mg/kg) over the monitored period were normalized by dividing by the lead level (530 mg/kg) of the surface street particle layer.

Both the measured lead and captured particulate matter estimated from the macroscopic depth filtration model exhibit top-heavy media profiles. However, the lead profile was much sharper than that of the estimated particulate matter. Below the 20 cm depth, the lead concentrations appears to be equal to the media background concentrations, indicating that both particulate and dissolved lead did not significantly penetrate beyond 20 cm. The disagreement between the two estimates indicates that depth filtration only accounts for part of the particle removal mechanism. The obvious street particle layer at the entrance ponding area of the

monitored facility implies that straining, sedimentation, and cake filtration also contribute to particle removal.

The observed TSS input of the monitored field bioretention was approximately 160 mg/ L (geometric mean). To estimate a TSS loading, it is assumed that annual precipitation to the facility is 102 cm (Washington DC, NWS 2006), and the runoff coefficient of the drainage area = 0.9. As a result, the annual runoff loading to the facility is 700 m^3/yr, and the total solids loading is 113 kg/yr or 6.6 kg/yr-m^2. Comparing the total solids loading for the field facility to the intermittent column tests for Soil I and Soil II/ Silt and Mixture inputs (6.3-14.5 kg/m^2, Trials 16, 17, and 19, Table 3), the estimated time span for the media clogging is 1 to 2 yr. However, media clogging did not occur during the 1.5-yr monitoring period. The vegetation and fauna (e.g., earthworms) present in the bioretention facility may act upon the media, loosening the media structure and regaining the permeability; these processes are not considered in the column tests. As such, the total solids loading data obtained from the column tests may be an underestimate for media clogging prediction in biologically rich systems.

Additionally, a coarser-media surface mulch layer may help field bioretention media delay the cake layer formation (compared to the underlying media), which is not considered in the column tests. (Soil I and II were pre-mixed with mulch, but not in a separated-layers configuration, the media mix ratios are unknown.) However, previous studies (Arias et al. 2001, Hsieh and Davis 2005) have mentioned that the more heterogeneous nature of a mulch layer (compared to other media layers) may

reduce infiltration rates and speed the media clogging, which will trigger cake layer formation if it occurs.

Further, most entrance ponding areas in field bioretention are not laid out with vegetation and mulch layers, partly because of the harsh conditions resulting from incoming runoff impact and excessive water. Entrance ponding areas are the location where most incoming runoff particles settle, compared to other zones in bioretention cells, and therefore are critical for media clogging and cake layer formation. Results of the column tests in this study can be applied to improve bioretention design and maintenance for these critical zones.

4.4 Summary

Through laboratory column tests and field observations, this chapter examines particle filtration phenomena for bioretention media and reaches the following conclusions:

1. Bioretention media appear to be clogging-limited due to their fine grain size, which indicates that media clogging will always occur before TSS penetration and limit the life expectancy for bioretention facilities.
2. Incoming TSS cannot significantly penetrate through 5-20 cm of bioretention media. Depth/cake filtration and surface straining all contribute to particulate capture.
3. Intermittent inflow conditions allow more particulate capture capacity in bioretention media before clogging than those of continuous inflow conditions.

4. Clay-sized components of incoming TSS exert a controlling effect on media clogging compared to components of other texture-size.
5. Media stratification in terms of particle deposition and permeability reduction along the runoff percolation depth is a characteristic of bioretention; as such, periodic surface media replacement can be used as an effective measure in bioretention maintenance.

Chapter 5: Bioretention Filtration – Theory and Model Development

5.1 Introduction

This chapter presents a theoretical and mechanistic evaluation of particle capture through bioretention media. In Chapter 4, laboratory and field observations demonstrated that (1) most captured suspended solids deposit within the very top layers (surface to 5-20 cm) of bioretention media, (2) bioretention filter media are clogging-limited instead of breakthrough-limited, which indicates that media clogging will always occur before TSS penetration and control the life expectancy for bioretention facilities, and (3) both depth filtration and cake filtration significantly contribute to urban particle capture from stormwater.

As stormwater BMPs becomes increasingly adopted for nonpoint source pollution mitigation and post-development hydrological restoration, the need for a BMP analysis system to integrate performance information for different BMPs on a watershed basics is acute (Zhen et al. 2006), highlighting the importance of understanding and modeling different BMPs. This paper presents an analytical model to investigate several important issues in bioretention filtration performance, including the role of the cake layer, the appropriate media depth for TSS removal, estimates for bioretention media life expectancy (before clogging), and suggestions for bioretention maintenance procedures. By applying comprehensive modeling theory to address urban particle capture and hydraulics (which are both key elements for BMP integration) for bioretention and other similar types of BMPs, applications

of BMPs can be integrated throughout a large watershed to provide greater water quality and hydrology benefits.

The objectives of this modeling study are:

(1) To develop a bioretention filtration model employing existing sand filter theory and bioretention field / laboratory tests which can simulate both suspended solids capture and penetration, and media clogging.

(2) To evaluate the importance of model parameters through pre-sensitivity analysis and calibrate the model parameters with laboratory column test results.

(3) To assess the feasibility of the developed model for variable flow conditions and different media/TSS type combinations.

(4) To apply the developed theory to predict effluent quality and headloss development, maintenance procedures (media replacement), and life expectancy (before media clogging) of bioretention facilities through simulation and long term scenario analyses. Based on results obtained from these simulations, recommendations for improved bioretention facility design and maintenance procedures can be offered.

5.2 Model Development

As noted in Chapter 4, both cake filtration and depth filtration are important mechanisms for urban solids removal in bioretention. Modeling of cake and depth filtration has been extensively studied in many areas, but predominantly in separate analyses. A few attempts, however, have been made to connect them (Swartzendruber 1960, Mein and Larson 1973, Swartzendruber and Uebler 1982,

Mays and Hunt 2005). Furthermore, urban particle loadings from stormwater runoff are intermittent, while most filtration studies are based on assumptions that the inflow rate and incoming TSS concentration are relatively steady. The proposed bioretention filtration model includes the following assumptions:

1. Only downward flow was considered (one dimensional flow).
2. The pore volume inside the deposited solids in the filter media is neglected.
3. Dispersion and the variation of pore-suspension concentration are neglected.
4. A homogeneous deposit with a constant cake layer porosity is assumed.

Those assumptions have been used in previous studies regarding depth filtration (Tien 1989, Mays and Hunt 2005) and cake filtration (Mays and Hunt 2005).

5.2.1 Particulate penetration depth

The profile of suspension concentration (C, the TSS) within the media depth (Z) in depth filtration studies is often expressed as a first order relationship (e.g., Iwasaki 1937):

$$\frac{\partial C}{\partial Z} = -\lambda C \tag{5-1}$$

where λ is the filter coefficient with dimension of reciprocal length. It is generally assumed that λ is independent of suspension concentration, but dependent on time, position, and specific deposit (Tien 1989). Equation (5-1) implies a sharp, exponential suspended solids vertical profile in the infiltrating liquid. However, employing a mass balance this profile also can be used to express the solids deposition within the filter media and demonstrate that the vertical profile of

volumetric specific deposit is approximately the same as the suspension concentration profile in the flow (Ives 1963):

$$\frac{C}{C_0} = \frac{\sigma_v}{\sigma_{v0}} \tag{5-2}$$

where C_0 is the suspension concentration in the incoming flow, σ_v is the volumetric specific deposit (the volume of deposited particles per unit filter volume), and σ_{v0} is the volumetric specific deposit at depth = 0, respectively. A similar concept was also presented in Mays and Hunt's (2005) work.

The filter coefficient λ varies with σ_v and other factor such as filter media porosity. Several expressions have been proposed to quantify these λ relationships. In this study, a simple linear dependence was used (Tien 1989):

$$\lambda = \lambda_0 + b\sigma_v \tag{5-3}$$

where λ_0 is the clean bed filter coefficient and b is an empirical constant which can be positive or negative.

5.2.2. Filtration equations

The classical macroscopic depth filtration model can be described as (e.g., Herizig et al. 1970):

$$q\frac{\partial C}{\partial Z} + \frac{\partial \sigma}{\partial t} = 0 \tag{5-4}$$

which is an approximation of the particulate mass balance, neglecting the minor terms of dispersion and pore-suspension concentration variation. Here q represents the approach velocity of the suspension, σ is the specific deposit (mass of deposited particles per unit filter volume, = $\sigma_v\rho_s$, where ρ_s is particle density), and t is time.

However, to evaluate filter head loss due to the solids accumulation, other parameters are needed. Mays and Hunt (2005) analyzed 43 experiments from 6 filtration studies with a simplified version of the O'Melia and Ali (1978) clogging model and successfully described the increased clogging that is always observed in the top segment of a filter using a relationship between headloss and specific deposit:

$$\Delta H / \Delta H_0 = [1 + \gamma \sigma_v]^2 \tag{5-5}$$

In this equation, ΔH is the head loss of the filter bed, ΔH_0 is the clean bed head loss, and γ, which represents the clogging parameter, can be described by (O'Melia and Ali 1978, Mays and Hunt 2005):

$$\gamma = \frac{\beta' d_m}{6(1-\varepsilon)} \frac{A_p}{V_p} \tag{5-6}$$

where β' is the specific area parameter, which is an empirical coefficient representing the fraction of retained particles contributing to the increased specific area, ε is the porosity of the clean filter composed of spherical collectors of diameter d_m, A_p is the surface area per particle, and V_p is the volume per particle. Previous studies have indicated that γ is quantified as a power law relationship of approach velocity (Mays and Hunt 2005). Using Darcy's law, Equation (5-5) is expressed in terms of hydraulic conductivity:

$$\frac{K}{K_0} = \frac{1}{(1+\gamma \sigma_v)^2} \tag{5-7}$$

where K is the hydraulic conductivity, and K_0 is the clean bed hydraulic conductivity.

5.2.3. Bioretention filtration

As discussed in Chapter 4, due to the fine size of bioretention media, incoming particles cannot significantly penetrate beyond 5-20 cm media depth. Therefore, media stratification in terms of suspended solids deposition and permeability reduction occurs along the runoff percolation path. As a result, the bioretention soil media is modeled as three distinct layers: layer a (bottom) – the pristine soil media, layer b (middle) - the media working accumulation zone, and layer c (top) - the cake layer, as shown in Figure 5-1. Incoming stormwater transports solids onto the media; a fraction of the solids penetrate the media and deposit in the upper media working zone (layer b), creating an exponential decline of deposited particle accumulation with depth as described in Equations (5-1) and (5-2). Eventually, solids accumulate on the surface of the filter media and gradually form a cake layer (layer c). Beneath the working zone, the filter media is assumed pristine and denoted as layer a.

A differential mass balance is used to describe the partitioning of deposited solids among the layers, with no accumulation in layer a:

$$dM = (L_a + L_b) A_c d\sigma + (1 - \varepsilon_c) \rho_s A_c dL_c \tag{5-8}$$

integrating to :

$$M = (L_a + L_b) A_c \sigma + (1 - \varepsilon_c) \rho_s A_c L_c \tag{5-9}$$

where M is cumulative captured mass, and L_a, L_b, and L_c represent the thickness of layers a, b and c, respectively. A_c is the cross-sectional area of the filter, and ε_c is the porosity of the cake layer c. The first terms on the right of Equations (5-8) and (5-9) represent the suspended solids removed by depth filtration and the second terms are the removal via cake filtration.

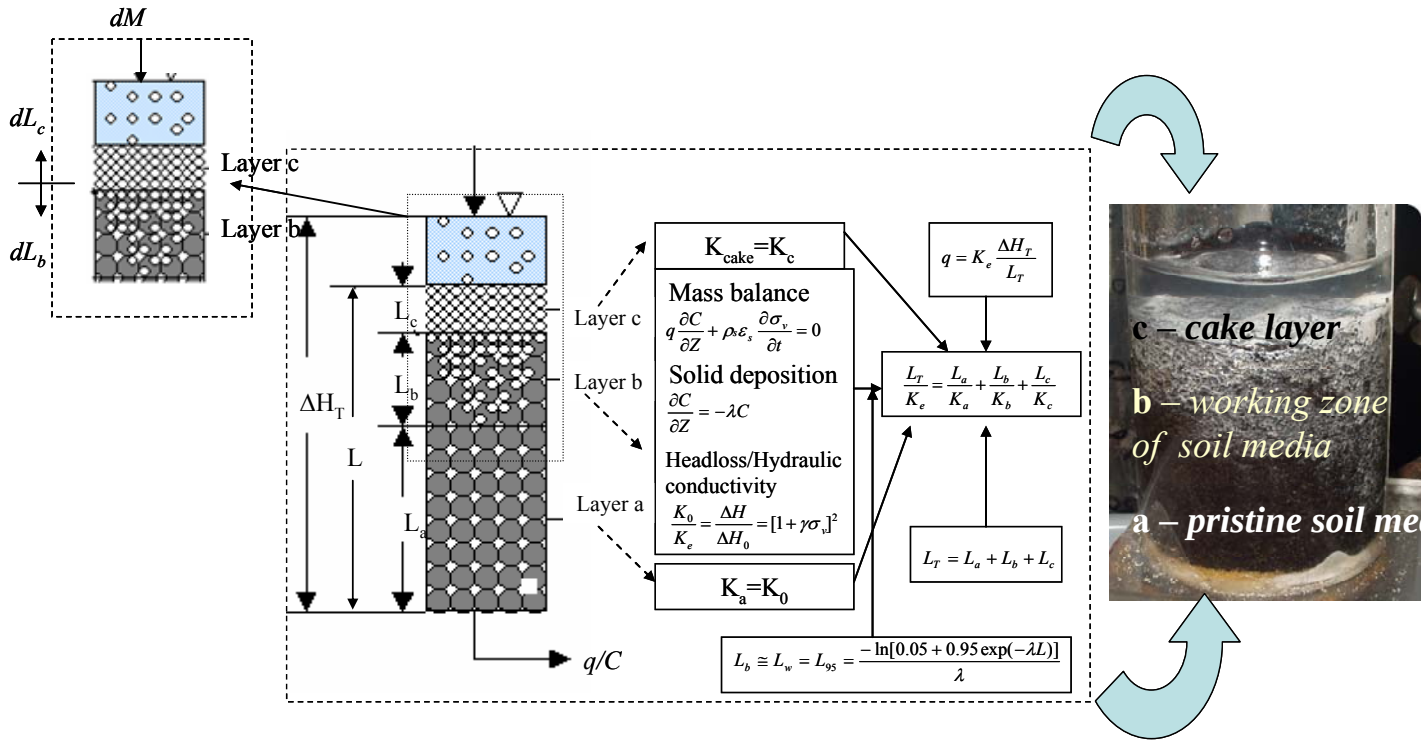

Figure 5-1. The three layer approximation of a bioretention media column. The soil media column photo shows the column test of Soil I media and Kaolin suspension (Chapter 4, Trial 1).

The decrease in infiltration flow resulted from the permeability reduction during the filtration process can also assist in separation of suspended solids from the input water before penetration into the media. Therefore a cake layer is formed even with fine-sized suspended solids, which have more significant repercussions on effluent quality and media permeability than coarse-sized solids. As a result, this model development considers only the fine-sized cake layer formed due to decrease in media permeability, and the decrease of media hydraulic conductivity was used to predict cake layer formation. After the cake thickness L_c develops to critical value, the cake filtration mechanism will dominate the overall filtration efficiency.

Previous studies (Swartzendruber 1960, Swartzendruber and Uebler 1982) show the equivalent hydraulic conductivity of the three-layer K_e as:

$$\frac{L_T}{K_e} = \frac{L_a}{K_a} + \frac{L_b}{K_b} + \frac{L_c}{K_c} \tag{5-10}$$

where K_a, K_b, and K_c represent the hydraulic conductivities of layers a, b, and c, respectively, and :

$$L_T = L_a + L_b + L_c \tag{5-11}$$

5.2.4. Approximation of filter working zone

Critical to understanding the filtration process is to approximate the thickness of the filter working zone L_b. This can be accomplished with Equations (5-1) and (5-2), which can be transformed as:

$$C / C_0 = \sigma / \sigma_0 = \exp(-\lambda Z) \tag{5-12}$$

Using Equation (5-12), a clogging-limited filter occurs when a filter fails due to media clogging instead of effluent quality deterioration because of TSS breakthrough.

At a given time t, the captured solids deposit M_d through depth filtration within the total length of the soil column L ($L = L_a + L_b$) can be represented as:

$$M_d(t) = \int_0^L \sigma(z,t) A_c dz = \int_0^L \sigma_0(0,t) e^{-\lambda z} A_c dz = \frac{\sigma_0(0,t)}{\lambda}(1 - e^{-\lambda L}) A_c \tag{5-13}$$

Operationally, the working zone (layer b) is defined as the upper part of the media filter volume in which 95% of the accumulated specific deposit is captured:

$$0.95 M_d(t) = \frac{\sigma_0(0,t)}{\lambda}(1 - e^{-\lambda L_b}) A_c \tag{5-14}$$

Comparing Equations (5-13) and (5-14) gives,

$$0.95 = \frac{(1 - e^{-\lambda L_b})}{(1 - e^{-\lambda L})} \tag{5-15}$$

or

$$L_b = \frac{-\ln[0.05 + 0.95 \exp(-\lambda L)]}{\lambda} \tag{5-16}$$

which is the approximated thickness of the filter working zone, L_b. The stratification and headloss profile in a bioretention soil filter can be obtained by solving Equations (5-7), (5-9), (5-10), (5-11), (5-12), and (5-16) with Darcy's law, as in Figure 5-1.

By assuming a homogeneous deposit with constant porosity in the cake layer, the cake growth can be related to the average specific deposit and TSS input from Equation (5-9):

$$L_c = \frac{\dfrac{M}{\rho_s A_c} - L\sigma}{(1 - \varepsilon_c)} \tag{5-17}$$

The media hydraulic conductivity reduction was used to predict cake layer formation. The ratio of K_e (overall) to K_0 (initial) of the media at which the cake was

first visually observed, $(K_e/K_0)_{bc}$, was selected to be the predicting parameter for filtration mechanism transition.

5.2.5. Bioretention maintenance- media replacement

Removal and replacement of a shallow surface media layer has been suggested as an effective maintenance procedure for bioretention, eliminating accumulated pollutants. Similar to Equation (5-15), the removal and replacement depth for bioretention media can be formulated as:

$$X = \frac{(1 - e^{-\lambda L_X})}{(1 - e^{-\lambda L})} \tag{5-18}$$

or

$$L_x = \frac{-1}{\lambda} \ln\left[1 - X(1 - e^{-\lambda L})\right] \tag{5-19}$$

where X represents the fraction of captured solids deposit that is removed from the facility through removal and replacement, and L_x is the replacement depth. However, Equations (5-18) and (5-19) will be an underestimate of X if a cake layer exists. With the inputs of the model parameters (λ_0, b, ε_c, γ, K_c, $(K_e/K_0)_{bc}$, L, A_c, K_o, and ρ_s) and forcing functions (C_0(t) and $q(t)$), this modeling theory can calculate the bioretention output TSS levels (C_0(t)) and media hydraulic conductivity ($K_e(t)$), as well as the length (L_a, L_b, and L_c) and hydraulic conductivity (K_a, K_b, and K_c) of the three layers (layers a, b, and c), which can be evaluated to interpret key phenomena for the fundamental features of bioretention media, as shown in Figure 5-2.

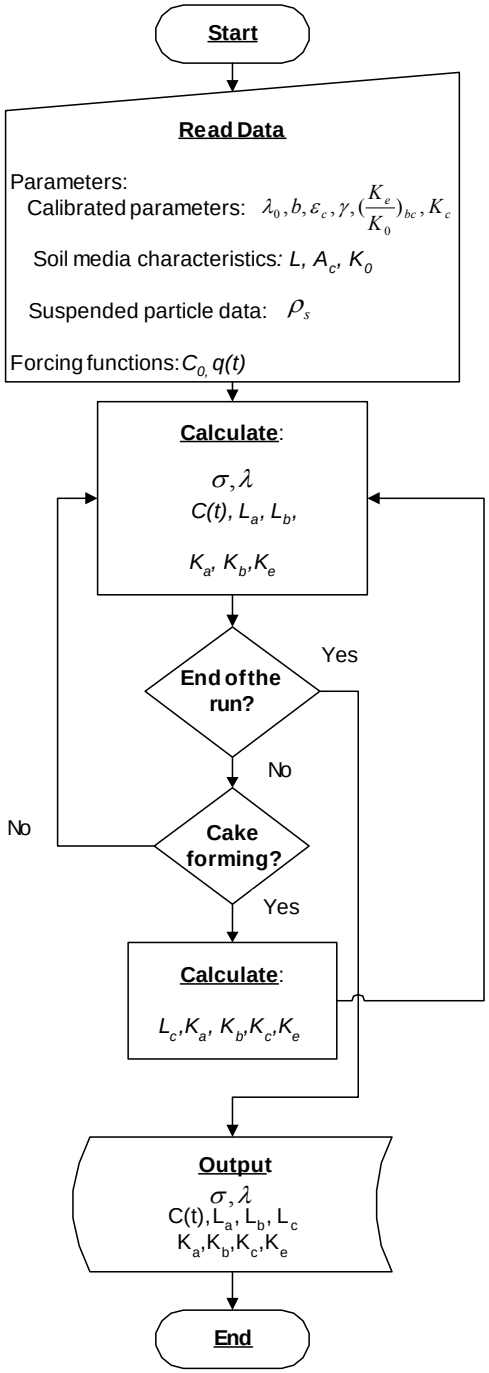

Figure 5-2. Flowchart of the modeling program.

5.3 Methodology

Laboratory column tests and field bioretention monitoring were used for the model calibration, simulations, and scenario analyses; experimental details and methodologies are described in Chapter 4. In the laboratory study, 20 column trials were employed with different media (Soil I and Soil II) and TSS type (kaolin, montmorillonite, silt, sand, and mixture = 80% silt + 5% montmorillonite + 5% kaolin + 10% sand) under both continuous and intermittent flow conditions to simulate bioretention filtration. Details are listed in Table 5-1. The complete results of all 20 column tests are shown in Appendix 3.

5.3.1. Computer program algorithm and input data

A computer program was created for model calibration, sensitivity analysis, and simulation in Matlab 6.5 with application to EXCEL 2003. The algorithm flowchart is shown in Figure 5-2. Input data include soil media depth and cross-sectional area, clean bed hydraulic conductivity, average density of runoff suspended solids, and estimated or calibrated parameters λ_0, b, ε_c, γ, K_c, and $(K_e/K_0)_{bc}$, as well as forcing functions (input runoff flow rates and TSS concentrations (as a function of time)). An example of the source code of the computer program is listed in Appendix 4.

5.3.2. A priori sensitivity analysis

An analysis was performed prior to the model calibration to rank the sensitivity of the model parameters, and therefore to reduce the number of trials necessary for calibration; however, it should be noted that the parameter interdependence was ignored in this procedure (Campo et al. 2006a). The Soil I / Kaolin (Trials 1-9)

combination had the greatest number of test trials and was used for the sensitivity analysis.

Data for model calibration were obtained from column studies as described in Chapter 4 and are presented in Tables 5-1 and 5-2. The data from Trials 1-7 were used to estimate model parameters. Values for λ were obtained through Equation (5-1) from input / output TSS levels of each trial. Thereafter, λ_0 and b were estimated through the curve fitting of Equation (5-3) before the cake build-up (when depth filtration was the only TSS removal mechanism) with the σ_v values obtained from the mass balance (Equation (5-9)), as well as K_b from Equation (5-10) and subsequently γ from curve-fitting of Equation (5-7).

The hydraulic conductivity at which the cake started to build up was used in calculating $(K_e/K_0)_{bc}$; after cake formation, the K_c values were calculated by Equation (10) with an assumption that K_b remains unchanged after cake build-up. The cake porosity ε_c was obtained through Equation (5-9). For each trial, single values of λ_0, b, and γ were obtained from curve fitting, a single $(K_e/K_0)_b$ was calculated, and an averaged K_c and ε_c were produced. This is known as the prior estimate process. The parameter ranges from analysis of Trials 1-7 are listed in Table 5-2. Mean values from the data sets over the ranges were used as the initial (default) values for the sensitivity analysis and calibration for each parameter.

Sensitivity analysis was performed to investigate the model output (C and K_e) to changes of the parameters (λ_0, b, ε_c, γ, K_c, and $(K_e/K_0)_{bc}$) by evaluating Trial 8, holding all prior estimated parameters constant while one was systematically varied over the parameter ranges described above. The default parameter values used in the

sensitivity analysis were obtained from the calibration process (of Trial 8), which is described in the following section. For each parameter, 6-9 inputs were assigned, distributed evenly in its range, with 90-135 outputs generated. The parameter sensitivity was quantified using a sensitivity coefficient (*SC*), which is defined as the ratio of the coefficient of variation of the model output to the coefficient of variation of a parameter, as defined by previous studies (e.g., Campos et al. 2006a).

Table 5-1. Conditions for the column tests (Chapter 4)

Trial #	Media	Suspended solids	Flow rate (cm/hr)	Media depth (cm)	Input TSS (mg/L)	Media size d_m (d_{50}, μm)	Suspended solid size d_p (d_{50} or interval, μm)	d_m/d_p (-)	Hydraulic conductivity (cm/hr)		Solids loading (kg/m^2)	Average filter coefficient λ (cm^{-1}) Eqn(1)	Layer thickness (cm)		
									Clean bed	At run end			L_a	L_b[3]	L_c
Continuous column tests															
1	Soil I	Kaolin	4.8	5.5	134±9	340	<1	>340	45	3	2.4	0.78 (0.52-1.03)	2.0	3.5	0-0.3
2			4.9	10.5	130±8	340			44	3	1.5	0.39 (0.30-0.53)	3.5	7.0	0-0.4
3			9.5	5.5	132±29	340			44	4	3.3	0.59 (0.47-0.78)	1.4	4.1	0-0.3
4			9.5	10.5	132±29	340			44	3	3.3	0.35 (0.28-0.48)	3.1	7.4	0-1.0
5			19.8	5.5	126±7	340			46	5	2.3	0.74 (0.58-0.88)	1.8	3.7	0-0.3
6			19.7	10.5	121±5	340			48	6	2.6	0.41 (0.37-0.46)	3.8	6.7	0-0.6
7			20.1	5.5	36±7	340			44	7	1.2	0.55 (0.31-0.68)	1.2	4.3	0-0.2
Intermittent loading tests															
8	Soil I	Kaolin	20.8 →9.0	10.5	49-1062	340	<1	>340	44	5	5.5	0.36 (0.31-0.43)	3.2	7.3	0-0.7
9			9.1→ 18.9	10.5	15-261				131	11	3.7	0.36 (0.20-0.51)	3.2	7.3	0-0.6
10	Soil I	Mont [1]	19.0	10.5	114-161	340	<1	>340	43	7	0.9	0.41 (0.36-0.47)	3.8	6.7	0
11			9.3	10.5	94-202				60	6	0.9	0.31 (0.24-0.37)	2.6	7.9	0
12	Soil II	Kaolin	19.6	10.5	31-195	570	<1	>570	45	8	1.0	0.40 (0.33-0.47)	3.6	6.9	0
13	Soil II	Kaolin	10.3 → 19.7	10.5	48-133				52	8	1.0	0.38 (0.30-0.44)	3.4	7.1	0-0.5

Table 5-1. (Continued) Conditions for column tests

Trial #	Media	Suspended solids	Flow rate (cm/hr)	Media depth (cm)	Input TSS (mg/L)	Media size d_m (d_{50}, μm)	Suspended solid size d_p (d_{50} or interval, μm)	d_m/d_p (-)	Hydraulic conductivity (cm/hr)		Solids loading (kg/m^2)	Average filter coefficient λ (cm^{-1}) Eqn(1)	Layer thickness (cm)		
									Clean bed	At run end			L_a	L_b[3]	L_c
Intermittent loading tests															
14	Soil II	Mont [1]	19.6	10.5	118-166	570	<1	>570	164	7	0.9	0.33 (0.16-0.46)	2.8	7.7	0
15			9.1	10.5	110-134	570	<1	>570	48	3	0.4	0.37 (0.29-0.46)	3.3	7.2	0
16	Soil I	Silt	19.9 →9.8 → 20.4	10.5	21-6030	34	3	113	51	9	14.5	0.38 (0.16-0.57)	3.4	7.1	0-0.2
17	Soil II	Silt	18.5	10.5	140-1774	570	3	190	49	7	6.3	0.52 (0.47-0.58)	4.6	5.9	0-0.4
18	Soil I	Sand	19.0	10.5	35-1729	340	75-425	1-5	55	7	6.4	0.39 (0.25-0.53)	3.5	7.0	0-0.5
19	Soil I	Mixture [2]	18.5 →9.8	10.5	28-1535	340	<1-425	1->34	59	6	7.5	0.39 (0.18-0.63)	3.5	7.0	0-0.6
Hydraulic conductivity restoration tests															
20	Soil II	Mont [1]	-	10.5	39-588	570	<1	>570	72	1	1.8	0.37 (0.18-0.54)	3.3	7.2	0-0.2
20-1	Original media		19.9						72						0
20-2	Replacing top 3 cm		8.3						36						0-0.2
20-3	Replacing top 5 cm		9.6						39						0
20-4	Replacing top 7 cm		8.1						43						0-0.1

[1]Montmorillonite, [2]80% silt+ 5% montmorillonite+ 5% kaolin+ 10% sand. [3]Estimated from average λ.

Table 5-2. Data sets allocation for calibration and simulation and the parameter values.

Media	TSS type	Parameter							Flow condition
			λ_0 cm^{-1}	$(K_e/K_0)_{bc}$ (-)	γ (-)	ε_c (-)	K_c cm/hr	b cm^{-1}	Trial	
Soil I	Kaolin	Prior estimated	0.65	0.08	133	0.90	1.0	14.5	1	Continuous
			0.29	0.09	495	0.95	0.4	39.8	2	
			0.63	0.11	72	0.88	0.6	-3.0	3	
			0.63	0.10	155	0.94	0.7	-5.7	4	
			0.83	0.17	93	0.83	1.0	-13.1	5	
			0.37	0.19	185	0.89	0.66	14.3	6	
			0.66	0.17	149	0.96	4.9	-24.2	7	
			0.32	0.11	166	0.85	1.4	8.0	8	
		Calibrated	0.34	0.13	200	0.65	5.6	2.0	8	
			0.34	0.13	200	0.65	5.6	2.0	9 (prediction)	
	Montmorilllonite	Prior estimated	0.46	-[2]	409	-[2]	-[2]	-28.6	10	Intermittent
		Calibrated	0.49	-[2]	438	-[2]	-[2]	-28.5	10	
			0.49	0[2]	438	-[2]	-[2]	-28.5	11 (prediction)	
	Silt	Prior estimated	0.34	0.23	12	0.50	0.5	1.1	16	
		Calibrated	0.48	0.31	14	0.40	0.5	1.1	16	
	Sand	Prior estimated	0.37	0.13	56	0.50	0.6	-3.4	18	
		Calibrated	0.55	0.53	61	0.70	0.5	-9.4	18	
	Mixture (Silt+Kaolin+ sand+ Montmorillonite)	Composite	0.48	0.31	49	0.42	0.7	-1.4	19 (prediction)	
		Prior estimated	0.31	0.10	85	0.50	4.1	7.1	19	
		Calibrated	0.45	0.20	82	0.54	4.1	7.1	19	
Soil II	Kaolin	Prior estimated	0.49	-[2]	222	-	-	2.0	12	
		Calibrated	0.40	0.13[1]	216	0.65[1]	5.6[1]	0.1	12	
			0.40	0.13[1]	216	0.65[1]	5.6[1]	0.1	13 (prediction)	
	Montmorilllonite	Prior estimated	0.48	-[2]	1015	-[2]	-[2]	-78.8	14	
		Calibrated	0.50	0[2]	1319	-[2]	-[2]	-80.0	15 (prediction)	
			0.50	0[2]	1319	-[2]	-[2]	-80.0	20 (prediction)	
	Silt	Prior estimated	0.48	0.26	0.12	0.50	0.7	-5.7	17	
		Calibrated	0.43	0.34	96	0.87	0.7	-7.8	17	

[1] Using the calibrated cake properties from Trial 8 (No cake formed in Trial 12) [2] No cake data available from the montmorillonite calibration trials

The *SC* values of the six parameters for *C* and K_e are presented in Figure 5-3. For the effluent TSS prediction, the sensitivity order is $\lambda_0 > (K_e/K_0)_{bc} > \gamma > b > \varepsilon_c > K_c$; for the hydraulic conductivity prediction, the order is $(K_e/K_0)_{bc} > \lambda_0 > \gamma > K_c > \varepsilon_c > b$. The effects of K_c, ε_c, and *b* to the model are minor compared to the other three parameters.

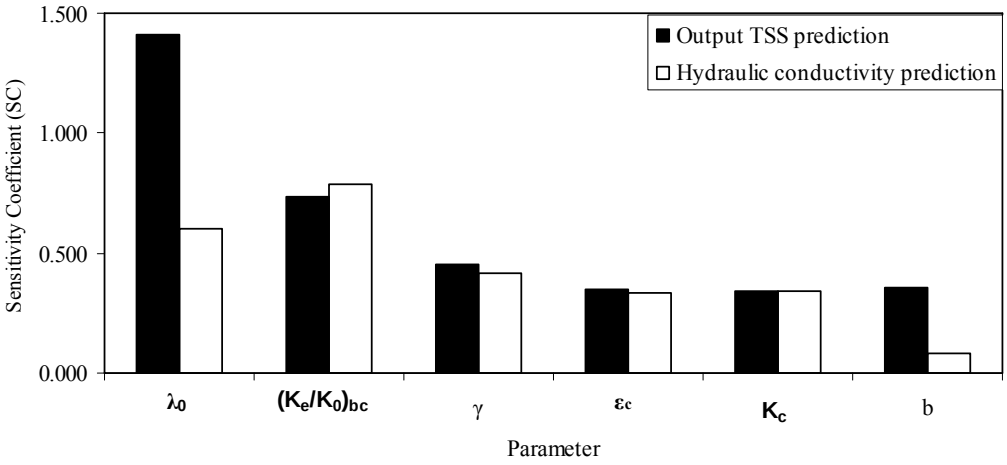

Figure 5-3. The sensitivity coefficients of the parameters in the modeling theory.

5.3.3. Calibration and simulation

The prior estimated parameters were used as the initial values for model input. The difference between experimental data and model prediction for an output variable is quantified using a least squares function (sum of squared errors, SSE). The objective function for parameter calibration was to minimize the product of the SSE for *C*, K_e, or L_c (Campos et al. 2006a, b). To evaluate the impact of intermittent vis-à-vis continuous loadings, the mean parameters prior estimated from Trials 1-7 were compared with the prior estimated parameters from Trial 8 (intermittent); two calibration processes followed with Trial 8 data using the mean prior estimated

parameters from Trials 1 -7 and prior estimated Trial 8 parameters as the initial model parameter estimates (starting values), respectively. Both calibrations reached the same calibrated parameter values. Subsequently, the prior estimated parameters from intermittent loading trials were used as the sole initial model parameter estimates for calibration processes. The Trial 8 calibrated parameters were used in the Trial 9 simulation. For Soil I / Montmorillonite, the parameters prior estimated, then calibrated from Trial 10, were used to simulate Trial 11. For Soil I/Mixture, a set of weighted composite (prior estimated then calibrated) parameters was used to simulate Trial 19; however, parameter calibration was also performed for Trial 19 specifically to compare between the composite and calibrated parameters. For Soil II / Kaolin, prior estimated / calibrated parameters from Trial 12 were used for Trial 13 simulation. For Soil II/Montorillonite, prior estimated / calibrated parameters from Trial 14 were used to simulate Trials 15 and 20 (the hydraulic conductivity restoration test). For Soil I / Silt (#16), Soil I / Sand (#18), and Soil II / Silt (#17), only parameter prior estimates / calibrations were completed. A summary of data set allocation to model calculation, calibration and simulation are listed in Table 5-2.

The parameter calibration was carried out by comparing the experimental data (output TSS C, media equivalent hydraulic conductivity K_e, and cake thickness L_c (if a cake layer is predicted or actually formed)) with values predicted by the model, similar to that by Campos et al. (2006a, b). According to the parameter sensitivity rank, the parameter calibration began with the most important parameter, with a sequence of λ_0, $(K_e/K_0)_{bc}$, γ, ε_c, K_c, and b. However, in the cases in which obvious cake layers were not expected to form (Trials 10-12, 14, and 15), K_c and ε_c were

skipped and a $(K_e/K_0)_{bc}$ of zero was used. Additionally, the goodness of fit between experimental data and model prediction (simulation) were quantified using the ratio of SSE to the number of data points *N*. The calibrated parameter values for each trial are listed in Table 5-2.

5.4 Result of Model Simulation

5.4.1. Effluent concentration and media hydraulic conductivity profile

Results of all the 20 column tests are shown in Appendix 3. The effluent TSS levels C were ≤ 30 mg/L in all tests (the influent TSS C_0 ranged from 15-6030 mg/L), with a C/C_0 <0.01-0.26, which demonstrates excellent TSS removal. Model validation is illustrated through comparing measured output TSS and K_e with model predictions using prior estimated parameters for Trials 1, 5, and 7 as shown in Figure 5-4, which indicate good agreement between model and experimental data. From the results of continuous flow trials (Table 5-2, Trials 1-7), it is suggested that the difference in media depth (Trials 1, 5, 7 with 5.5 cm vis-à-vis Trials 2, 4, 6 with 10.5 cm) affect the effluent quality prediction in terms of the clean bed filter coefficient λ_0.

After the model validation, the hydraulic conductivity profiles for layers a, b, and c (K_a, K_b, and K_c, respectively) were computed by the model and are illustrated in Figure 5-5 for Trial 1 (Soil I / Kaolin). At the end of the run, $K_a > K_b > K_c$, which indicates that the cake layer was the least permeable for runoff infiltration; the working zone (layer b) had a low conductivity as well. These values are about an order of magnitude less than K_a, the original media. The simulated conductivity profiles of all of the 20 trials are listed in Table 5-3, which also show the same trend of surface clogging; that is, the lowest hydraulic conductivities are exhibited by the

cake and working zone. The conductivity profile suggests that top-raking or top-removal of the cake layer and part of the working zone (with refill) may be a maintenance recommendation for bioretention permeability restoration.

As mentioned, most filtration models have been developed based on an assumption of relatively constant inflow rates; however, runoff inputs to bioretention cells are intermittent in nature. After the model validation with constant flow inputs, intermittent flow inputs were used to test model performance. Results of the model prediction performance are exemplified with a comparison of the experimental results and model prediction in Figure 5-6. The modeling exercise produced good predictions for the outflow TSS (with the SSE/N = 0-75 $(mg/L)^2$), K_e (0.4-59 $(cm/h)^2$), and L_c (0-0.04 cm^2) in all trials, as shown in Table 5-4. Figures 5-7 and 5-8 show the model prediction and experimental data for Trials 11 (Soil I / Montmorillonite) and 13 (Soil II / Kaolin); good predictions of outflow TSS (Trial 13) and K_e (Trial 11) were also noted.

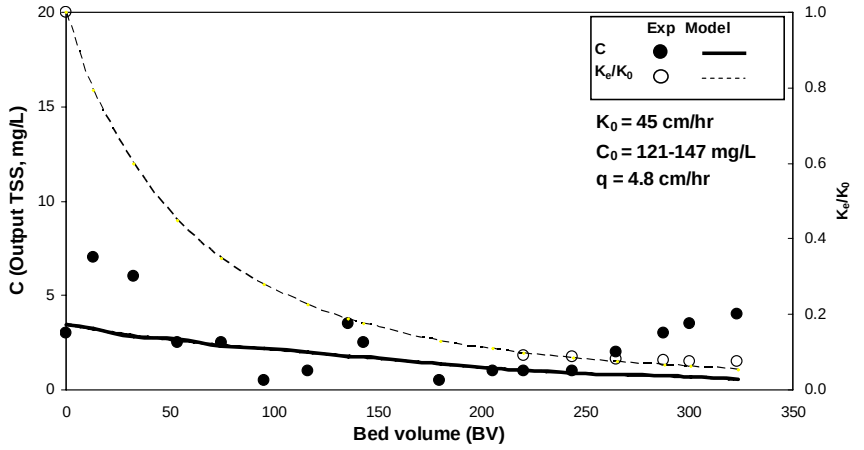

(a)

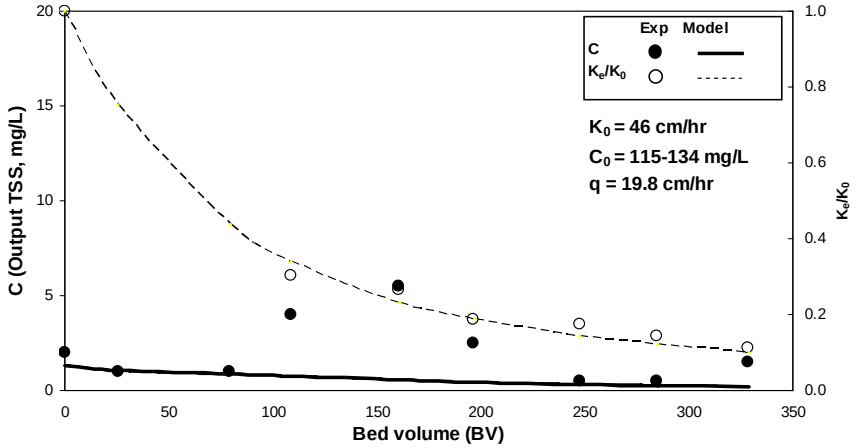

(b)

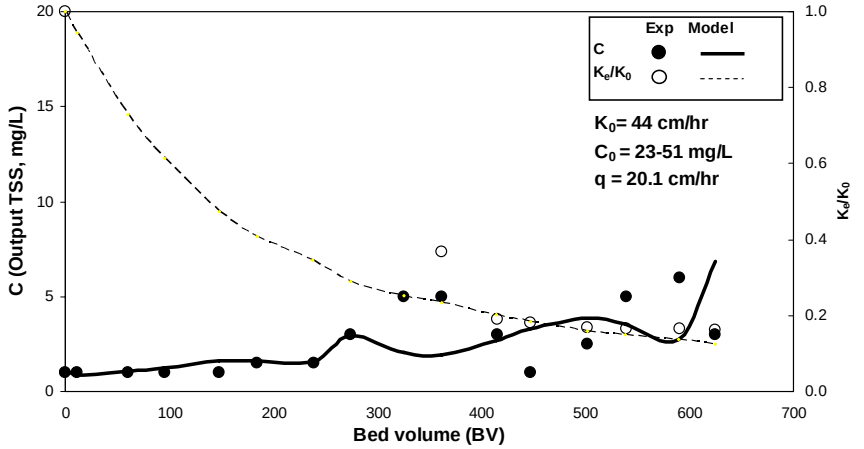

(c)

Figure 5-4. Illustrations of model validation using Trials #1 (a), 5 (b), and 7 (c) for Soil I/Kaolin with experimental data and model fit, media depth = 5.5 cm.

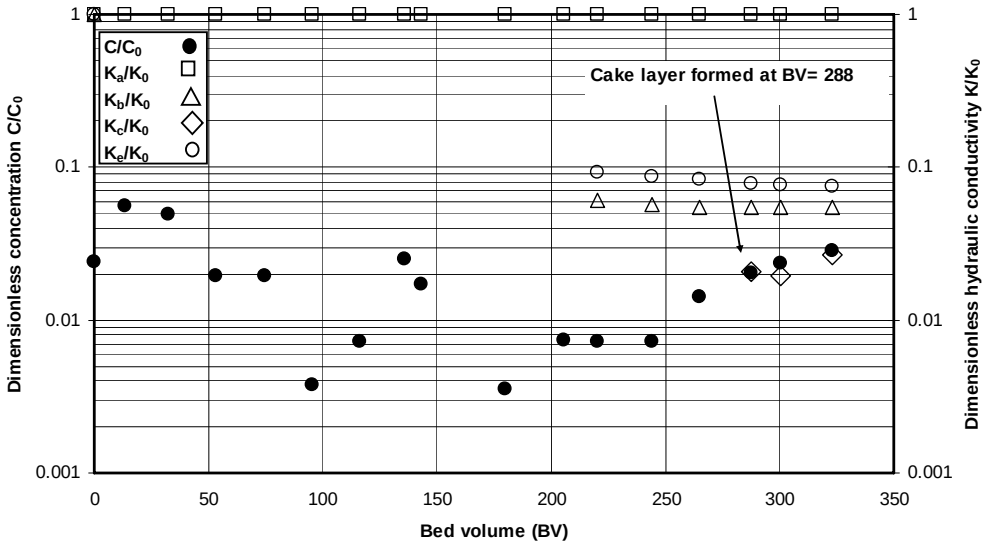

Figure 5-5. Effluent quality (measured) and hydraulic conductivity profile (simulated) of Trial 1 (Soil I/Kaolin), inflow rate = 4.8 cm/hr, input TSS=134±9 mg/L, media depth = 5.5 cm. The conductivity order of the different layers is $K_a > K_b > K_c$.

Table 5-3. Hydraulic conductivity profile for layers a-c in all of the 20 column tests, the permeability among the three layers followed the order of $K_a > K_b > K_c$.

Trial	Media/TSS	Hydraulic conductivity (cm/hr)		
		K_a	K_b	K_c
1	Soil I/Kaolin	45.0	45.0→2.5	0.9-1.2
2		44.0	44.0→2.9	0.3-0.6
3		44.2	44.0→4.0	0.3-0.9
4		44.0	44.0→3.4	0.5-0.9
5		46.0	44.0→6.2	0.6-1.4
6		48.0	48.0→7.5	0.6-0.8
7		43.5	43.5→5.8	4.2-5.6
8	Soil I/Kaolin	44.0	44→5.1	1.3
9		131.0	131.0→12.0	0.7-2.2
10	Soil I/Montmorillonite	42.7	42.7→4.9	-
11		60.0	60.0→4.4	-
12	Soil II/Kaolin	45.0	45.0→5.4	-
13		51.6	51.6.0→5.9	3.7-12.7
14	Soil II/Montmorillonite	164.0	164.0→5.5	-
15		48.0	48.0→2.2	-
16	Soil I/Silt	51.0	51.0→10.9	0.5
17	Soil II/Silt	49.0	49.0→10.9	0.5-1.0
18	Soil I/Sand	55.1	55.1→13.9	0.6
19	Soil I/Mixture	58.6	58.6→4.5	4.1
20	Soil II/Montmorillonite	72.0	72.0→4.0	0.1

Table 5-4. The goodness of fit between the experimental data and model simulation for model outputs (C, K_e, and L_c).

Trial	Media/TSS	Packing length (cm)	SSE/N		
			C(mg/L)^2	K_e(cm/h)^2	L_c(cm^2)
8	Soil I/Kaolin	10.5	3	48.1	0.0320
9		10.5	4	41.9	0.0194
10	Soil I/Montmorillonite	10.5	0	0.5	0.0000
11		10.5	38	11.1	0.0000
12	Soil II/Kaolin	10.5	1	8.6	0.0000
13		10.5	1	25.3	0.0342
14	Soil II/Montmorillonite	10.5	0	10.7	0.0000
15		10.5	3	2.9	0.0000
16	Soil I/Silt	10.5	75	2.5	0.0035
17	Soil II/Silt	10.5	55	0.4	0.0414
18	Soil I/Sand	10.5	3	3.3	0.0004
19*	Soil I/Mixture	10.5	11	26.7	0.0006
19**			8	0.2	0.0006
20	Soil II/Montmorillonite	10.5	59	59.0	0.0035

* Simulation with composite parameters. ** Simulation with Trial 19-calibrated parameters.

During the parameter calibration process, which seeks the least sum of square errors for the three output predictions (outflow TSS, hydraulic conductivity, and the cake layer thickness), the calibrated parameters may be the best fit overall yet deviate for one output prediction as a compromise in some occasion. Additionally, although Figures 5-4 and 5-6 through 5-8 indicate that both the continuous and intermittent flow conditions can be simulated with the proposed model, parameter adjustment may be needed to address intermittent flow conditions. A comparison of the clogging parameter γ between the continuous trials 2, 4, and 6 with intermittent flow trial 8 (with the same media depth of 10.5 cm) suggests that the γ values were higher under continuous flow conditions (prior estimated γ = 155 - 495, average = 278) than the intermittent flow condition (prior estimated γ =166 and calibrated γ = 200). The dormant periods seemed to allow the bioretention media to amend for a less-resistant

flow path and integrate with the captured particles in shape. This may have helped the media columns to partially regain their permeability between runoff loadings (Chapter 4).

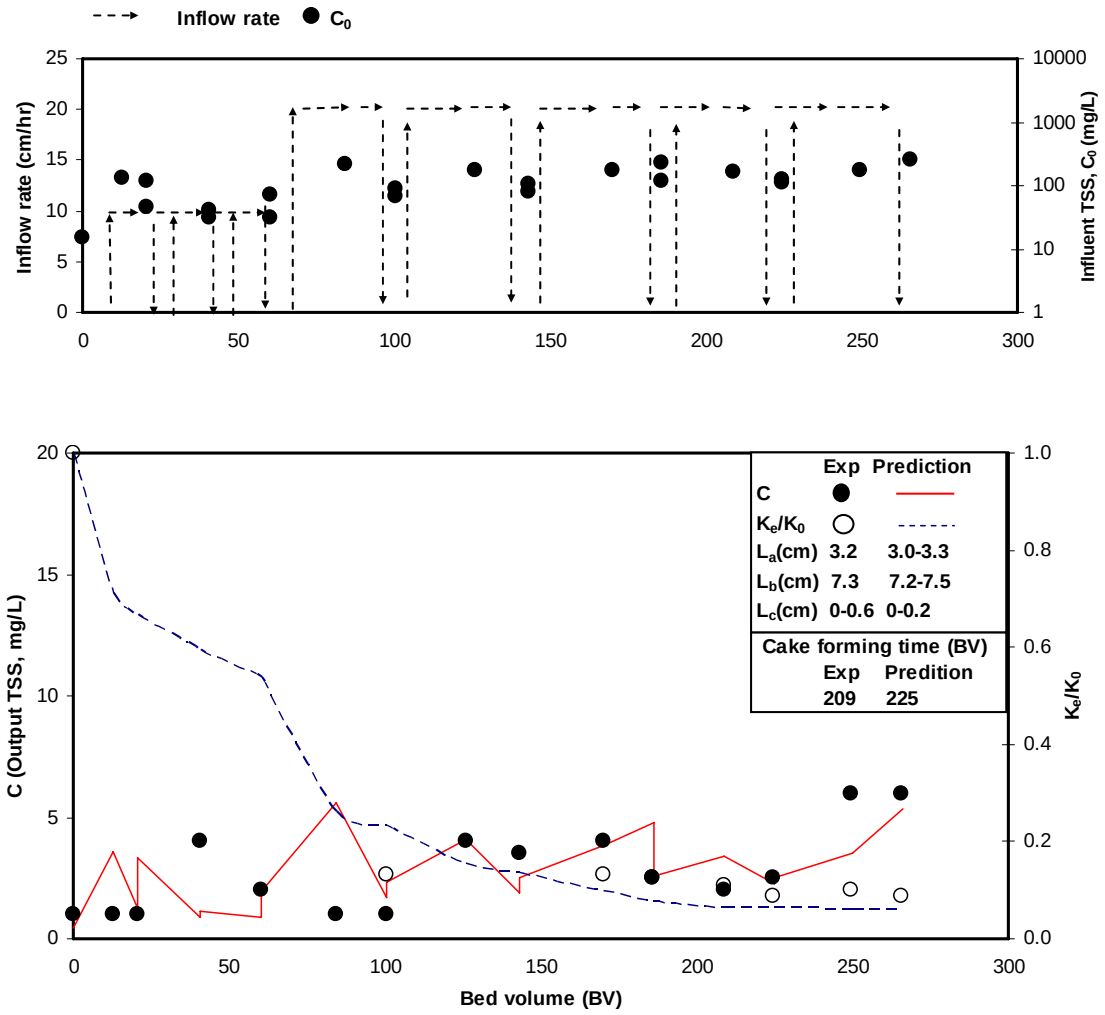

Figure 5-6. Comparison of effluent quality and hydraulic conductivity between the experimental data and model prediction for Trial 9 (Soil I / Kaolin).

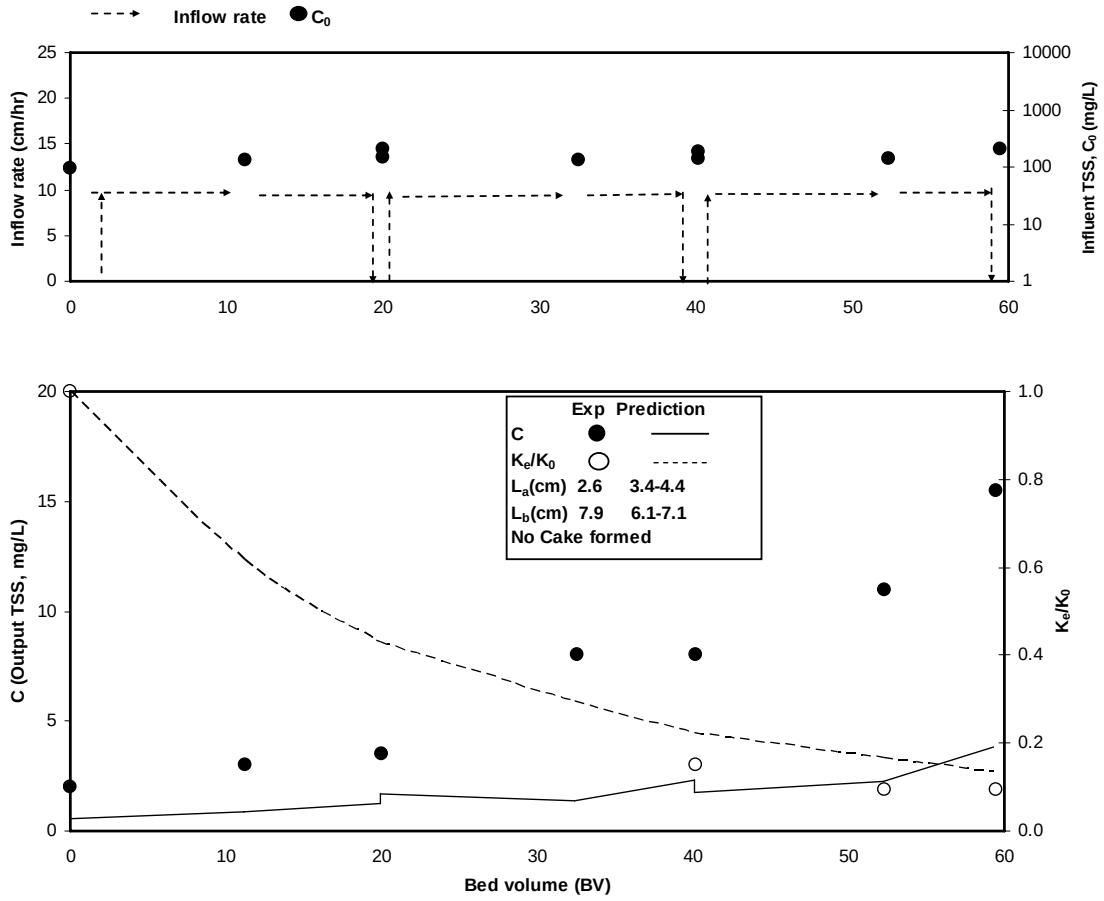

Figure 5-7. Comparison of effluent quality and hydraulic conductivity between the experimental data and model simulation for Trial 11 (Soil I / Montmorillonite).

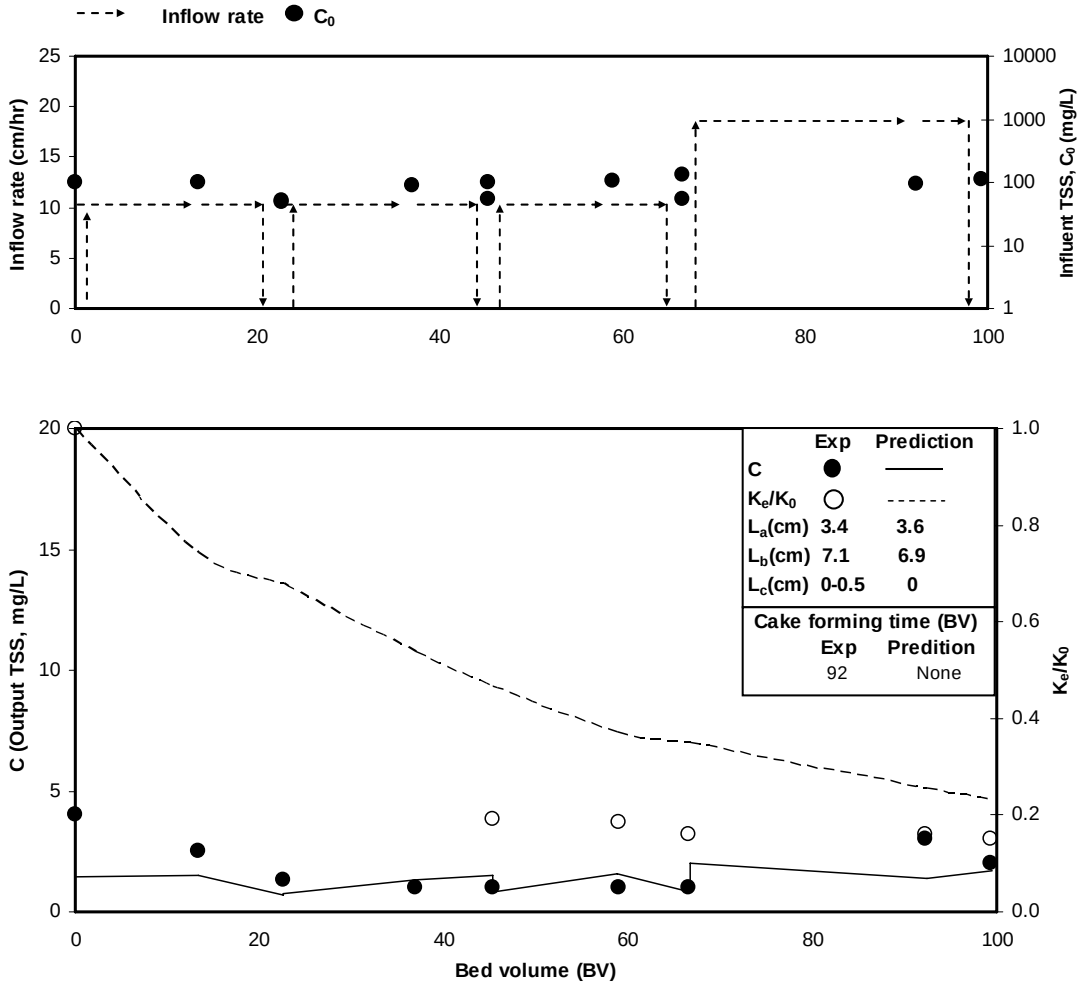

Figure 5-8. Comparison of effluent quality and hydraulic conductivity between the experimental data and model simulation for Trial 13 (Soil II / Kaolin).

In all 20 tests, L_b, the media depth in which 95% of captured particles were deposited, was estimated by the model as L_b=3.5-4.3 cm (out of 5.5 cm media depth) or 5.9-7.7 cm (10.5 cm media), as listed in Table 5-1. Media size analyses after the column tests demonstrated that most incoming particulates were captured within a 5 cm media depth (Chapter 4). As a result, both modeling theory and physical evidence suggests a very short penetration depth of incoming particles in the soil media.

5.4.2 Effects of TSS types and media characteristics

The TSS types exert a strong influence upon the permeability reduction of the media, which is quantified by the clogging parameter γ. For Soil I, the order of γ values (higher values indicate stronger tendency to clog the media) for different TSS types was Silt (calibrated γ = 14) < Sand (61) < Kaolin (200) < Montmorillonite (438); for Soil II, the order is the same, Silt (96) < Kaolin (216) < Montmorillonite (1319) (Table 5-2). Literature γ values were documented by Mays and Hunt (2005) through a variety of researchers and test conditions, and ranged from 10^1 to 10^4. In general, finer particles indicated a stronger tendency to clog the media, in concurrence with previous study regarding hydraulic conductivity and soil particle size (Boadu 2000). Montmorillonite showed a higher potential to clog the media than Kaolin, which agrees with its more pronounced swelling behavior as compared to Kaolin when they are wetted (Hillel 1998). This can lead to filling more media pore volume and more drastically reducing the permeability.

TSS type also influenced the cake formation, as indicated by $(K_e/K_0)_{bc}$. The sequence for different TSS are Montmorillonite (no cake formation) < Kaolin (calibrated $(K_e/K_0)_{bc}$=0.13) < Silt (0.31) < Sand (0.53) in Soil I (Table 5-2). In Soil II, cake layer formation only occurred in 2 trials out of 6 for Montmorillonite (Trial 20 is counted as 4 trials) and 1 out of 2 trials for Kaolin (Table 5-4). As a result, no calibrated $(K_e/K_0)_{bc}$ values are available for clays in Soil II, which suggests that the relatively larger particle size distribution of the Soil II media (d_{50} = 570 μm, Table 5-1) compared to Soil I (d_{50} = 340 μm) reduced the likelihood of the cake filtration. The calibrated $(K_e/K_0)_{bc}$ for Soil II/Silt was 0.34; no test of Soil II / Sand was

performed. These data indicate that coarser TSS particles had a stronger tendency to build up a cake layer, as previous studies have mentioned (McDowell-Boyer et al. 1986, Teng and Sansalone 2004). Teng and Sansalone (2004) have indicated that the ratio of the media diameter (d_m) to the street particle diameter (d_p), d_m/d_p (both d_{50}) of 10 is the index value to differentiate between cake filtration (d_m/d_p <10) and depth filtration (d_m/d_p >10). However, Trial 18 (Soil I / Sand) had a d_m/d_p of 1 to 5 (Table 5-1), yet significant TSS removal through depth filtration was still observed before build up of a cake layer.

Nonetheless, the value of d_m/d_p representing the "transition regime" from depth filtration to cake filtration will need further investigation for stormwater filtration. The predicted trend of the TSS capture mechanism shifting from depth filtration to cake filtration as the d_m/d_p decreases agrees with experimental results. This study indicates that both d_m/d_p and the media hydraulic conductivity reduction (in terms of K_e/K_0) during the filtration process affect the timing of the transition from the dominance of depth to cake filtration.

5.4.3. Polydispersed TSS

The model prediction of poly-dispersed TSS (Trial 19, 80% Silt + 5% Montmorillonite + 5% Kaolin + 10% Sand) performance using weighted average combinations of the calibrated parameters of Silt / Montmorillonite / Kaolin / Sand according to the input proportion (the composite parameters, Table 5-2) is presented in Figure 5-9. The simulation demonstrated a good prediction to the experimental data; the goodness of fit between the simulation and experimental data in terms of SSE/N is similar with other trials (Table 5-4), which implies that the linear

combination of performance parameters can be used in poly-dispersed systems for practical purposes.

However, a linear combination may not be the best fit for the parameters. The experimentally obtained parameters were prior estimated / calibrated for Trial 19, and compared with the composite parameters (Table 5-2), providing a better fit (Table 5-4). The calibrated clogging parameter γ, was found to be equal to 82, as compared to the value of 48 prior estimated from the weighted composite data. This suggests that the parameter combination may be non-linear in nature and the fine clay particles employ a stronger influence to clog the media compared to other particle textures, which agrees with the experimental description in terms of total solids loading (Chapter 4). However, it should be noted that the difference between γ values may also be attributed to sample variations and more trial replicates are desirable. The finer particles also dominated the cake layer formation, which was indicated by the lower calibrated $(K_e/K_0)_{bc}$ (= 0.20) than the weighted composite used for simulation $(K_e/K_0)_{bc}$ (= 0.31). As such, a best fit combination with more weight on the clay components is reasonable and warrants further studies.

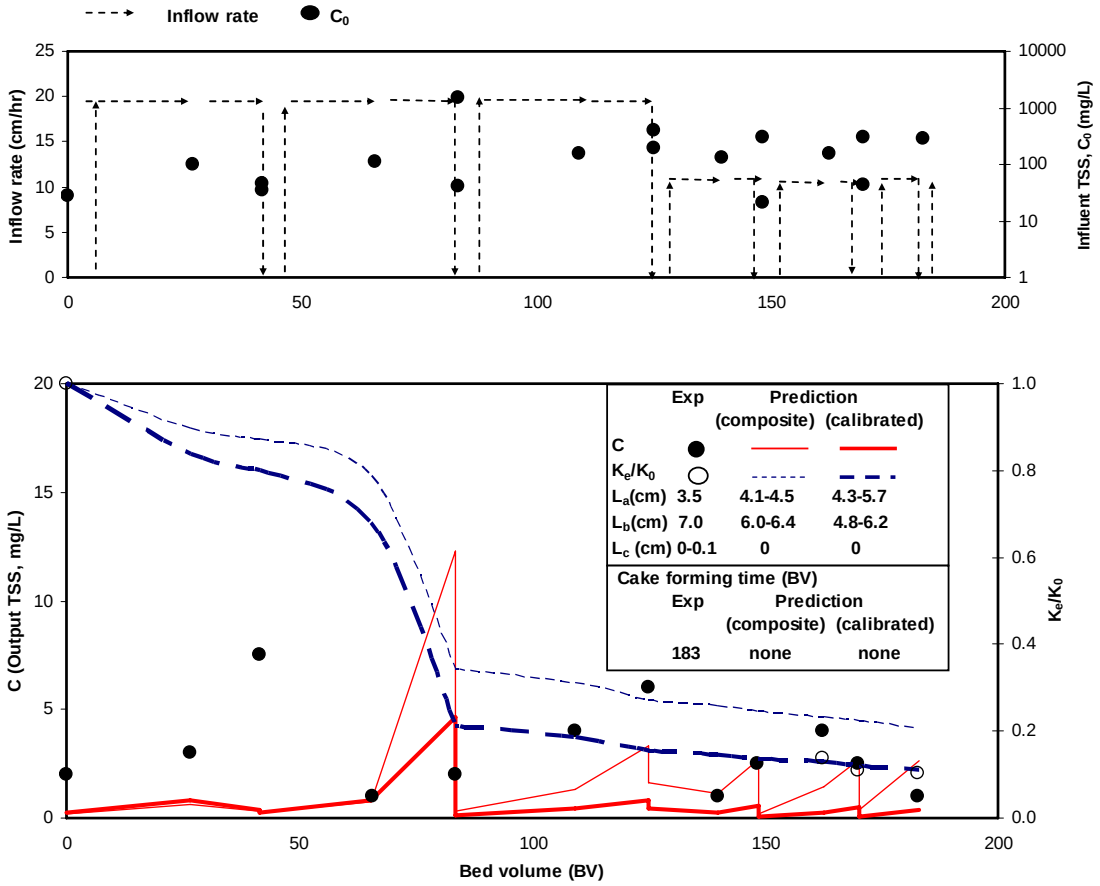

Figure 5-9. Simulation for Trial 19 (Soil I/Mixture) using the composite and calibrated parameters. Both simulations demonstrated good prediction for effluent TSS and permeability reduction.

5.4.4. Media replacement (hydraulic restoration) test

The simulation and experimental data of the hydraulic restoration test (Trial 20, Soil II / Montmorillonite) are presented in Figure 5-10. The clean bed hydraulic conductivity K_0 was equal to 72 cm/hr. After renewing the top 3 cm, 5 cm, and 7 cm of the media (10.5 cm total), the measured hydraulic conductivity was restored to 36, 39, and 43 cm/hr, respectively. The model underestimated the conductivity restoration for the top 3 cm and 5 cm media renewal (predicted to restore to 15 and 12 cm/hr, respectively), but produced a better prediction for the top 7 cm renewal (which

was near to the predicted working zone depth L_b = 7.2 cm), in which the model predicted hydraulic conductivity restoration to 52 cm/hr. The model predictions for C, K_e and L_c in Trial 20 exhibited similar or poorer goodness of fit with experimental data compared to other trials (Table 5-4). The replacement of media likely disturbed the media structure and resulted in change of the media behavior.

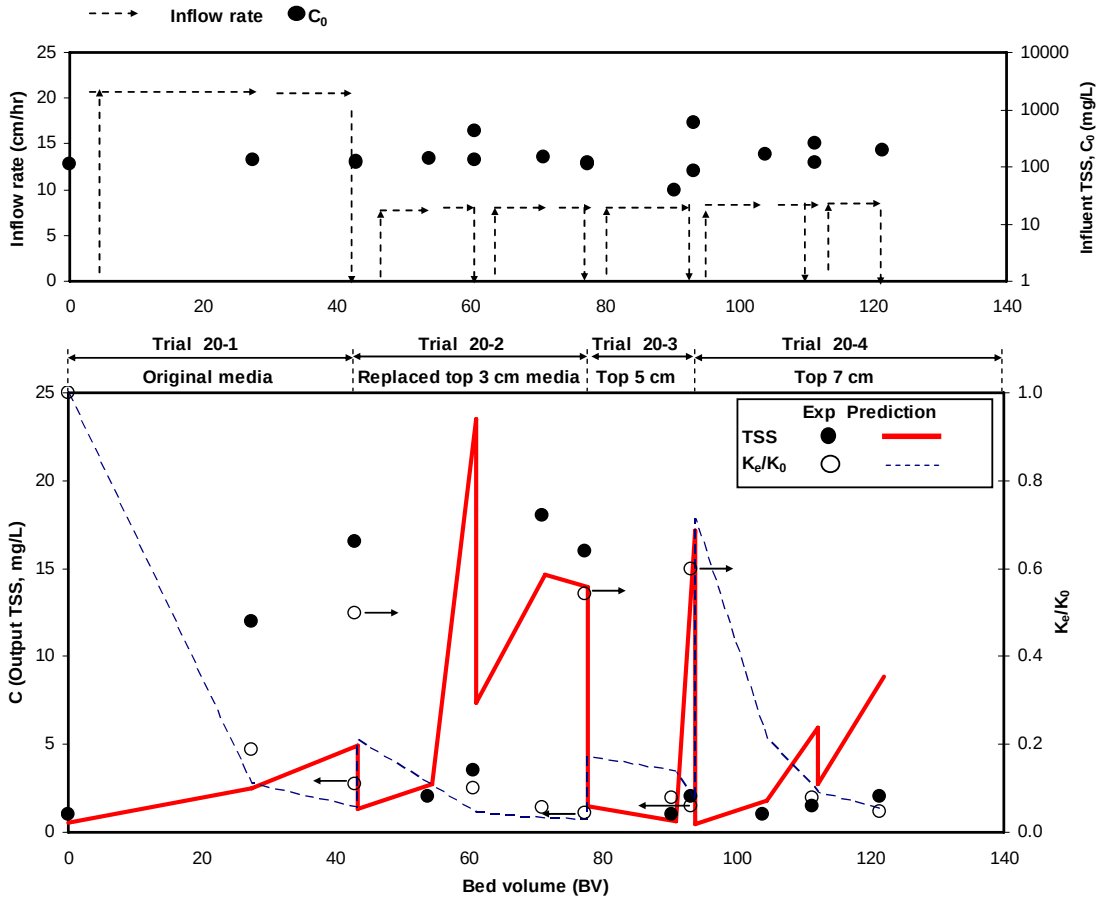

Figure 5-10. Simulation and experimental data for the hydraulic conductivity restoration test (Trial 20). Media depth= 10.5 cm, clean bed conductivity K_0 = 72 cm/hr. After removal and refilling for top 3 cm (20-2), 5 cm (20-3), and 7 cm (20-4) of the media, the hydraulic conductivity was restored to 36, 39, and 43 cm/hr, respectively.

5.4.5. Filtration mechanisms

Table 5-5 lists the experimental TSS loadings before cake layer formation and the overall loadings until filter failures. Assuming that the cake filtration mechanism became operative after the cake layers were formed, the percentages of TSS treated via the depth filtration and cake filtration can be estimated. As previously mentioned, the d_m/d_p values had strong influence on particle removal mechanisms, as well as the permeability reduction during the filtration process. The percentages of the TSS captured via cake filtration were significant (24±23% average, range = 0-80%), which implies that the captured TSS spatial profile is even more vertically sharp than the estimate based only on depth filtration theory, as Chapter 4 discussed.

Table 5-5. Profile of the TSS loading treated via depth and cake filtration.

Trial #	Media	TSS	$d_m/d_{p\,(-)}$	TSS loading (kg/m^3)			Filtration mechanism (%)	
				Overall	Depth filtration	Cake filtration	Depth filtration	Cake filtration
1	Soil I	Kaolin	>340	2.4	2.0	0.5	81	19
2			>340	1.5	1.0	0.6	64	36
3			>340	3.3	2.6	0.6	81	19
4			>340	3.3	2.4	0.8	75	25
5			>340	2.3	1.4	0.9	61	39
6			>340	2.6	1.2	1.3	48	52
7			>340	1.2	1.0	0.2	82	18
8			>340	5.5	5.0	0.6	90	10
9			>340	3.7	2.3	1.3	64	36
10	Soil I	Montmorillonite	>340	0.9	0.9	0.0	100	0
11			>340	0.9	0.9	0.0	100	0
12	Soil II	Kaolin	>570	1.0	1.0	0.0	100	0
13			>570	1.0	0.6	0.4	60	40
14	Soil II	Montmorillonite	>570	0.9	0.9	0.0	100	0
15			>570	0.4	0.4	0.0	100	0
16	Soil I	Silt	11	14.5	11.8	2.7	81	19
17	Soil II	Silt	190	6.3	1.3	5.0	20	80
18	Soil I	Sand	1-5	13.0	5.1	7.9	39	61
19	Soil I	Mixture	1->340	3.7	3.5	0.2	94	6
20	Soil II	Montmorillonite	>570	-	-	-	-	-
							average	24

5.4.6. Discussion on the media permeability

Bioretention can also be effective removing nutrients such as nitrogen and phosphorus species from runoff via complex chemical and biological processes (Davis and McCuen 2005), which need longer hydraulic retention time for infiltrating runoff. Hunt et al. (2006) attempted to improve bioretention performance for nitrogen removal by employing low permeability media with hydraulic conductivity of 0.2 to 7.9 cm/hr (depth = 1.2 m) and / or creating an anoxic media zone (using upturned elbows in underdrain pipes), and obtained maximum annual nitrogen mass removal of 40%. However, as discussed above, bioretention capture of TSS from runoff reduces the media permeability and may cause media clogging and filter failure. As such, the design of media hydraulic conductivity may be a trade-off between runoff nutrient removal and TSS treatment capacity.

5.5 Scenario Analysis for Long Term Bioretention Performance

A bioretention facility located along the Anacostia River in the southeast quadrant of the District of Columbia, USA (Chapter 4), was used in the scenario analysis for long term bioretention performance in this study. The design drainage area is 0.077 ha. The facility has sides of 2.9, 5.4, and 6.3 m (trapezoid-shaped), and a media depth of about 1.1 m. The original media consisted of 50% (by volume) sand, 30% top soil, and 20% mulch. Seven storm events were monitored using grab samples for cell input and output runoff from January 2005 to May 2006 with subsequent TSS analyses. The observed input TSS level was 160 mg/L, and the TSS removal efficiency was 73% (both are geometric means). It is assumed that annual precipitation to the facility is 102 cm (Washington DC, NWS 2006), the average

density of the urban particles = 2.3 g/cm^3, and the runoff coefficient of the drainage area = 0.9. As a result, the estimated runoff loading to the facility is 700 m^3/yr, the TSS loading is 113 kg/yr (0.05 m^3/yr particle volume), and the volumetric specific deposit at 73% removal efficiency is 1.9x10^{-3}/yr.

Using representative clogging parameters from different trials in the column tests (γ = 82 (Mixture, Trial 19), 96 (Silt, Trial 17), 200 (Kaolin, Trial 8), and 1319 (Montmorillonite, Trial 14, Table 5-2) and Equation (5-7), the long term hydraulic conductivity reduction (K_e/K_0) can be estimated, as presented in Figure 5-11. If the clogging behavior of the incoming urban particles is similar to the mixture or silt used in the laboratory tests, the field permeability is predicted to decrease to 50% of the original value within the first three years, and to 25-30% by the end of the fifth year. Additionally, laboratory studies suggest the formation of cake at (K_e/K_0) of about 0.2 to 0.3, shown as the shaded area in Figure 5-11. This is predicted occur at the end of the fifth year. If the clogging behavior of the incoming urban particles is similar to clays, the clogging and cake formation is predicted occur at the end of the second year. However, media clogging was not noticed during the 1.5-yr monitoring period. The vegetation and fauna (e.g., earthworms) present in the bioretention facility may contribute in loosening the media structure and maintaining the permeability. As such, the clogging parameter γ obtained from the laboratory tests may be an underestimate for media permeability prediction. This physical model (Equations (5-6) and (5-7)) dictates the media hydraulic conductivity to decrease with constant and positive γ values; however, media biota function may render the media with diminishing or even negative γ values, which help maintain the media permeability.

Relationships between γ and media flora and fauna activities for media clogging warrant further studies.

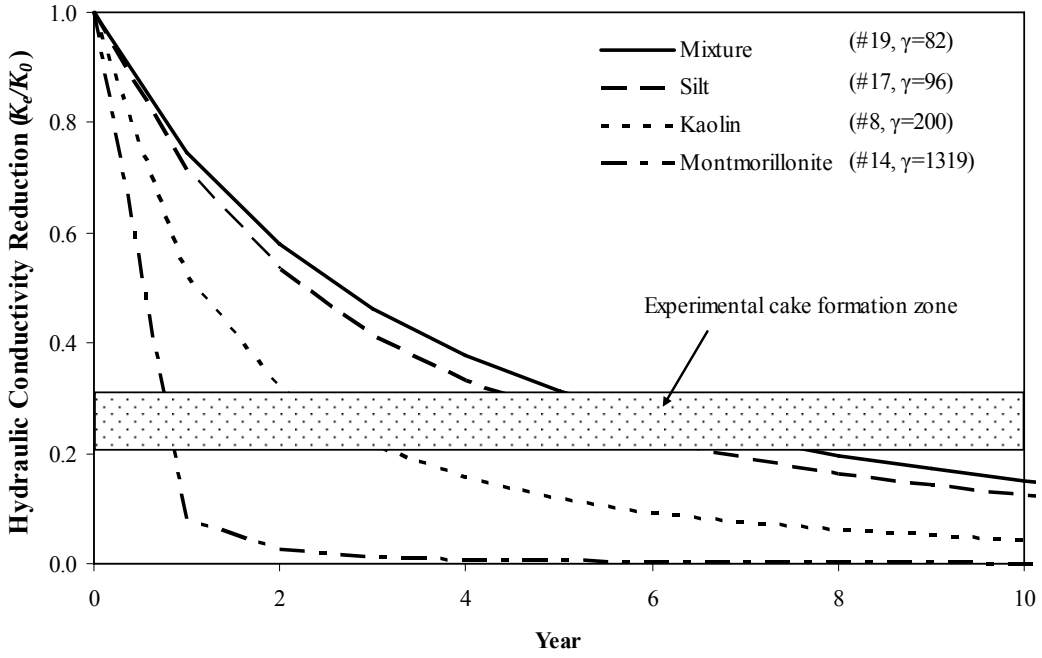

Figure 5-11. Long term estimate of the permeability reduction for the field bioretention filter using different clogging parameters γ. The shaded area represents projected cake layer build-up.

5.6 Application of the Clogging Parameters in Field Bioretention

Following Section 5.5, this section endeavors to illustrate the application of different clogging parameters γ in field bioretention. From the bioretention filtration theory developed in this study, bioretention media permeability depends on the designed treatment capacity, facility layout, and the clean filter bed hydraulic conductivity. Davis and Ravirajan (2005) measured the hydraulic conductivity of core media samples for newly constructed bioretention facilities using a constant head

permeameter; the results were between 115 to 356 cm/hr. Assuming a bioretention cell has a designed water quality volume for a 2.54 cm rainfall, with a 5% cell surface area to drainage area ratio (MDE 2000) implies a 51 cm/hr designed treatment capacity. The cell would have a ponding storage depth of 15 cm (0.5 ft) and a media depth of 76 cm (2.5 ft) (MDE 2000), producing a maximum hydraulic gradient of 1.20. As a result, the minimum required media hydraulic conductivity is $K = 43$ cm/hr.

Assume that the cell had a clean bed hydraulic conductivity $K_0 = 115$ cm/hr, which produces a minimum $K/K_0 = 0.37$. With data modeling the relationship between the clogging parameters γ and particulate loadings of the bioretention cell (similar to those shown in Figure 5-11), the bioretention maintenance frequency for clogging prevention can therefore be determined. For example, if the illustrated bioretention cell has a particulate loading and clogging relationship similar to that of Figure 5-11, and the incoming particles have similar clogging behaviors with silt or mixture in the column tests, a $K/K_0 = 0.37$ will lead to a 4-yr periodic media maintenance for clogging prevention. If the clogging parameters γ are appropriately incorporated with media biota functions, the media conductivity prediction can become more accurate.

5.7 Summary

The proposed theory in this study is the most comprehensive model representation of stormwater BMP filtration to date, addressing particulate penetration, permeability decrease, and cake layer formation. By applying this model to laboratory and field

test results employing different media / input particle combinations, the dominant filtration mechanism (cake and depth filtration), the fate of media (breakthrough-limited or clogging-limited), and possible media maintenance procedures for bioretention are obtained, providing information for modifying current design and maintenance procedures for bioretention.

Chapter 6: Media Analysis of Field Stormwater BMP Filters

6.1 Introduction

Filtration BMPs include bioretention facilities (Davis et al. 2001b, 2003), infiltration basins (Dechesne et al. 2005), sand filters (Urbonas 1999 and Barrett 2003), and others. Mechanisms of pollutant removals in these filters include sedimentation, filtration, adsorption, precipitation, and possibly biological transformations. A major advantage inherent to many filtration BMPs is an ability to remove pollutants at both particulate and dissolved forms through adsorptive filtration (Davis and McCuen 2005).

However, issues related to long-term accumulation of pollutants captured in BMP filters have been only minimally addressed. Heavy metals are found in urban runoff originating from a variety of sources (Davis et al. 2001a), and laboratory studies have indicated excellent removal of metals using bioretention media (Davis et al. 2003). Studies regarding total phosphorus (TP) removal in stormwater BMPs were divided, from good removal (e.g., Barrett 2003 in Austin Sand Filter, Davis et al. 2006 in bioretention), variable removal (Hsieh and Davis 2005 in bioretention), to export (Dietz and Clausen 2005, 2006 for bioretention, Pradhan 2006 for bioinlets). Nonetheless, the fate and spatial profiles of captured toxic and persistent pollutants within BMP media and the possibilities of re-entrainment into infiltrating runoff are of great concern with respect to BMP performance, as well as to design and maintenance issues. Top-heavy metal pollutant profiles have been noted in media of stormwater infiltration basins (Dechesne et al. 2005), and the profile can have major

implications on pollutant buildup and the degree (depth) of maintenance required for a BMP. However, this pollutant profile needs to be authenticated for other common BMPs and mechanisms that are responsible for the profile have not been adequately discussed. This chapter presents the results of media analyses for heavy metals and phosphorous for a bioretention cell and a District of Columbia Sand Filter, which were implemented over 1 yr-period in the Anacostia River watershed in the District of Columbia, USA.

6.2 Methodology

6.2.1. BMP site description and media collection

The bioretention cell and sand filter are located along the Anacostia River in the southeast quadrant of the District of Columbia, USA (Figure 6-1). The bioretention cell (DC bioretention, design drainage area = 0.077 ha) is located in an active parking lot. The cell is trapezoid-shaped (sides = 2.9, 5.4, and 6.3 m), with a media depth of about 1.1 m. The original media consisted of 50% (by volume) sand, 30% top soil, and 20% mulch. No official document is available for the exact date for the cell completion, however, the best estimate is Summer 2001.

The District of Columbia sand filter (DC sand filter) is located in the backside service area of a strip shopping mall. It is contained in a three-chamber underground concrete vault. The first is an entrance sedimentation chamber. The second chamber is the sand filter bed, which consists of three layers. The top layer is 15 cm of gravel, the middle is 35 cm of fine sand, and the bottom underdrain layer is gravel (its thickness data was unavailable), each separated by a filter cloth. No official document is available for the exact date for the filter completion, but a cell full

restoration (replacement of all filter media) was performed before the monitoring began. The media samples were taken from the top two layers. Details of the two BMPs are shown in Figures 6-2 and 6-3.

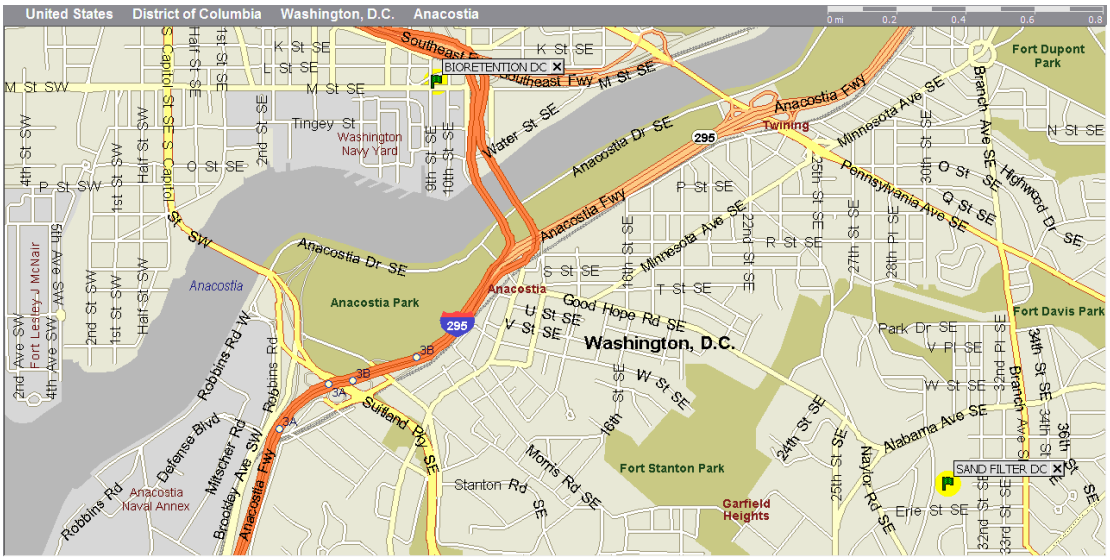

Figure 6-1. The locations of the two BMPs monitored in this study in District of Columbia, U.S.A. The DC bioretention cell is on the northwest side of Anacostia River; the DC sand filter is on the southeast side (the map is from Microsoft Streets and Trips).

A Hoffer soil sampler corer (2 to 2.54 cm inner diameter, 90 cm length, BFK manufacturer, Ohio) was used in the sampling of the bioretention media. The corer was submerged in 15% Na_2-EDTA solution (Fisher Scientific) overnight before it was used, flushed with deionized water and air dried. The core samples were taken from the surface to 85-90 cm deep. Each 10 or 20 cm segment was separated with a pre-cleaned knife to examine the vertical profile of pollutants (heavy metals and phosphorus) in the cell matrix. An additional sample was taken from an obvious collection of street particles (which has a different color than the media) near one runoff entrance. The sand filter media samples were collected by hand from the top

two layers of the media. Nitrile gloves were worn during all sampling and the collected samples were double bagged. Media samples were air dried, sieved at 2-mm, and heated at 103 to 105 ˚C for three days before further analysis.

Figure 6-2. The DC bioretention cell investigated in this study. The core samples for media analysis were taken in area A and C, B is the manhole for effluent discharge.

The first media samplings were carried out in December 2004 for the bioretention cell and June 2005 for the sand filter. The second media sampling for both BMPs occurred in December 2005, employing the same procedure as the first at the same general locations

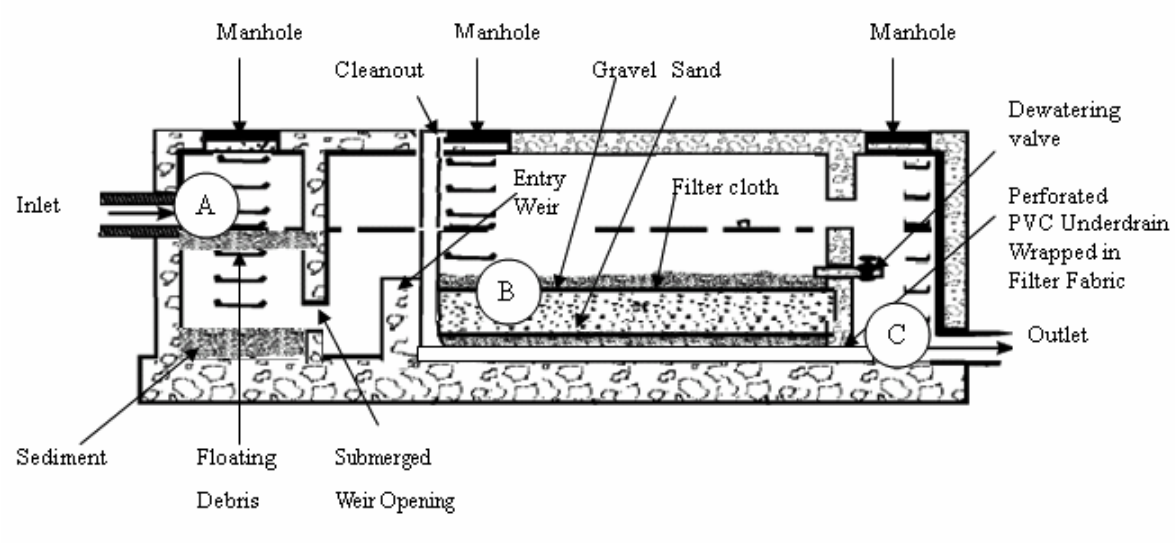

Figure 6-3. The schematic of the DC sand filter investigated in this study. The influent runoff enters at A. The effluent water discharges at C, and the core samples for media analysis were taken in filter bed B. The top filter bed layer was gravel, over a fine sand layer, separated by a filter cloth. The thickness of top gravel layer was 15 cm. The supportive fine sand layer was 35 cm.

6.2.2. Characterization of media samples

The pH of the media was determined by adding 25 mL of deionized water to 5 g of a medium sample, stirring intermittently for 1 h, and then left standing for 0.5 h. Approximately 400 g of soil from the second bioretention media sampling was sent to the University of Delaware Soil Testing Program for characterization.

Five trace metals (beryllium, cadmium, copper, lead, and zinc) were analyzed employing a sequential extraction technique for the media. The procedures are modified from the metal extraction optimization process from Ahnstrom and Parker's work (1999) for cadmium (Table 6-1). Unless otherwise noted, all chemicals used in the sequential extraction were American Chemical Society reagent-grade or better. All labware were acid-washed and thoroughly rinsed with deionized water. For each sample, about 0.5 g of dried media was used. At the end of each extraction, the

sample was centrifuged at 3000 rpm for 10 min. Afterwards, the supernatant and residue were separated by a 0.2 μm membrane disk filter (Pall Corporation). The supernatant was diluted to 50 mL with deionized water for the subsequent metal analyses.

Table 6-1. Sequential extraction scheme for fractionation of trace metals (beryllium, cadmium, copper, lead, and zinc) within the BMP media.

Step	Fraction	***Extraction procedure***	***Solid/liquid ratio (g/mL)***
F1	*"Soluble-exchangeable"*	0.1 M $Sr(NO_3)_2$ (4 hr)	1:16
F2	*"Sorbed-carbonate"*	1 M Na-acetate (pH 5, 5 hr)	1:16
F3	*"Oxidizable"*	5% NaOCl (pH 8.5, 1.5 hr @ 90-95 ^oC)	1:8
F4	*"Reducible"*	0.2 M oxalic acid + 0.2 M NH_4 oxalate + 0.1 M ascorbic acid (pH 3, 1.5 hr @ 90-95 ^oC)	1:25
F5	*"Residual"*	Aqua regia (HCl + HNO_3, 1.5 hr @ 70^oC)	1:16

Between each step the residue was suspended with 1.5 mL of 0.1 M NaCl to displace entrained solution and minimize metal re-adsorption. A drop of toluene was added to the F4 extract to inhibit bacteria growth (Ahnstrom and Parker 1999). Metal analyses were carried out on a Perkin-Elmer 5100ZL atomic absorption spectrophotometer. Beryllium, cadmium, copper, and lead concentrations were determined on the furnace module, according to Standard Method 3110 (APHA 1995). Zinc concentrations were determined on the flame module using an air /

acetylene flame, according to Standard Method 3111 (APHA 1995). Analytical standards were prepared using 1000 mg/L stock solutions for each metal (Fisher Scientific or VWR Scientific Products).

Water soluble phosphorus (WSP) was quantified by mixing 0.5 g of media sample with 5 mL of deionized water for 1 h (Maguire and Sims 2002). Mehlich III extractable P (M3P) was determined by shaking 0.5 g of media sample with 5 mL of Mehlich III reagent (0.2 N CH_3COOH + 0.25 N NH_4NO_3 + 0.015 N NH_4F + 0.013 N HNO_3 + 0.001M EDTA) for 15 min (Mehlich 1984). The residue and supernatant were separated by centrifugation and filtration as in the extractions above, then diluted to 40 mL. Aqueous P concentrations in all extracts were analyzed spectrophotometrically at 882 nm using the Murphy and Riley (1962) method. The P standards were made using a phosphate standard solution of 50 mg/L as P (Labchemical Inc.).

Duplicates were employed for each media sample extraction. Reagent blanks for all extractants were analyzed in parallel with samples and found to be below the detection limits of metals and phosphorus in all cases. During analyses, a standards check was performed for every ten samples and only deviations less than 5% were accepted. The quantification limits were 1 mg/kg (Be), 0.2 mg/kg (Cd, Cu, and Pb), 5 mg/kg as P (WSP and M3P), and 5 mg/kg (Zn).

6.3 Results and Discussion

6.3.1. Media characteristics

Characteristics of soil media in the DC bioretention cell are listed in Table 6-2 (measured by the University of Delaware Soil Testing Program). The soil is a sandy

loam with a pH of 6.5 and an organic matter content of 2%. Measurement of pH at various layers yielded pH 6.8-6.9 for the surface street particle layer, 6.8 in the top 10 cm layer, 5.8-6.0 for the depth of 10–60 cm, and 4.9–5.3 for the depth of 60–90 cm. The higher pH in the surface and top layers may be attributed to runoff of concrete particles, and residues of fill materials (Smolders and Degryse 2002). Sansalone and Buchberger (1997) found runoff pH to be buffered to 6.7-7.5 by Portland cement concrete pavement. The pH of the sand filter media was 5.6 to 5.7.

Table 6-2. Characteristics of the soil media in the bioretention cell, December 2005.

Characteristics	Level	Characteristics	Level (mg/kg)
Soil texture:		Mehlich III extraction:	
Sand (%)	79	M3-Ca	738
Silt (%)	11	M3-Mg	84
Clay (%)	10	M3-Mn	16
Texture	Sandy loam	M3-Zn	7
		M3-Cu	2
pH	6.5	M3-Fe	271
Organic matter (%)	2	M3-B	1
Mehlich III extraction (mg/kg):		M3-S	6
M3-P	39	M3-Al	335
M3-K	50		

Media samples from two locations were assumed representative of captured street particles. One location was the surface layer at the entrance gravel zone of the DC

bioretention cell. The other was the upper layer of the DC sand filter, in which the gravel media are larger than 2 mm. As a result, when processed with a 2-mm sieve, material passed through the sieve was almost all accumulated street particles from runoff, and not original BMP media. Street particles consist of a mixture of naturally occurring sediments and anthropogenic materials such as worn tire treads / brake pads and atmospheric deposition solids. Previous studies have demonstrated that street particles are a significant contributor to stormwater runoff pollutants such as heavy metals (Lau and Stenstrom 2005, Brown and Peake 2006).

6.3.2. Pollutant extraction results

Zinc profile and sequential extraction results for the DC bioretention media are shown in Figure 6-4. A top-heavy profile is clearly noted, especially in the more recent profile, which agrees with previous related studies. Turer et al. (2001) found that soil heavy metal contamination along an urban highway was concentrated in the top 15 cm layer (Pb: 1989 mg/kg, Zn: 1430 mg/kg) and fell off notably with depth. Dechesne et al. (2005) also reported similar pollutant profiles for soil columns collected from stormwater infiltration basins (maximum Cu: 355 mg/kg, Pb: 930 mg/kg, Zn: 2605 mg/kg). In this study, high concentrations occurred in the surface street particle layer (e.g., 111-532 mg/kg of Zn) and the top 10 cm layer. Below 10 cm, the zinc levels were as low as expected for background soil concentrations (overall 8-138 mg/kg, Logan and Miller 1983, Deng and Jennings 2006, NRCS 2005). Zinc enrichment over the one-year sampling interval primarily occurred in the surface street particle layer (421 mg/kg/yr). Similar profiles also were seen for lead (Figure 6-5, 399-660 mg/kg) with accumulation of 260 mg/kg/yr in the surface layer;

background Pb levels are 4-209 mg/kg. Upward migration of the heavy metals from plant uptake had been considered as a part of the metal enrichment at the media surface; however, literature indicates that the upward flux is minor in bioretention media (Sun and Davis 2007).

The copper values are presented in Figure 6-6, which were close to background concentrations (1-49 mg/kg). The surface accumulation layer was less well-developed at 29-75 mg/kg and copper affiliated with the lower media layers decreased over one year. A parallel water quality monitoring study was conducted for the two BMPs during approximately the same period (1.5 yr) using grab samples, (auto-samplers were not used in the two BMPs because of site conditions, and therefore the measured pollutant levels did not represent as EMCs as in Chapter 3), these values are listed in Appendix 5. Grab sample results demonstrated effluent copper levels higher than the influent in 4 out of 7 monitored events for the DC bioretention cell, confirming the release of copper from the media. The phenomena agree with the EMC results for copper concentrations at Cells CP and SS (Chapter 3). Literature indicates that the affiliation between copper and soil media is weaker than that of lead and zinc, copper also tends to associate with soil organic matters and thus is more likely to be dissolved out into soil solution than lead and zinc (Sauvé et al. 2000).

Heavy metal media profiles in the DC sand filter were similarly top-heavy (Figures 6-7 to 6-9). The upper street particle layer had the highest zinc levels (Figure 6-7). The profile and accumulation of copper for the DC sand filter were similar (Figure 6-8). The lead profile in the sand filter was also top-heavy, but no

significant accumulation occurred during the sampling interval (Figure 6-9). Beryllium and cadmium levels detected in the media of the two BMPs were minor (Be: < 1.0 mg/kg, and Cd: < 4.2 mg/kg) and are not discussed further.

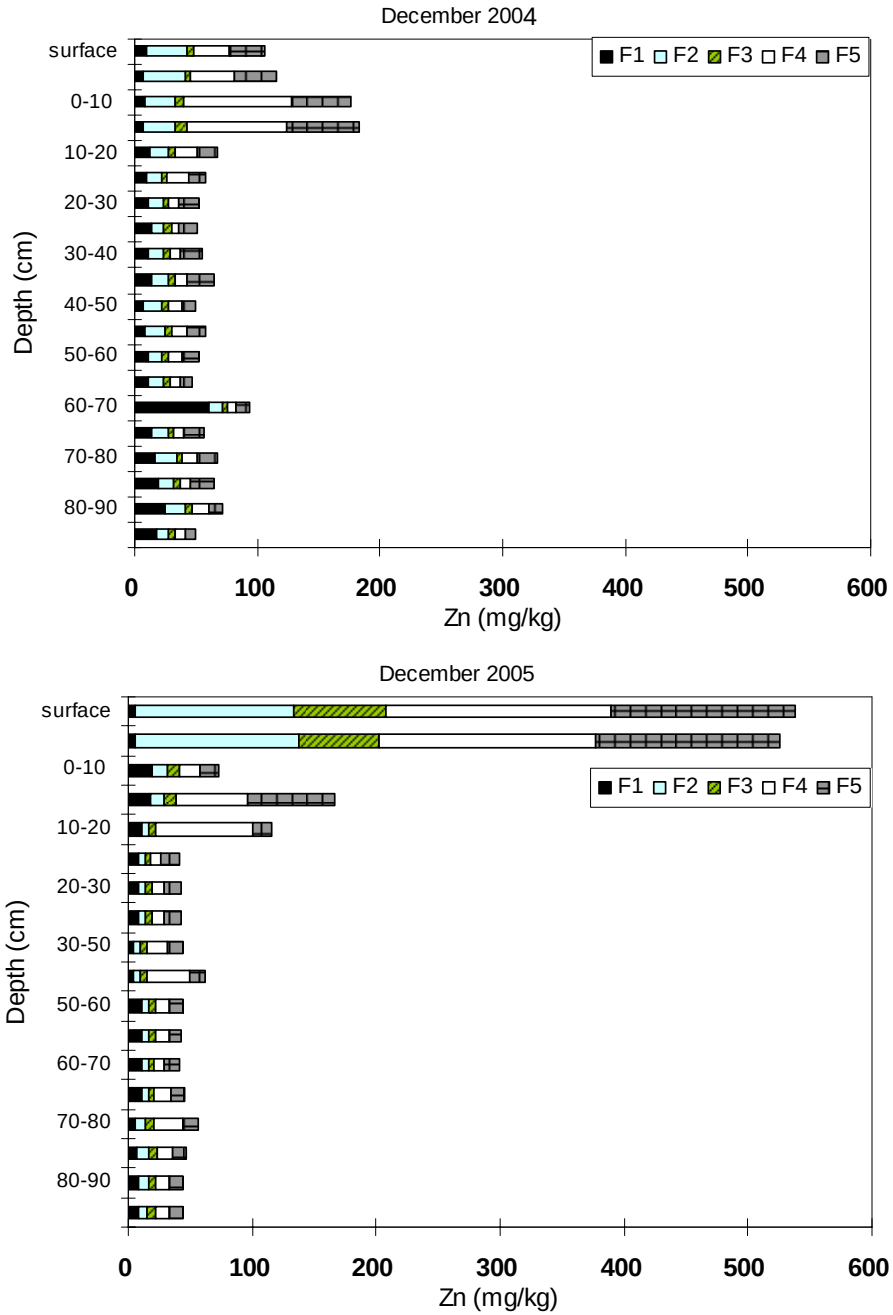

Figure 6-4. Zinc profiles in the DC bioretention cell, top-heavy in most cases. The surface layer is primarily captured street particles. Significant zinc enrichment occurred on the surface layer during one year.

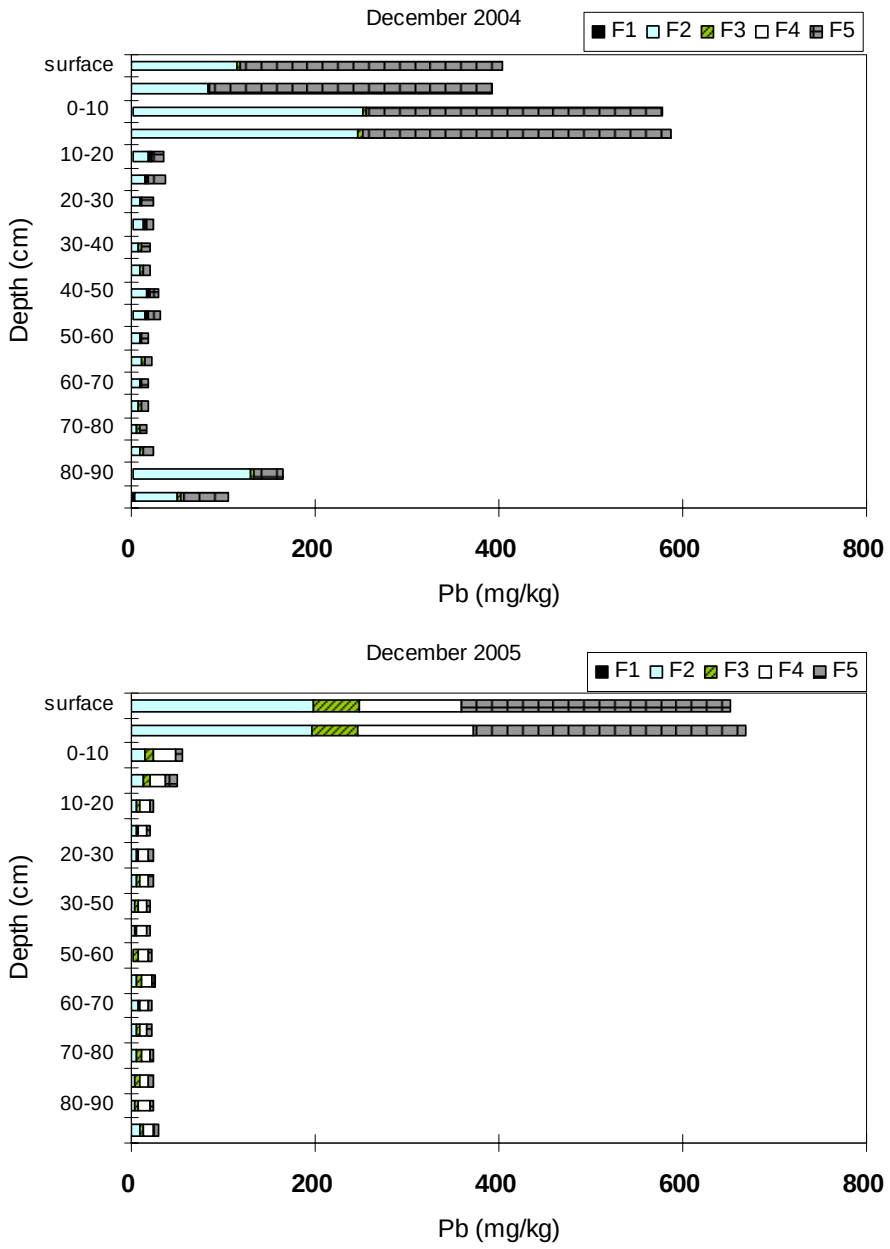

Figure 6-5. Lead profiles in the DC bioretention cell. The surface layer is primarily captured street particles. Lead accumulations on the surface layer were observed.

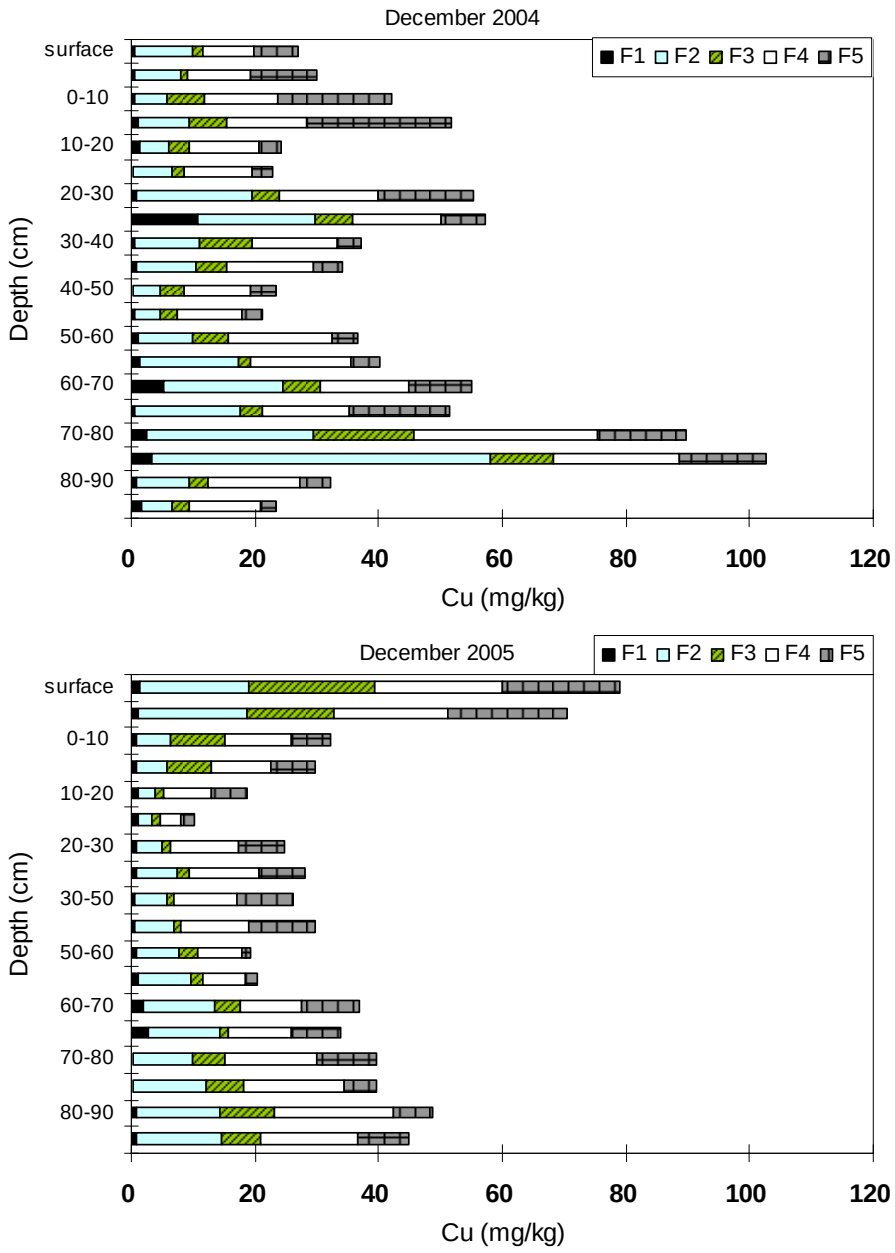

Figure 6-6. Copper profiles in the DC bioretention cell. The surface layer is primarily captured street particles. The concentration- depth profile of copper converted to a top-heavy profile during the one-year monitoring period.

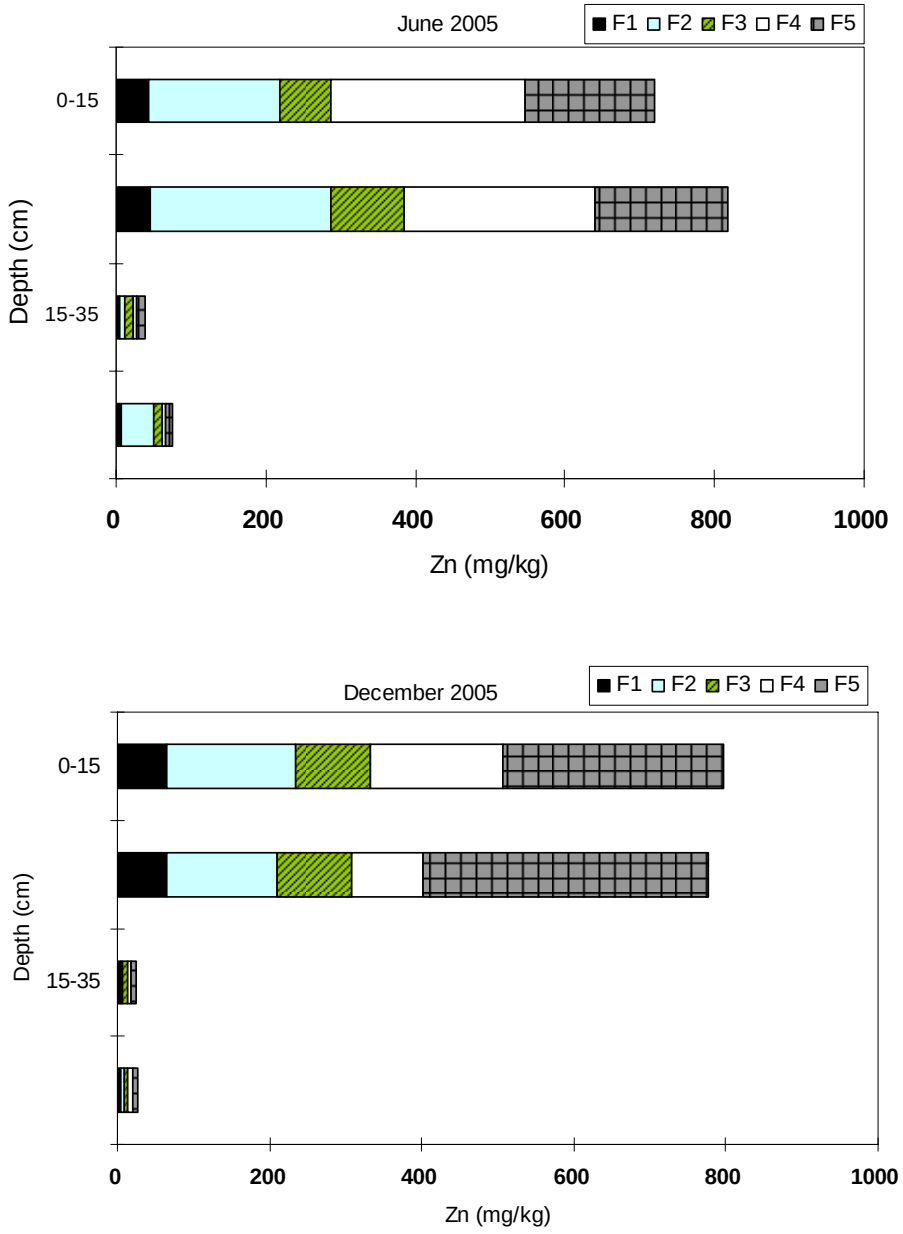

Figure 6-7. Zinc profiles in the DC sand filter, top-heavy in all cases. The surface layer is primarily captured street particles. A significant amount of zinc became bound more tightly from F4 to F5 in the upper layer within six months.

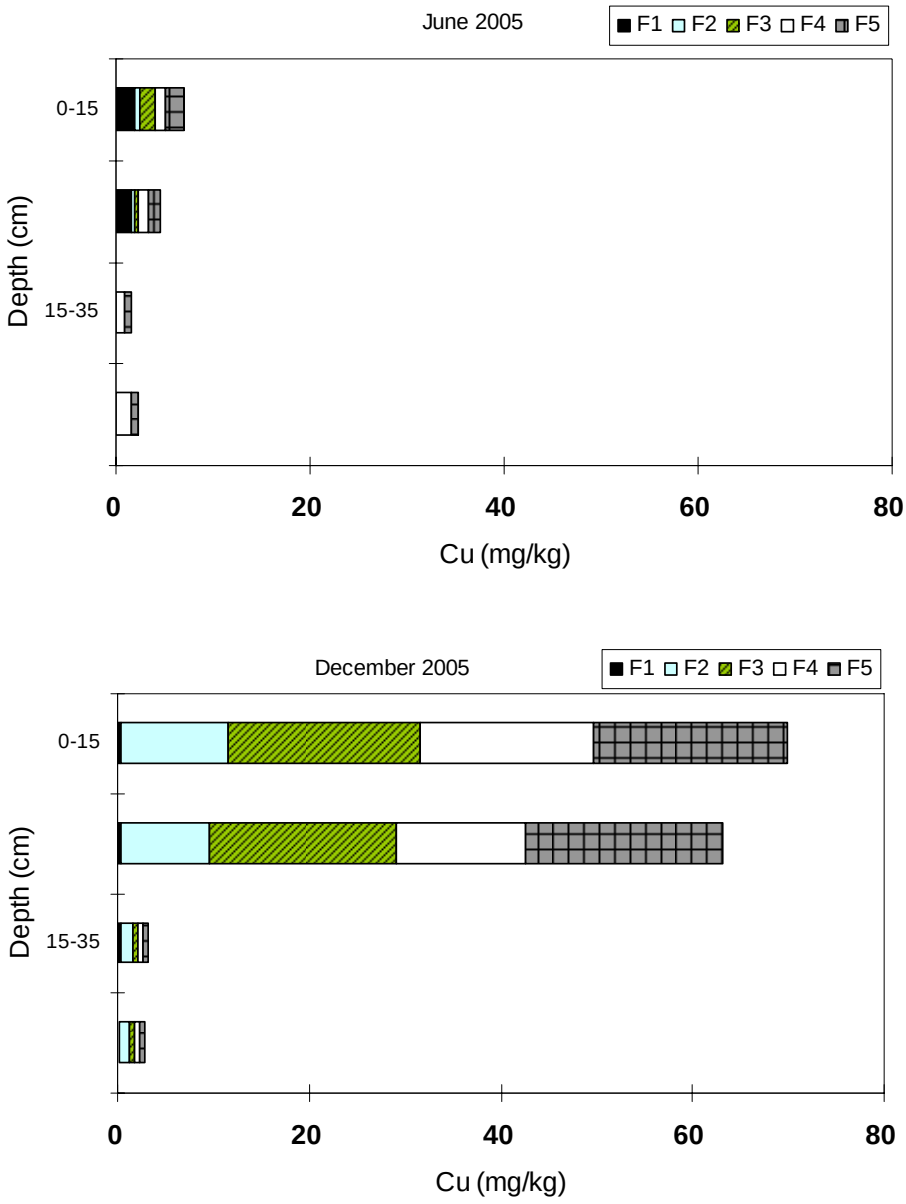

Figure 6-8. Copper profiles in the DC sand filter, top-heavy in all cases. The surface layer is primarily captured street particles. Copper accumulation occurred in the upper layer. The fraction of the most mobile copper (F1) shifted to the more strongly-bound fractions.

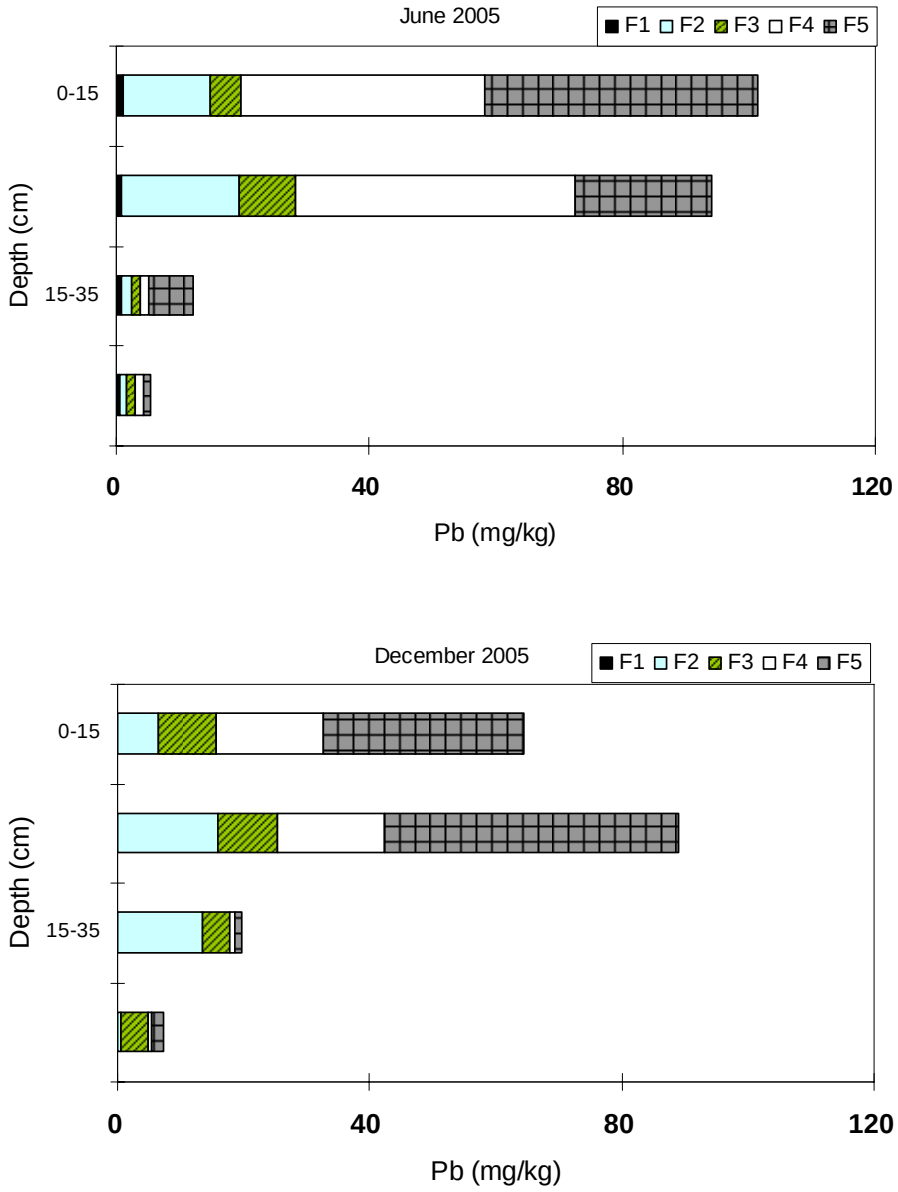

Figure 6-9. Lead profiles in the DC sand filter, top-heavy in all cases. The surface layer is primarily captured street particles. No significant accumulations of lead occurred.

The phosphorus profiles of the DC bioretention cell are presented in Figure 6-10. The profiles were rather uniform compared to those of the metals, implying weaker bonding between phosphorus and the street particles / soil media. Significant reduction in media phosphorus was found between the two samples. Uniform

phosphorus profiles and significant media phosphorus losses in the DC sand filter over 6 months (Figure 6-11) were similar to those noted in the DC bioretention cell. In the water quality monitoring previously mentioned, the effluent total phosphorous (TP) levels were often higher than the influent in the two BMPs (5 out of 7 events for DC bioretention cell, and 2 out of 6 for DC sand filter), which agrees with the EMC results at Cells CP and SS (Chapter 3). Although the effluent concentrations were low (effluent levels = 0.30-0.83 (bioretention) and <0.05-0.26 (sand filter) mg/L as P).

A descriptive model illustrating heavy metal and phosphorus capture in a filter-type BMP is depicted in Figure 6-12. The incoming runoff carries both dissolved and particulate-bound pollutants. Total metal levels in urban runoff generally follow the order: Zn (20-5000 μg/L) > Cu ≈ Pb (5-200 μg/L) > Cd (<12 μg/L) (Davis et al. 2001a). Sansalone and Buchberger (1997) reported that cadmium, copper, and zinc are mainly in dissolved form, while lead is primarily particulate-bound in urban roadway stormwater runoff. Tire-tread material, which contains about 1 wt% of zinc (Councell et al. 2004), is worn and flushed with runoff. Studies examining partitioning of these four metals indicate an affinity order of Pb > Cu> Cd > (or ≈) Zn for surfaces of soils (Sauvé 2002, Sauvé et al. 2003, Covelo et al. 2004), and sediments (Howari and Banat 2001).

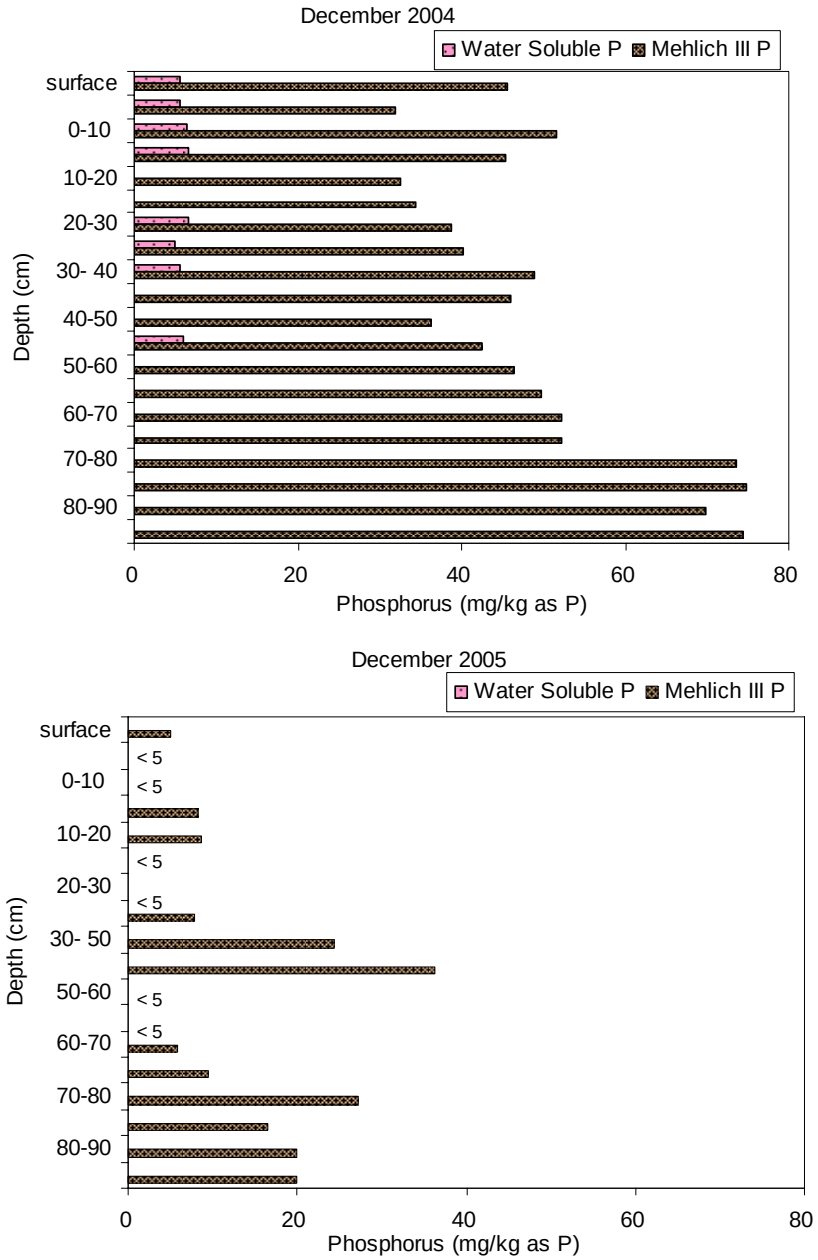

Figure 6-10. WSP and M3P profiles in the DC bioretention soil media. At some sample points, no WSP or M3P was detected (<5 mg/kg). Significant phosphorus loss had occurred over the 1 yr-test.

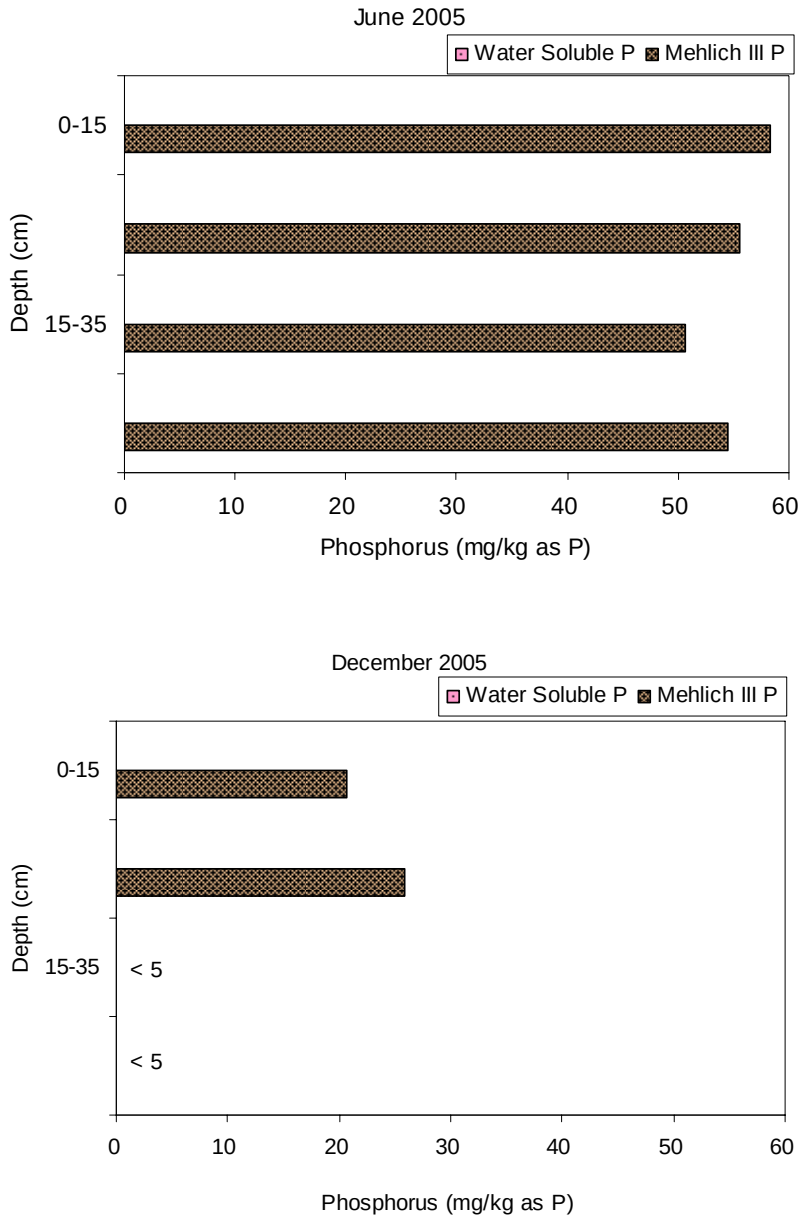

Figure 6-11. WSP and M3P profiles in the DC sand filter media. At some sample points, no WSP or M3P was detected (<5 mg/kg). Significant phosphorus loss had occurred over the 0.5 yr-test.

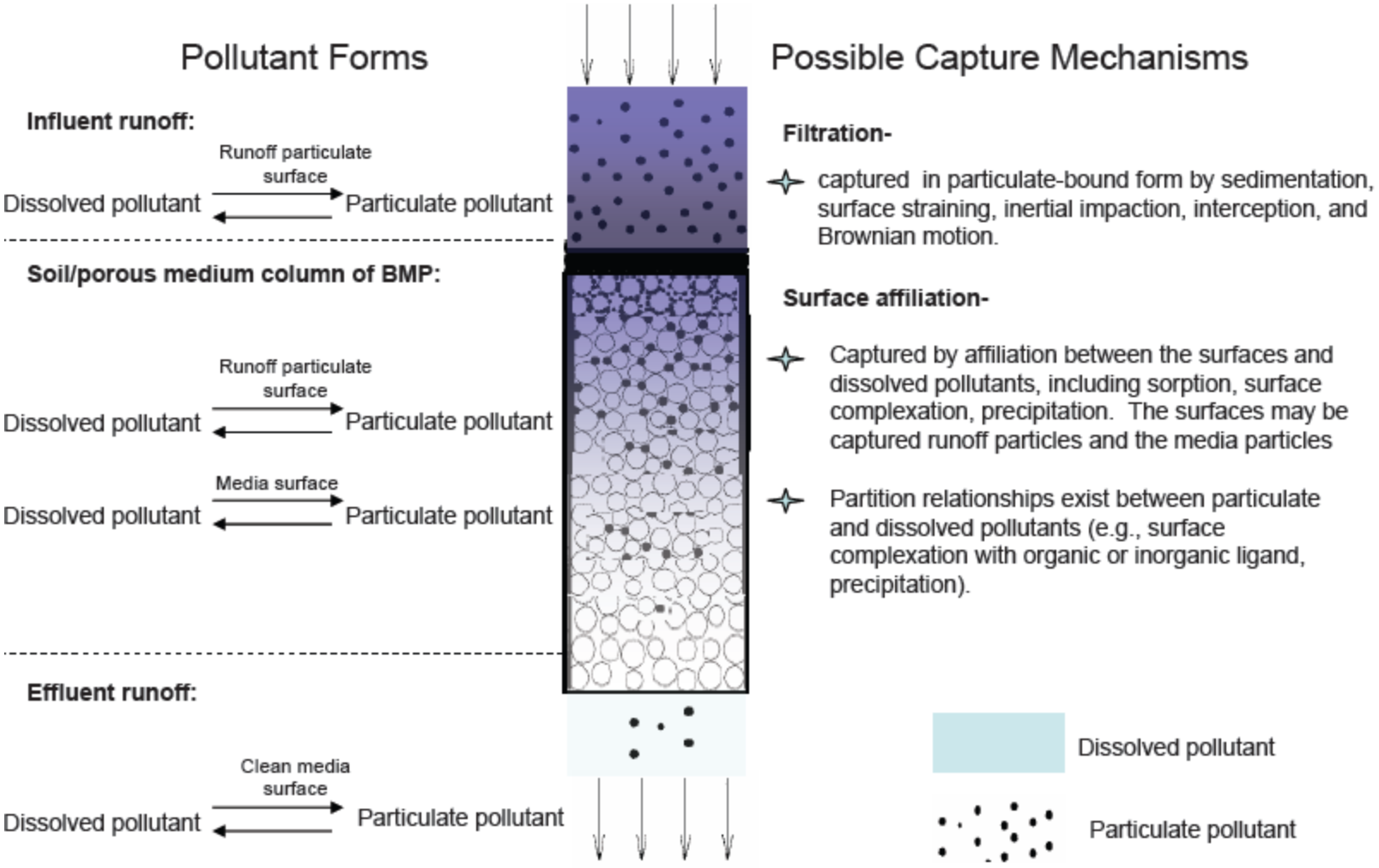

Figure 6-12. A descriptive model for dissolved/particulate pollutant capture in a filter-type BMP.

As runoff percolates through the media column, particulate metals are trapped through filtration processes (sedimentation, interception, and diffusion). As mentioned, a first-order relation with depth can be used to describe the depth profile of captured particles within the BMP media (e.g., Iwasaki 1937):

$$m / m_0 = \exp(-\lambda Z) \tag{6-1}$$

where m is the concentration of particles collected within the media, m_0 is the concentration of particles at the media surface, Z is the vertical media depth, and λ is the filter coefficient.

Equation (6-1) represents an exponentially sharp decay for incoming runoff particle concentrations. The relative small size of the media in bioretention cells (compared to rapid sand filters, which mostly use sand, gravel, and anthracite media) should result in a sharper profile, as previously mentioned. The particulate-bound pollutants in incoming runoff will deposit along with the runoff particles.

Dissolved pollutants also have greater chance to interact with the solid surfaces of deposited street particles and the top layer soil media, which can be interpreted with the simple one-dimensional advection / dispersion / adsorption transport equation (Bedient et al. 1999):

$$\frac{\partial C}{\partial t} = D(\frac{\partial^2 C}{\partial Z^2}) - u(\frac{\partial C}{\partial Z}) - (\frac{\rho}{\varepsilon})(\frac{\partial C_s}{\partial t}) \tag{6-2}$$

C and C_s are the dissolved and particulate pollutant concentrations, respectively; t is time, D is the pollutant dispersion coefficient, u is the average runoff velocity, and ρ and ε are the bulk mass density and porosity of the media column, respectively. A

simple linear-isotherm can be proposed for the adsorption term (Sauvé 2002), as previously mentioned:

$$K_d = \left(\frac{C_s}{C} \right) \tag{6-3}$$

where K_d is the distribution coefficient (L/kg). Previous studies have indicated that the metal adsorption on solid surface is non-linear in nature; however, linear expressions are still used because of their simplicity and easiness in comparison for regulatory or other purposes (Sparks 1995, Sauvé 2002). Dissolved pollutants will affiliate with the surface of media / runoff particles through sorption processes and can be retained. Solution of Equation (6-2) with Equation (6-3) employing an initial condition ($C = 0$ initially) and boundary conditions of a constant influent metal concentration C_0 and a semi-infinite soil column ($C = 0$ at $z = \infty$), results in an expression containing a combination of complimentary error functions and exponential functions (Bedient et al. 1999):

$$C(z,t) = \frac{C_0}{2}[erfc(\frac{Rz - ut}{2\sqrt{RDt}}) + \exp(\frac{uz}{D})erfc(\frac{Rz + ut}{2\sqrt{RDt}})] \tag{6-4}$$

where $R = [1 + (\rho/\varepsilon) K_d]$ = the retardation factor. Depending on the value of K_d, dissolved pollutants may affiliate with the surface of media/ runoff particles through sorption and can be retained. Equation (6-4) indicates a sharp dissolved pollutant concentration profile. Consequently, dissolved pollutants are also retained at the very top of the media column. Pilot-scale bioretention water quality data have indicated that below the surface media (e.g., 20 cm), the percolating runoff contains very low concentrations of heavy metals (Davis et al. 2003). Dynamic sorption / precipitation / ligand surface complexation processes dictate solid-solution partitioning between

dissolved pollutants and particulate pollutants in the influent runoff suspension and the media column.

Models such as Equations (6-1) and (6-4) illustrate that below the top surface layer, the metal load in runoff is very low. Consequently, the metal reactions shift to attempt to equilibrate pollutants with the background soil media (whether the system has reached equilibrium or not). Since the ratio of a bioretention cell area to its drainage area typically is about 5%, as previously mentioned (in the monitored DC bioretention cell, about 2%), during a rain event, about 20-fold depth of runoff flushes through the media column. Below the thin "working" depth at the surface of the soil column, large runoff volumes with low heavy metal content "wash" the soil media. Background metals and phosphorus may leach out, but at concentrations much lower than in the top layers. Below the surface layer, the accumulated bioretention media metal contents were generally negative, indicating washout, equal to -57 to 19 mg/kg/yr (Cu), -530 to 3 mg/kg/yr (Pb), and -59 to 15 mg/kg/yr (Zn). The unreasonably large values for metal loss below the surface layer in some cases (e.g., -530 mg/kg for Pb) may be attributed to some inadvertent mixing of the surface layer and the 0-10 cm layer in the first media sampling, but largely the lower layers exhibited slight metal loss over one year, compared to the large heavy metal enrichment in the surface layer during the same period.

The spatial profiles of captured heavy metals in the DC bioretention cell and sand filter agree with the proposed theories. Higher levels of captured metals are sorbed in the very top layers of the media columns, together with the filtered/captured street

runoff particles. In the bioretention cell, the soil media below 20 cm appear to be virtually unused for metal removal.

6.3.3. Pollutant strength of affiliation

The fraction of soluble-exchangeable (F1) captured trace metals may be considered as an indicator for its potentials of leaching and bioavailability (Turer et al. 2001*)*, although soil metal bioavailability is far from an accurate science (Sauvé 2002*)*, and is sensitive to biotic activity (Wen et al. 2004*)*. In the two BMPs (all layers), zinc generally had the highest F1 fraction (average 18% for the bioretention, 10% for the sand filter), which indicates a higher mobility than copper (3% and 11%) and lead (1% and 2%). This agrees with previous studies regarding solid-solution partitioning *(*Howari and Banat 2001, Sauvé 2002, Sauvé et al. 2003, Covelo et al. 2004*)*. Smolders and Degryse (2002) reported on the fate of zinc from soil-applied tire debris, showing that 10-40% of the zinc was released to the labile pool (the zinc quantity in soil which has the same solid-liquid distribution as the recently added labeled Zn^{2+} salt in that soil, Smolders and Degryse 2002) after one-year weathering. However, the parallel increase in soil pH due to runoff of concrete particles and residues of fill materials limits the mobilization of zinc in soil. As the most abundant and mobile metal, zinc had larger F1 fractions in the subsurface layers (20-90 cm) of the DC bioretention cell (average 21%) than the surface and top 10 cm layers (average 7%). This increase in zinc mobility along the depth also coincided with the pH decrease. Copper and lead mobility in the subsurface layers were also lower than zinc (F1 average 3% and 1%, respectively). In the upper street particle layer of the sand filter, a significant amount of zinc became bound more tightly, from F4 to F5

within six months as shown in Figure 6-7. Overall, the relatively low F1 fractions indicate that the captured metals were tightly bound with street particles and BMP media.

Copper and lead were largely bound to F2 (sorbed-carbonate), F4 (reducible), and F5 (residual) fractions in both BMPs. Zinc was distributed uniformly across all fractions except for a lower F3 (oxidizable fraction). This affiliation pattern is different from those previously described in the literature. Norrstrőm and Jacks (1998) reported that lead and zinc occurred in roadside soils mostly associated with the "oxide bound" fraction, while copper mostly bound with the "organic" fraction. Bäckstrőm et al. (2004) reported that lead was mostly associated with roadside soil in the "reducible" and "oxidizable" fractions. Preciado and Li (2006) suggested that the "residual" soil metal fractions were deposited via geological rather than anthropogenic processes, implying that anthropogenic metal inputs are characterized by an increase in the sum of exchangeable, oxide, and organic fractions. Supporting this, copper was released fairly readily from simple leaching of automobile break dust (Hur et al. 2003), and zinc from tire debris (Smolders and Degryse 2002). In this study, the percentages of the sums of F1 to F4 fractions to the total metal accumulations (F1-F5) for the surface layers (in which the most metal accumulations occurred) of the DC bioretention cell over time were 78% for copper, ~100% for lead, and 72% for zinc. The F1-F4 percentage for copper in the DC sand filter was 69% (lead and zinc did not significantly accumulate in the sand filter). These high percentages suggest that the origins of the captured metals were mostly anthropogenic. As a result, the heavy metal background levels at the surface media of

the both BMP filter were minor compared to the anthropogenic heavy metals input from incoming runoff. Furthermore, the capture metals exhibited strong affiliation with the media. These imply downstream water quality improvement for heavy metal pollution.

Figures 6-10 and 6-11 indicate that WSP (<5.0-6.7 mg/kg) was much lower than M3P (<5.0-74.9 mg/kg) in the two BMPs and was not detected in the second sample, suggesting that WSP was washed out with infiltrating runoff over time, or consumed by plant uptake as a nutrient supply. The WSP test was developed to simulate the soil solution, estimating the amount of easily-desorbed phosphorus in soil. M3P was originally designed for the optimization of soil phosphorus for crop production, but recently has been used for non-point phosphorus pollution management (Sim et al. 2001). The M3P values were generally below the optimal range (50-100 mg/kg) that supports agricultural production while minimizing environment risks (Sim et al. 2001). Although the observed WSP and M3P losses can be attributed to plant uptake and wash-out, the uniform phosphorus profiles compared to those of the heavy metals and the higher effluent TP levels than those of the influents observed in the parallel water quality monitoring study (Appendix 5 for the DC bioretention and Chapter 3 for Cells CP and SS) imply a relatively weak phosphorus affiliation with the media. Phosphorus has strong affiliation with heavy metals (especially lead) in soil media and can help soil metal stabilization (e.g., Zwonitzer et al. 2004); however, excess soil phosphorus also can leach out into soil solution. Hunt et al. (2006) observed that TP concentrations in the effluent of several bioretention facilities were higher than the influents, and concluded that those bioretention media had high phosphorus contents,

which caused the TP export. As such, the bioretention media selection must be based on the target pollutants. Low phosphorus content media should be used in phosphorus removal (Hunt et al. 2006); nonetheless, low phosphorus soil media may not be favorable for vegetation growth in rain gardens.

6.3.4. Risk considerations for heavy metal accumulation

A simple risk evaluation for metal accumulation in the BMPs is presented in Table 6-3. Guidance values for heavy metals in residential soils for 30 states in the U.S. have been compiled by Petersen et al. (2006). An average value from this database is used for each metal as a representative regulatory limit (Cu: 3700 mg/kg, range 25-20000 mg/kg, Pb: 350 mg/kg, 61-500 mg/kg, Zn: 28000 mg/kg, 20-170000 mg/kg). The risk assessment for residential soil pollution usually is based on children's soil exposure at home or other corresponding locations (Petersen et al. 2006). Stormwater filtration BMPs are not necessarily located in residential areas, but may be available to child exposure. Measured total metal levels in the DC bioretention cell surface layer indicate that lead exceeded the mean limit. The total metal levels in the sand filter were well below the limits.

From the differences of the total metal concentrations over 0.5-1 yr, the annual metal loadings were calculated in mg/kg/yr (Table 6-3). From the data set, it can be roughly estimated that both BMP media still have enough capacity for copper and zinc capture. However, lead accumulation is expected to reach the guidance value within 1.3 yr in the DC bioretention, no lead accumulation in the DC sand filter top layer was noted.

6.3.5. Environmental Significance

Street particle samples in both BMPs exhibited the highest heavy metal concentrations and enrichment over time. However, without collection and concentration via the BMPs, these street particles would have been transported and dispersed into various water bodies, possibly leading to long-term environmental challenges. Collection as a thin layer on the surface of BMP media, while burdensome, allows relative ease of cleanup and management compared to alternatives. Nonetheless the results of this assessment suggest a fairly high maintenance frequency for the removal of the thin surface street particle layer.

Table 6-3. Estimates of accumulated heavy metal levels in the street particle layers of the two BMPs (see text for details).

	Cu	Pb	Zn
DC bioretention:			
Total metal concentration of surface media, Dec 2004 (mg/kg)	29	399	111
Total metal concentration of surface media, Dec 2005 (mg/kg)	75	660	532
Annual metal loading of surface media (mg/kg/yr)	46	261	421
Average guidance values for residential soils (mg/kg)	3700	350	28000
DC sand filter:			
Total metal concentration of top media, Jun 2005 (mg/kg)	6	98	769
Total metal concentration of top media, Dec 2005 (mg/kg)	66	77	787
Annual metal loading of top media (mg/kg/yr)	120	-42	36
Average guidance values for residential soils (mg/kg)*	3700	350	28000

(* Petersen et al. 2006)

For the DC bioretention cell, since most captured pollutants accumulated on the surface and in the top 10 to 20 cm layer, a more shallow media design of 20 to 40 cm is proposed. A reduction in the depth for the planting soil will significantly reduce construction costs and increase the feasibility for BMP installation, such as in places with an elevated groundwater table and / or shallow stormwater infrastructure. The shallow cell design should not limit the use of large shrubs and trees in bioretention,

as they can be allowed to penetrate the native soils. The media selection is pollutant dependent, a low phosphorus content media should be used in locations at which phosphorus removal is most important; otherwise higher media phosphorus levels can help in stabilization of the heavy metals captured in the media and nourishing the rain garden vegetation.

A simple assessment for long-term metal accumulation of the DC bioretention cell indicates that lead is the limiting heavy metal. Although lead levels for the majority of the media in the cell may be below levels of concern, the top-heavy lead profile characteristics may dictate the need for frequent maintenance for the cell surface layer to eliminate high lead-containing materials. Similarly, more frequent partial restoration (surface layer) instead of full restoration is recommended for sand filter maintenance.

Chapter 7: Conclusions and Recommendations

7.1 Conclusions

Field monitoring in this study has demonstrated good hydrological performance in delaying / reducing peak flow and promoting infiltration for bioretention facilities. As such, with proper deployment bioretention facilities can be used as a beneficial and practical infrastructure component for flood control, channel erosion protection, and groundwater recharge for small urban drainage systems (such as parking lots). A large cell surface area: drainage area ratio and media volume design can further enhance the hydrological performance. Hydrological performance also closely correlates with water quality benefits for bioretention cells, since flow attenuation also significantly contributes to pollutant mass removal.

Bioretention facilities studied in this work have exhibited good effluent quality in nearly all monitored pollutants, except for copper and TP (total phosphorus) at Cells CP (College Park) and SS (Silver Spring). Results indicated that particulate pollutants and other heavy metals were effectively captured in bioretention media through concentration reduction and flow attenuation. Nutrients (nitrogen species and TP) concentrations slightly increased after treatment at monitored bioretention cells with net removal (Cell SS) or net export (Cell CP) after consideration of flow attenuation. TOC (total organic carbon) and chloride were leaked from the media. The minor increases in nutrients and TOC concentrations are attributed to biological activity within the media; the significant export of chloride results is attributed to de-icing reagent application. The soil organic matter leaching also prompted copper

dissolution at low concentrations (which demonstrated net removal through flow attenuation). Bioretention also reduced the mass discharge of dissolved copper to some extent, indicating a metal toxicity control function. Pathogen indicator removals (*E. Coli.* and Fecal Coliform) were inconclusive and need further studies.

The increase of copper adsorption capacity of the runoff particles (in terms of K_d values) at Cells CP and SS after treatment can be attributed to the addition of media organic matter and media loss. From the column tests and field study at the DC bioretention cell, particulate pollutants (in terms of TSS) cannot penetrate beyond 5-20 cm of the media; as such, the majority of effluent particles should originate from the media loss, also rendering the effluent obviously different in color. Depth / cake filtration and surface straining all contribute to particulate capture. Therefore, a shallower bioretention design is feasible. However, trade-offs between different pollutant removals (e.g., TSS, lead, and zinc can be effectively removed solely with concentration reduction, while nutrients and copper may need flow attenuation); or trade-offs between construction ease (e.g., cost or site selection) and the hydrological performance need further analysis on a case-by-case base.

The column tests also indicate that bioretention media appear to be clogging-limited due to their fine grain size, which suggests that media clogging will always occur before TSS penetration for bioretention facilities. Intermittent inflow conditions allow greater particulate capture capacity in bioretention media before clogging than those of continuous inflow conditions. The dormant dry periods seemed to allow the media to amend for a less-resistant flow path and may have helped the media columns to partially regain their permeability between runoff loadings.

However, the effects of vegetation on media clogging have not been included and warrant further studies.

Upland soil texture and media size also are also of critical importance to bioretention media clogging. The clay-sized components exert a controlling effect on media clogging compared to components of other texture-size. Media stratification from particle deposition and permeability reduction along the runoff percolation depth is a characteristic of bioretention; periodic surface media replacement can be used as an effective measure in bioretention maintenance.

The bioretention filtration theory developed in this study is the most comprehensive model representation of stormwater BMP filtration to date, addressing particulate penetration, permeability decrease, and cake layer formation. By applying this model to laboratory and field test results employing different media / input particle combinations, the dominant filtration mechanism (cake and depth filtration), media performance (breakthrough-limited or clogging-limited), and possible media maintenance procedures for bioretention are obtained. Information is provided for modifying current design and maintenance procedures for bioretention.

The media analyses for the DC bioretention cell and sand filter demonstrate the relation and the importance of managing street particles for filter-type stormwater BMPs. For the bioretention cell, since most captured metal pollutants accumulated on the surface and in the top 10 to 20 cm layer, a shallow cell design is again demonstrated feasible for heavy metal capture. The top-heavy profile and low soluble-exchangeable fraction of heavy metals in the DC bioretention cell and sand filter media indicate a strong affiliation between bound-metal and media / captured

particles. However, weak phosphorus-media affiliation was observed, which may be attributed to excess soil media phosphorus. Selection of a low phosphorus media can enhance runoff TP capture, but media phosphorus may assist metal stabilization and support vegetation growth. Again, a trade-off evaluation is needed. Simple risk evaluation for metal accumulation in the DC bioretention and sand filter also reveals the possibility of heavy metal enrichment at the surface media, which dictates the need for regular maintenance for the cell surface layer to eliminate high metal-containing materials.

7.2 Recommendations

7.2.1. Recommendations for bioretention design and maintenance

The media analyses demonstrate that most captured metal pollutants accumulated on the surface and in the top 10 to 20 cm layer of the media. The laboratory bioretention column tests also noted that particulates cannot penetrate 5-20 cm of the media. As such, a shallow cell design is offered for urban particle and heavy metal control, as shown in Figure 7-1. A current design has the cell depth of 0.8 to 1.2 m (2.5 to 4 ft) for planting soil (MDE 2000). This new design has the cell depth of 0.2 to 0.4 m (0.7 to 1.3 ft). A reduction in the depth for the planting soil will significantly reduce the construction costs and increase the feasibility for BMP installation, such as in places with an elevated groundwater table and stormwater infrastructure. The shallow cell design should not limit the use of large shrubs and trees in bioretention, as they can be allowed to penetrate the native soils with appropriate layout. Of course, concerns other than particle and heavy metals capture (such as other pollutants, vegetation survival, and hydrological performance) may dictate different

depth recommendations. To avoid clogging, the minimum use of filter cloth over the perforated underdrain pipe is suggested, a layer of surrounding gravels can also serve as an alternative.

Site inspection and media replacement are also recommended for reducing the risk of metal accumulation and media clogging prevention. Based on the results of the modeling theory, field / laboratory experiments, and the long term scenario analysis of the DC bioretention facility, a bioretention media depth of 5-20 cm is recommended for media replacement. A field inspection frequency (once or twice a year) and media maintenance (top-raking or top media replacement) every 5 yr are also suggested. Regular media analyses of the top media layer for heavy metal content are also desirable for cells that may be subject to intensive heavy metal inputs.

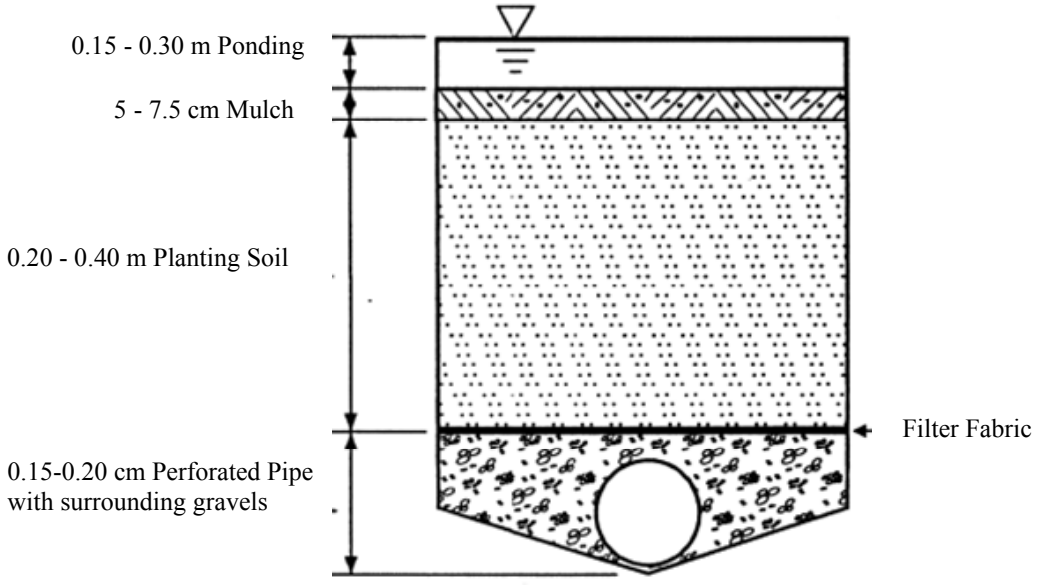

Figure 7-1. Recommendation bioretention design for particle and heavy metal removal.

7.2.2. Recommendations for Washington DC sand filter

Current practice for Washington DC sand filter maintenance includes partial restoration (which includes pumping out all standing water, removing the upper gravel layer, the underlying filter cloth, and the top 10 to 15 cm of sand under the filter cloth from the sand chamber), and full restoration (which includes the partial restoration tasks plus the replacement all of the sand, gravel, and filter cloth). The frequency of these restorations depends on the age of the sand filter or condition. Since no significant pollutant was captured or accumulated in the sand media below the fabric filter cloth during the six-month monitoring, two recommendations are made: One is to more frequently use the partial restoration instead of the full restoration. The other is to modify the procedure of the partial restoration to pumping out all standing water and removing the upper gravel layer and the underlying filter cloth. If the old filter cloth is intact by visual inspection, then the top 10-15 cm of the sand in the lower layers does not need replacement. The frequency for a full restoration can be determined by a future long term study, similar to the process used in this study. By reducing the frequency of the restoration and making the partial restoration procedures more flexible as described, maintenance costs can be cut without compromising the effluent water quality.

Appendix 1: Hydrological Data for Bioretention Cells CP and SS

1. Hydrological data of Cell CP

Date	Rain Duration	Influent	Effluent	precipitation (cm)	influent volume (l)		effluent volume (l)	Peak influent rate		Peak effluent rate	Peak influent flow time	Peak effluent flow time
	(hr)	duration (hr)	duration (hr)					l/s		l/s	(min)	(min)
					(1)		(2)	(3)		(4)	(5)	(6)
4/3/2006	2.60	2.33	10.87	0.45	10358		7097	5.29		0.35	2	360
4/17/2006	4.57	0.83	0.00	0.15	1812		0	1.30		0.00	18	-
4/21/2006	9.57	5.60	6.30	0.28	4435		3094	1.08		0.18	18	552
6/14/2006	0.20	0.17	0.00	0.03	487		0	0.83		0.00	2	-
6/19/2006	3.63	2.47	16.83	0.62	10465		16484	12.65		0.95	8	214
6/23/2006	2.53	0.27	0.00	0.16	1598		0	1.69		0.00	8	-
6/24/2006	1.13	0.80	8.93	0.20	2900		9589	5.29		0.59	2	30
7/4/2006	0.73	0.70	13.90	0.83	11510		29966	14.62		4.24	8	46
9/1/2006	24.90	20.40	50.80	2.05	38881	>	166747	3.04	>	5.56	598	-
9/5/2006	13.73	6.90	28.43	1.31	29060	>	91187	6.36	>	5.56	374	-
9/14/2006	10.50	10.00	7.33	0.43	17288		14603	1.30		1.01	78	604
10/5/2006	17.40	14.83	14.17	1.12	18310		12949	1.46		1.17	666	698
12/22/2006	17.00	9.60	7.43	0.77	20794		2714	1.46		0.24	566	596
2/25/2007	-	21.60	-	8.4 snow+1.9 rain	123626		22875	12.69		0.35	468	1072

2. Hydrological data of Cell SS

Date	Rain Duration (hr)	Influent duration (hr)	Effluent duration (hr)	precipitation (cm)	influent volume (l)		effluent volume (l)	Peak influent rate l/s		Peak effluent rate l/s	Peak influent flow time (min)	Peak effluent flow time (min)
					(1)		(2)	(3)		(4)	(5)	(6)
4/3/2006	2.30	2.20	2.23	1.40	12354		1431	7.57		0.41	2	188
4/21/2006	27.70	25.47	8.77	4.47	42023	>	34699	10.6	>	2.1	1386	-
6/14/2006	0.03	0.00	0.00	0.03	0		0	-		-	-	-
6/19/2006	2.27	2.13	0.00	0.25	736		0	1.9		0.0	124	-
6/23/2006	1.03	0.00	0.00	0.18	0		0	-		-	-	-
6/24/2006	15.00	2.63	2.27	3.02	26410	>	15052	9.4	>	2.1	44	-
7/4/2006	0.50	0.33	3.80	1.60	19916	>	11465	36.9	>	2.1	14	-
7/5/2006	4.53	2.23	13.37	5.33	60705	>	80839	30.9	>	2.1	8	-
7/22/2006	3.57	0.10	0.00	0.23	1396		0	6.7		0.0	0	-
8/7/2006	7.17	1.60	0.00	1.07	8659		0	12.1		0.0	6	-
8/20/2006	0.03	0.00	0.00	0.03	0		0	-		-	-	-
8/29/2006	0.03	0.00	0.00	0.03	0		0	-		-	-	-
9/1/2006	32.27	21.63	18.37	5.36	69697	>	21296	6.8	>	2.1	664	-
9/5/2005	14.27	6.23	8.57	3.73	51835	>	30691	14.1	>	2.1	322	-
9/14/2006	10.67	5.70	1.83	1.68	22200		220	4.7		0.1	314	634
9/28/2006	3.97	4.10	5.37	2.62	41121		11963	30.3		1.6	2	76
10/1/2006	2.93	0.20	0.00	0.15	971		0	1.5		0.0	2	-
10/5/2006	18.57	19.70	14.47	4.04	78250		33951	3.6		1.9	604	740
10/7/2006	9.60	0.10	0.00	0.23	622		0	1.4		0.0	0	-
10/12/2006	0.33	0.17	0.00	0.08	1099		0	2.3		0.0	2	-
10/17/2006	8.93	5.93	5.87	1.93	34383		5986	4.8		0.6	34	238
10/19/2006	12.83	4.73	0.00	1.02	16904		0	5.3		0.0	4	-
10/27/2006	14.90	14.20	12.07	3.71	70364		37363	6.8		1.9	794	846
11/2/2006	3.87	2.97	0.00	0.86	13913		0	3.9		0.0	12	-
11/7/2006	8.93	6.13	11.87	4.17	83809	>	52903	7.2	>	2.1	154	236
11/12/2006	18.03	15.77	9.20	2.29	44035		10760	4.1		0.9	118	428
11/16/2006	7.20	6.03	13.83	4.75	82969	>	67325	44.2	>	2.1	232	-
11/22/2006	13.53	8.13	8.73	2.16	33124		11919	4.3		1.0	430	542
12/13/2006	6.40	0.13	0.00	0.20	392		0	2.0		0.0	8	-
12/22/2006	15.87	1.57	4.93	2.16	11432		3428	5.6		0.4	6	138
12/25/2006	8.80	3.00	0.00	0.94	11590		0	2.1		0.0	2	-
12/31/2006	15.00	8.80	12.07	2.51	45989		20542	12.7		1.6	14	196
1/5/2007	4.37	2.47	0.00	0.61	7788		0	4.1		0.0	128	-
1/7/2007	16.03	16.00	4.10	1.52	40658		375	2.6		0.1	42	1056
1/21/2007	-	0.00	0.00	3 snow + 0.83 rain	0		0	-		-	-	-
1/23/2007	3.13	0.00	0.00	0.51	0		0	-		-	-	-
1/25/2007	-	-	-	Trace amount	0		0	-		-	-	-
2/2/2007	13.97	0.20	-	0.36	959		0	1.5		0.0	6	-
2/13/2007	N/A	N/A	N/A	5.6 snow + 2.12 rain	N/A		N/A	N/A		N/A	N/A	N/A
2/25/2007	-	9.33	14.80	8.4 snow+1.9 rain	35397		12231	6.3		1.2	450	864

Appendix 2: Water Quality Data for Bioretention Cells CP and SS

1. Pollutant analyzing methods used by the WSSC laboratory

Pollutant	Analyzing Method [a]
Total arsenic	EPA 200.9 [b]
Total cadmium	EPA 200.9 [b]
Chloride	Lachat 10-117-07-1 B [c]
Total chromium	EPA 200.8 [b]
Total copper	EPA 200.8 [b]
E. Coli.	Standard Method 9223 B [d]
Fecal Coliform	Standard Method 9221 E2 [e]
Total lead	EPA 200.8, EPA 200.9 [b]
Total mercury	EPA 245.1 [b]
Nitrate	EPA 353.2 [f]
Nitrite	EPA 353.2 [f]
TKN	EPA 351.2 [f]
Oil &Grease	EPA 1664 [g]
Total phosphorus	EPA 365.1 [f]
Total organic carbon	Standard Method 5310 C [h]
Total suspended solids	Standard Method 2540 D [e]
Total zinc	EPA 200.8 [b]

[a] provided by the laboratory subcontractor, [b] USEPA 1994, [c] Lachat Instrument 2001, [d] APHA et al. 1999, [e] APHA et al. 1992, [f] USEPA 1993, [g] USEPA 1999b, [h] APHA et al. 1995.

2. Water quality data summary

BMP	Event date			Arsenic (mg/L)				Cadmium (mg/L)			
		Detention limit		0.002				0.002			
		Inflow volume (L)	Outflow volume (L)	In	Out	EMC removal (%)	Mass removal (%)	In	Out	EMC removal (%)	Mass removal (%)
CP Bioretention	04/03/06	10358	7097	<0.002	<0.002	-	-	<0.002	<0.002	-	-
	04/21/06	4435	3094	<0.002	<0.002	-	-	<0.002	<0.002	-	-
	06/24/06	2900	9589	<0.002	0.0021	<-5	<-247	<0.002	<0.002	-	-
	07/04/06	11510	29966	<0.002	<0.002	-	-	<0.002	<0.002	-	-
	09/14/06	17288	14603	<0.002	<0.002	-	-	<0.002	<0.002	-	-
	10/05/06	18310	12949	<0.002	<0.002	-	-	<0.002	<0.002	-	-
	12/22/07	20794	2714	<0.002	<0.002	-	-	<0.002	<0.002	-	-
	02/25/07	123626	22875	0.002	<0.002	>13	>84	<0.002	<0.002	-	-
SS Bioretention	04/03/06	12354	1431	<0.002	<0.002	-	-	<0.002	<0.002	-	-
	04/21/06	42023	>34699	<0.002	0.003	<-45	<-20	<0.002	<0.002	-	-
	06/24/06	26410	>15052	<0.002	0.0033	<-65	<6	<0.002	<0.002	-	-
	07/04/06	19916	>11465	<0.002	0.0034	<-70	<2	<0.002	<0.002	-	-
	09/14/06	22200	220	<0.002	<0.002	-	-	<0.002	<0.002	-	-
	10/05/06	78250	33951	<0.002	<0.002	-	-	<0.002	<0.002	-	-
	12/22/07	11432	3428	<0.002	<0.002	-	-	<0.002	<0.002	-	-
	02/25/07	35397	12231	0.006	<0.002	>66	>88	<0.002	<0.002	-	-
BMP	Event date			chloride (mg/L)				Chromium (mg/L)			
		Detention limit		1				0.002			
		Inflow volume (L)	Outflow volume (L)	In	Out	EMC removal (%)	Mass removal (%)	In	Out	EMC removal (%)	Mass removal (%)
CP Bioretention	04/03/06	10358	7097	143	448	-213	-115	0.014	0.005	68	78
	04/21/06	4435	3094	8	84	-918	-661	0.004	0.005	-49	-4
	06/24/06	2900	9589	4	28	-623	-2290	0.004	0.004	8	-205
	07/04/06	11510	29966	4	29	-628	-1796	<0.002	0.003	<-40	<-265
	09/14/06	17288	14603	4	7	-60	-35	0.003	0.003	16	29
	10/05/06	18310	12949	2	6	-314	-193	<0.002	0.002	<0	<29
	12/22/07	20794	2714	2	4	-115	72	0.003	0.002	39	92
	02/25/07	123626	22875	N/A	N/A	-	-	0.013	0.002	85	97
SS Bioretention	04/03/06	12354	1431	8	3	64	96	0.004	<0.002	>46	>94
	04/21/06	42023	>34699	<1	11	<-960	<-775	0.005	0.003	46	<55
	06/24/06	26410	>15052	2	7	-282	<-118	<0.002	<0.002	-	-
	07/04/06	19916	>11465	<1	3	<-179	<-61	<0.002	<0.002	-	-
	09/14/06	22200	220	3	3	18	99	<0.002	<0.002	-	-
	10/05/06	78250	33951	2	2	31	70	<0.002	<0.002	-	-
	12/22/07	11432	3428	13	2	83	95	<0.002	<0.002	-	-
	02/25/07	35397	12231	13	16	-29	55	0.006	<0.002	>65	>88

BMP	Event date			Copper (mg/L)				Escherichia coli (#/100mL)			
		Detention limit		0.01 or 0.002				1			
		Inflow volume (L)	Outflow volume (L)	In	Out	EMC removal (%)	Mass removal (%)	In	Out	EMC removal (%)	Mass removal (%)
CP Bioretention	04/03/06	10358	7097	0.042	0.020	53	68	43	4	91	93
	04/21/06	4435	3094	0.019	0.035	-84	-29	N/A	N/A	-	-
	06/24/06	2900	9589	0.016	0.015	6	-212	307.6	1145	-272	-1131
	07/04/06	11510	29966	0.013	0.016	-25	-226	N/A	N/A	-	-
	09/14/06	17288	14603	0.013	0.009	32	43	N/A	N/A	-	-
	10/05/06	18310	12949	0.009	0.010	-5	25	N/A	N/A	-	-
	12/22/07	20794	2714	0.019	0.011	41	92	44	22	51	94
	02/25/07	123626	22875	0.041	0.034	16	85	139	1	99	>99
SS Bioretention	04/03/06	12354	1431	0.015	<0.01	>35	>92	2	1	50	94
	04/21/06	42023	>34699	0.016	0.017	-5	<13	N/A	N/A	-	-
	06/24/06	26410	>15052	0.013	0.014	-9	<38	>2420	5475	>-126	-
	07/04/06	19916	>11465	0.010	0.014	-38	<21	N/A	N/A	-	-
	09/14/06	22200	220	0.009	0.007	19	99	N/A	N/A	-	-
	10/05/06	78250	33951	0.007	0.007	-6	54	N/A	N/A	-	-
	12/22/07	11432	3428	0.011	0.011	2	71	5	58	-1008	-232
	02/25/07	35397	12231	0.019	0.005	74	91	<1	<1	-	-
BMP	Event date			Fecal Coliforms (MPN/100mL)				Mercury (mg/L)			
		Detention limit		2				0.0002			
		Inflow volume (L)	Outflow volume (L)	In	Out	EMC removal (%)	Mass removal (%)	In	Out	EMC removal (%)	Mass removal (%)
CP Bioretention	04/03/06	10358	7097	110	4	96	98	<0.0002	<0.0002	-	-
	04/21/06	4435	3094	N/A	N/A	-	-	<0.0002	<0.0002	-	-
	06/24/06	2900	9589	900	1600	-78	-488	<0.0002	<0.0002	-	-
	07/04/06	11510	29966	N/A	N/A	-	-	<0.0002	<0.0002	-	-
	09/14/06	17288	14603	N/A	N/A	-	-	<0.0002	<0.0002	-	-
	10/05/06	18310	12949	N/A	N/A	-	-	<0.0002	<0.0002	-	-
	12/22/07	20794	2714	170	70	59	95	<0.0002	<0.0002	-	-
	02/25/07	123626	22875	80	4	95	99	<0.0002	<0.0002	-	-
SS Bioretention	04/03/06	12354	1431	2	2	0	88	<0.0002	<0.0002	-	-
	04/21/06	42023	>34699	N/A	N/A	-	-	<0.0002	<0.0002	-	-
	06/24/06	26410	>15052	>1600	1600	>0	-	<0.0002	<0.0002	-	-
	07/04/06	19916	>11465	N/A	N/A	-	-	<0.0002	<0.0002	-	-
	09/14/06	22200	220	N/A	N/A	-	-	<0.0002	<0.0002	-	-
	10/05/06	78250	33951	N/A	N/A	-	-	<0.0002	<0.0002	-	-
	12/22/07	11432	3428	13	70	-438	-61	<0.0002	<0.0002	-	-
	02/25/07	35397	12231	<2	<2	-	-	<0.0002	<0.0002	-	-

BMP	Event date			Lead (mg/L)				Nitrate (mg /L as N)			
		Detention limit		0.002				0.05			
		Inflow volume (L)	Outflow volume (L)	In	Out	EMC removal (%)	Mass removal (%)	In	Out	EMC removal (%)	Mass removal (%)
CP Bioretention	04/03/06	10358	7097	0.018	0.004	77	84	0.78	1.98	-155	-75
	04/21/06	4435	3094	0.003	0.007	-97	-38	0.43	1.03	-139	-67
	06/24/06	2900	9589	0.0062	0.0028	55	-49	0.09	0.27	-194	-872
	07/04/06	11510	29966	<0.002	<0.002	-	-	0.23	0.49	-111	-450
	09/14/06	17288	14603	<0.002	<0.002	-	-	0.32	0.60	-84	-55
	10/05/06	18310	12949	<0.002	<0.002	-	-	0.12	0.80	-556	-364
	12/22/07	20794	2714	0.003	<0.002	>41	>92	0.35	0.81	-133	70
	02/25/07	123626	22875	0.013	<0.002	>85	>97	2.59	2.04	21	85
SS Bioretention	04/03/06	12354	1431	0.005	<0.002	>61	>95	0.49	0.05	90	99
	04/21/06	42023	>34699	0.007	0.003	60	<67	0.06	<0.05	>17	>32
	06/24/06	26410	>15052	0.002	<0.002	>0	-	0.10	<0.05	>51	-
	07/04/06	19916	>11465	<0.002	<0.002	-	-	0.12	0.05	61	<78
	09/14/06	22200	220	<0.002	<0.002	-	-	0.34	0.29	14	99
	10/05/06	78250	33951	<0.002	<0.002	-	-	0.20	<0.05	>75	>89
	12/22/07	11432	3428	<0.002	<0.002	-	-	0.72	0.10	86	96
	02/25/07	35397	12231	<0.002	<0.002	-	-	0.54	<0.05	>91	>97
BMP	Event date			Nitrite (mg /L as N)				TKN (mg /L as N)			
		Detention limit		0.02				0.2			
		Inflow volume (L)	Outflow volume (L)	In	Out	EMC removal (%)	Mass removal (%)	In	Out	EMC removal (%)	Mass removal (%)
CP Bioretention	04/03/06	10358	7097	0.05	<0.02	>58	>72	2.2	0.8	62	74
	04/21/06	4435	3094	0.04	0.04	-4	27	1.2	1.2	0	30
	06/24/06	2900	9589	<0.02	0.03	<-29	<-325	<0.2	0.6	<-182	<-832
	07/04/06	11510	29966	<0.02	<0.02	-	-	1.2	0.7	38	-71
	09/14/06	17288	14603	0.05	0.04	27	38	0.6	1.0	-67	-41
	10/05/06	18310	12949	<0.02	<0.02	-	-	<0.2	0.5	<-146	<-74
	12/22/07	20794	2714	0.02	0.03	-48	81	1.0	0.8	20	90
	02/25/07	123626	22875	0.12	0.08	34	88	2.2	1.1	49	91
SS Bioretention	04/03/06	12354	1431	<0.02	<0.02	-	-	0.7	0.3	58	95
	04/21/06	42023	>34699	<0.02	<0.02	-	-	0.9	1.1	-26	<-4
	06/24/06	26410	>15052	<0.02	<0.02	-	-	<0.2	0.4	<-109	<-19
	07/04/06	19916	>11465	<0.02	<0.02	-	-	<0.2	0.8	<-282	<-120
	09/14/06	22200	220	0.03	0.04	-5	99	0.5	0.6	-33	99
	10/05/06	78250	33951	<0.02	<0.02	-	-	<0.2	0.6	<-201	<-30
	12/22/07	11432	3428	0.03	0.03	-8	68	0.5	0.5	1	70
	02/25/07	35397	12231	0.05	<0.02	>62	>87	0.6	0.4	40	79

BMP	Event date			Total Nitrogen (mg /L as N)				Oil & Grease (mg/L)			
		Detention limit		-				5			
		Inflow volume (L)	Outflow volume (L)	In	Out	EMC removal (%)	Mass removal (%)	In	Out	EMC removal%	Mass removal%
CP Bioretention	04/03/06	10358	7097	3.0	2.8	7	36	<5	<5	-	-
	04/21/06	4435	3094	1.7	2.3	-35	6	<5	<5	-	-
	06/24/06	2900	9589	0.1	0.9	-836	-2994	<5	<5	-	-
	07/04/06	11510	29966	1.4	1.2	14	-140	<5	<5	-	-
	09/14/06	17288	14603	1.0	1.7	-68	-42	<5	<5	-	-
	10/05/06	18310	12949	0.1	1.3	-961	-651	<5	<5	-	-
	12/22/07	20794	2714	1.3	1.6	-21	84	<5	<5	-	-
	02/25/07	123626	22875	4.9	3.2	34	88	N/A	N/A	-	-
SS Bioretention	04/03/06	12354	1431	1.2	0.3	76	97	<5	<5	-	-
	04/21/06	42023	>34699	1.0	1.1	-18	<3	<5	<5	-	-
	06/24/06	26410	>15052	0.1	0.4	-309	<-133	<5	<5	-	-
	07/04/06	19916	>11465	0.1	0.8	-567	<-284	<5	<5	-	-
	09/14/06	22200	220	0.9	1.0	-13	99	<5	<5	-	-
	10/05/06	78250	33951	0.2	0.6	-203	-31	<5	<5	-	-
	12/22/07	11432	3428	1.2	0.6	50	85	<5	<5	-	-
	02/25/07	35397	12231	1.2	0.4	70	89	N/A	N/A	-	-
BMP	Event date			TSS (mg/L)				TOC (mg/L			
		Detention limit		1				0.4			
		Inflow volume (L)	Outflow volume (L)	In	Out	EMC removal (%)	Mass removal (%)	In	Out	EMC removal (%)	Mass removal (%)
CP Bioretention	04/03/06	10358	7097	128	2	98	99	N/A	9.0	-	-
	04/21/06	4435	3094	30	1	97	98	11.4	17.5	-53	-7
	06/24/06	2900	9589	78	8	90	66	1.6	9.5	-492	-1856
	07/04/06	11510	29966	16	10	39	-59	4.4	14.0	-218	-727
	09/14/06	17288	14603	16	3	83	86	6.8	9.2	-35	-14
	10/05/06	18310	12949	7	3	53	67	2.2	7.4	-237	-139
	12/22/07	20794	2714	63	9	85	98	2.1	6.5	-212	59
	02/25/07	123626	22875	200	2	99	>99	N/A	N/A	-	-
SS Bioretention	04/03/06	12354	1431	48	<1	>98	>99	7.9	1.0	88	99
	04/21/06	42023	>34699	150	30	80	<83	2.4	16.8	-598	<-476
	06/24/06	26410	>15052	32	4	88	<93	1.8	7.0	-277	<-115
	07/04/06	19916	>11465	16	14	13	<50	3.4	21.5	-524	<-259
	09/14/06	22200	220	8	2	75	99	4.5	2.9	35	99
	10/05/06	78250	33951	6	3	49	78	3.0	7.1	-141	-4
	12/22/07	11432	3428	17	13	20	76	4.9	5.2	-6	68
	02/25/07	35397	12231	6	<1	>83	>94	-	-	-	-

BMP	Event date			Zinc (mg/L)				TP (mg/L)			
		Detention limit		0.005 or 0.002				0.1			
		Inflow volume (L)	Outflow volume (L)	In	Out	EMC removal (%)	Mass removal (%)	In	Out	EMC removal (%)	Mass removal (%)
CP Bioretention	04/03/06	10358	7097	0.174	0.010	94	96	0.3	0.5	-76	-21
	04/21/06	4435	3094	0.036	0.014	61	73	0.2	0.4	-122	-55
	06/24/06	2900	9589	0.047	0.0112	76	21	<0.1	0.4	<-287	-1180
	07/04/06	11510	29966	0.015	0.012	22	-103	<0.1	0.3	<-161	<-580
	09/14/06	17288	14603	0.033	0.011	65	71	<0.1	0.2	<-78	<-50
	10/05/06	18310	12949	0.016	0.009	47	62	<0.1	0.2	<-56	<-10
	12/22/07	20794	2714	0.071	0.006	92	99	0.3	0.1	59	95
	02/25/07	123626	22875	0.157	0.017	89	98	0.7	0.3	57	92
SS Bioretention	04/03/06	12354	1431	0.046	<0.005	>89	>99	0.2	0.1	55	95
	04/21/06	42023	>34699	0.067	0.008	89	<91	0.2	0.1	24	<38
	06/24/06	26410	>15052	0.0095	<0.005	>47	<70	<0.1	<0.1	-	-
	07/04/06	19916	>11465	0.007	0.005	24	<56	<0.1	0.1	<-20	<31
	09/14/06	22200	220	0.025	0.011	56	<99	<0.1	<0.1	-	-
	10/05/06	78250	33951	0.011	<0.005	>55	>80	<0.1	<0.1	-	-
	12/22/07	11432	3428	0.014	0.002	85	96	<0.1	<0.1	-	-
	02/25/07	35397	12231	0.015	0.003	80	93	<0.1	<0.1	-	-

3. Pollutant probability plots

Chromium

Cell CP

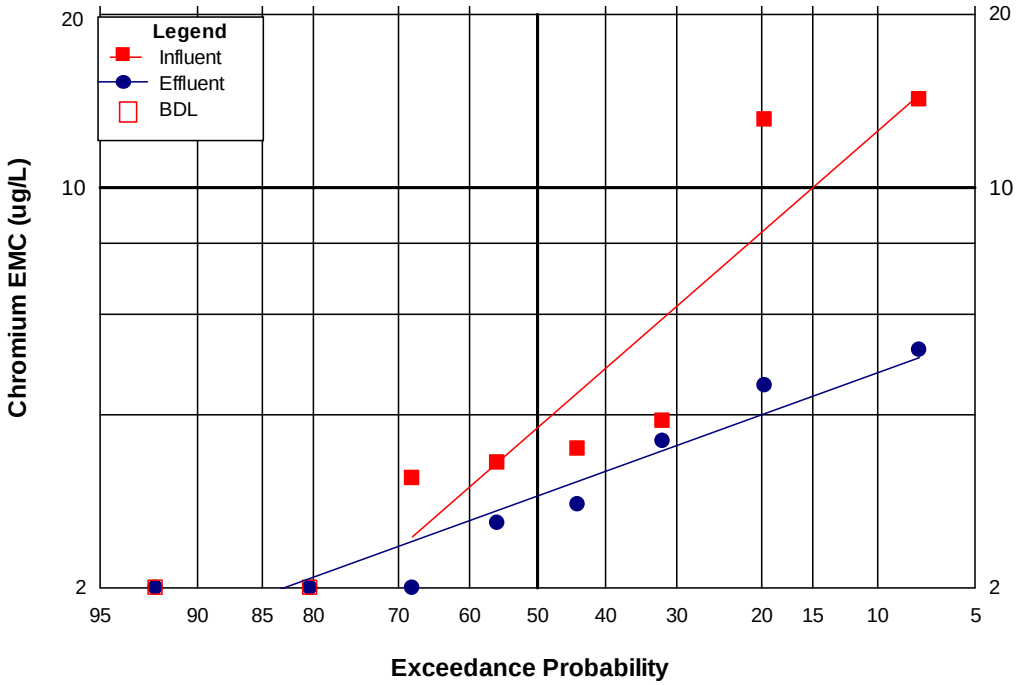

Cell SS

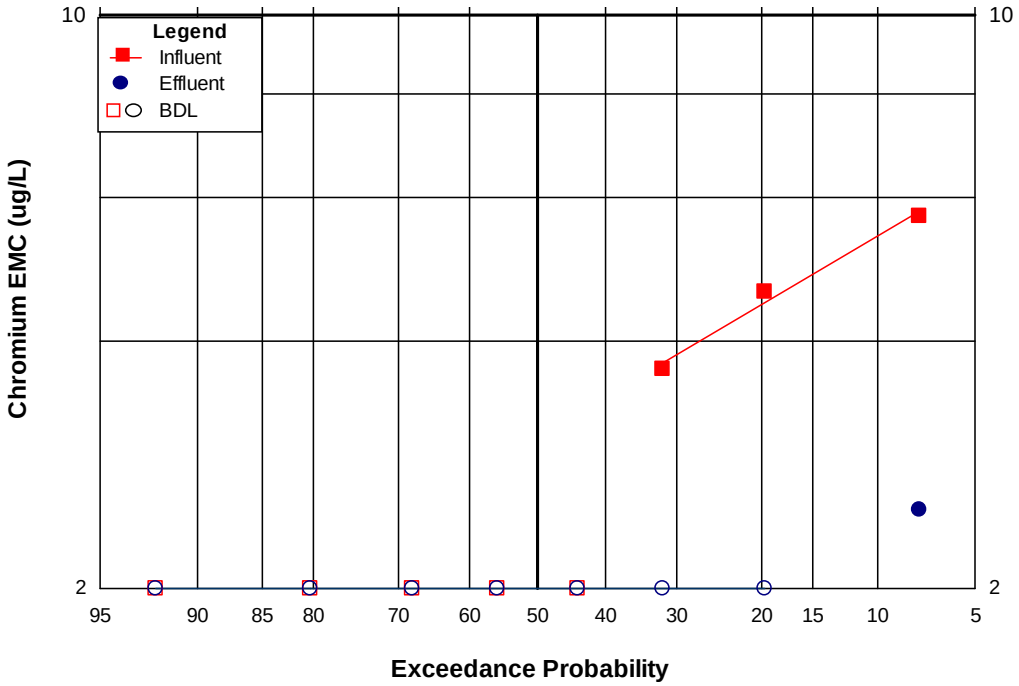

Copper

Cell CP

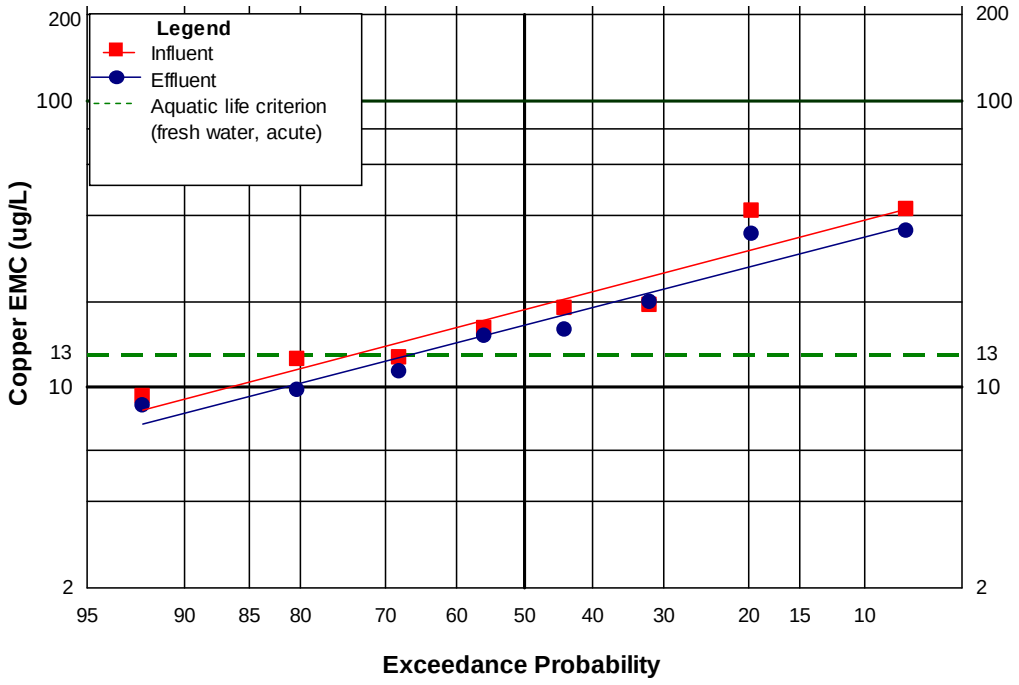

Cell SS

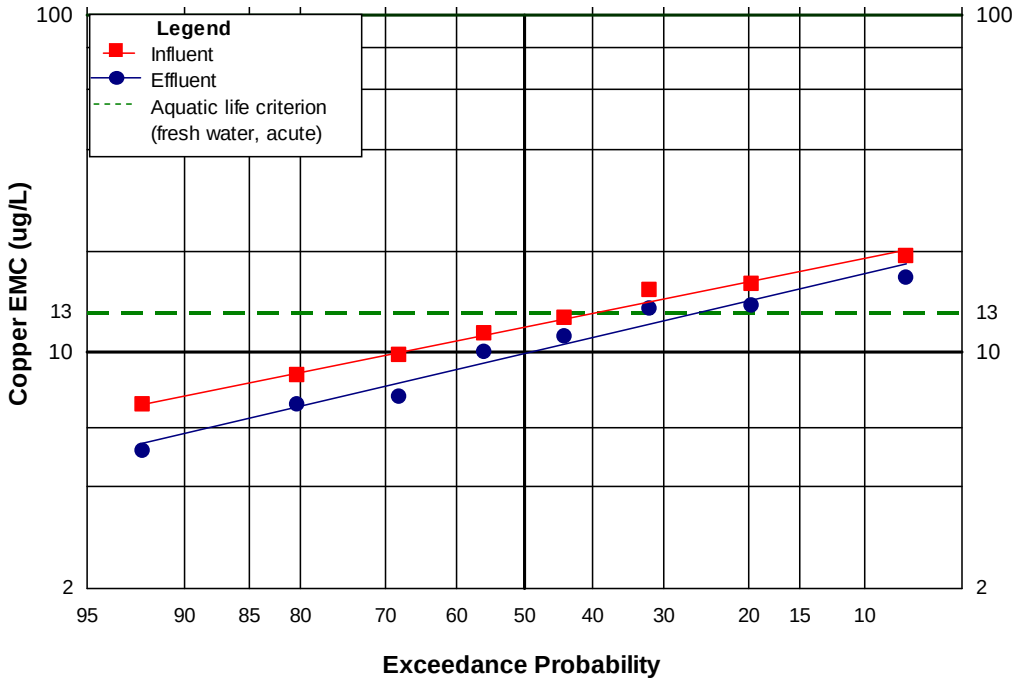

Lead

Cell CP

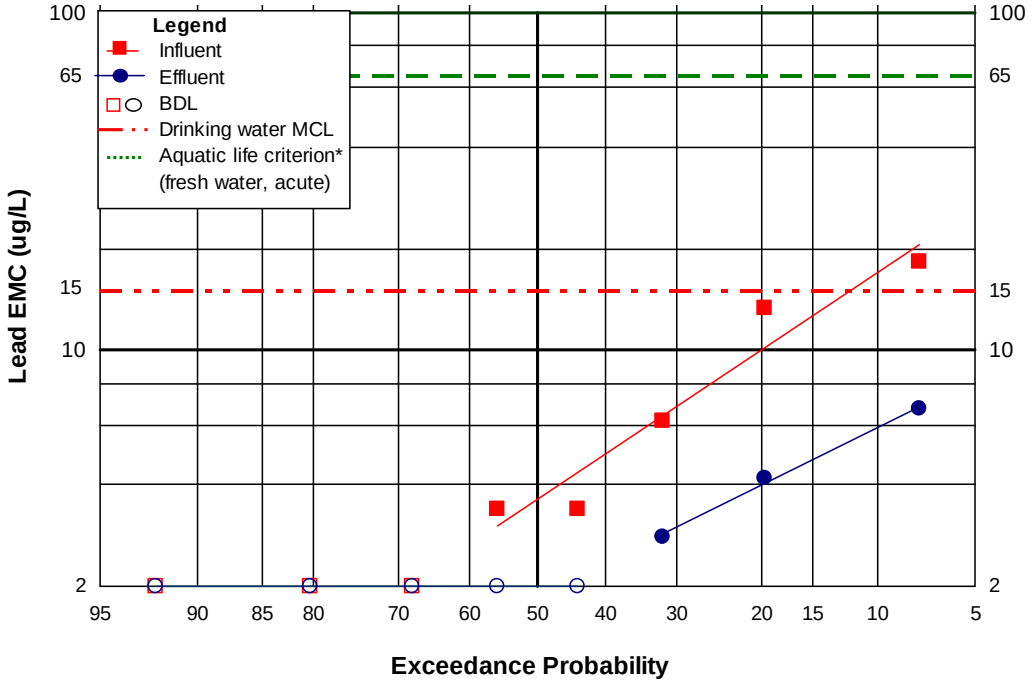

Cell SS

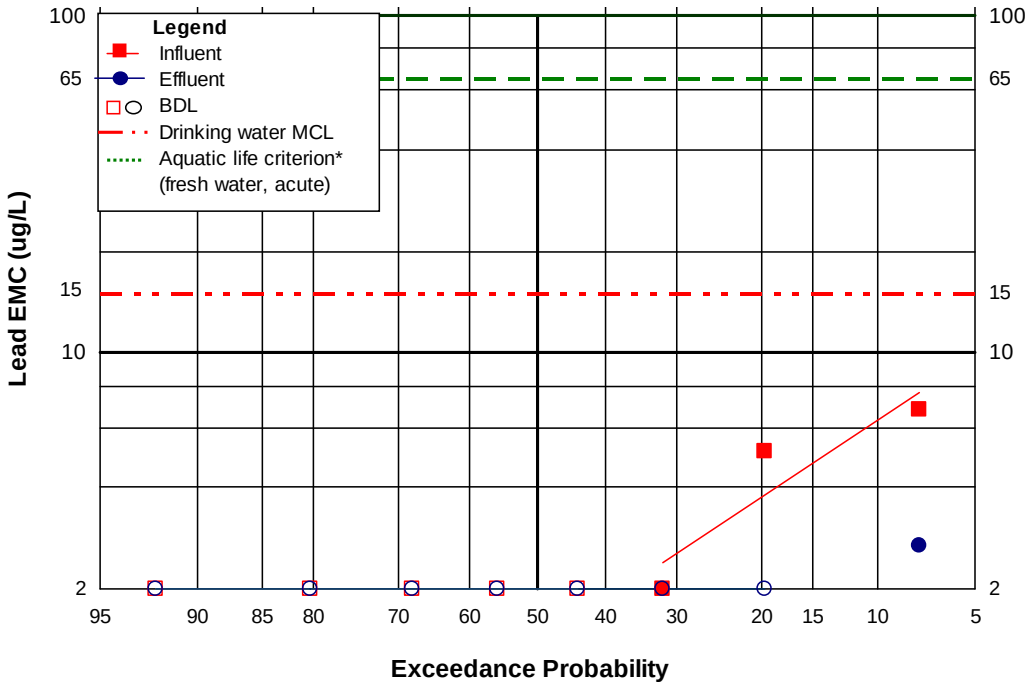

Nitrate

Cell CP

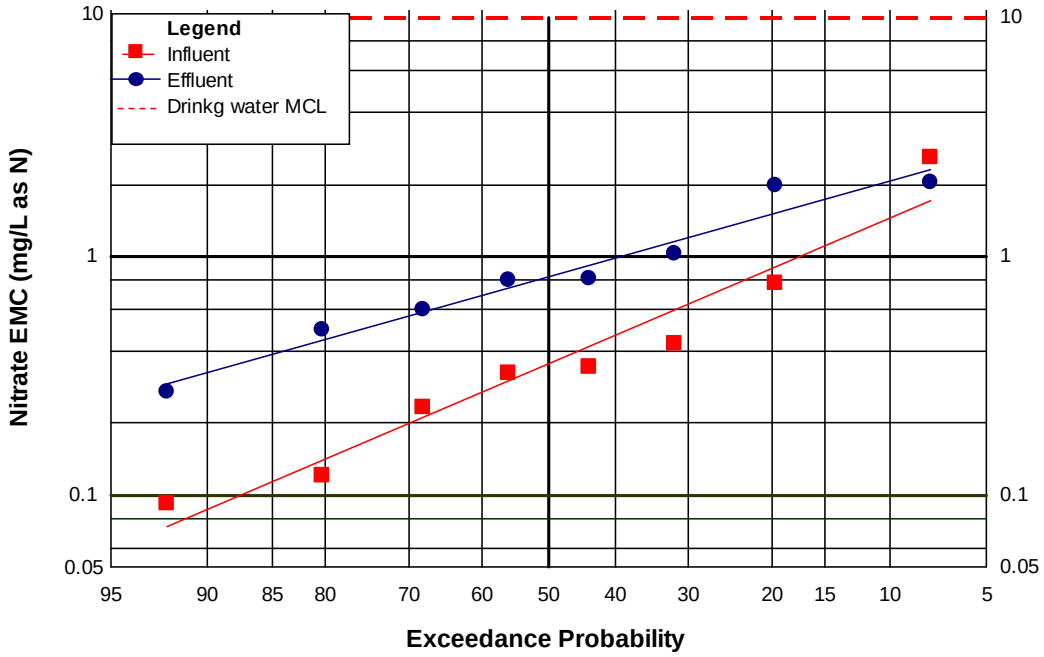

Cell SS

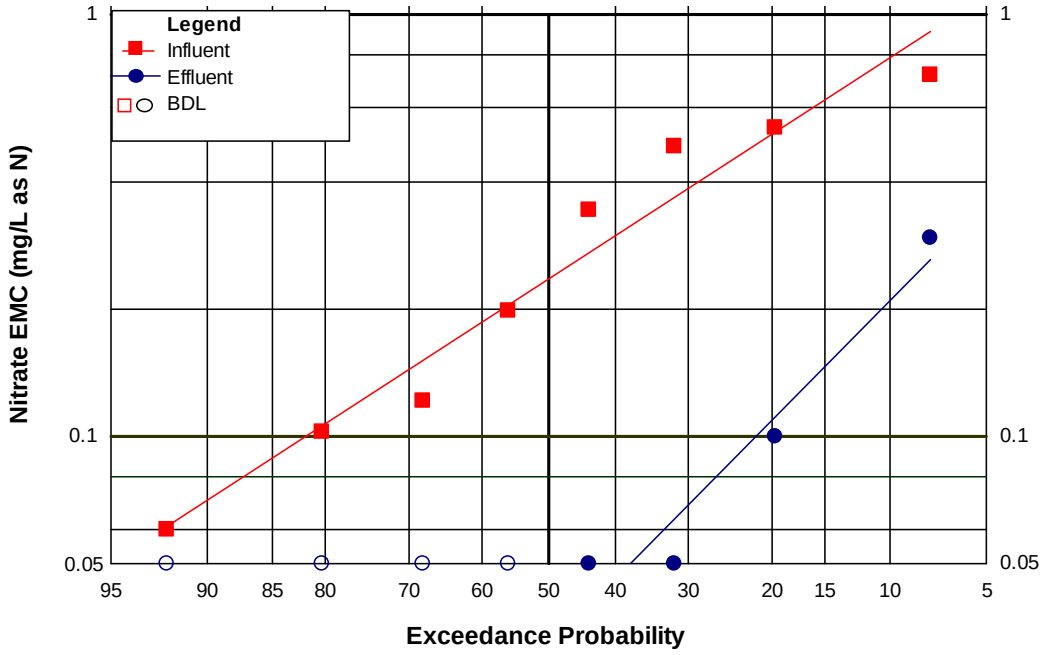

Nitrite

Cell CP

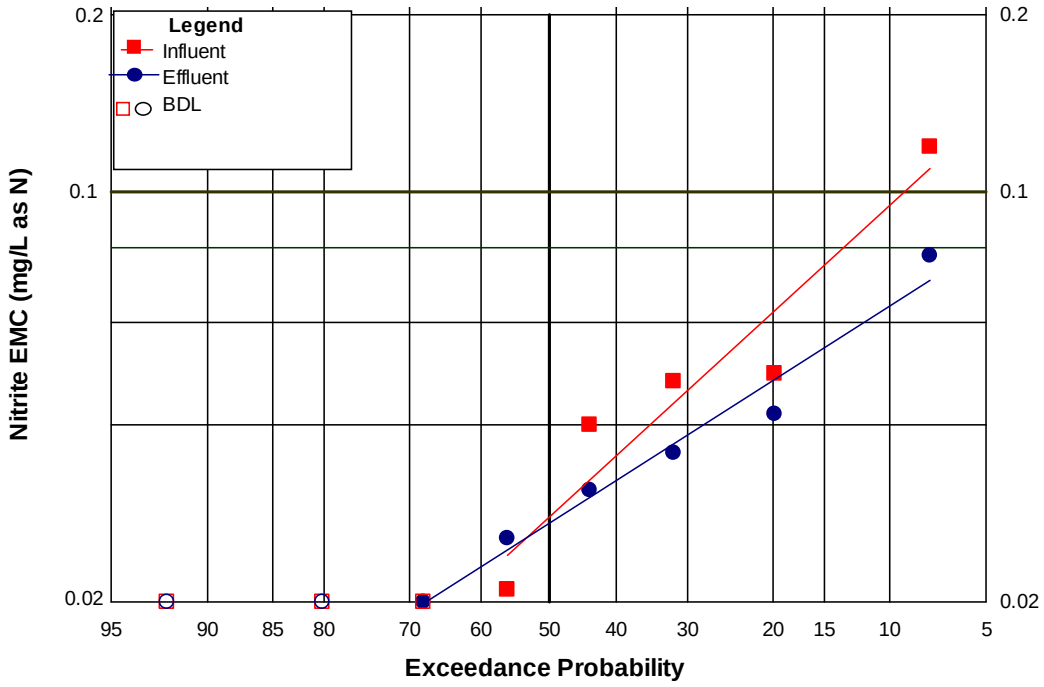

Cell SS

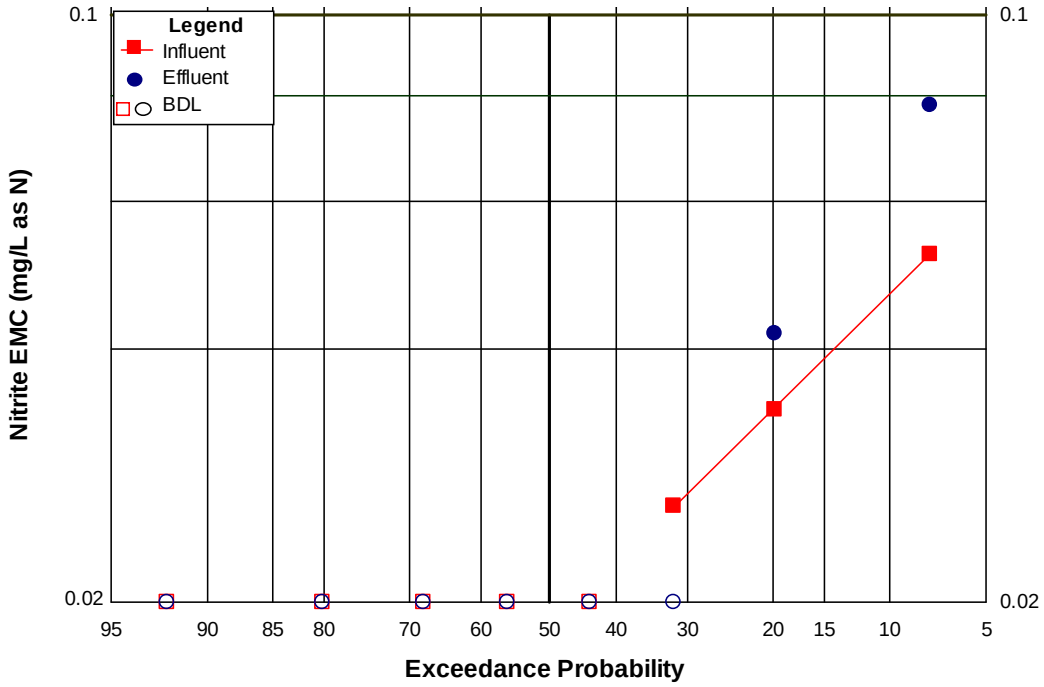

TKN

Cell CP

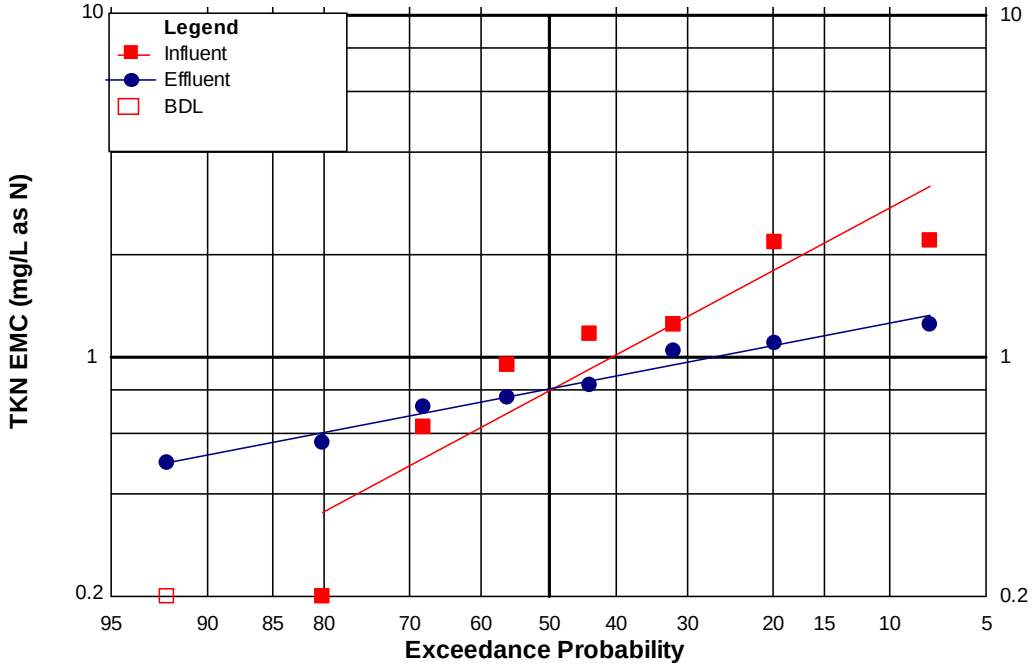

Cell SS

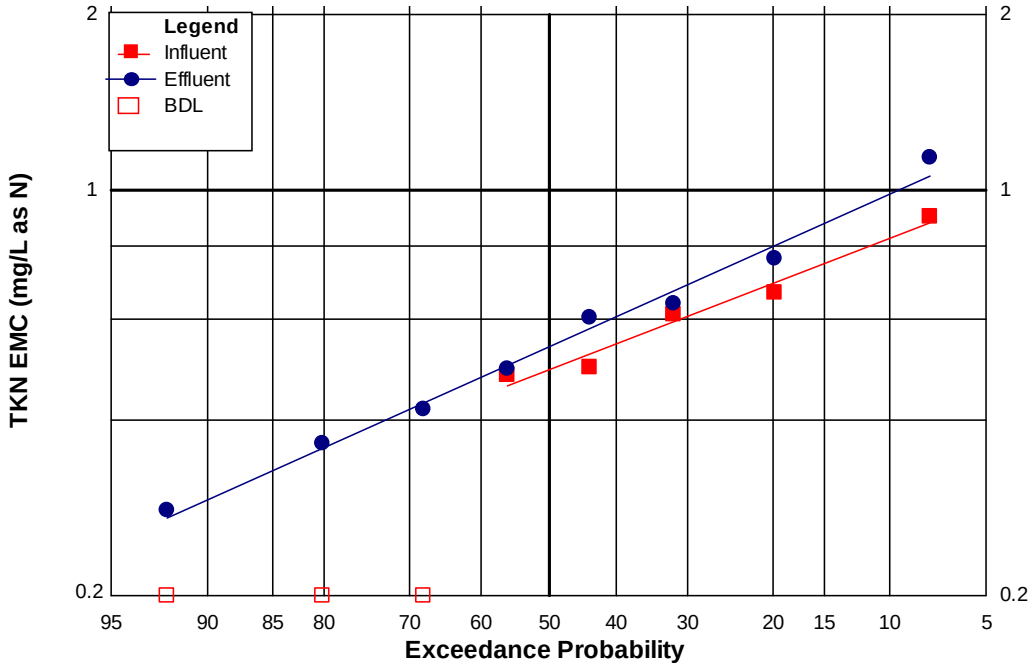

TN

Cell CP

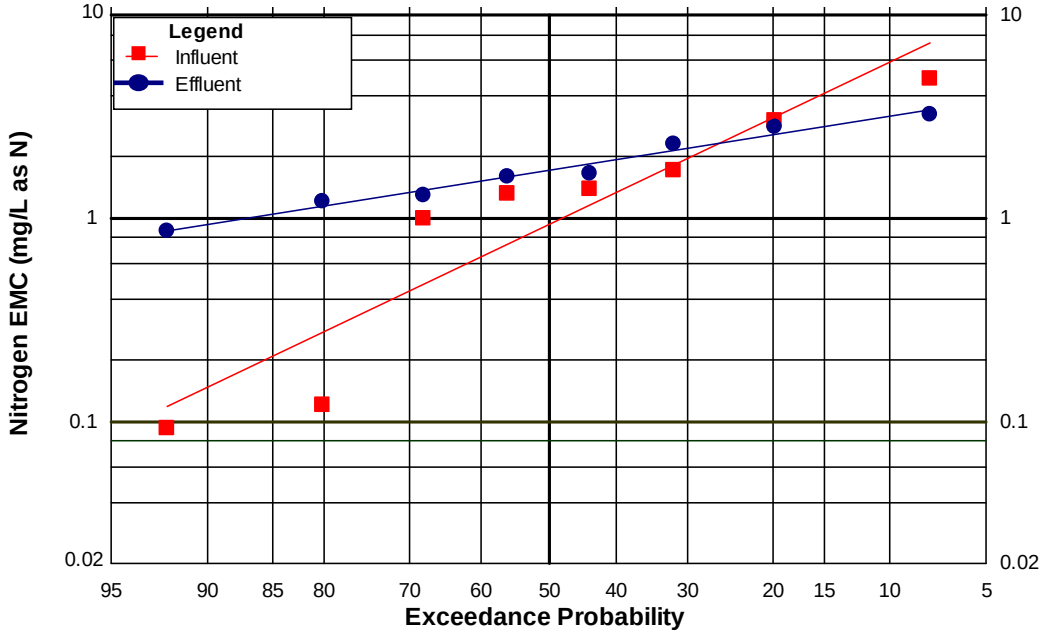

Cell SS

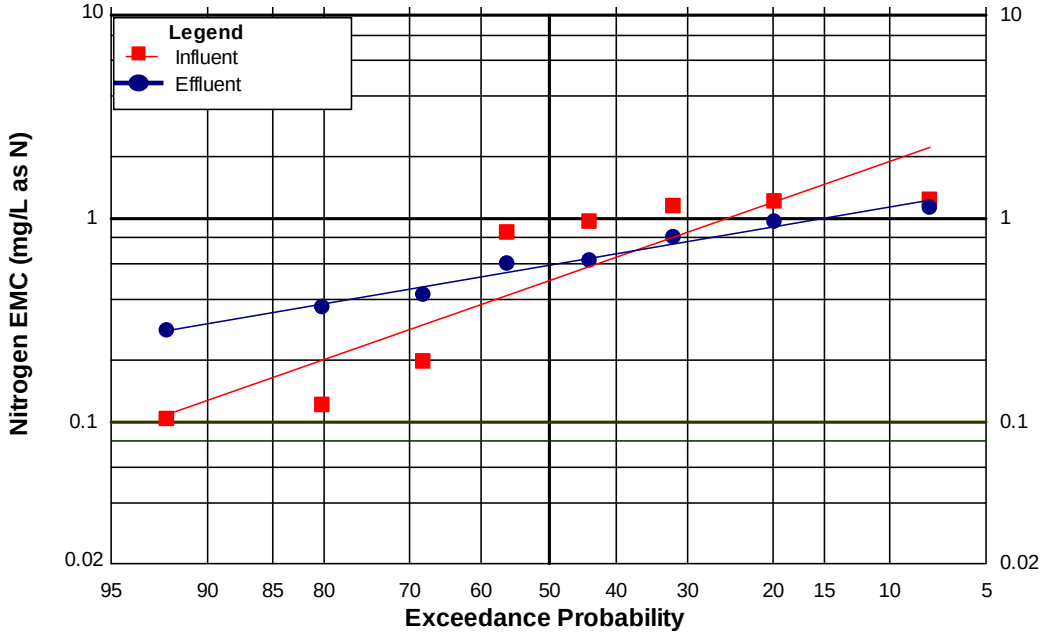

TP

Cell CP

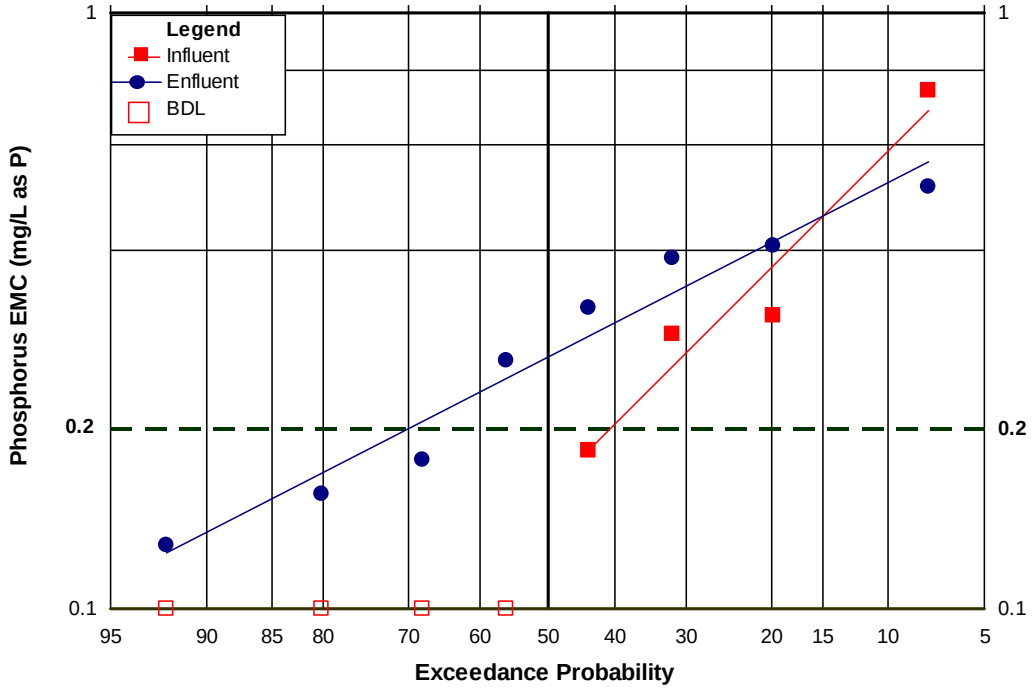

Cell SS

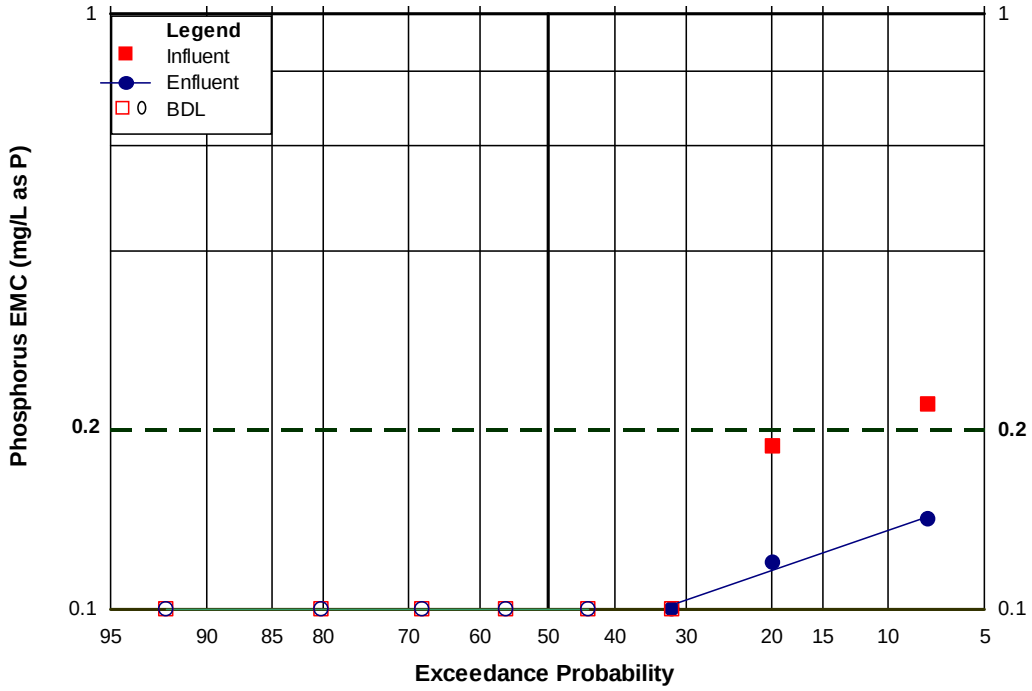

TOC

Cell CP

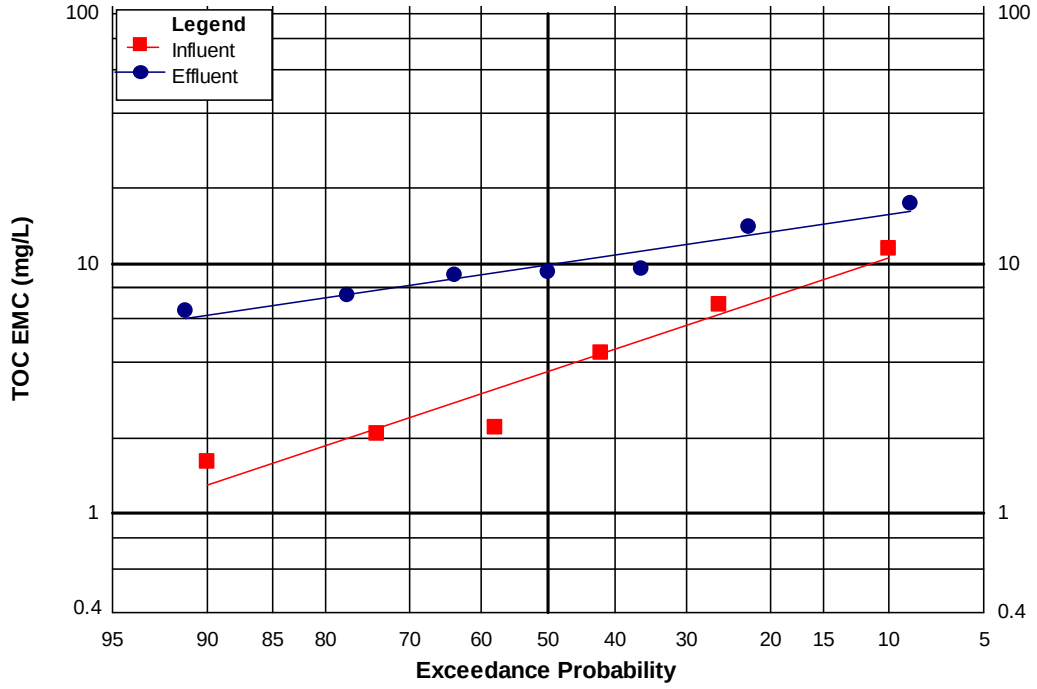

Cell SS

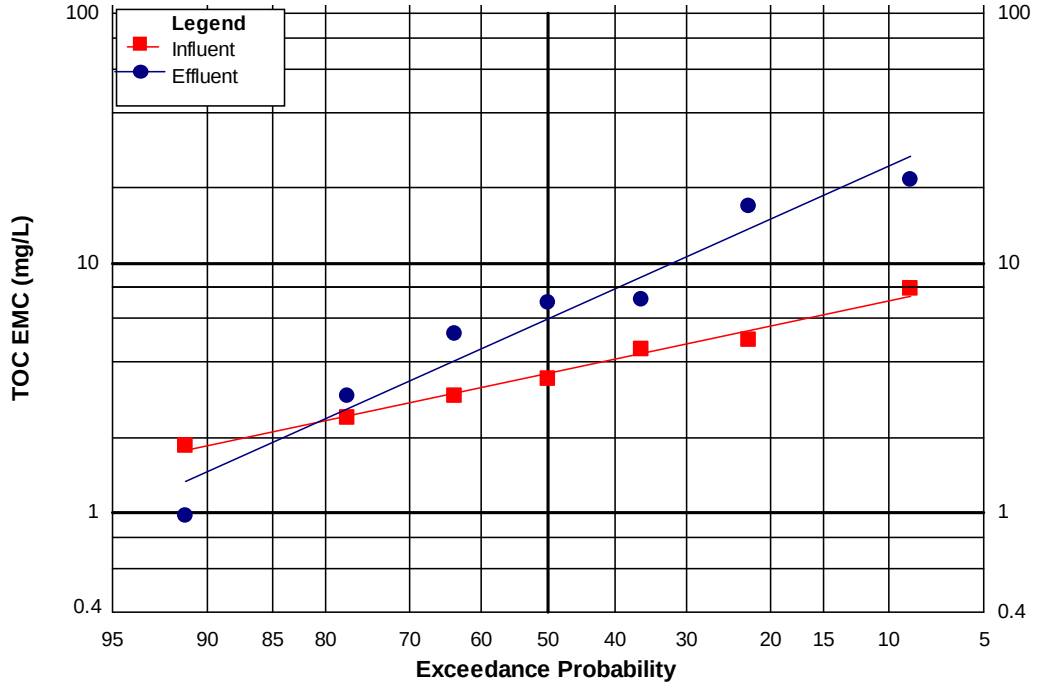

Chloride

Cell CP

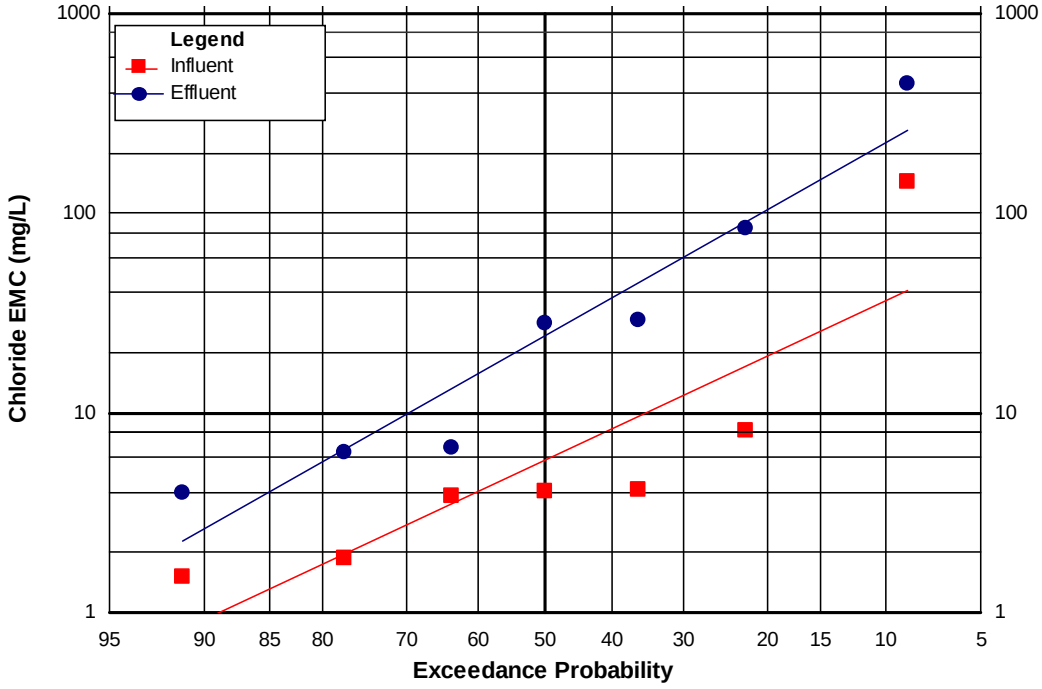

Cell SS

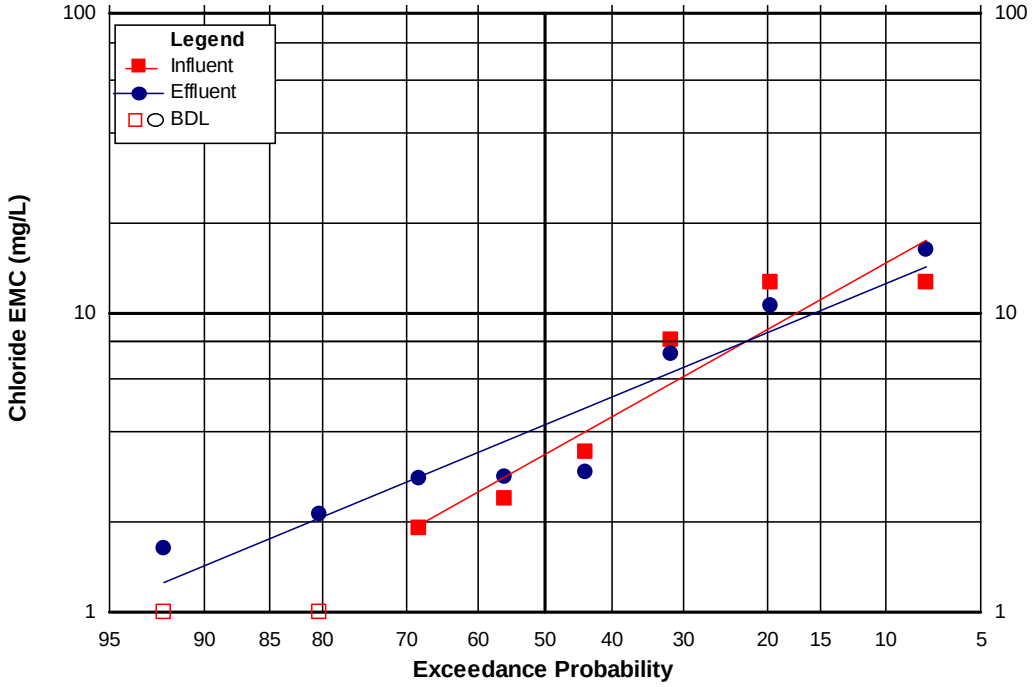

E. Coli.

Cell CP

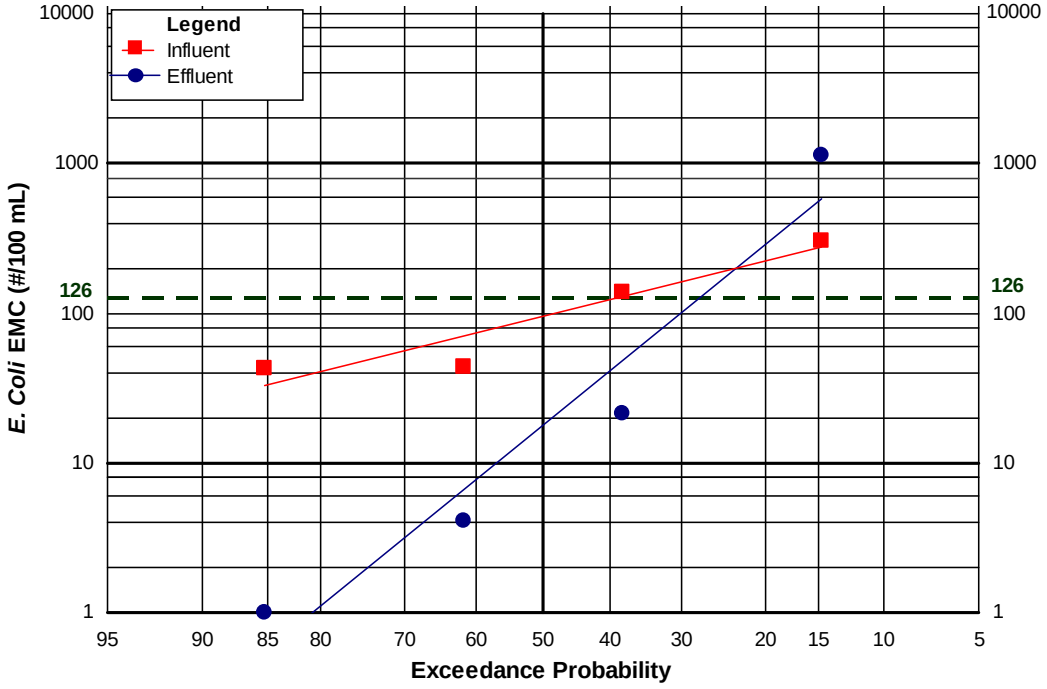

Cell SS

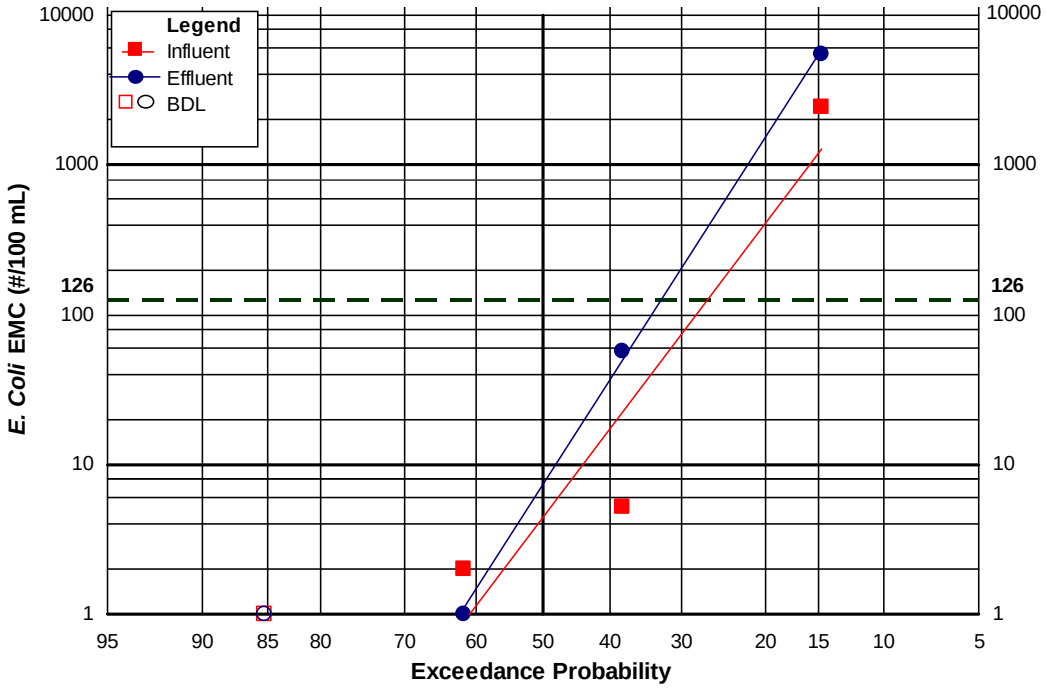

Fecal Coliform

Cell CP

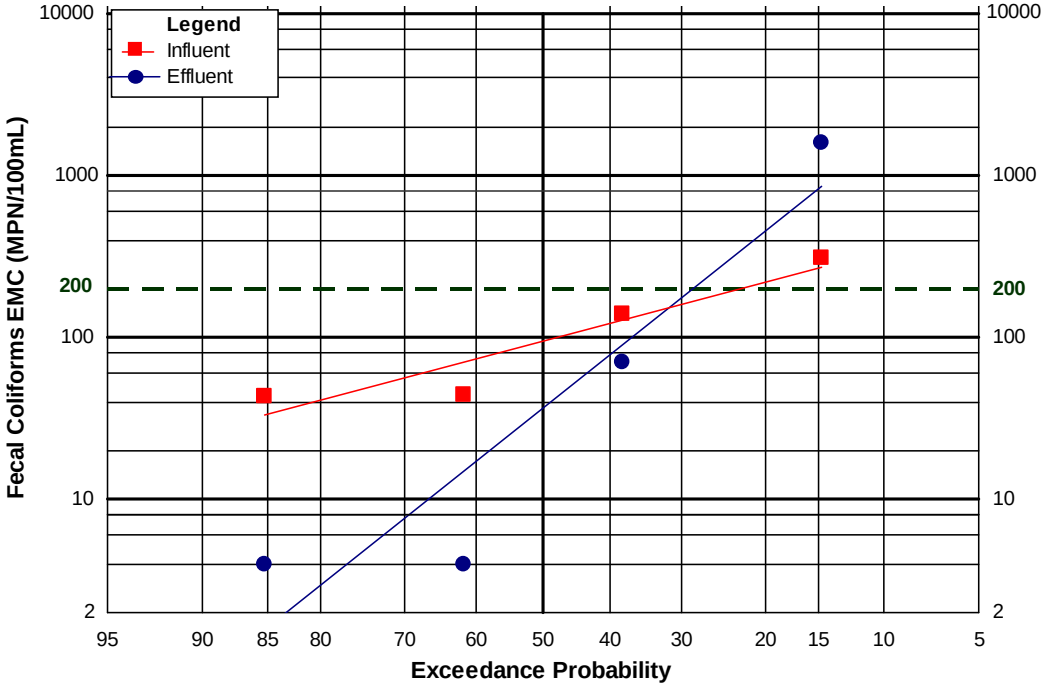

Cell SS

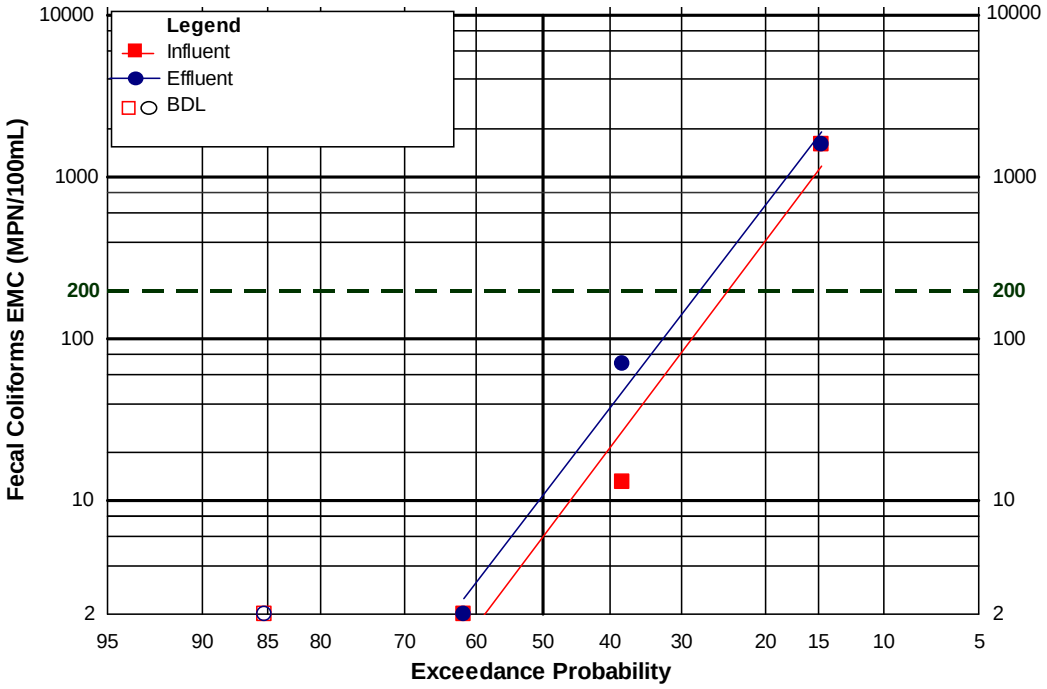

Appendix 3: Bioretention Column Test Results

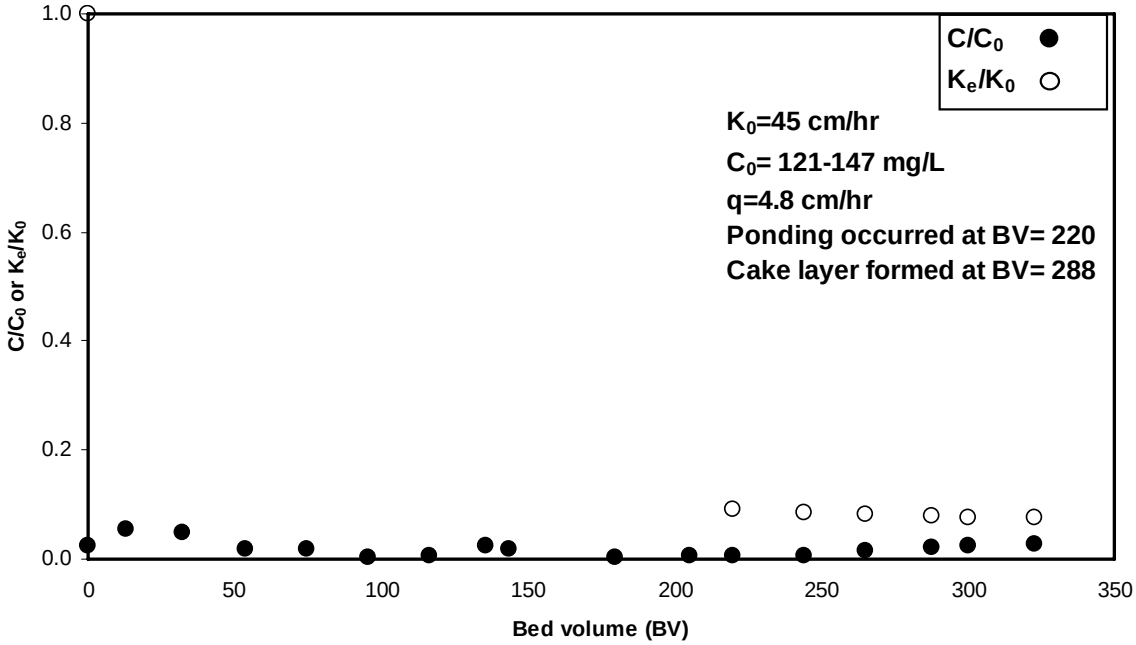

Trial 1 (Soil I/Kaolin), inflow rate = 4.8 cm/hr, input TSS=134±9 mg/L, media depth = 5.5 cm.

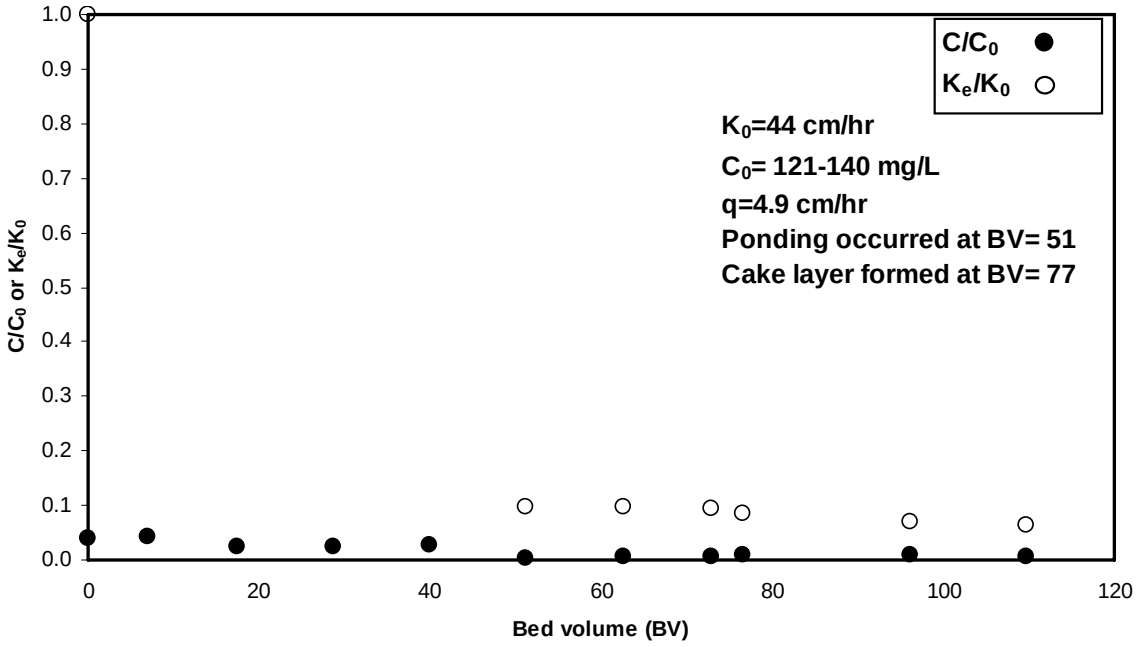

Trial 2 (Soil I/Kaolin), inflow rate = 4.9 cm/hr, input TSS=130±8 mg/L, media depth = 10.5 cm.

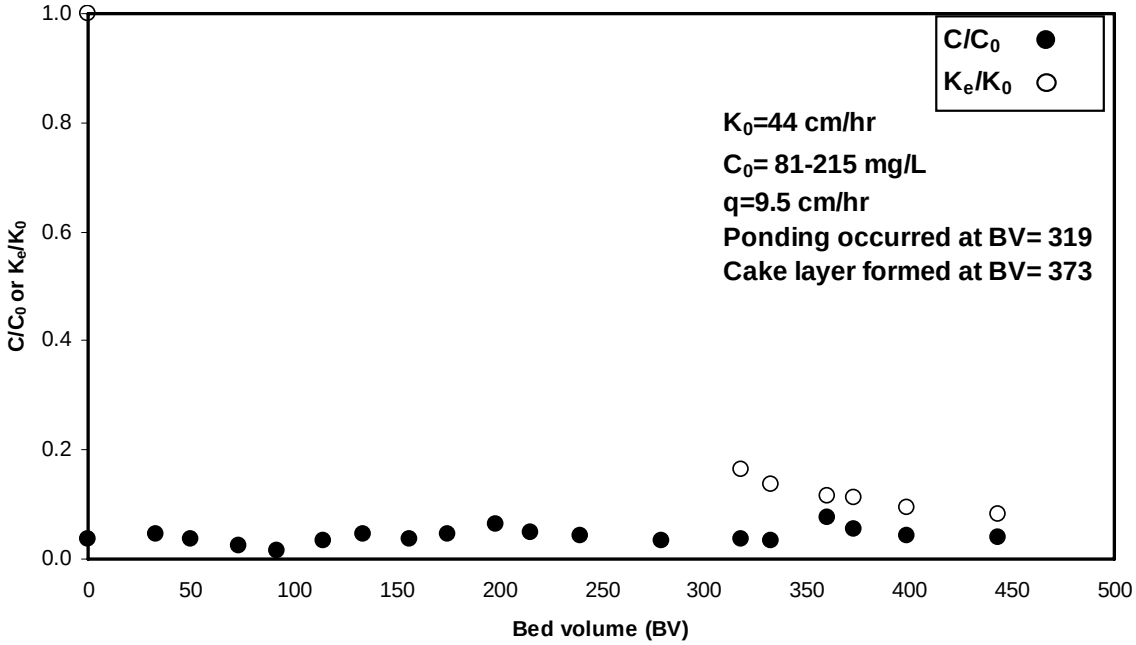

Trial 3 (Soil I/Kaolin), inflow rate = 9.5 cm/hr, input TSS=132±29 mg/L, media depth = 5.5 cm.

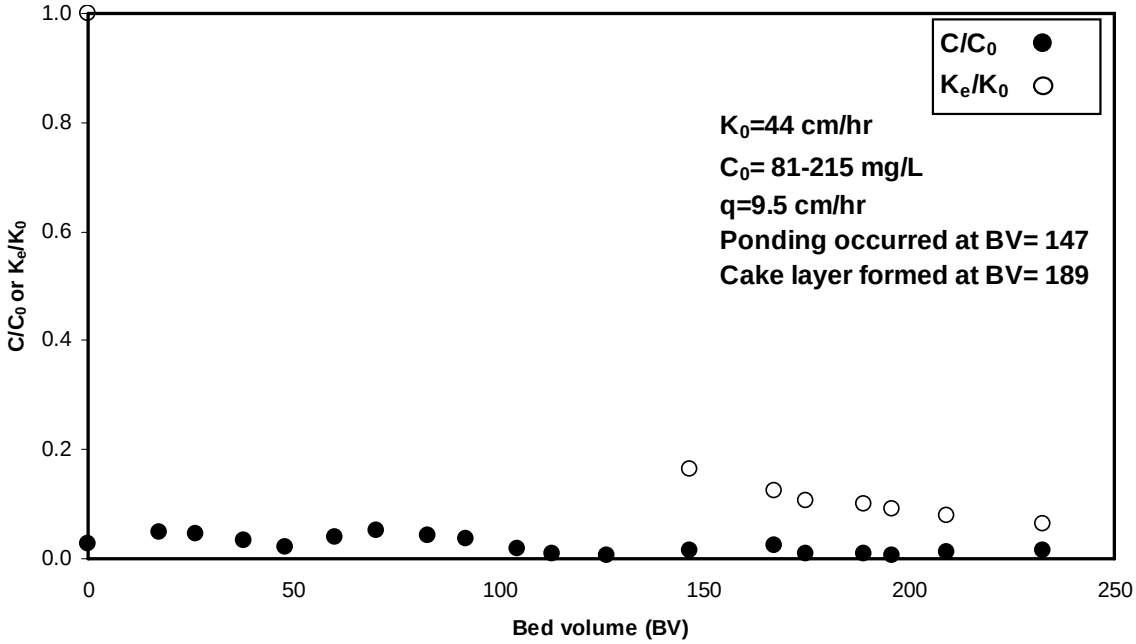

Trial 4 (Soil I/Kaolin), inflow rate = 9.5 cm/hr, input TSS=132±29 mg/L, media depth = 10.5 cm.

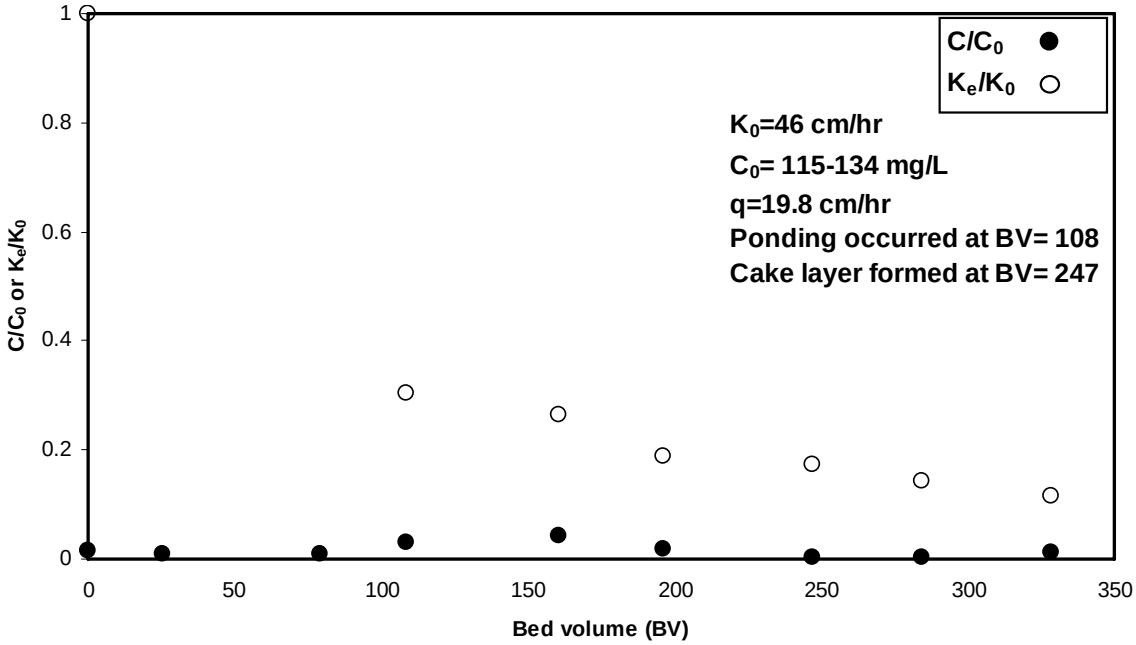

Trial 5 (Soil I/Kaolin), inflow rate = 19.8 cm/hr, input TSS=126±7 mg/L, media depth = 5.5 cm.

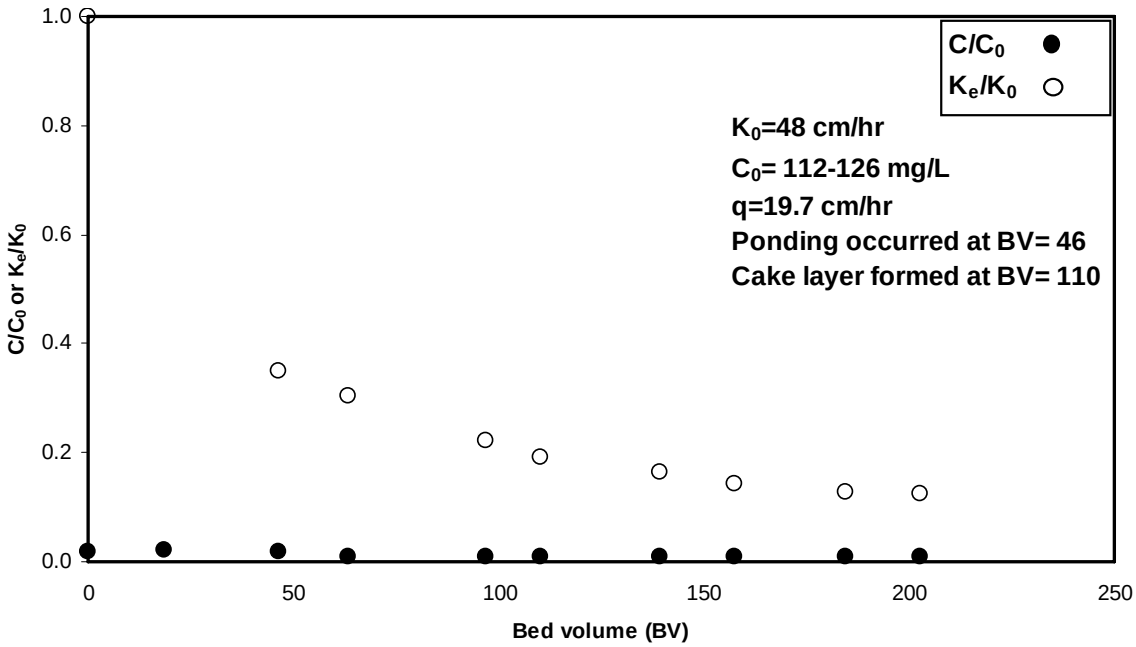

Trial 6 (Soil I/Kaolin), inflow rate = 19.7 cm/hr, input TSS=121±5 mg/L, media depth = 10.5 cm.

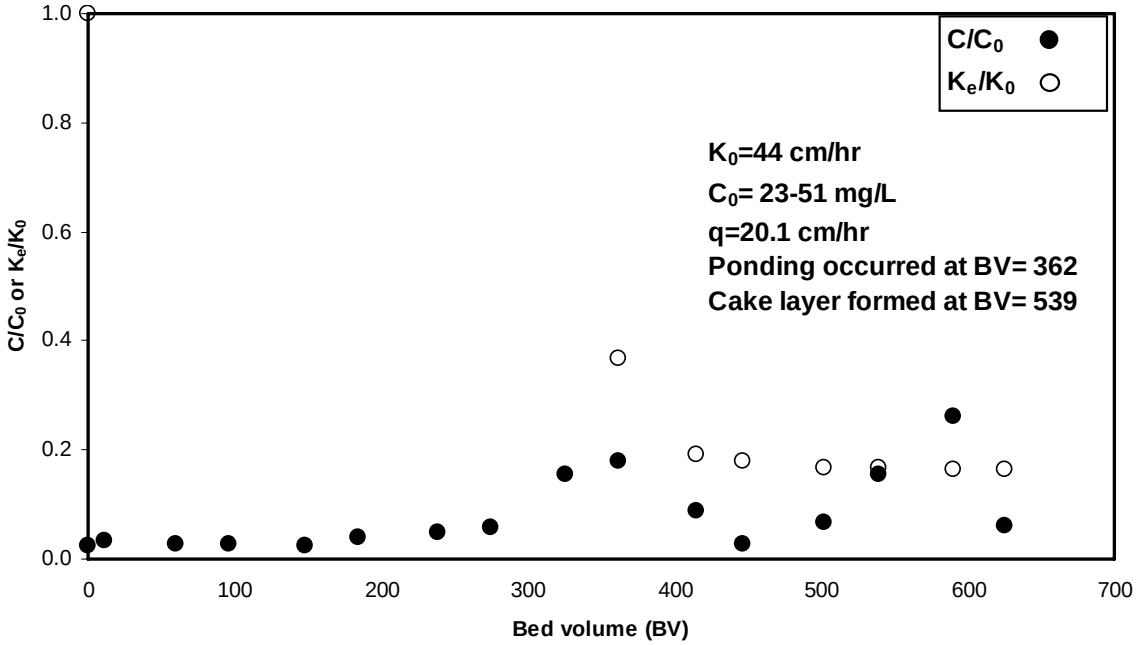

Trial #7 (Soil I/Kaolin), inflow rate = 20.1 cm/hr, input TSS=36±7 mg/L, media depth = 5.5 cm.

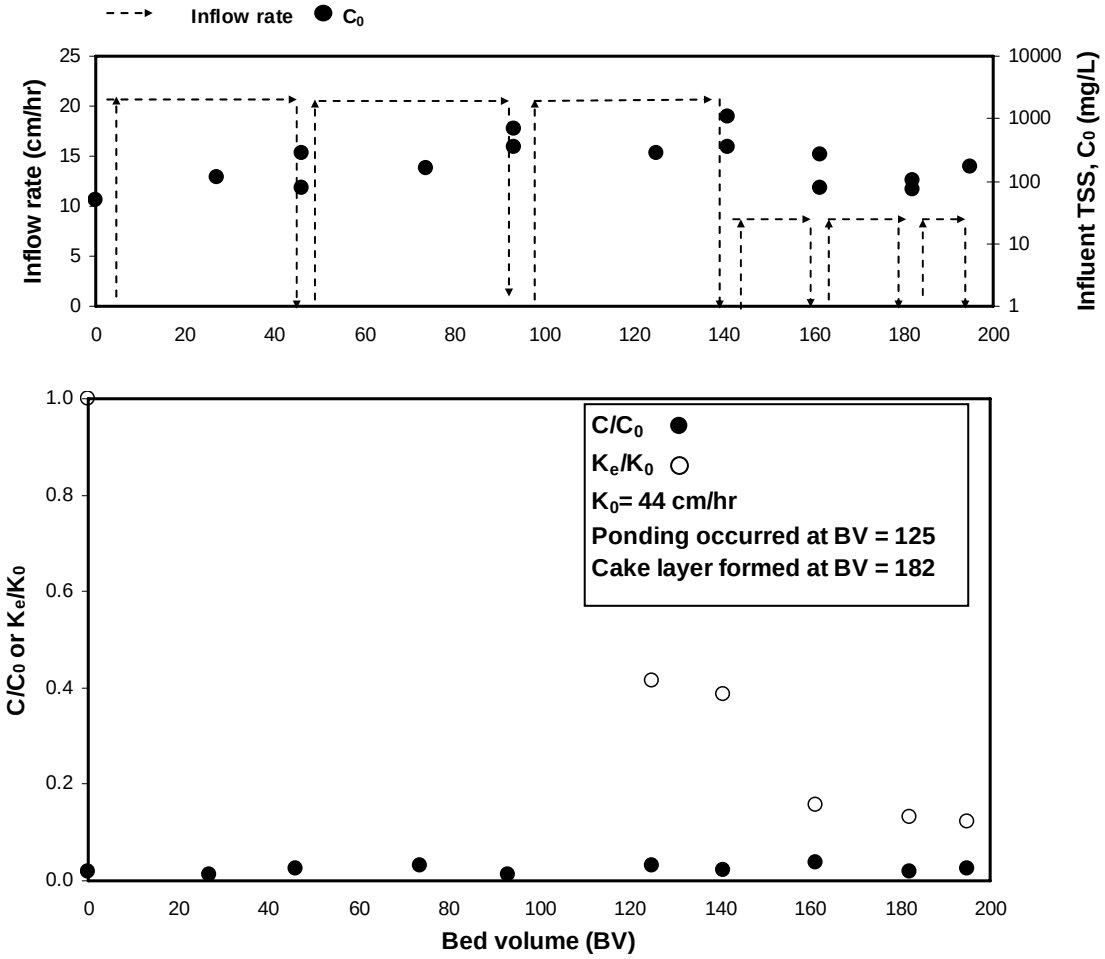

Trial 8 (Soil I/Kaolin), inflow rate = 20.8→9.0 cm/hr (intermittent), input TSS=49-1062 mg/L, media depth = 10.5 cm.

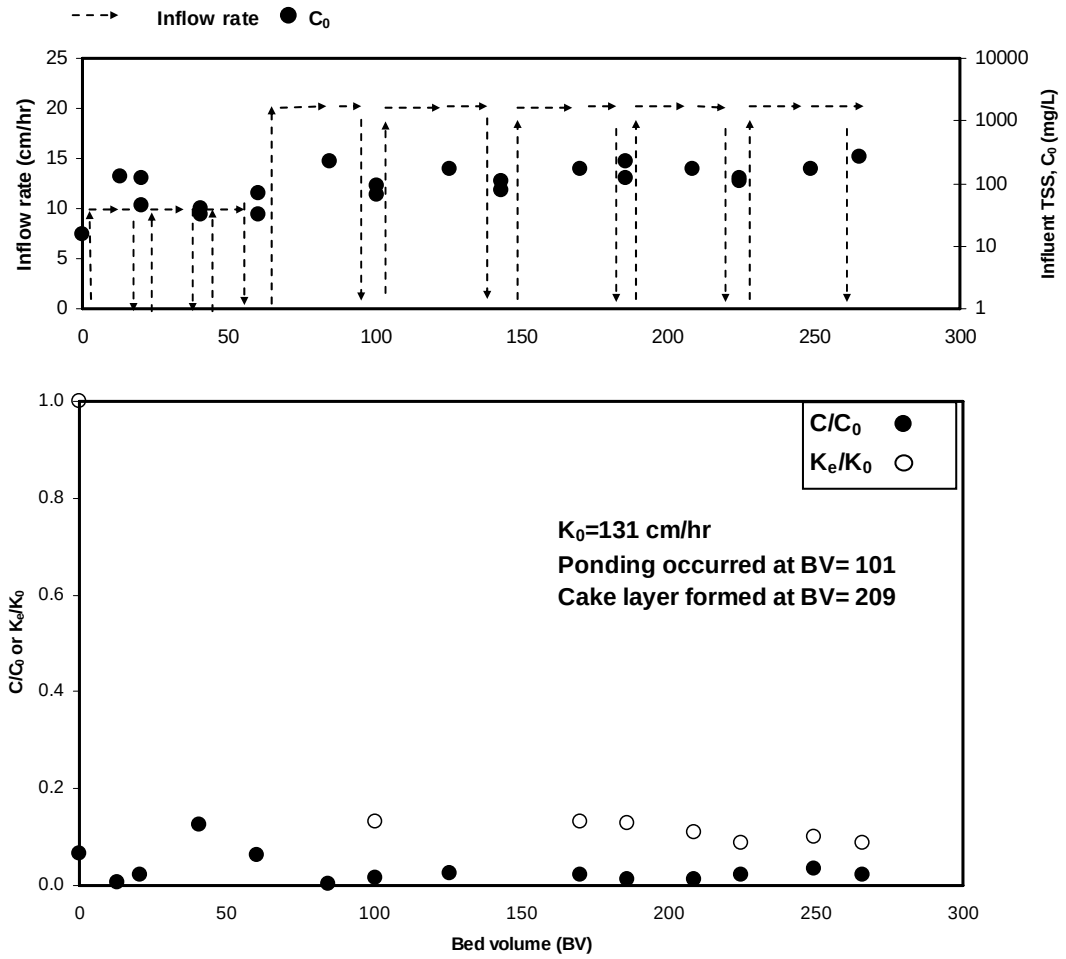

Trial 9 (Soil I/Kaolin), inflow rate = 9.1→18.9 cm/hr (intermittent), input TSS=15-261 mg/L, media depth = 10.5 cm.

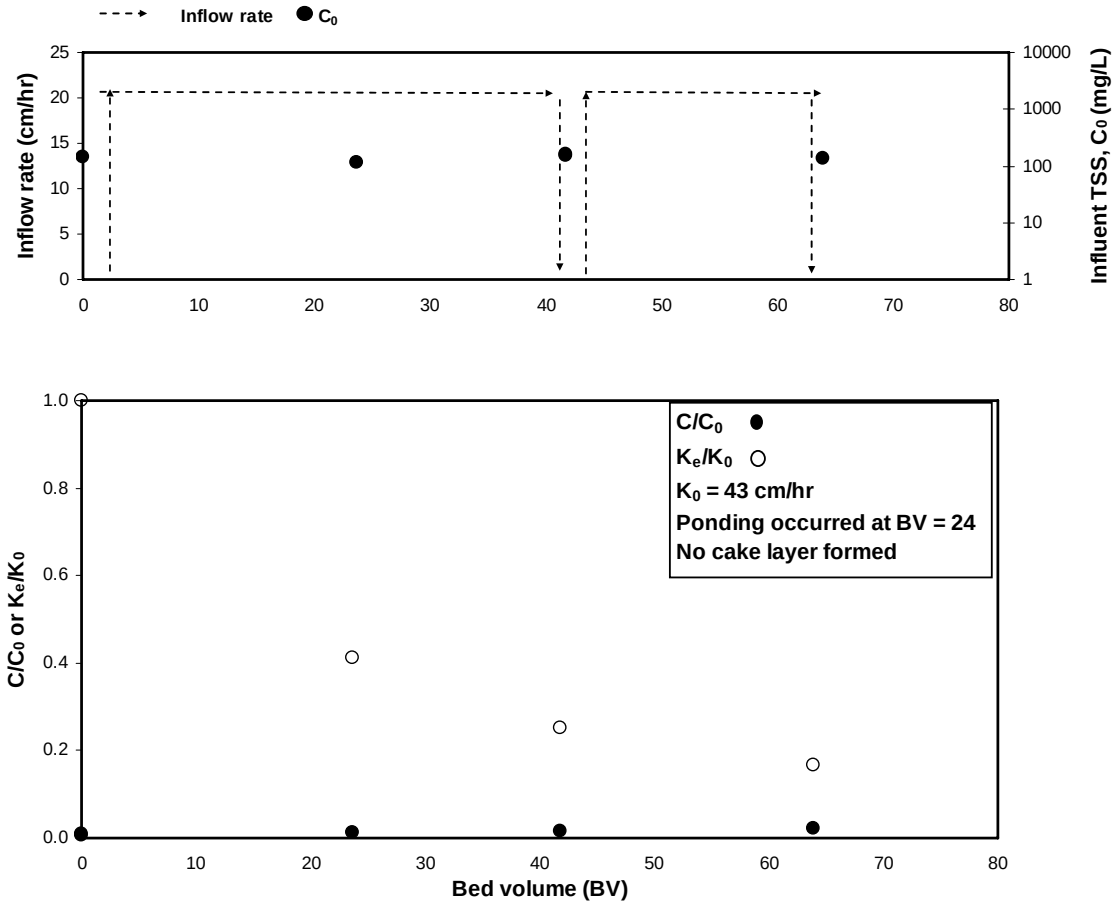

Trial 10 (Soil I/Montmorillonite), inflow rate = 19.0 cm/hr (intermittent), input TSS=114-161 mg/L, media depth = 10.5 cm.

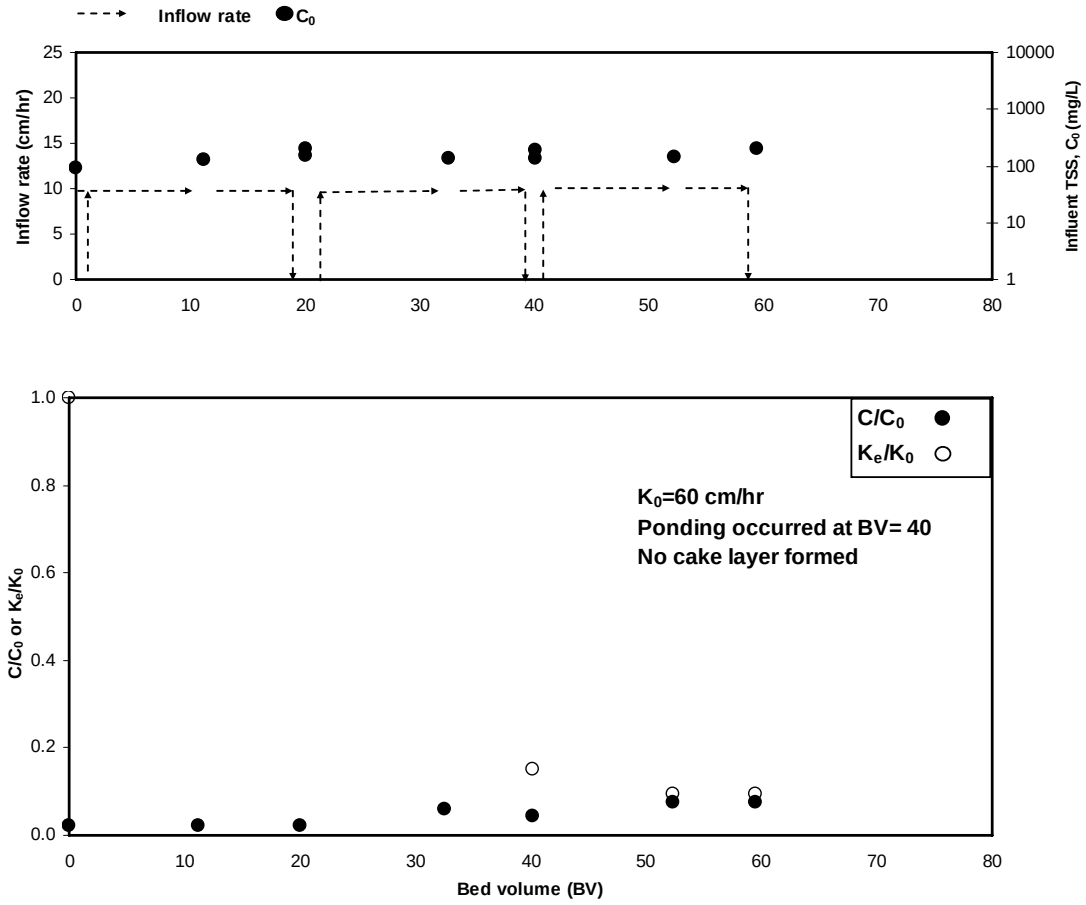

Trial #11 (Soil I/Montmorillonite), inflow rate = 9.3 cm/hr (intermittent), input TSS=94-202 mg/L, media depth = 10.5 cm.

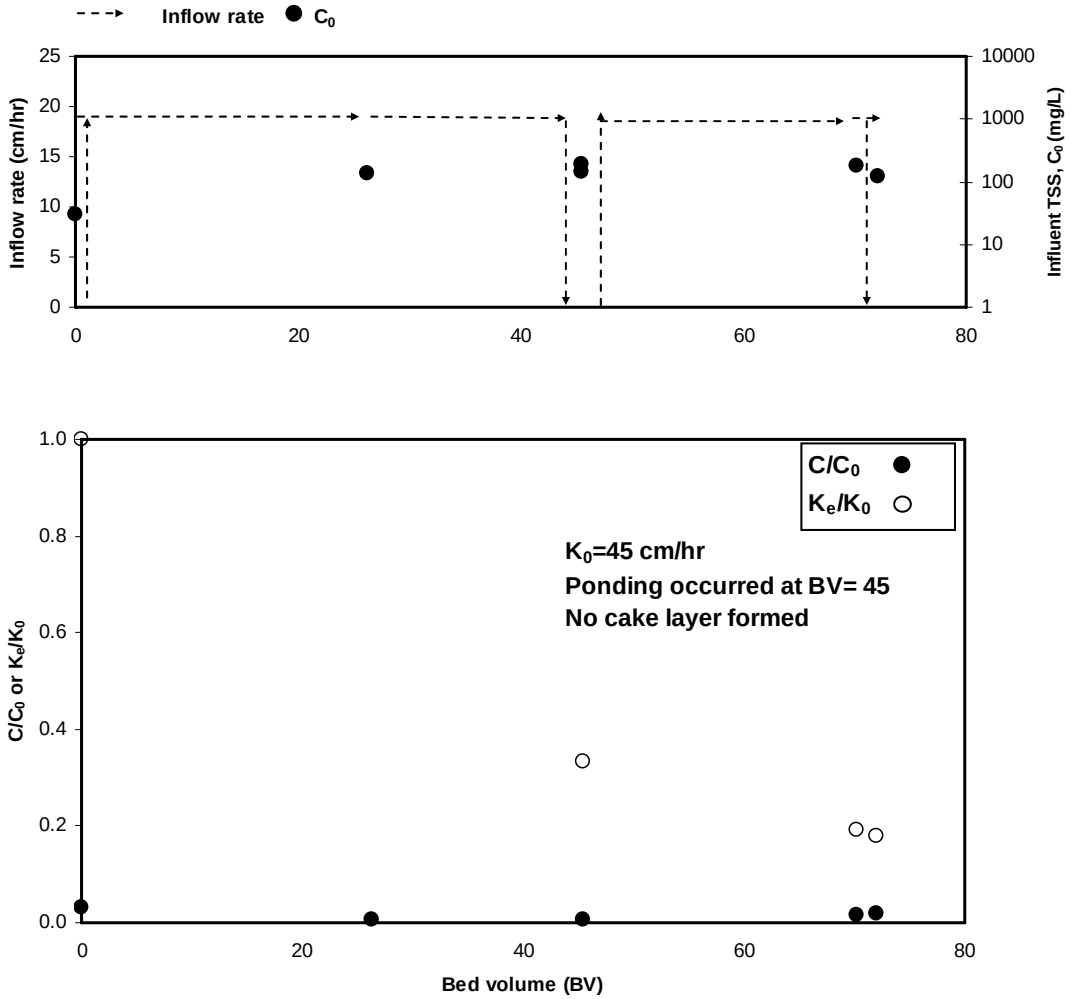

Trial 12 (Soil II/Kaolin), inflow rate = 19.6 cm/hr (intermittent), input TSS=31-195 mg/L, media depth = 10.5 cm.

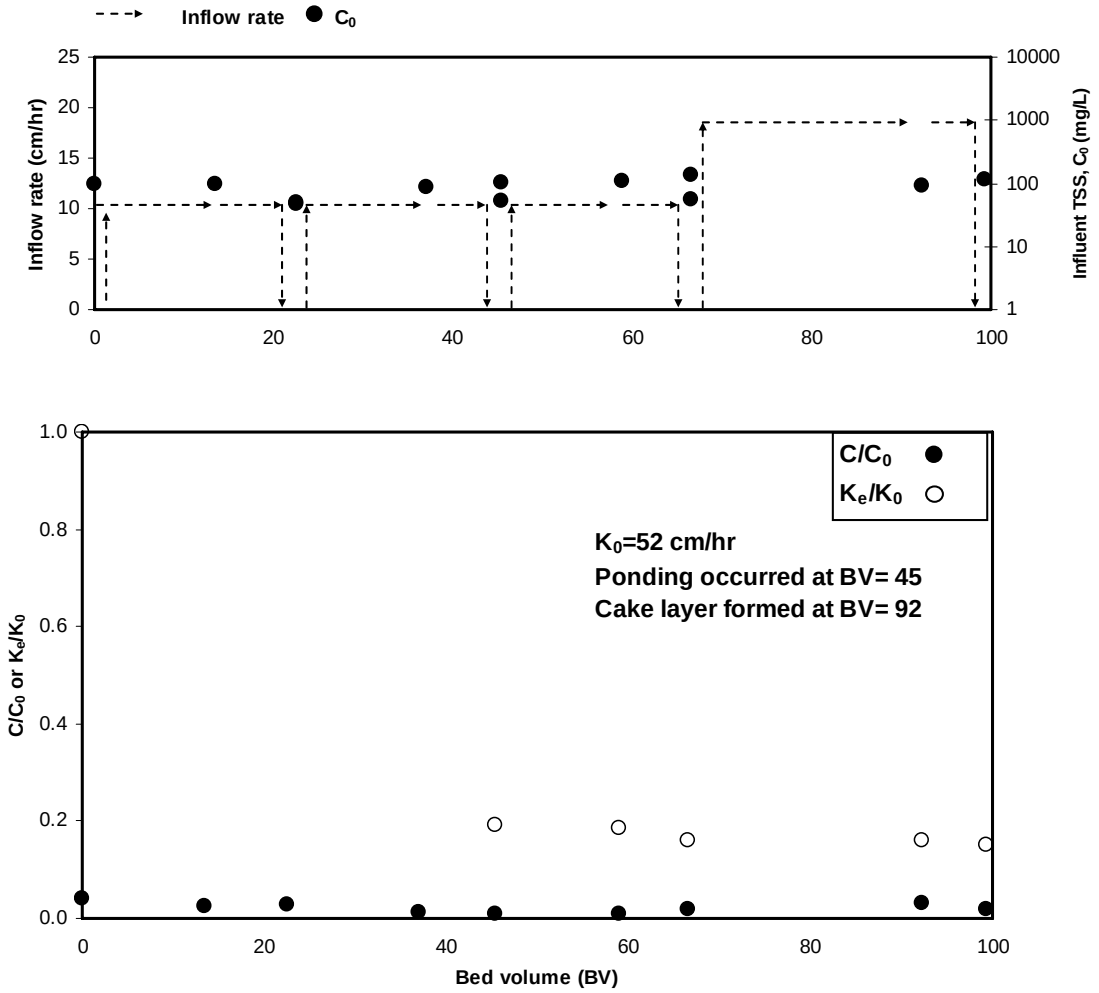

Trial 13 (Soil II/Kaolin), inflow rate = 10.3→19.7 cm/hr (intermittent), input TSS=48-133mg/L, media depth = 10.5 cm.

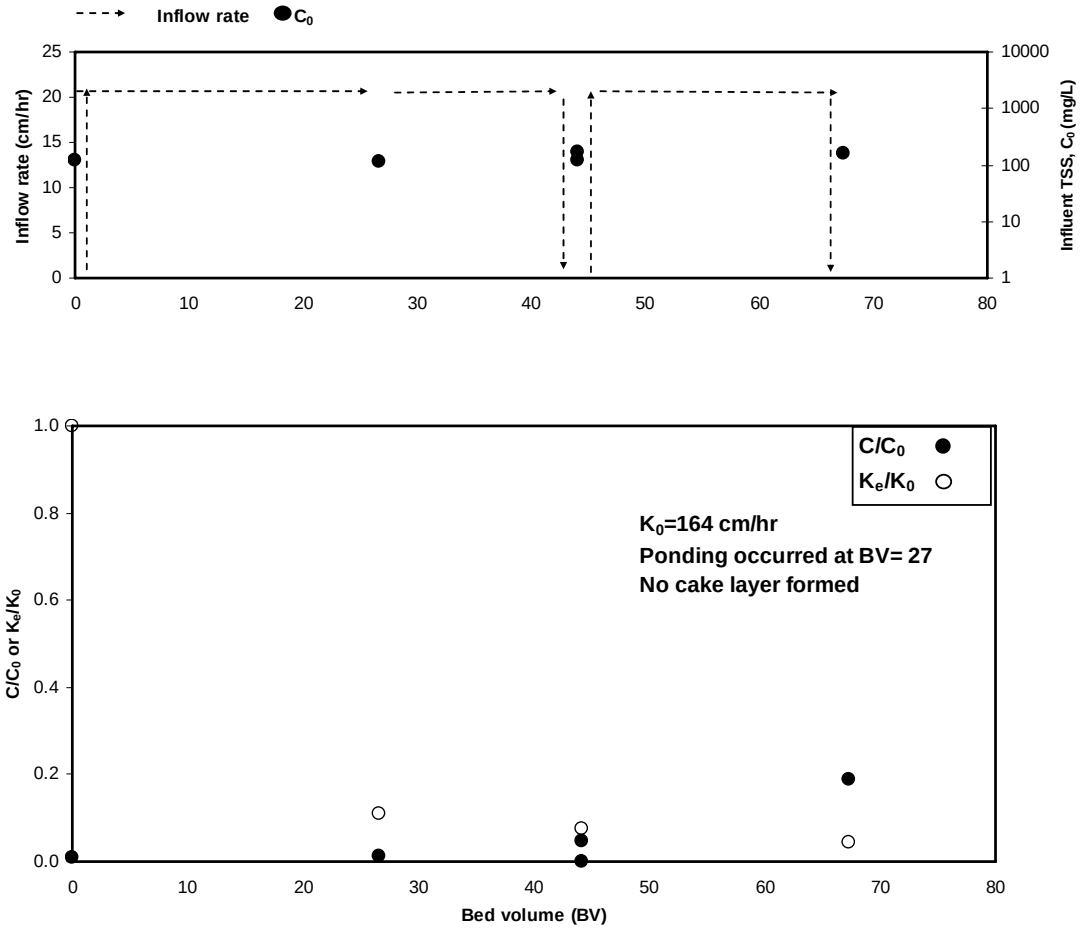

Trial 14 (Soil II/Montmorillonite), inflow rate = 19.6 cm/hr (intermittent), input TSS=118-166 mg/L, media depth = 10.5 cm.

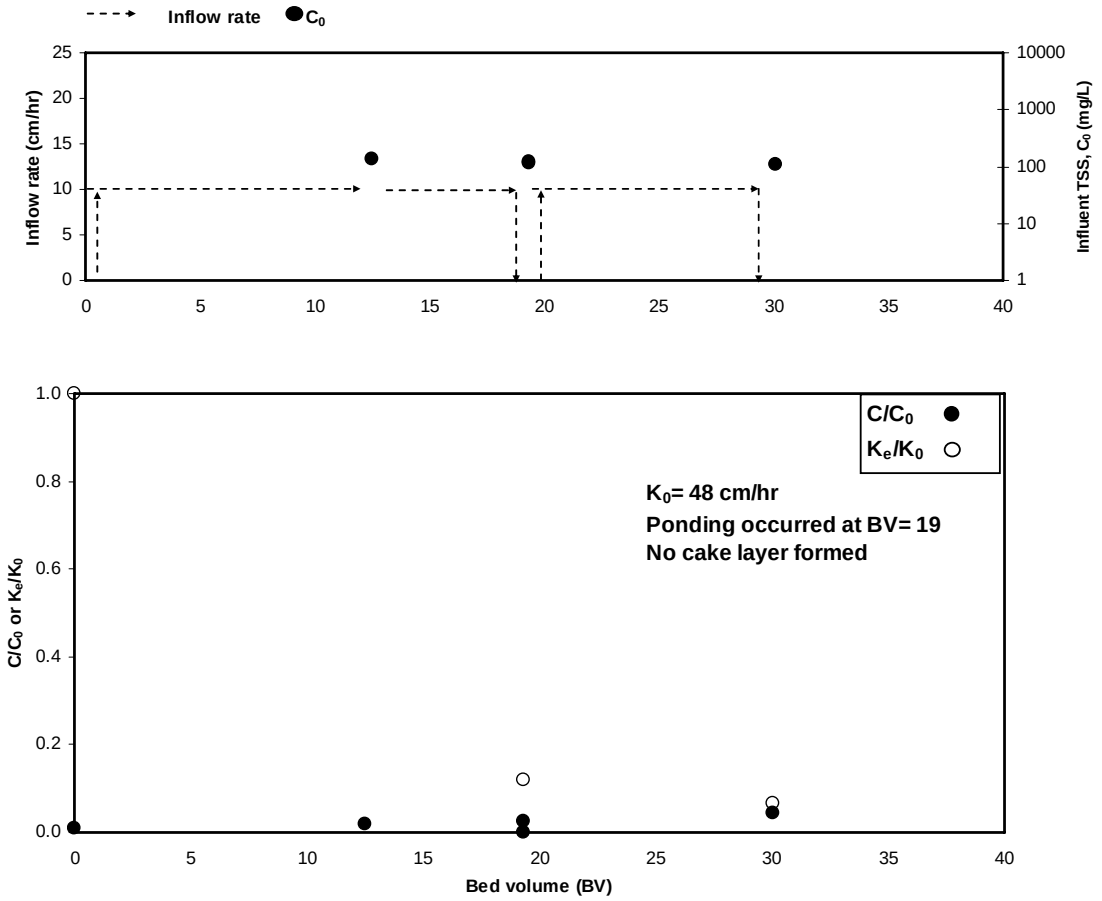

Trial 15 (Soil II/Montmorillonite), inflow rate = 9.1 cm/hr (intermittent), input TSS=110-134 mg/L, media depth = 10.5 cm.

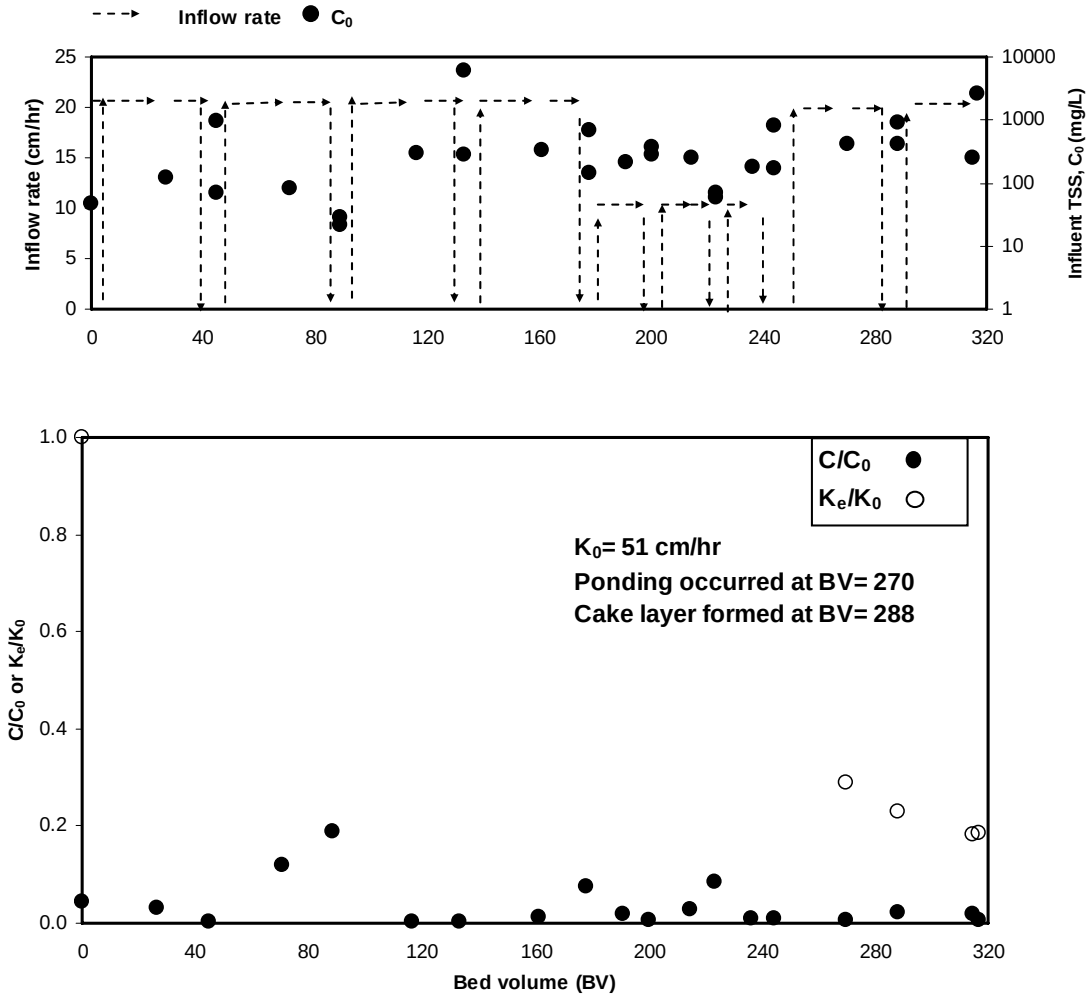

Trial 16 (Soil I/Silt), inflow rate = 19.9→9.8→20.4 cm/hr (intermittent), input TSS=21-6030 mg/L, media depth = 10.5 cm.

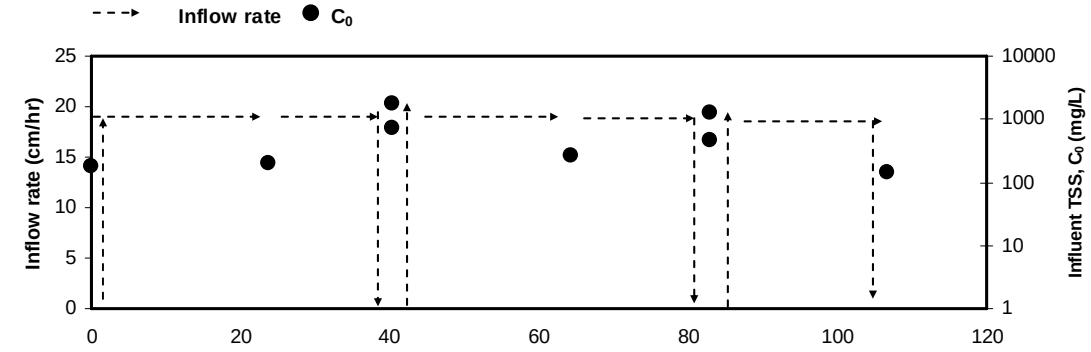

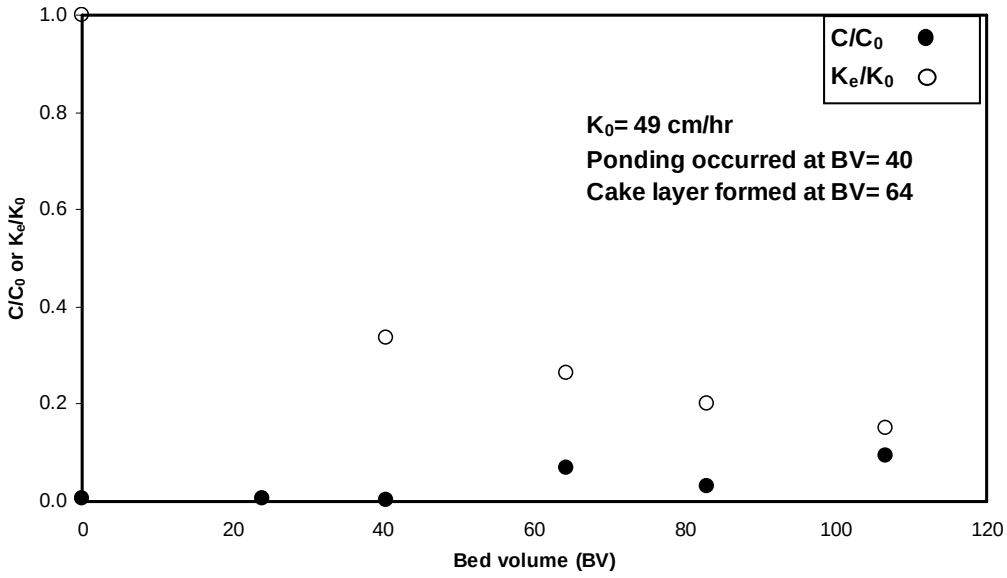

Trial #17 (Soil II/Silt), inflow rate = 18.5 cm/hr (intermittent), input TSS=140-1774 mg/L, media depth = 10.5 cm.

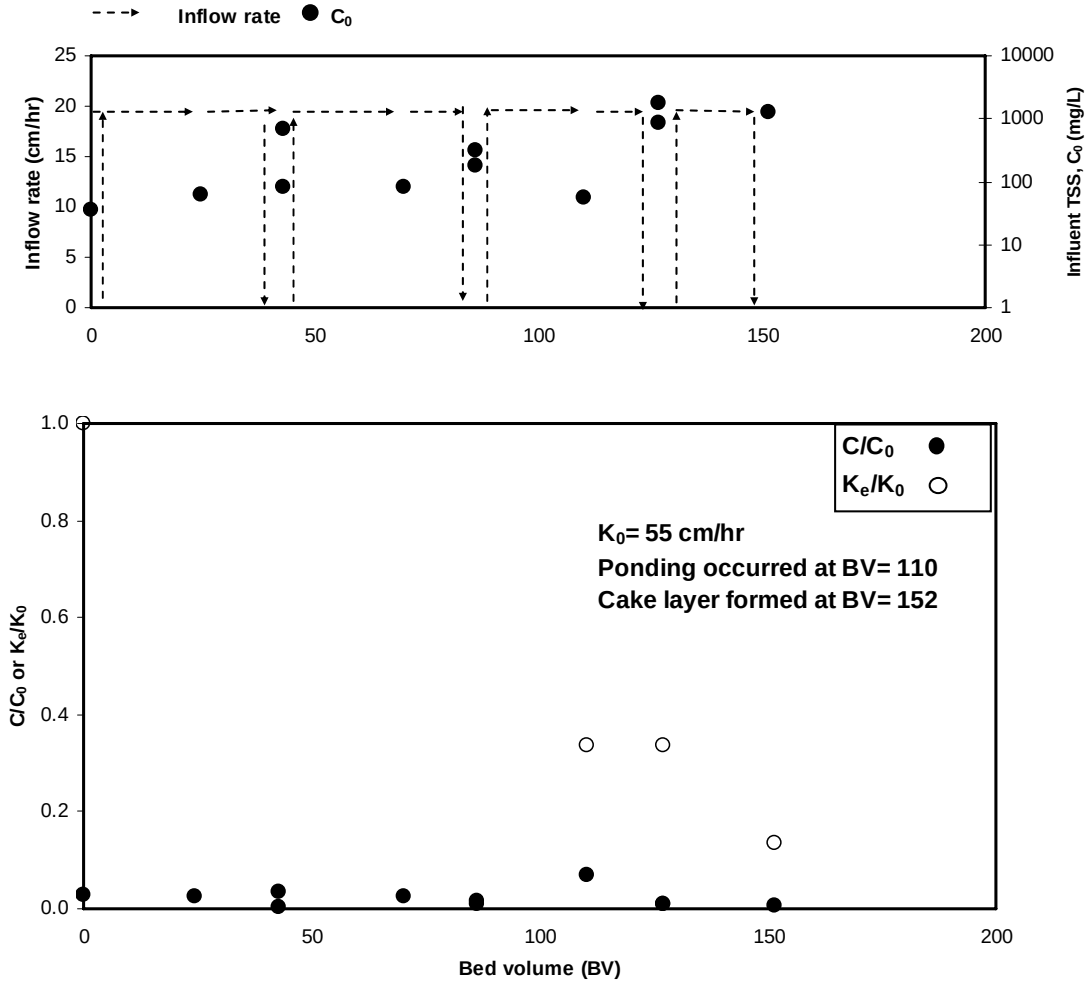

Trial 18 (Soil I/Sand), inflow rate = 19.0 cm/hr (intermittent), input TSS=35-1729 mg/L, media depth = 10.5 cm.

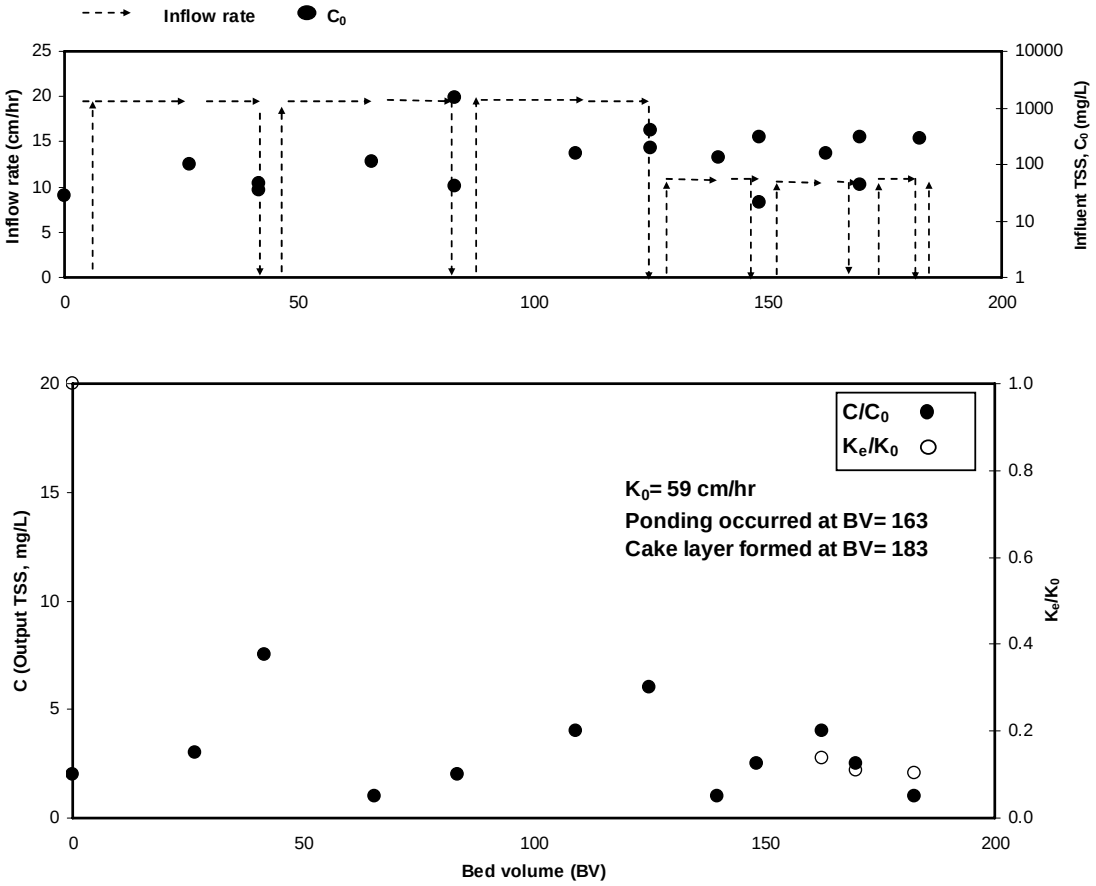

Trial 19 (Soil I/Mixture: 80% Silt+10% Sand+5% Kaolin+5% Montmorillonite) versus model predition, inflow rate = 18.5→9.8 cm/hr (intermittent), input TSS=28-1535 mg/L, media depth = 10.5 cm.

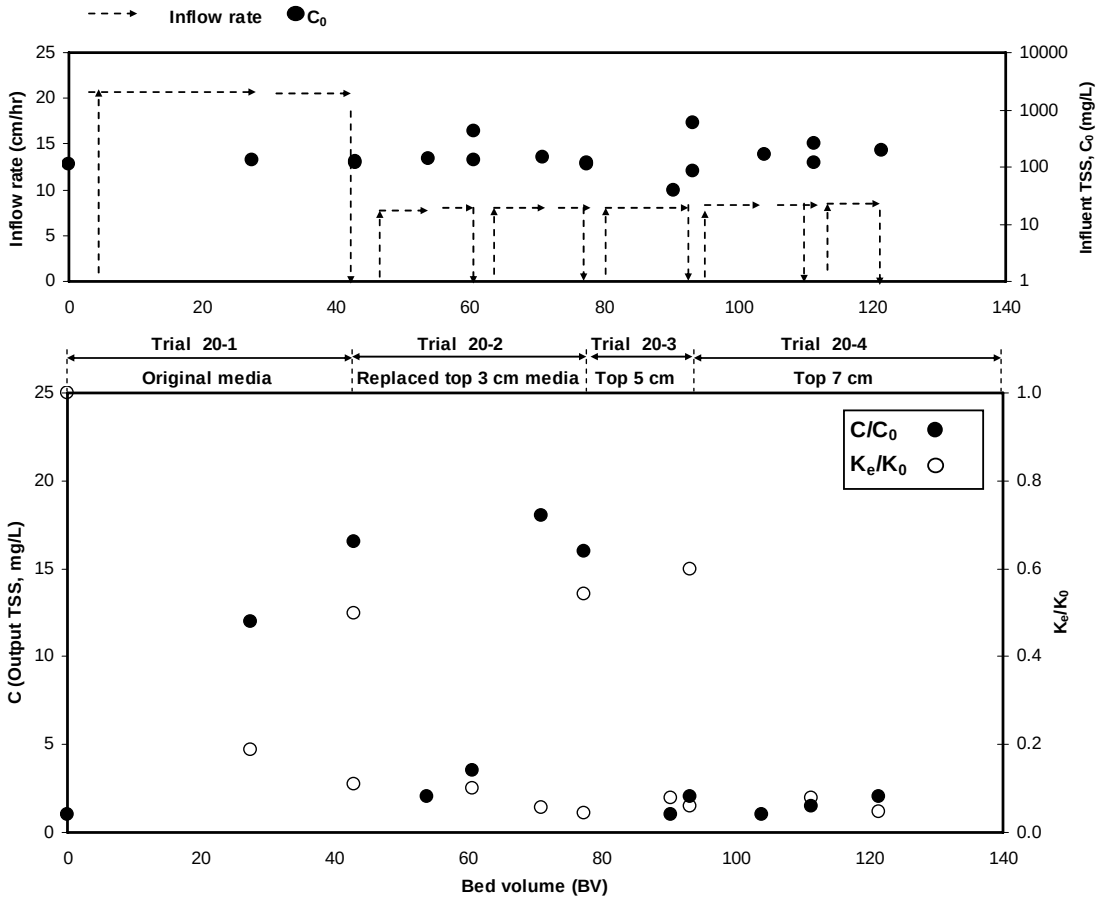

20 (Soil II/Montmorillonite) versus model prediction, inflow rate = 19.9→8.3→9.6→8.1 cm/hr (intermittent), input TSS=28-1535 mg/L, media depth = 10.5 cm.

Appendix 4: An Example for the Source Code of the Computer Program for Model Simulation

```
% Depth and cake filtration modeling

% Suspended solids removal, particles retained, and hydraulic conductivity

% in engineered bioretention

% Used in simulation of column test # 9.
%

% //////////////////
function sim_Kao_Soil_I
clear;
% input the bioretention cell characteristics(unit: cm)
% assumed column shape

L = 10.5;   % depth of media (unit: cm)
LT(1) = L;
Dc = 2*2.54;  % diameter of column (unit: cm)
Ac = pi/4*Dc*Dc; % (Cross-sectional area of filter bed)
dm = 520; % median diameter of packed media (?m)
% \\\\\\\\\\\\\\\\\\

%//////////////////

% input runoff suspended solids characteristics
% Suspended soilds type: kaolin (?s=1.8 in g/cm^3)

densityS = 1.8; %(?=1.8 in g/cm^3)
dp = 1; % median diameter of TSS (um), actually <1 in Kaolin and Montmorillonite
% //////////////////

% //////////////////
% input hydraulic and depth filtration model parameter
% Media- Soil I, TSS- Kaolin
K0 = 131.0 % clean bed hydraulic conductivity, when K0 is determined with experiment (cm/hr)
Ka(1)= K0;
Kb(1)= K0;
Ke(1)= K0;
Gamma = 200; % dimensionless
Lambda0= 0.34; % ?0=clean bed filter coefficient for certain packing length (1/cm)
Lambda (1) = Lambda0;
b= 2.0; % As in Lambda = Lambda0+b(Sigmav), in 1/cm;
%//////////////////////

% //////////////////
% input cake layer characteristics
porosityC = 0.65; % ?c as the cake layer porosity, dimensionless;
Kc= 5.6; % hydraulic conductivity of cake layer, in cm/hr;
```

```
EBC= 0.13; %E=Ke/K0 when EBC<=E, cake build up;
% ////////////////////////

% ///////////////////
% input precipitation/inflow data

% input time as hours.

inflowdata = xlsread ('inflowdata.xls');
Tin = inflowdata(:,1);   % unit: hour
Qin = inflowdata(:,2);   % unit: cm^3/hr

% discretize the time and bedvolume domain:

n = length (Tin);

dt(1)=Tin(2)-Tin(1);
tmax = max(Tin);

dBV(1) = ((dt*Qin(1)-0)*Ac)/L/Ac; % first delta bed volume (unit: cm^3)
BV(1) = 0; % Bed volume (BV, in cm^3)

for i= 2 : n;
   dt(i)= Tin(i)-Tin(i-1);

end


for i = 2:n;
   dBV(i) = (dt(i)*Qin(i)*Ac)/L/Ac;
   BV(i) = dBV(i)+ BV(i-1);
end
% ///////////////////

% input inflow TSS data

% input time as hours

Cinss = inflowdata(:,3);    % unit: mg/L

% \\\\\\\\\\\\\\\\\\\


% ///////////////////
% Calculate specific deposit
dSolidloading(1)=0;
dSigma (1) = 0;
Sigma (1) = 0;
Sigmav (1) = 0;

for i= 2:n;
   dSolidloading(i) = (dBV(i)*Ac*L/1000)*(Cinss(i)/1000);
   dSigma (i) = dSolidloading(i)/Ac/L; % in g/cm^3;
   Sigma (i) = dSigma (i)+ Sigma (i-1);
   Sigmav(i)= Sigma (i)/ densityS;
   Lambda (i)=Lambda0 + b*Sigmav (i); % Calculate Lambda;
```

```
end
% ////////////////////////////////

% \\\\\\\\\\\\\\\\\\\\
% Depth filtration;
Lc(1) = 0;
La(1) = L;
Lb(1) = 0;
C (1)= Cinss(1)*exp(-Lambda(1)*L);
for i = 2:n;
   Ka(i)=K0;
   Lb (i)= (log(0.05+0.95*exp(-Lambda(i)*L)))/(-Lambda(i));
   La (i)= L-Lb(i);
   C(i)=Cinss(i)*exp(-Lambda(i)*L);
   Ke(i)=K0/(1+Gamma*Sigmav(i))^2;
   Kb(i)= Lb(i)/(L/Ke(i)-La(i)/Ka(i));
   Kcc(i)=0;
   Lc(i)=0;
end
% ////////////////////

 %
% ////////////////////
% calculate mass capture
M(1)=0;

for i= 2: n;
   dM(i)= (dBV(i)*Ac*L/1000)*((Cinss(i)-C(i))/1000);% in gram
   M(i)=  M(i-1)+dM(i); % Total TSS captured
end
% ////////////////////////////



% ////////////////////
% Transition zone between depth filtration (headlosss buildup) to cake
% filtration
% ////////////////////////////////////////////////////////
A(1)=1;%=Ka(1)/K0;
B(1)=1;%=Kb(1)/K0;
E(1)=1;%=Ke(1)/K0;
Lc(1)=0;
for i = 2: n;
   Ka (i)=K0;
   A(i)=Ka(i)/K0;
   B(i)=Kb(i)/K0;
   E(i)=Ke(i)/K0;
   Lc (i) = 0;
   if E(i)<=EBC;
      Sigma(i)=Sigma(i-1);
       Lc (i) = (M(i)/densityS/Ac-L*Sigma(i))/(1-porosityC);
       if Lc(i)<0;
          Lc(i)=0; % Buffer for the transitional regime of depth filtration/cake filtration,
       else
          Sigma(i)=Sigma(i-1);
          Sigmav(i)=Sigmav(i-1);% Cake filtration mechanism takes over.
```

```
        Lambda (i)=Lambda0 + b*Sigmav (i); % Re-Calculate Lambda;
        Lb (i)= Lb(i-1);
        La (i)= L-Lb(i);
        C(i)=Cinss(i)*exp(-Lambda(i)*L); % Recalculate C
        Kb(i)= Kb(i-1)
      end
   LT(i)=L+Lc(i);
   Kcc(i)=Kc;
   Ke(i)= LT(i)/(La(i)/Ka(i)+Lb(i)/Kb(i)+Lc(i)/Kcc(i));
end
end
% ////////////////////////////


% ////////////////////////////
% calculate mass capture through cake filtration and depth filtration
Md(1)=0;
Mc(1)=0;

for i= 2: n;
   Mc(i)=Lc(i)*Ac*(1-porosityC)*densityS; % TSS capture through cake filtration;
   Md (i)= M(i)-Mc(i); % TSS capture through depth filtration;
end


% Plot the results

figure(1)

plot(BV,C);

% Add information to the plot

title ({'Effllluent TSS'})

xlabel ('Bed Volume')

ylabel ('TSS, mg/L')

hold            % clears display for next plot.

figure(2)


plot(BV,Ke,'b')

hold            % allows other curves to be added
% Add information to the plot
title ({'Soil column conductivity'})

xlabel ('Bed volume')

ylabel ('Hydraulic conductivity, cm/hr')

hold
```

```
% Output
% Tranapose matrix for the same row number to output

OutBV = transpose (BV);
OutLambda = transpose (Lambda);
OutC = transpose (C);
OutLa = transpose (La);
OutLb = transpose (Lb);
OutLc = transpose (Lc);
OutKa = transpose (Ka);
OutKb = transpose (Kb);
OutKc = transpose (Kcc);
OutKe = transpose (Ke);
OutM = transpose (M);
OutMc = transpose (Mc);
OutMd = transpose (Md);
OutSigmav = transpose (Sigmav);
output = [Tin, OutBV, OutLambda, OutC, OutLa, OutLb, OutLc, OutKa, OutKb, OutKc, OutKe,
OutM, OutMc,OutMd, OutSigmav];
export = strcat('export', '.xls');
save ([export], 'output', '-ascii', '-tabs');
```

Appendix 5: Water Quality Data of the DC Bioretention and Sand Filter Grab Samples

BMP	Pollutant	Influent			Effluent			Removal efficiencies (%)		
		Median	Minimum	Maximum	Median	Minimum	Maximum	Median	Minimum	Maximum
DC bioretention	TSS (mg/L)	119	22	9031	13	10	225	70	55	>99
	Copper (µg/L)	45	23	195	47	20	73	-9	-107	79
	Lead (µg/L)	91	5	734	15	9	20	77	-91	97
	Zinc (µg/L)	145	19	995	18	15	30	83	18	97
	TP (mg/L as P)	0.185	0.084	1.588	0.514	0.301	0.826	-180	-546	48
DC sand filter	TSS (mg/L)	5	<1	10	3	<1	30	8	-2920	75
	Copper (µg/L)	<25	12	108	<20	<10	41	35	-5	62
	Lead (µg/L)	<2	<2	3	<2	<2	2	-	-	-
	Zinc (µg/L)	200	131	471	68	62	182	63	52	87
	TP (mg/L as P)	0.071	<0.050	0.249	71	<0.050	0.259	-1	<-58	73

Bibliography

AASHTO (American Association of State Highway and Transportation Officials). (1993). *Standard Specification for Transportation Materials and Methods of Sampling and Testing.* 16 ed. p. 145, Washington, DC.

Adin, A. and Rebhun, M., (1977). "A model to predict concentration and head-loss profiles in filtration." *J. Am. Water Works Assoc*. 69 (8), 444-453.

Akgiray, Ö., and Saatci, A. M., (1998), "An algorithm for bank operation of declining rate filters." *Wat. Res.*, 32 (7), 2095-2105.

Ahnstrom, Z. S. and Parker, D. R. (1999). "Development and assessment of a sequential extraction procedure for the fractionation of soil cadmium," *Soil Sci. Soc. Am. J.*, 63, 1650-1658.

APHA; AWWA; and WPCF. (1992). *Standard Methods for the Examination of Water and Wastewater*. 18th Ed., Washington, D. C.

APHA; AWWA; and WPCF. (1995). *Standard Methods for the Examination of Water and Wastewater*. 19th Ed., Washington, D. C.

APHA; AWWA; and WPCF. (1999). *Standard Methods for the Examination of Water and Wastewater*. 20th Ed., Washington, D. C.

Arias, C. A., Bubba, M. D., and Brix, H. (2001). "Phosphorus removal by sands for use as media in subsurface flow constructed reed beds." *Water Res.*,35(5), 1159–1168.

Atherholt, T. B., LeChevallier, M. W., Norton, W. D., Rosen, J. S. (1998). "Effect of rainfall on *Giardia* and *Cryptosporidium*." *J. Am. Water Works Assoc.* 90(9), 66–80.

AWWA (American Water Work Association). (1999). *Water Quality & Treatment Handbook.* 5th Ed. McGraw-Hill, New York.

Bäckstrőm, M., Karlsson, S., and Allard, B. (2004). "Metal leachability and anthropogenic signal in roadside soils estimated from sequential extraction and stable lead isotopes," *Environ. Monit. Assess.*, 90, 135-160.

Bardin, J. P., Gautier, A., Barraud, S., and Chocat, B. (2001). "The purification performance of infiltration basins fitted with pretreatment facilities: a case study." *Wat. Sci. Tech.* 43 (5), 119-128.

Barrett, M. E., Irish Jr., L. B., Malina Jr., J. F., Charbeneau, R. J. (1998). Characterization of highway runoff in Austin, Texas, Area," *J. Environ. Eng.*, 124 (2), 131-137.

Barrett, M. E. (2003). "Performance, cost, and maintenance requirements of Austin sand filters." *J. Water Resour. Plann. Manage.*, 129 (3), 234-242.

Barrett, M. E. (2005). "Performance comparison of structural stormwater best management practices," *Water Environ. Res.*, 77 (1), 78-86.

Bedient, P. B., Hanadi, S. R., and Newell, C. J. (1999). *Ground Water Contamination- Transport and Remediation.* 2nd ed. Prentice-Hall, New Jersey, 172-173.

Blaisdell, F. W. (1994). "Results of Parshall flume tests." *J. Irrig. Drain. Eng.*, 120 (2). 278-291

Boadu, F. K. (2000). "Hydraulic conductivity of soils from grain-size distribution: new models." *J. Geotech. Geoenviron. Eng.*, 126 (8), 739-746.

Bohart, G. S. and Adams, E. Q. (1920). "Some aspects of the behavior of charcoal with respect to chlorine." *Journal of the American Chemical Society*. 42. 523-544.

Brown, J. N. and Peake, B. M. (2006). "Sources of heavy metals and polycyclic aromatic hydrocarbons in urban stormwater runoff," *Sci. Total Environ.*, 359, 145-155.

Campos, L. C., Smith, S. R., and Graham, N. J. D. (2006a). "Deterministic-based model of slow sand filtration. I: Model development." *J. Environ. Eng.* 132 (8), 872-886.

Campos, L. C., Smith, S. R., and Graham, N. J. D. (2006b). "Deterministic-based model of slow sand filtration. I: Model application." *J. Environ. Eng.* 132 (8), 887-894.

Chaudry, F. H., (1987a), "Theory of declining rate filtration I: continuous operation." *J. Environ. Eng*., 113 (4), 834-851.

Chaudry, F. H., (1987b), "Theory of declining rate filtration II: bank operation." *J. Environ. Eng.*, 113 (4), 852-867).

COMAR (Code of Maryland Regulations) (2006). 26.08.04.01-1. <http://www.dsd.state.md.us/comar/26/26.08.02.03%2D2.htm>, (8/28/2006)

Cookson, J. T. (1995). *Bioremediation Engineering: Design and Applications*. McGaw-Hill, New York.

Councell, T., Duckenfield, K. U., Landa, E. R., and Callender, E. (2004). "Tire-wear particles as a source of zinc to the environment," *Environ. Sci. Technol.*, 38 (15) 4206-4214.

Covelo, E. F., Andrade, M. L., and Vega, F. A. (2004). "Heavy metal adsorption by humic umbrisols: selectivity sequences and competitive sorption kinetics," *J. Colloid Interface Sci.*, 280 (1), 1-8

Cunnane, C. (1978). "Unbiased plotting positions- a review," *J. Hydrology*, 37, 205-222.

Cushing, R. S., and Lawler, D. F., (1998). "Depth filtration: fundamental investigation through three-dimensional trajectory analysis." *Environ. Sci. Technol.*, 32, 3793-3801.

Das, B. M. (1992). *Soil Mechanics Laboratory Manual*, 4th ed., Engineering Press, San Jose.

Davis, A. P., Shokouhian, M., and Ni, S. (2001a). "Loading estimates of lead, copper, cadmium, and zinc in urban runoff from specific sources," *Chemosphere.* 44, 997-1009.

Davis, A. P., Shokouhian, M., Sharma, H., and Minami, C. (2001b). "Laboratory study of biological retention for urban storm water management," *Water Environ. Res.*, 73 (1), 5-14.

Davis, A. P., Shokouhian, M., Sharma, H., Minami, C., and Winogradoff, D. (2003). "Water quality improvement through bioretention: lead, copper, and zinc removal," *Water Environ. Res*., 75 (1), 73-75.

Davis, A. P. (2005). "Green engineering principles promote low impact development," *Environ. Sci. Techno.*, 39 (16), 338A-344A.

Davis, A. P. and McCuen, R. H. (2005). *Stormwater management for smart growth*, Springer, New York.

Davis, A. P. and Ravirajan, K. (2005). *Hydraulic Conductivity Analysis of Bioretention Media*. Final report prepared for Highway Hydraulics Division of Maryland State Highway Administration. Department of Civil and Environmental Engineering, University of Maryland, College Park, USA.

Davis, A. P., Shokouhian, M., Sharma, H., Minami, C., and Minami, C. (2006). "Water quality improvement through bioretention media: nitrogen and phosphorus removal," *Water Environ. Res*., 78 (3), 284-293.

Davis, A. P. (2007a). "Field performance of bioretention: hydrology impacts." *J. Hydrology*, *in press.*

Davis, A. P. (2007b). "Field performance of bioretention: water quality." *Environ. Eng. Sci.*, *in press.*

Dean, C. M., Sansalone, J.J., Cartledge, F. K., and Pardue, J. H. (2005). "Influence of hydrology on rainfall-runoff metal element speciation" *J. Environ. Eng.,*131 (4), 632-642

Dechesne, M., Barraud, S., and Bardin, J. (2005). "Experimental assessment of storm water infiltration basin evolution," *J. Environ. Eng*., 131 (7), 1090-1098.

Deng, X. and Jennings, A. A. (2006). "Evaluating an electrokinetically driven extraction method for measuring heavy metal soil contamination," *J. Environ. Eng.*, 132 (4), 527-537.

Dietz, M. and Clausen, J. C. (2005). "A field evaluation of rain garden flow and pollutant treatment." *Water, Air, and Soil Pollution*, 167, 123-138.

Dietz, M. and Clausen, J. C. (2006). "Saturation to improve pollutant retention in a rain garden." *Environ. Sci. Technol*, 40, 1335-1340.

Drexler, J. Z., Snyder, R. L., Spano, D., and Paw U, K. T. (2004). "A review of models and micrometeorological methods used to estimate wetland evapotranspiration." *Hydrol. Processes*, 18(11), 2071-2101.

Eldor, P. A. (2007). *Soil microbiology, ecology, and biochemistry.* Academic Press, 3rd ed., Boston.

Fischer, D., Charles, E. G., Baehr, A. L. (2003). "Effects of stormwater infiltration on quality of groundwater beneath retention and detention basins." *J. Environ. Eng.*, 129 (5), 464-471.

Flint, K. R. (2004). *Water Quality Characterization of Highway Sstormwater Runoff from an Ultra Urban Area*. Master Thesis, Department of Civil and Environmental Engineering, University of Maryland, College Park.

Furumai, H., Balmer, H., and Boller, M. (2002). "Dynamic behavior of suspended pollutants and particle size distribution in highway runoff." *Water Sci. Technol.*, 46 (11-12), 413-418.

Gannon, J. J. and Busse, M. K. (1989). "*E. coli* and enterococci levels in urban stormwater, river water, and chlorinated treatment plant effluent." *Water Res*. 23 (9), 1167–1176.

Grace, H. P. (1953). "Resistance and compressibility of filter cakes." *Chemical Engineering Progress*, 49 (6), 303-318.

Grant, D. M. and Dawson, B. D. (2001). *Isco Open Channel Flow Measurement Handbook*. 5th ed. Isco, Lincoln, NE.

Harter, H.L. (1984). "Another Look at Plotting Positions," *Commun. Statist.-Theor. Meth.,* 13 (13), 1613-1633.

Herzig, J. P. and Leclerc, D. M., and Le Goff, P. (1970). "Flow of suspensions through porous media: application to deep filtration." *Ind. Eng. Chem.* 64 (5), 8-35.

Hillel, D. (1998). *Environmental Soil Physics*, Academic Press, San Diego, USA.

Howari, F. M., and Banat, K. M. (2001). "Assessment of Fe, Zn, Cd, Hg, and Pb in the Jordan and Yarmouk river sediments in relation to their physicochemical properties and sequential extraction characteriszation," *Water, Air, and Soil Pollution*, 132, 43-59.

Hsieh, C-h. and Davis, A. P. (2005). "Evaluation and optimization of bioretention media for treatment of urban storm water runoff," *J. Environ. Eng.*, 131 (11), 1521-1531.

Hunt, W. F., Jarrett, A. R., Smith, J. T., and Sharkey, L. J. (2006). "Evaluation bioretention hydrology and nutrient removal at three field sites in North Carolina." *J. Irrig. Drain. Eng.*, 132 (6), 600-608.

Hur, J., Yim, S., and Schlautman, M. A. (2003). "Copper leaching from brake wear debris in standard extraction solutions," *J. Environ. Monit.*, 5, 837-843.

Ives, K. J. (1963). "Simplified rational analysis of filter behavior." *Instn. Civ. Engrs. – Proc.*, 25, 345-364.

Iwasaki, T. (1937), "Some notes on sand filtration," *J. Am. Water Works Assoc*., 29, 1591-1597

Jacobs, J. M., Myers, D. A., Anderson, M. C., and Diak, G. R. (2002). "GOES surface insolation to estimate wetlands evapotranspiration ." *J. Hydrology*, 266(1-2), 53-65.

Kau, S. M. and Lawler, D. F., (1995). "Dynamics of deep bed filtration: velocity, depth and media," *J. Environ. Eng.*, 121 (12), 850-859.

Kreeb, L.B. (2003). *Hydrologic Efficiency and Design Sensitivity of Bioretention Facilities*. Honors Research, University of Maryland, College Park, MD.

Kunze, G. W. and Dixon, J. B. (1989). *Pretreatment for mineralogical analysis, methods of soil analysis, Part 1-Physical and mineralogical method.* 2nd ed., Agronomy Society of America and Soil Science of America, Madison, WI.

Lachat Instruments (2001). *Chloride in Waters*, Lachat Instrument, (Method Number 10-117-07-1-B).

Lau, S. and Stenstrom, M. K. (2005). "Metals and PAHs adsorbed to street particles," *Wat. Res.*, 39, 4083-4092.

Lehner, B., Doll, P., Alcamo, J., Henrichs, T., and Kaspar, F. (2006). "Estimating the impact of global change on flood and drought risks in Europe: A continental, integrated analysis." *Climate Change*, 75 (3), 273-299.

Logan, T. and Miller, R. (1983). *Background levels of heavy metals in Ohio farm soils*. <http://www.ag.ohio-state.edu/~ohioline/rc275/index.html>, (9/15/2003).

Logan, B.E., Jewett, D.G., Arnoid, R. G., Bouwer, E. J., and O' Melia, C. R, (1995). "Clarification of clean-bed filtration models." *J. Environ. Eng.*, 121 (12), 869-873.

Maguire, R.O. and Sims, J.T. (2002). "Soil Testing to Predict Phosphorus Leaching," *J. Environ. Qual.*, 31, 1601-1609.

Martin, M. J., Logan, B. E., Johnson, W. P., Jewett, D. G., and Arnold R. G. (1996). "Scaling bacterial filtration rates in different sized porous media." *J. Environ. Eng*., 122(5), 407-415.

Mays, D. C., and Hunt, R. H., (2005), "Hydrodynamic aspects of particle clogging in porous media," *Environ. Sci. Technol.*, 39, 577-584.

McCuen, R. H. (1985). *Statistical Methods for Engineers.* Prentice-Hall, New Jersey.

McDowell-Boyer, L. M., Hunt, J. R., and Sitar, N. (1986), "Particle transport through porous media," *Water Resour. Res.* 22(13), 1901-1921.

McGhee, T. J., (1991), *Water Supply and Sewage*, 6th ed., McGraw-Hill, Singapore (International edition)

MDE (Maryland Department of the Environment). (2000). *2000 Maryland Stormwater Design Manual, Volume I & II*, MDE, Baltimore, MD

Mehlich, A. (1984). "Mehlich 3 soil test extractant: a modification of Mehlich 2 extractant," *Commun. In Soil Sci. Plant Anal.*, 15 (12), 1409-1416.

Mein, R. G.. , and Larson, C. L. (1973). "Modeling infiltration during a steady rain," *Water Resour. Res.* 9, 384-393.

Merkley, G. P. (2004). *Irrigation and Conveyance and Control: Flow Measurement and Structure Design*. (Lecture note of BIE 6300). p.p. 23-27. Biological and Irrigation Engineering Department, Utah State University, Logan, Utah. <http://ocw.usu.edu/Biological_and_Irrigation_Engineering/Irrigation___Conveyance_Control_Systems>, (April 2007).

Mikkelsen, P. S., Häfliger, M., Ochs, M., Jacobsen, P., Tjell, J. C., and Boller, M. "Pollution of soil and groundwater from infiltration of highly contaminated stormwater- a case study." *Wat. Sci. Tech.*, 36 (8-9), 325-330.

Murpy, J. and Riley, J. P. (1962). "A modified single solution method for the determination of phosphate in natural waters," *Anal. Chim. Acta.*, 27, 31-36.

Norrstrőm, A. C. and Jacks, G. (1998). "Concentration and fractionation of heavy metals in roadside soils receiving de-icing salts," *Sci. Total Environ.*, 219, 161-174.

NRCS (Natural Resources Conservation Service). (2005). *Soil Geochemistry Spatial Database.* United States Department of Agriculture (sampling in 2003 at Baltimore County, Maryland) , <http://soils.usda.gov/survey/geochemistry>, (May 2005).

NWS (National Weather Service) (2006), <*http//:www.nws.noaa.gov*>. (August 2006).

O'Melia, C. R. and Ali, W. (1978). "The role of retained particles in deep bed filtration." *Prog. Wat. Tech.*, 10 (5/6), 167-182.

Petersen, E., Jennings, A. A., and Ma, J. (2006). "Screen level risk assessment of heavy metal contamination in Cleveland area commons," *J. Environ. Eng.*, 132 (3), 392-404.

Pradhan, A. U. (2006). *Field Evaluation of Low Impact Development Practices for Treatment of Highway Runoff in an Ultra Urban Area.* Master Thesis, Department of Civil and Environmental Engineering, University of Maryland, College Park.

Preciado, H. F. and Li, L. Y. (2006). "Evaluation of metal loadings and bioavailability in air, water and soil along two highways of British Columbia, Canada," *Water, Air, and Soil Pollution*, 172, 81-108.

Sansalone, J. J., and Buchberger, S. G. (1997). "Partitioning and first flush of metals in urban roadway storm water," *J. Envionr. Eng*., 123(2), 134-143.

Sansalone, J. J., Koran, J. M., Smithson, J. A., and Buchberger, S. G. (1998). "Physical characteristics of urban roadway solids transported during rain events." *J. Environ. Eng*., 124(5), 427-440.

Satti, A. M., (1989), "Harmonic mean conductivity in declining rate filters." *J. Environ. Eng.*, 115 (2), 462-467.

Satti, A. M., (1990), "Application of declined rate filtration theory- continuous operation." *J. Environ. Eng.*, 116 (1), 87-105.

Sauvé, S., Hendershot, H., and Allen, H. E. (2000), "Solid-solution partitioning of metals in contaminated soil: Dependence on pH, total metal burden, and organic matter," *Environ. Sci., Technol.*, 34, 1125-1131.

Sauvé, S. (2002). *Speciation of Metals in Soils, In Bioavailability of Metals in Terrestrial Ecosystems: Importance of Partitioning for Bioavailability to Invertebrates, Microbes and Plants*, Allen, H. E. ed., SETAC, Pensacola, 7-38.

Sauvé, S., Manna, S., Turmel, M. L., Roy, A., and Courchesne, F. (2003), "Solid-solution partitioning of Cd, Cu, Ni, Pb, and Zn in the organic horizons of a forest soil," *Environ. Sci., Technol.*, 37, 5191-5196.

Schueler, T. (1987). "Controlling urban runoff: a practical manual for planning and designing urban BMPs." Metropolitan Washington Council of Governments, Washington, DC.

Sims, J.T., Leytem, A.B., and Gartley, K.L. (2001), *Interpreting Soil Phosphorus Tests,* Coop. 14 Bull, NM-04, College of Agric. and Natural Resource, University of Delaware, Newark, DE.

Smolders, E. and Degryse, F. (2002). "Fate and effect of zinc from tire debris in soil," *Environ. Sci. Technol.*, 36 (17), 3706-3710.

Sparks, D. L. (1995). *Environmental Soil Chemistry*., Academic Press, San Diego.

Stagge, J, H. (2006). *Field evaluation of hydrologic and water quality benefits of grass swales for managering highway runoff.* Master Thesis, Department of Civil and Environmental Engineering, University of Maryland, College Park.

Stotz, G. (1987). "Investigations of the properties of the surface water runoff from federal highways in the FRG," *Sci. Total Environ*., 59, 329-337.

Strecker, E. and Quigley, M. (1999). *ASCE/EPA Determining Urban Stormwater Best Management Practice (BMP) Removal Efficiencies. Technical Memorandum - Task 3.1 Development of Performance Measures*. <http://www.bmpdatabase.org/docs/task3_1.pdf>, (11/27/2006)

Strecker, E., Quigley, M., and Howell, J. (2000). *ASCE/EPA Determining Urban Stormwater Best Management Practice (BMP) Removal Efficiencies. Task 3.4 – Final Data Exploration and Evaluation Report* <http://www.bmpdatabase.org/docs/task3_4.pdf>, (11/27/2006)

Strecker, E., Quigley, M. Urbonas, B., Jones, J., and Clary, J. (2001). "Determing urban storm water BMP effectiveness." *J. Water Resour. Plann. Manage.*, 127 (3), 144-149.

Strecker, E., Quigley, M., Urbonas, B., and Jones, J. (2004). "Analyses of the expanded EPA/ASCE international BMP database and potential implications for BMP design." *Proceedings of the World Water and Environmental Congress 2004*, June 27-July 1, 2004, Salt Lake City, UT, <http://www.bmpdatabase.org/docs/BMP%20Database%20Analysis%20and%20Design%20Implications%202004.pdf>, (November 2006)

Sun, X. and Davis, A. P, (2007). "Heavy metal fates in laboratory bioretention systems." *Chemosphere*, 66, 1601-1609.

Swartzendruber, D. (1960). "Water flow through a soil profile as affected by the least permeable layer," *J. Geophys. Res.* 65, 4037-4042.

Swartzendruber, D. and Uebler, R. L. (1982). "Flow of kaolinite and sewage suspensions in sand and sand-silt: II. Hydraulic conductivity reduction," *Soil Sci. Soc. Am. J.*, 46, 912-916.

Tchobanoglous, G., Burton, F. L., and Stensel, H. D. (2003). *Wastewater Engineering: treatment and reuse/Metcalf & Eddy*, McGraw-Hill, 4th ed. New York.

Teng, Z. and Sansalone, J. J. (2004). "In situ partial exfiltration of rainfall runoff. II: Particle separation," *J. Environ. Eng.,* 130 (9), 1008-1020.

Tien, C. (1989). *Granular filtration of aerosols and hydrosols*, Butterworths, Boston.

Tien, C. and Bai, R. (2003), "An assessment of the conventional cake filtration theory." *Chem. Eng. Sci.*, 58, 1323-1336.

Tufenkji, N. and Elimelech, M. (2004). "Correlation equation for predicting single-collector efficiency in physicochemical filtration in saturated porous media." *Environ. Sci. Technol.*, 38, 529-536.

Turer, D., Maynard, J. B., and Sansalone, J. J. (2001). "Heavy metal contamination in soils of urban highways: comparison between runoff and soil concentrations at Cincinnati, Ohio," *Water, Air, and Soil Pollution*, 132, 293-314.

UNHSC (University of New Hampshire Storm Center). (2006). *2005 Data Report.* Durham, NH, <http://ciceet.unh.edu/news/releases/stormwater_report_05/Stormwater_05-03-06.pdf>, (12/20/2006).

Urbonas, B.R. (1999). "Design of a sand filter for stormwater quality enhancement," *Water Environ. Res*., 71 (1), 102-112.

USEPA (1986). *Ambient Water Quality Criteria for Bacteria – 1986*. EPA440/5-84-002. United States Environmental Protection Agency. Washington DC, <http://www.epa.gov/OST/beaches/files/1986crit.pdf >, (4/13/2007).

USEPA (1993). *Methods for the Determination of Inorganic Substances in Environmental Sample,* United States Environmental Protection Agency. EPA-600-R-93-100, Ohio.

USEPA (1994). *Methods for the Determination of Metals in Environmental Samples – Supplement I.* United States Environmental Protection Agency. EPA-600-R-94-111. Ohio.

USEPA (1999a). *Preliminary data summary of urban stormwater best management practices*. EPA-821-R-99-012. United States Environmental Protection Agency. Washington, DC.

USEPA (1999b). *Method 1664 Revision A: N-Hexane Extractable Material (HEM) (HEM; Oil and Grease) and Silica Gel Treated N-Hexane Extractable Material (SGT-HEM; Non-polar Material) by Extraction and Gravimetry*. United States Environmental Protection Agency. EPA-821-R-98-002,

Washington DC., <http://www.epa.gov/waterscience/methods/16640514.pdf >, (5/21/2007).

USEPA (2003). *Drinking Water Contaminants.* (Webpage materials), United States Environmental Protection Agency, <http://www.epa.gov/safewater/mcl.html#mcls>, (8/26/2006).

USEPA (2005). *Stormwater Phase II: final rule, an overview* EPA-833-F-00-001. United States Environmental Protection Agency. Washington, DC.

Van Buren, M.A., Watt, W.E, and Marsalek, J. (1997). "Application of the log-normal and normal distributions to stormwater quality parameters," *Wat. Res.*, 31 (1), 95-104.

Wen, B., Hu, X., Liu, Y., Wang, W., Feng, M., and Shan X. (2004). "The role of earthworms (*Eisenia fetida*) in influencing bioavailability of heavy metals in soils," *Biol. Fertil. Soils*, 40, 181-187.

Willis, M. S. and Tosun, I. (1980). "A rigorous cake filtration theory." *Chem. Eng. Sci.*, 35, 2427-2438.

Wu, J. S., Allan, C. J., Saunders, W. L., and Evett, J. B. (1998). "Characterization and pollutant loading estimation for highway runoff," *J. Environ. Eng*., 124 (7), 584-592.

Yao, K. M., Habibian, M. T., and O'Melia, C. R. (1971). "Water and waste water filtration. Concepts and applications." *Environ. Sci. Technol.*, 5 (11). 1105-1112.

Zar, J. H. (1996). *Biostatistical Analysis*. 3rd ed. Prentice-Hall, New Jersey.

Zhen, J., Shoemaker, L., Riverson, J., Alvi, K., and Cheng, M-s. (2006), "BMP analysis system for watershed-based stormwater management." *J. Environ. Sci. Health., Part A*, 41, 1391-1403.

Zwonitzer, J. C., Pierzynski, G. M., Hettiarachchi, G. M. (2004). "Effects of phosphorus additions on lead, cadmium, and zinc bioavailabilities in a metal-contaminated soil." *Water, Air, and Soil Pollution*, 143, 193-209.